QPRTASE: QUINOLINIC ACID ANALOGUE SYNTHESIS AND NON-ENZYMIC DECARBOXYLATION OF N-ALKYLQUINOLINIC ACIDS

Andrew M. Allsebrook

A Thesis Submitted for the Degree of PhD
at the
University of St Andrews

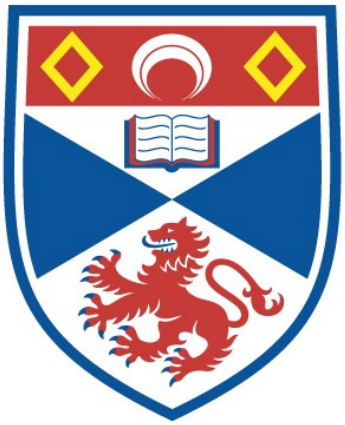

1998

QPRTase: Quinolinic acid Analogue Synthesis and Non-enzymic Decarboxylation of *N*-alkylquinolinic acids

A thesis presented for the degree of
Doctor of Philosophy
to the
University of St. Andrews
in August 1998

by
Andrew M. Allsebrook

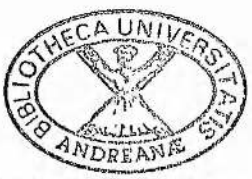

ProQuest LLC.
789 East Eisenhower Parkway
P.O. Box 1346
Ann Arbor, MI 48106 – 1346

i) I, Andrew Michael Allsebrook, hereby certify that this thesis, which is approximately 40 000 words in length, has been written by me, that it is the record of work carried out by me and that it has not been submitted in any previous application for a higher degree.

date 28.8.98 signature of candidate

ii) I was admitted as a research student in October, 1994 and as a candidate for the degree of Ph.D. in August, 1998; the higher study for which this is a record was carried out in the University of St. Andrews between 1994 and 1997.

date 28.8.98 signature of candidate

iii) I hereby certify that the candidate has fulfilled the conditions of the Resolution and Regulations appropriate for the degree of Ph.D. in the University of St. Andrews and that the candidate is qualified to submit the thesis in application for that degree.

date 28.8.98 signature of supervisor

In submitting this thesis to the University of St. Andrews I understand that I am giving permission for it to be made available for use in accordance with the regulations of the University Library for the time being in force, subject to any copyright vested in the work not being affected thereby. I also understand that the title and abstract will be published, and that a copy of the work may be made and supplied to any *bona fide* library or research worker.

date 28.8.98 signature of candidate

ACKNOWLEDGEMENTS

Firstly, I would like to thank Dr. Nigel Botting, for all his help, support and ideas, both throughout my time at St. Andrews, and in the past months whilst I have been away. It was a pleasure working for him, and I have learnt a great deal from him. The Zimmers will struggle to find such a prolific partnership again! Thank you very much, Nigel.

Avril has been such a tower of strength since we met, I don't know how I managed before. Long may it continue.

I have to thank Roger Spark for all his help and friendship (and lifts), especially whilst I was injured.

Mostly, though, I have to thank my Mother and Father, for giving me the opportunity to succeed. They have always supported me in all my decisions, I couldn't have done it without them.

To Mum and Dad,

Thank you for all you've done

Abbreviations

The following common abbreviations have been used throughout the thesis.

AIDS	Auto Immune Deficiency Syndrome
AMP	Adenosine Monophosphate
AMPA	3-(5-Methylisoxazol-4-yl) propionic acid
APRTase	Adenine phosphoribosyltransferase
ATP	Adenosine Triphosphate
AZT	Azidothymine
BMP	Barbituric monophosphate
CSF	Cerebrospinal fluid
DME	1,2-Dimethoxyethane
DMF	*N,N*-Dimethylformamide
DMG	Directed metallation group
DMSO	Dimethyl sulfoxide
EAA	Excitatory amino acid
FAD	Flavin adenine dinucleotide
3-HAO	2-Hydroxyanthraniliate oxygenase
HD	Huntington's disease
HIV	Human Immunodeficiency Virus
HPLC	High Pressure Liquid Chromatography
KAT	Kynurenine aminotransferase
KHMDS	Potassium hexamethyldisilazide
LDA	Lithium diisopropylamide
LTMP	Lithium 2,2,6,6-tetramethylpiperidide
MTT	3-(4,5-dimethylthiazolyl)-2,5-diphenyltetrazolium
MW	Molecular weight

NaADN	Nicotinic acid adenine dinucleotide
NAD	Nicotinamide adenine dinucleotide
NADP(H)	Nicotinamide adenine dinucleotide phosphate
NAMN	Nicotinic acid mononucleotide
NAmPRTase	Nicotinamide phosphoribosyltransferase
NAPRTase	Nicotinic acid phosphoribosyltransferase
NMDA	*N*-Methyl-D-aspartic acid
NMN	Nicotinamide mononucleotide
NMR	Nuclear Magnetic Resonance
ODase	Orotate decarboxylase
OMP	Orotidine-5'-monophosphate
OPRTase	Orotate phosphoribosyltransferase
PLP	Pyridoxal-5'-phosphate
PNC	Pyridine Nucleotide Cycle
PRPP	5-Phosphoribosyl-1-pyrophosphate
PRTase	Phosphoribosyltransferase
QPRTase	Quinolinic acid phosphoribosyltransferase
tlc	Thin layer chromatography
THF	Tetrahydrofuran
TMEDA	*N, N, N', N'*,-tetramethyl-1,2-ethanediamine
UMP	Uridine-5'-monophospate

QPRTase: QUINOLINIC ACID ANALOGUE SYNTHESIS AND NON-ENZYMIC DECARBOXYLATION OF *N*-ALKYL QUINOLINIC ACIDS

CONTENTS

Abstract

Quinolinate phosphoribosyltransferase (QPRTase, E.C. 2.4.2.19) is considered to be a unique enzyme in that it is thought to catalyse two distinct chemical reactions. Both the transfer of a phosphoribosyl group from 5-phosphoribosyl-1-pyrophosphate onto the nitrogen of quinolinic acid and the subsequent decarboxylation of the intermediate to form nicotinic acid mononucleotide are thought to be catalysed by the QPRTase system.

Analogues of quinolinic acid were designed as potential inhibitors of QPRTase. These contain acidic groups at the 2- and 3- positions but are unable to decarboxylate. However, such compounds may be able to undergo the phosphoribosyl transfer reaction, potentially increasing their inhibitory potency. These compounds may be useful as "biological tools" allowing the neurological effects of an increase in quinolinic acid levels to be investigated. The compounds may show anti-fungal activity blocking the kynurenine pathway for NAD production.

2-Sulfonicotinic acid was synthesised by the oxidation of 2-mercaptonicotinic acid by either basic potassium permanganate, or iodine, with the structure was confirmed by X-ray crystallography. In biological testing the acid was shown to be neither an agonist or antagonist of the NMDA receptor, or to be neurotoxic.

A number of synthetic routes towards 2-phosphononicotinic acid, an alternative quinolinic acid analogue, were attempted though none were successful. These included orthometallation strategies and palladium coupling reactions to incorporate the phosphonic acid group at the 2- position. Nucleophilic addition routes, methods of building up the pyridine ring and including non-selective phosphonic acid addition were also examined. However, a related derivative, 2-(phosphonomethyl)nicotinic acid, was successfully synthesised.

The non-enzymic decarboxylation of *N*-alkyl quinolinic acids was investigated, for comparison with the decarboxylation reaction catalysed by QPRTase. Both *N*-methyl and *N*-ethylquinolinic acid were synthesised, and the pH versus rate profiles measured. The rate maximum for both compounds was at pH 1.5, with the rate decreasing both above and below the maximum. *N*-Methylquinolinic acid was 10 times faster than quinolinic acid itself, demonstrating the effect of the nitrogen substituent. The *N*-ethyl derivative decarboxylated a further 1.5 times faster, showing the effect of increasing the size of the substituent. An Arrhenius plot was also carried out, giving an activation energy for the reaction of 153 kJ mol^{-1}. Attempts to prepare the *N*-propyl derivative were unsuccessful, as decarboxylation occurred very readily to give *N*-propylnicotinic acid.

CHAPTER 1

1. QPRTase - the enzyme

1.1 Background

Quinolinate phosphoribosyltransferase (QPRTase, E.C. 2.4.2.19) is an important enzyme of the *de novo* NAD biosynthetic pathway in both prokaryotes and eukaryotes. QPRTase is unique as it is considered to catalyse two distinct chemical reactions. The first of these is the phosphorylation of quinolinic acid (**1**) with 5-phosphoribosyl-1-pyrophosphate (PRPP) (**2**) as the phosphorylating agent, in the presence of Mg^{2+}, to give the intermediate quinolinic acid mononucleotide (**3**). Subsequent decarboxylation of this intermediate at the 2- position of the pyridine ring yields nicotinic acid mononucleotide (**4**) (Scheme 1.1).

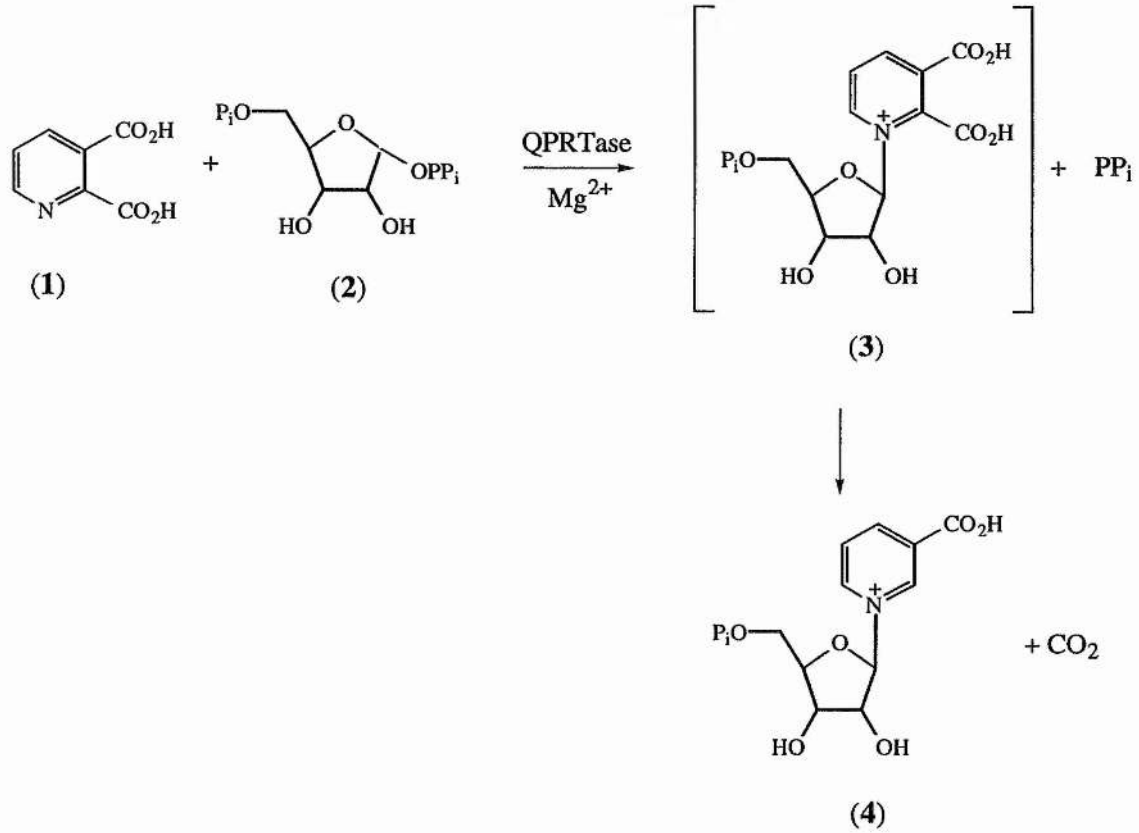

Scheme 1.1: QPRTase catalysed reaction

QPRTase is therefore essential for metabolism of quinolinic acid, which is the first intermediate in the biosynthesis of NAD common to all organisms. From this point in the pathway all biological systems, animals, plants and micro-organisms, follow the same route to formation of NAD. The metabolism of quinolinic acid is important due to its potency as a neurotoxin. It is an agonist of the NMDA receptor, and high levels of the acid have shown to be present in the brain and CSF of patients with neurodegenerative diseases such as Huntington's Disease and AIDS (see Section 1.9).

1.2 Introduction

It was first suggested that quinolinic acid was simply a side product of 3-hydroxyanthranilate metabolism, rather than an intermediate in nicotinic acid mononucleotide (NAMN) biosynthesis.[1] Nishizuka and Hayaishi showed the presence of an enzyme that would convert 3-hydroxyanthranilate to NAMN, via quinolinic acid as an intermediate.[2] Using ^{14}C-labelled quinolinic acid, $^{14}CO_2$ was detected in cat and rat liver. Later that year the same group demonstrated that nicotinic acid was not an intermediate in this pathway, and that quinolinic acid is not inert, but was a vital part.[3]

Nakamura *et al*[4] first isolated and purified an enzyme from rat liver acetone powder and demonstrated that free nicotinic acid is not involved in the PRPP-dependent NAMN formation from quinolinic acid. They found that a single enzyme was responsible for the reaction to form NAMN, and gained no evidence for the formation of quinolinic acid mononucleotide as an intermediate. This group named the enzyme "quinolinate transphosphoribosylase". The NAMN formed was isolated, and the amount of $^{14}CO_2$ measured along with the concentration of remaining quinolinic acid. The results of this experiment gave the stoichiometry of the reaction. The amount of quinolinic acid consumed corresponded directly to the amount of NAMN and $^{14}CO_2$ consumed. Thus one mole of quinolinic acid leads to the formation of one mole of NAMN with the additional loss of one mole of $^{14}CO_2$. When their experiments were

repeated without PRPP no quinolinic acid was consumed, no NAMN formed and no $^{14}CO_2$ detected. The same results were obtained when Mg^{2+} was the only component missing, and when all the components were present, but the enzyme had been boiled first, showing that both Mg^{2+} and PRPP are required for the reaction to take place.

The assay used involved measuring the PRPP-dependent evolution of $^{14}CO_2$ from [^{14}C]-quinolinic acid.[3] The synthesis of [$^{14}C]_4$-quinolinic acid is given below (Scheme 1.2). Labelled aniline (**5**) was condensed with glycerol to form quinoline (**6**), which in the presence of divalent copper cations was oxidised to [$^{14}C]_4$-quinolinic acid with hydrogen peroxide. Acidification, extraction and then treatment with H_2S produced the required free acid.

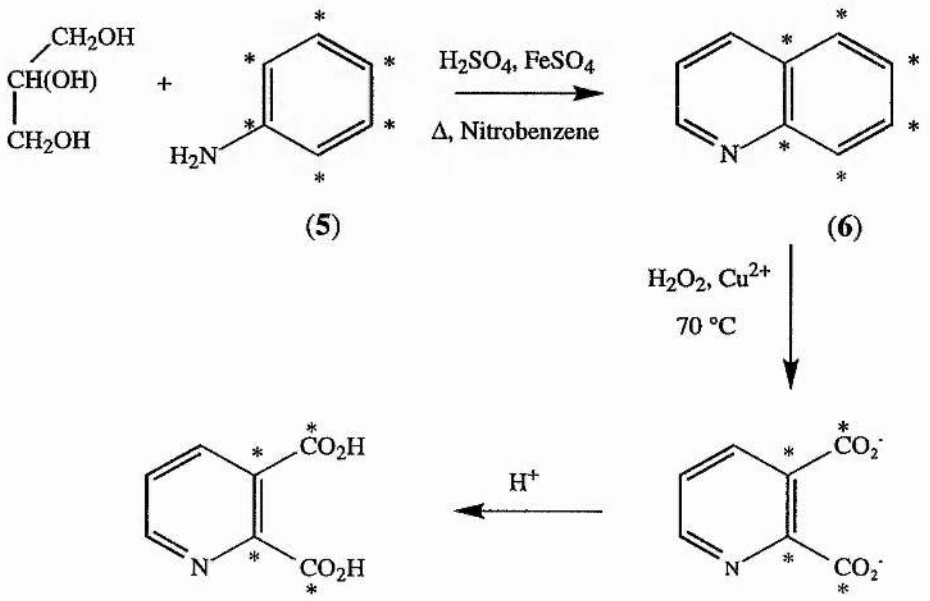

Scheme 1.2: Synthesis of [$^{14}C]_4$-quinolinic acid

Gholson *et al* confirmed that only one enzyme is required for the transformation when they also found no evidence for the presence of quinolinic acid mononucleotide.[5] From the relatively high rate of reaction, and the low K_m value for quinolinic acid, it was proposed that quinolinic acid was an intermediate in the transformation of tryptophan to NAD and the biosynthesis of pyridine nucleotides from tryptophan.

A single enzyme thus appeared to be responsible for both the phosphoribosyl transfer and decarboxylation, but it was also suggested that the decarboxylation reaction could be non-enzymic. Increased electronegativity at position two,[6] as the pyridine ring nitrogen becomes quaternary on addition of the phosphoribosyl group, could facilitate loss of carbon dioxide.

Nakamura *et al* suggested that the enzyme was found only in the liver and kidney of rat and mouse, but not in any other tissues or organs.[4] They also found that "quinolinate transphosphoribosylase" was widely distributed in micro-organisms, fungi and plants, including *Pseudomonas fluorescens*, *E. coli*,[7] *Neurospora crassa*,[1] yeast and cucumber. Since this initial discovery, QPRTase has been isolated and purified from many sources. Iwai and Taguchi observed high activity for the enzyme in a wide range of organisms with persimmon leaf, Shiitake mushroom, Enshitake mushroom, bakers' yeast and *Pseudomonas riboflavin* being revealed as sources of the enzyme for the first time.[8] *Ricinius communis* (castor bean) endosperm,[9] hog liver[10,11] and kidney,[12,13] *Alicagenes eutrophus*,[14] the root and leaves of the tobacco plant *Nicotiniana tobaccum*,[15] rat brain[16] and human brain and liver,[17,18] and *Salmonella typhimurium*[19] have all since been identified as sources of QPRTase.

1.3 Physical properties

1.3.1 Molecular weight

Depending upon the source of the enzyme, QPRTase has been shown to have a range of molecular weights. Initial reports of QPRTase from a pseudomonad[20] revealed a molecular weight (MW) of 178 000. Further work by the same researchers[21] modified this to a MW of 165 000, which they could be irreversibly dissociated into inactive protein units of MW 54 000. Electrophoresis on the enzyme from the castor bean endosperm (*Ricinius communis*) demonstrated that two subunits both of approximately 35 000 were present.[9] Hog liver QPRTase[10] was found to have five subunits of 34 200, giving a total MW of around 172 000. However the X-ray diffraction analysis of the enzyme from hog liver[22] indicated that there were actually six identical subunits, all of 34 200, and the MW was re-evaluated to between 202 000 - 210 000. Interestingly, the enzyme from *Alicagenes eutrophus* nov subsp. *quinolinicus*[14] was shown to have a MW 210 000 - 222 000, but in this case consisted of eight identical subunits of 27 500. Rat QPRTase was purified from liver and brain sources,[16] and was found to have a MW of 160 000, with five subunits of 32 000, whilst purification of human QPRTase[18] revealed a MW of 170 000, again with five subunits. The most recent QPRTase to be purified is that from *Salmonella typhimurium* nad C gene,[19] which shows a MW 72 000 with two subunits in this case.

Overall there seems to be a pattern of the enzyme existing either in the form of a dimer or a pentamer, depending on the evolutionary history.

1.3.2 Variation of activity with pH

As with the molecular weight the optimum pH for QPRTase varies according to the particular source of the enzyme. From beef liver[4] maximum activity was seen at pH 6.2. If the source was a pseudomonad, the optimum pH was 6.8, with 50% of maximal activity at pH 6.2, and 80% at pH 8.0, whilst another *Pseudomonas sp.* gave optimum activity at pH 7.1. In contrast to these sharp pH optima, QPRTase from castor bean endosperm was active over a wide pH range,[9] with optimum activity between 6.5 and 7.7. Interestingly, *Alicagenes eutrophus* nov subsp. *quinolinicus* QPRTase had an optimum pH of 8.5 - 9.0, and optimum temperature of 60 °C while that of hog liver[14] only pH 6.1, and crystalline hog kidney enzyme pH 5.5. Human liver QPRTase[18] showed a maximum activity at approximately pH 6.5.

The optimum pH for maximum activity of the enzyme thus appears to differ as much according to the location of the enzyme within the organism as it does from organism to organism.

1.4 Inhibition studies

Investigation into the inhibition of an enzyme system is an extremely important part of understanding the enzyme. The use of inhibitors is vital, not just to prevent the enzyme from functioning, but also to examine possible mechanisms for the catalysed reaction. QPRTase is no exception and several inhibition studies have been reported.

1.4.1 Cations

The study of Nakamura *et al* showed that the enzyme from beef liver gave maximum activity with a $MgCl_2$ concentration of 5×10^{-4} M.[4] As the concentration of Mg^{2+} increased, an increase in inhibition was observed, with 90-95% inhibition at 2×10^{-2} M. Inhibition by high concentrations of Mg^{2+} can be easily reversed by adding a boiled crude enzyme extract preparation,[23] suggesting that a substance which is able to chelate Mg^{2+} is present in the crude extract. It was also confirmed that the presence of Mg^{2+} is absolutely required for the activity of the enzyme.

Other divalent cations also inhibited the enzyme. Thus Hg^{2+}, Co^{2+}, Cu^{2+}, Ba^{2+}, Mn^{2+} and Ca^{2+} all inhibited by almost 100% at 10^{-3} M, while Zn^{2+} and Fe^{2+} inhibited by 40-70% at this level. Further studies showed that Cd^{2+} also inhibited enzyme activity by 20-40% at 10^{-3} M.[23]

Shibata and Iwai reported that with QPRTase from hog kidney, Mg^{2+} could actually be completely replaced by Mn^{2+} ions,[12] and that similar results could be obtained from the liver enzyme.[22] In *Alicagenes sp.*[14] and Shiitake mushrooms,[24] Mn^{2+} was only partially effective in replacing Mg^{2+}.

1.4.2 Nucleotides

It was discovered early on in QPRTase studies that the formation of NAMN from quinolinic acid was not reliant on ATP, as is its formation from nicotinic acid (NAPRTase).[23] In fact ATP actually inhibits QPRTase activity at 10^{-3}-10^{-4} M. NAD also inhibits the reaction, and initially this was thought to be some form of regulatory system.[5] Such negative feedback control is very well known in the metabolic pathways of micro-organisms,[25] but rarely occurs in higher organisms.

The reaction, at optimum Mg^{2+} concentration, is inhibited by other phosphorus containing compounds, including AMP, inorganic pyrophosphate, NAD and FAD at concentrations between 10^{-3}-10^{-4} M. Metal chelating agents, such as F^- also inhibit the reaction at 10^{-3} M. If, however, the Mg^{2+} is then increased (5 x 10^{-3} M and higher) then the inhibition brought about by these molecules disappears. This implies that inhibition by these compounds was not by interaction at the active site of the enzyme but rather by chelation of Mg^{2+} ions.

Okuno *et al* incubated purified liver QPRTase with [^{3}H]-NAMN and pyrophosphate under normal QPRTase assay conditions and showed that no production of [^{3}H]-quinolinic acid was observed by ion exchange chromatography.[18] This is a good indication that NAMN does not inhibit QPRTase. [^{3}H]-NAMN was prepared by the incubation of 1 μCi [^{3}H]-quinolinic acid with 1 mM PRPP, 4 mM $MgCl_2$ in a solution of 20 mM sodium acetate-acid buffer (pH 5.5), total volume 0.5 ml, at 37 °C for 2 hours.[26] Complete reaction of [^{3}H]-quinolinic acid was observed by HPLC and tlc.

1.4.3 Nicotinic acid and nicotinamide

In their studies on QPRTase from castor bean endosperm, Mann and Byerrum[9] examined the effect of pyridine nucleotide precursors nicotinic acid and nicotinamide, and showed that neither inhibited the enzyme, and that neither of them were affected by the enzyme at all. Studies by Packman and Jakoby on the enzyme from *Pseudomonas* confirmed this observation.[27] QPRTase is absolutely specific for quinolinic acid, and does not catalyse formation of any other pyridine nucleotides.

1.4.4 5-Phosphoribosyl-1-pyrophosphate analogues

Kunjara *et al* investigated the stereospecificity of the enzyme-PRPP binding site, and especially the metal-PRPP complex at this site.[28] They synthesised phosphorothioate analogues of PRPP and tested them as substrates of QPRTase, using either Mg^{2+}, Co^{2+} or Cd^{2+} as the cation. These analogues, previously synthesised by Smithers and O'Sullivan,[29] were phosphoribosyl-1-O-(2-thiodi-phosphate) (PRPPβS) and the diastereomers of phosphoribosyl-1-O-(1-thiodiphosphate) (PRPPαS). With Mg^{2+} PRPP was a better substrate than (PRPPαS), but the velocities were of a similar order. The S diastereomer was a better substrate with Mg^{2+}, whereas with Cd^{2+} the R diastereomer was better. The apparent reversal of enzyme stereospecificity with the change of divalent cation suggests that the metal ion remains ligated to the 1-P moiety in the rate determining step, as cations such as Mg^{2+} (hard) prefer ligation with oxygen, and soft Cd^{2+} prefers complexation with S.

Iwai *et al* found that potassium phosphate buffer inhibited QPRTase from *Alicagenes sp.*[14] The two salts constituting a potassium phosphate buffer were investigated individually, and as a result, KH_2PO_4 was shown to inhibit more than K_2HPO_4, which inhibits to the same extent as both KCl and K_3PO_4. The inhibition by $H_2PO_4^-$ was not affected by increased concentrations of phosphoribosyl pyrophosphate, and as the ionic strength increased so did the level of inhibition. It was

suggested from these results that the inhibition by $H_2PO_4^-$ is not only due to an increase in the ionic strength, but by some interaction with the protein, in particular the ionic binding between the enzyme and its substrate.

In their investigations into the effect of PRPP on hog kidney and liver QPRTase Shibata and Iwai demonstrated that increased PRPP concentrations affect the optimum pH for QPRTase activity,[30] and actually inhibited activity of the enzyme at alkaline pH and physiological pH. This inhibition of the enzyme was not recorded at acidic pH, although if 30% glycerol was present the same degree of inhibition was seen with a lower PRPP concentration than at alkaline pH.

A possible explanation for the inhibition at alkaline pH or physiological pH may be that the enzyme conformation is actually native at this pH range, as PRPP inhibits at physiological pH. Shibata and Iwai proposed that the enzyme protein may have two binding sites, one of which is capable of binding both quinolinic acid and PRPP, the other PRPP only.[30] This could alter at acidic pH, so that the binding site for quinolinic acid and PRPP may only bind quinolinic acid, thus removing PRPP inhibition properties.

Glycerol has been shown to affect the binding site of enzymes,[31] and has been observed to maintain, even at acidic pH, an active conformation of hog kidney and liver QPRTases.[22,32] This helps to explain why, in the presence of glycerol, PRPP can still inhibit the enzyme.

1.4.5 Quinolinic acid analogues as inhibitors

This is the area of QPRTase inhibition which has been most studied. The effect of these analogues on the rate of the QPRTase reaction should give information on the active site of the enzyme and the way in which the enzyme catalyses the reaction.

Mann and Byerrum investigated the effect of several quinolinic acid analogues on the rate of the enzymic reaction for the enzyme from castor bean endosperm.[9] Picolinic acid (**7**) was by far the most effective inhibitor of those tested, with a K_i of 10^{-3} M. The results demonstrated that a free carboxylate at the 2-position was required for effective inhibition. The methyl esters tested were not as effective inhibitors as the free acids. Interestingly the 2-methyl ester of quinolinic acid (**8**) does inhibit the enzyme, and more significantly than the other 2-methyl esters, methyl 3-aminopyridine-2-carboxylate (**9**) and methyl 3-cyanopyridine-2-carboxylate (**10**). This suggests that the 3-carboxylate is also important for substrate binding, but not as significant as the 2-carboxylate.

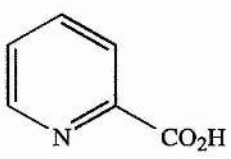

(**7**)

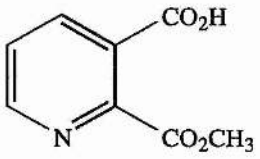

(**8**)

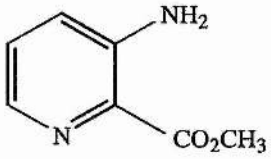

(**9**)

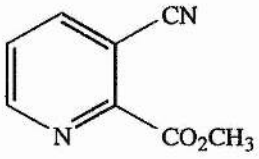

(**10**)

The effect of a 2-carboxylate was also demonstrated with inhibition studies on the positional isomers of quinolinic acid. The 2,4- (**11**) and 2,5-dicarboxylic acids (**12**) were mainly ineffective, but pyridine-2,6-carboxylic acid (**13**) and pyridine-3,4-carboxylic acid (cinchomeric acid) (**14**) did inhibit well. Pyridine-2,6-carboxylic acid (dipicolinic acid) acts like picolinic acid, showing the requirement for the 2-carboxylate.

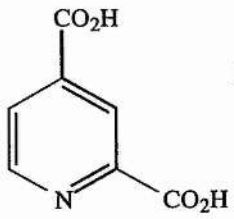

(11)

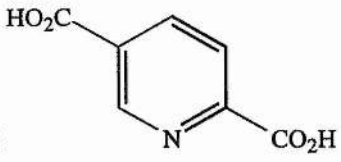

(12)

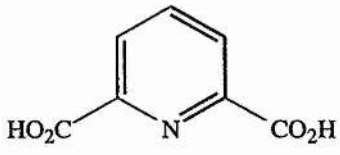

(13)

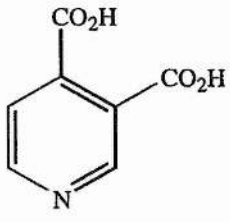

(14)

2-Hydroxynicotinic acid (**15**) did inhibit QPRTase activity, but not as much as analogues with a carboxylic acid group at the 2- position. 4-Hydroxyquinolinic acid (**16**) also inhibited quite well, the steric effect of the C-4 substituent appearing not to exclude the molecule from the active site.

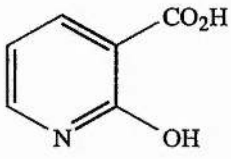

(15)

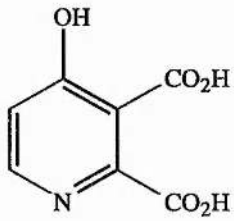

(16)

Shibata and Iwai also showed that dipicolinic acid inhibited the enzyme from this source, despite not inhibiting QPRTase from hog liver and *Alicagenes sp.*[14] Dipicolinic acid is known as a metal chelator, but in this case adding extra Mg^{2+} did not decrease inhibition to a significant extent. The same pattern was seen with pyrazine-2,3-dicarboxylic acid.

Taguchi and Iwai looked at inhibition of hog liver QPRTase by various quinolinic acid analogues.[24] Only phthalic acid had any significant inhibitory effect, the mode of inhibition for which was shown to be competitive and a K_i value of 1.7×10^{-4} M determined.

Shibata and Iwai tested a selection of carboxylic acids as inhibitors of QPRTase from *Alicagenes sp.* and again showed picolinic acid as an inhibitor. Phthalic acid also strongly inhibited enzyme activity, which suggests that the nitrogen of quinolinic acid

may not be required for binding of the substrate at the active site of the enzyme. However, as pipecolic acid (piperidine-2-carboxylic acid) does not inhibit, the pyridine ring may be essential. The type of inhibition for picolinic acid and phthalic acid was shown to be competitive for both with a K_i of 8.22 and 8.87 x 10^{-5} M respectively, while the esters of these inhibitors, methyl picolinate and dibutyl phthalate, did not inhibit. These results help to confirm the suggestion that C-2 carboxylate group is important in binding the substrate to the enzyme, and that having carboxylate groups adjacent to each other is also important.

K_i values for phthalic acid from all three sources show how potent an inhibitor it is and K_m values for quinolinic acid increase significantly when phthalic acid is added. The K_i value for phthalic acid as an inhibitor of brain QPRTase is 40-80 times lower than the values seen for inhibition in the liver or the enzyme from *Alicagenes sp.*, so either brain QPRTase is different or is subject to distinct regulatory influences.

Kalikin and Calvo synthesised a group of 2-substituted nicotinic acids and 2-substituted 3-nitropyridines to investigate their action as inhibitors (Table 1.1).[33] The four compounds used in the study were 2-hydroxynicotinic acid, 2-mercaptonicotinic acid (**17**), 2-hydroxy 3-nitropyridine (**18**) and 2-mercapto-3-nitropyridine (**19**). The mode of inhibition for 2-mercapto-3-nitropyridine was determined and shown to be competitive, with a K_i of 0.126 mM, which implies that it binds more tightly to the enzyme than quinolinic acid (K_i of 0.17 mM in this study). All of the compounds studied inhibited the enzyme, with varying effectiveness.

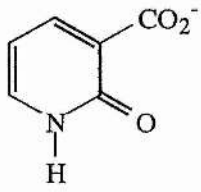

(15)

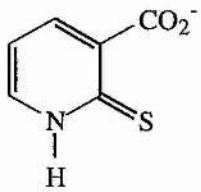

(17)

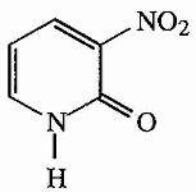

(18)

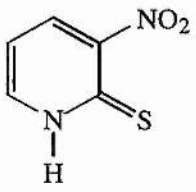

(19)

Such compounds, which are 2-hydroxy or 2-mercaptopyridines, can exist in a tautomeric form, where the ring exists as an unsaturated lactam. NMR studies in methanol have suggested that only about 4% of 2-hydroxynicotinic acid is present as the pyridine, while the amount of 2-mercaptopyridine as the thiol tautomer is slightly larger. With 3-nitro substituents, the effect is to even further increase the amount of hydroxyl or thiol tautomer relative to the lactam or thiolactam. Obviously both the hydroxyl and thiol groups can ionise. Due to the electron withdrawing effect of the nitro group, the pKa of these 3-nitropyridines is lower than that of the 3-carboxylate substituted compounds.

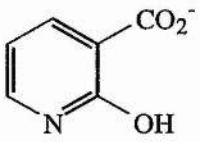

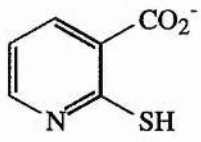

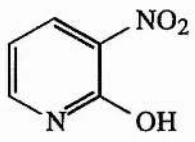

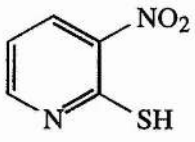

	(15)	**(17)**	**(18)**	**(19)**
pK_a	nd	nd	10.3	6.9
% Inhibition	0.0	8.3	16.0	95.0

Table 1.1: Inhibition of quinolinic acid analogues

It can be seen from the results of Table 1.1 that the actual degree of inhibition follows a definite pattern. 2-Mercapto-3-nitropyridine, the compound with the lowest pKa of these tested, showed the greatest inhibition, whilst 2-hydroxynicotinic acid inhibited the least, and was thought to have the highest pKa. So, as pKa increases, the degree of inhibition decreases. These results imply that a negative charge at position 2 is a big contributor to the tight binding of the inhibitor to the enzyme, as the compound with the lowest pKa is also the best inhibitor. Hence there may be some very important interaction between the negative charge and a positively charged group at the active site of the enzyme.

1.4.6 Amino acid modifications

Reagents that react specifically with sulfhydryl groups, such as *p*-chloromercurobenzoic acid, *N*-ethylmaleimide, dithiobis(2-nitrobenzoic acid) and monoiodoacetic acid all strongly inhibited the QPRTase catalysed reaction at 37 °C, suggesting SH groups have an important part to play in the reaction.[34] β-Naphthoquinone-4-sulfonic acid and 2,4,6-trinitrobenzenesulfonic acid are known to combine with lysine residues.[10] Diethyl pyrocarbonate and *p*-diazobenzene sulfonic acid combine with histidine residues and glyoxal with arginine. These all showed inhibitory effects at fairly low concentrations, which implied that lysine, histidine and arginine residues may also be involved at the active site of the enzyme. Reaction with β-naphthoquinone-4-sulfonic acid and *p*-diazobenzenesulfonic acid was inhibited by the presence of the substrate, although reaction with glyoxal was not.

Diisopropylfluorophosphate, 2-hydroxy-5-nitrobenzyl bromide and acetylimidazole are chemical modifying agents for serine, tryptophan and tyrosine residues respectively. None of these inhibited QPRTase activity to any degree, suggesting that these residues are not present at the active site.

1.5 Mechanisms

1.5.1 Kinetic mechanism

To date studies on the kinetic mechanism of QPRTase have resulted in no conclusive evidence for one particular mechanism. Depending on the source of the enzyme, conflicting conclusions have been produced.

For QPRTase from hog kidney double reciprocal plots of initial velocity versus a second substrate resulted in parallel, linear plots.[12] From these secondary plots, the K_m values of quinolinic acid and PRPP were calculated to be 4×10^{-5} M and 1.4×10^{-4} M respectively. This made it likely that the reaction mechanism for this source was of the "ping-pong" type. Similar results were found for both the hog liver enzyme, and QPRTase from *Neurospora crassa*.[22,35]

Those enzymes which do operate via a "ping-pong" mechanism require the loss of pyrophosphate prior to the binding of quinolinic acid. Alberty developed equations for analysis of reactions involving two substrates in which formation and decomposition of binary complexes occur, therefore ruling out ternary complexes.[36] If it is assumed that the initial reaction of QPRTase involves PRPP and the enzyme, a minimal formal sequence can be written:

$$\begin{aligned} E + PRPP &\rightleftharpoons E' \\ E' &\rightleftharpoons ERP + PP \\ ERP + QUIN &\rightleftharpoons E'' \\ E'' &\rightleftharpoons E + NAMN + CO_2 \end{aligned}$$

In contrast, the enzyme isolated from castor bean endosperm gave double reciprocal plots which were linear but non-parallel, representing an ordered reaction mechanism.[9] This means that both quinolinic acid and PRPP must be bound to the

enzyme before any product is released. This enzyme, therefore, seems to operate via a ternary complex mechanism, facilitated by random binding of the two substrates.

All of this evidence is very much superficial and so no definitive conclusions can be drawn from it.

1.5.2 Ylid mechanism for decarboxylation

The significance of the observations by Kilikin and Calvo lies in the chemical mechanism for the decarboxylation reaction of QPRTase. An intermediate nitrogen ylid mechanism was proposed by Brown and Moser after their studies on the decarboxylation of pyridine-2-carboxylic acids.[37] Hammick also postulated a nitrogen ylid intermediate in the decarboxylation of picolinic acids,[38] as did Beak and Siegel for the decarboxylation of orotic acid,[39] while Levine *et al* explained the inhibition of OMP decarboxylase by a barbiturate nucleotide in the same manner.[40]

If this mechanism is the method of decarboxylation for QPRTase, inhibition by the tautomeric forms of 2-hydroxy and 2-mercaptopyridine may also be due to the fact that the compounds resemble the intermediate ylid formed immediately after decarboxylation (see Scheme 1.3).

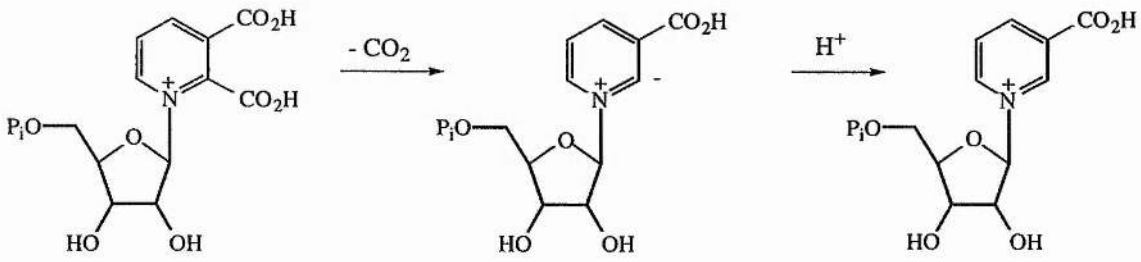

Scheme 1.3: Proposed ylid decarboxylation mechanism for QPRTase

Further work on the ylid mechanism is discussed in Section 3.1.

1.6 Crystal structure

The first crystallisation of QPRTase was completed by Packman and Jakoby in 1965.[20] Musick[41] crystallised the enzyme from hog liver, and investigated the space group and the molecular symmetry from this source, by X-ray crystallographic methods. In addition to the hexagonal apoenzyme crystals grown, a pseudo-ternary complex, containing the enzyme, Mg^{2+} ions, PRPP and phthalic acid, a known competitive inhibitor for the enzyme was obtained. This did not alter the crystal morphology, possibly implying that a conformational change does not occur when substrate binds to the enzyme. Upon investigation of the space group, the unit cell was found to accommodate only two or four molecules in special positions. This implied that the enzyme protein was hexameric, which is in direct contradiction to Taguchi and Iwai's proposal of a pentamer.[42] These results also lead to a molecular point symmetry of 32.

More recently the detailed crystal structure of QPRTase has been determined by Eads *et al* for the enzyme from *Salmonella typhimurium*.[43] The structure has been elucidated with bound quinolinic acid to 2.7 Å resolution, and with bound NAMN to 3.0 Å resolution. Thus the active site of the enzyme, and the amino acid residues involved with substrate binding have been identified. Interestingly, the 3-dimensional structure of the enzyme shows a completely new and novel fold for a phosphoribosyltransfer enzyme, one that has a two domain structure, a mixed α/β N-terminal domain and an α/β barrel like domain which contains seven β strands. The active site of QPRTase is present at the C-terminal ends of the β strands of the α/β barrel, and is bordered by the N-terminal domain of the second sub-unit of the dimer. The site is composed mainly of conserved charged residues, which are obviously important both for substrate binding and the actual catalysis.

1.6.1 α/β Barrel

The QPRTase α/β barrel is unlike others previously seen. Seven stranded α/β barrels have been previously reported, but the domain of the QPRTase barrel appears to be similar to the normal eight stranded α/β barrels. This is the result of a gap between the second (B5) and the third (B6) β strands, and this gap gives the appearance of there actually being eight strands. No H-bonding exists between B5 and B6 strands and the two lie almost orthogonal to each other.

1.6.2 Dimer

The structure of *S. typhimurium* QPRTase indicates that the dimer is required for full activity of the enzyme, as both parts contribute to the active site, and it has been shown that the dimer does exist in solution. Both subunits are very similar.

1.6.3 Active site - quinolinic acid bound

The quinolinic acid molecule is found near the centre of the α/β barrel close to the C-terminal end β strand B4, which is similar to that seen for other α/β barrel enzymes. This also means that the active site is bordered by the N-terminal domain of the other subunit in the dimer, which limits the solvent access to quinolinic acid to just 36 $Å^2$ of a possible 151 $Å^2$ van der Waals surface of quinolinic acid normally available.

The resolution of the data is such that it is difficult to orient quinolinic acid unambiguously. The 3-carboxylate group of quinolinic acid is within H-bonding distance of N_ε and N_η of Arg 175 and N_ε of Arg 152, whereas the 2-carboxylate group only H-bonds to the mainchain NH of Arg 152. It is also approximately 4 Å from the side chain of Lys 153 and Arg 118 from the other dimer. His 174 is near C-5 of quinolinic acid and also about 4 Å from the 3-carboxylate group, and these side chains form the basic pocket for anionic substrate binding. The active sites of the two

molecules of the dimers are different. In molecule A, Lys 153 is 3.8 Å from the C-2 carboxylate group of quinolinic acid, whereas in molecule B it is greater than 4 Å away. Lys is only approximately 4 Å away from the C-2 carboxylate in B, but in molecule A is much further away (> 6 Å). Both these facts help to explain the reason why quinolinic acid has a lower active site occupancy in molecule A.

The fact that there are positively charged residues close to the positions of the C-2 and C-3 carboxylate groups of quinolinic acid could certainly stabilise ylid formation, both by electron withdrawal of negative charge from the pyridine ring inductively via the C-3 carboxylate, or perhaps by direct stabilisation of the negative charge at position C-2 by interaction with Lys 185 or Arg 118.

Figure 1.1 below shows the active site of the enzyme with quinolinic acid bound, with the close proximity of lysine and arginine residues noted.

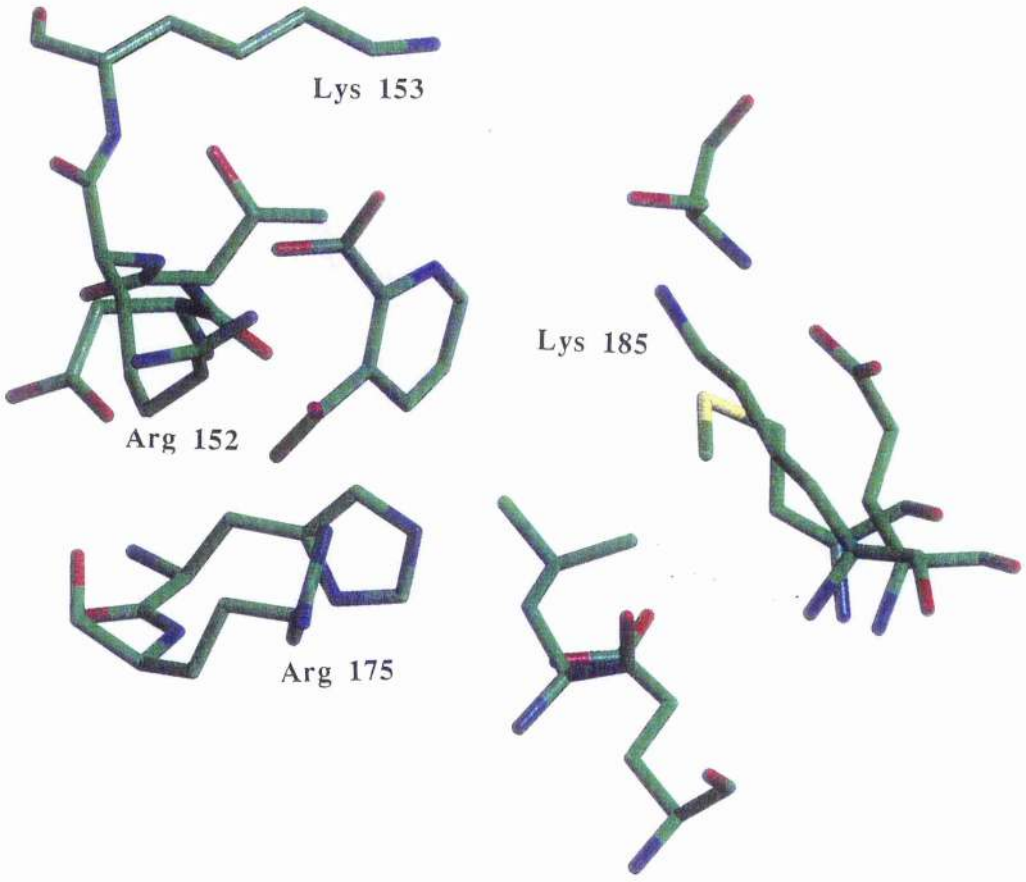

Figure 1.1: Active site structure of QPRTase

Having a negatively charged C-2 substituent has been shown to be vitally important for quinolinic acid binding. Nicotinic acid does not have this negative charge and has been shown not to be an inhibitor of QPRTase from *E. coli* or *S. typhimurium*.[7,19] Compounds with negative charge at position 2 of the pyridine ring have been shown to inhibit effectively.[33,9] From the crystal structure there seems to be no particular reason why this is so, as more interactions are seen at C-3 carboxylate than C-2. There is a possibility that Arg 118 and Lys 185 could move closer to C-2 upon binding or the flexibility which can be seen in the region 180 - 206 may bring Lys 185 to within H-bonding distance of C-2 carboxylate.

Mutant strains of QPRTase from *S. typhimurium* that are able to grow on nicotinic acid rather than quinolinic acid show a mutation at Lys 185, implying that this amino acid residue plays an important part in both QPRTase specificity and therefore NAD biosynthesis.

1.6.4 Active site - NAMN binding

Both subunits of the dimer bind NAMN equally. The nicotinic acid ring occupies a very similar position to that of quinolinic acid, and the bound ribose phosphate group extends across the barrel towards B9 and B10.

When quinolinic acid is bound to the enzyme, Asn 260 occupies a position which coincides with the phosphate binding site. When NAMN binds, Asn 260 is shifted. The C_α position moves 3 Å away from the phosphate group, the side chain atoms further, leading to a 2-3 Å shift of the whole of the 258 - 265 group. One of the side effects is a shift of 4 Å for C_α from Gly 259 as the backbone NH moves completely.

One of the outcomes is that the residues 258 - 265 in the NAMN-QPRTase complex is clearer from electron density maps, compared to the poorly defined density maps in the quinolinic acid-QPRTase complex.

Orotate PRTase, HGPRTase and Glutamine-PRPP aminotransferase all have a similar type I PRTase, but the thirteen amino acid residue motif is conserved. It is found at the centre of the fold and is vital in ribose-phosphate moiety of PRPP.

1.7 Phosphoribosyl Transfer Reaction

1.7.1 Chemical Mechanism

The chemical mechanism of the reaction catalysed by QPRTase is not fully understood. Addition of the phosphoribosyl group can be considered to be similar to that catalysed by other members of the PRTase family. However there is still no consensus of opinion concerning the mechanism of the PRTases. This group of enzymes catalyses the addition of a phosphoribosyl moiety to a nucleophilic nitrogen, with a resulting overall stereochemical inversion at the sugar centre implying that a direct displacement reaction takes place (Scheme 1.4).

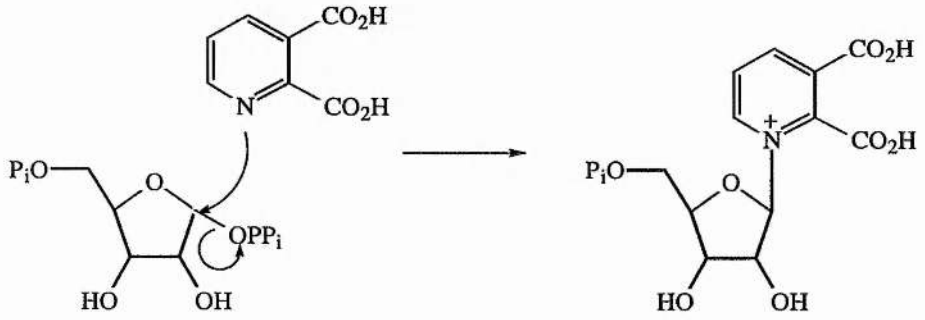

Scheme 1.4: Chemical mechanism

Goitein *et al* determined primary ^{14}C and secondary ^{3}H kinetic isotope effects for a series of phosphoribosyltransferases.[44] The common substrate PRPP was synthesised with ^{14}C at C-1 or with ^{3}H at the C-1 or C-5 carbon atoms. Pairs of these were then used to investigate the kinetic isotope effects for the reaction.

A carbocation like transition state arising from an sp^3 ground state generally has less total point energy, thus activation for the reaction of a molecule with a heavier hydrogen isotope is large, resulting in slower reaction of the substituted molecule.

^{3}H Kinetic isotope effects in the range 1.11 to 1.30 were obtained for the phosphoribosyltransferases. A typical S_N1 type reaction with a carbocation like transition state should have a ^{3}H kinetic isotope effect of around 1.41, compared to 1.0

for an S_N2 type reaction. However an ambiguity can arise in enzymic reactions, where an isotope effect close to 1 does not necessarily indicate an S_N2 mechanism being utilised. Some substrates display no significant effect due to steady state suppression of the isotope effect.

Determination of the primary ^{14}C kinetic isotope effect for these enzymic reactions leads to resolution of this ambiguity. Small primary ^{14}C kinetic isotope effects of 1.0 to 1.08 result from a carbocation like transition state, because of the asymmetric intermediate state, whereas an S_N2 type reaction, with a symmetric transition state, has a primary ^{14}C kinetic isotope effect of 1.09 to 1.15.[45-48]

The primary ^{14}C kinetic isotope effect for the phosphoribosyltransferases studied ranged from 1.01 to 1.05, which supports the theory that on chemical grounds a carbocation like S_N1 transition state is involved (Scheme 1.5).

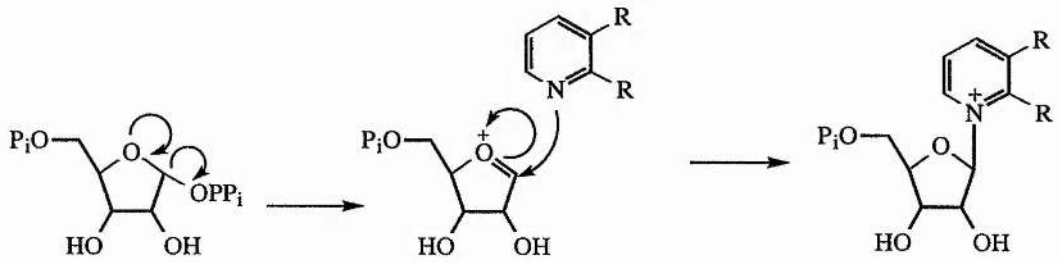

Scheme 1.5: S_N1 transition state

This evidence is consistent with the ternary complex kinetic mechanism, as it fits in with the idea of direct attack by the nucleophilic nitrogen. The "ping-pong" mechanism is less easy to rationalise as it implies the presence of a ribosyl-enzyme intermediate. Orotate and hypoxanthine phosphoribosyltransferases both use the "ping-pong" mechanism with the presence of a stable enzyme-bound ribosyl phosphate intermediate, but this also implies that stereochemistry is retained. This is obviously still a problem that needs to be investigated.

1.7.2 Other Phosphoribosyltransferases[49]

Phosphoribosyltransferase (PRTase) enzymes are a family of ten enzymes which are involved in the biosynthesis of purine, pyridine and pyrimidine nucleotides, and the aromatic amino acids histidine and tryptophan. Each of these enzymes is highly specific for an aromatic nitrogenous base, α-D-5-phosphoribosyl-1-pyrophosphate (PRPP) and a divalent metal ion. The general reaction catalysed by the PRTase family is the cleavage of the pyrophosphate group of the PRPP molecule, which by way of an anomeric inversion of the ribose ring results in a β-*N*-ribose monophosphate, e.g. the reaction catalysed by APRTase (Scheme 1.6).

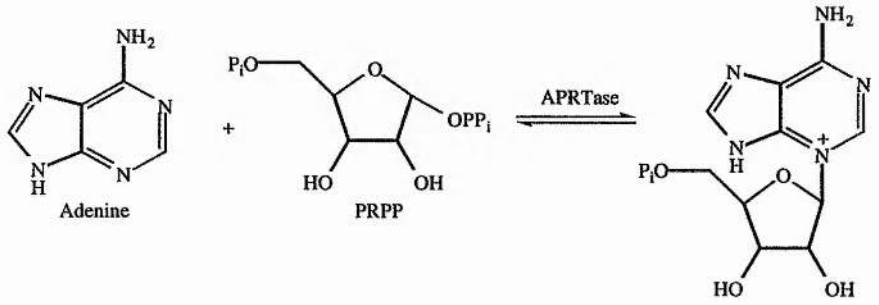

Scheme 1.6: APRTase reaction

1.7.3 Structures of other Phosphoribosyltransferase enzymes

The crystal structures of several of the PRTase family of enzymes have been resolved, and all have shown a common "PRTase" fold - a type I fold. This consists of a central parallel β sheet of 5 β strands, surrounded by α helices. Within the fold, a common recognition motif of 13 residues, critical for PRPP binding and catalysis is present. These 13 residues usually include four hydrophobic residues which form the β strand of the five stranded β sheet, two acidic residues, usually aspartic acid, which lie close to the ribose group of the substrate and therefore stabilise the positive charge of the transition state, two more hydrophobic residues and four more smaller amino acid

residues, including at least one glycine, which help to bind the 5-phosphate of PRPP and the nucleotide.

However none of QPRTase, NAPRTase and ATP-PRTase contain the thirteen residue motif, and so indicate the possibility of at least two PRTase fold types.

1.7.4 PRTase Reactions

PRTase enzymes are vitally important as they act as key control points on their respective metabolic pathways. They are allosterically regulated by a variety of effectors. In some cases the enzymes consist of sub-units which may occur as bi-functional complexes and act with an enzyme further down the pathway. Although distinct iso-enzymic species of the PRTases do not exist, physical and kinetic variations occur between PRTases in different organisms. Most PRTases in vertebrates are highly specific for just one organ, others are found in most tissues, while at the sub-cellular level in most organisms the PRTases are confined to the soluble cytoplasmic fractions. PRTases are active over a fairly broad pH range, with generally an alkaline pH optimum, and inactivation in more acidic conditions.

Although as a family they have similar catalytic and physical properties, these common structural features are probably dictated by divergent evolution, where the structural information is inherited from a common ancestral protein, rather than convergent evolution. There is probably a "core" protein, which is important for enzymic activity, as the enzymes have a wide range of subunit molecular weights.

Studies on ATP-PRTase, OPRTase and HGPRTase have shown β-glycoside formation occurs through an S_N1 carbocation reaction,[44] and both APRTase and OPRTase stabilise carbonium ions.[50,51] As this stabilisation can be performed by an ionised cysteine residue, it is consistent with the requirements for sulfhydryl reagents observed for most of the PRTases. Lysine also appears to be involved with binding at the active site, as described before for QPRTase.

1.7.5 Other Pyridine Nucleotide PRTases

Obviously this is the area of most interest in this study, as QPRTase is a member of this group of PRTase enzymes. The biosynthesis of NAD was first observed in the liver, and the enzyme thought to be responsible for its production, NAPRTase, isolated.[48] Further studies confirmed that quinolinic acid and nicotinamide were also precursors to NAD, and while quinolinic acid may be synthesised in the organ, nicotinic acid and nicotinamide were obtained exogenously. Therefore NAPRTase and NAmPRTase are known as salvage enzymes, and QPRTase a *de novo* pathway enzyme.

As described above, NAPRTase is involved in the salvage pathway of NAD biosynthesis. The enzyme has been isolated from many sources, which are split into three groups, those which are not affected by ATP, those that are dependent on ATP, and those that will use and cleave ATP, but are not reliant on it. In the latter case, the role of ATP is to reduce the Michaelis activity.[52,53]

Without nicotinic acid or PRPP, ATP phosphorylates the enzyme from bakers yeast,[49] after which the other substrates are added randomly and sequentially. Even in the presence of all substrates this mechanism is followed.

NAPRTase is highly specific for nicotinic acid and shows no activity with precursors of other PRTase enzymes.[52] ATP can be replaced in some cases by other purine nucleotides, and the thermal stability can be replaced by a range of nucleotide analogues.[54,55] This enzyme can be split into two forms, that from sources that require ATP absolutely, and that in which a lack of ATP can be overcome by an increase in PRPP and Mg^{2+} levels.[56] Indeed ATP has been shown to have an allosteric effect, and the turnover number for the rat liver enzyme has been estimated at less than 1 molecule of nicotinamide mononucleotide per hour.

1.7.6 Purine Nucleotide PRTases

Glutamine-amido PRTase catalyses the initial and rate determining step of the *de novo* purine nucleotide biosynthesis.[57,58] 5-Phosphoribosylamine, the product of this reaction can then be transformed to IMP via nine enzymatic steps. Modifications of this molecule leads to the production of other purine nucleotides guanine, adenine and xanthine. As with the pyridine nucleotides, they are also synthesised by salvage pathway enzymes, e.g. HGPRTase and APRTase, or by the degradation of nucleic acids. In this case purine nucleotide PRTases are not as specific, and the number of bases capable of occupying the enzyme active site is much larger.

1.7.7 Pyrimidine Nucleotide PRTases

The pathway to pyrimidine nucleotide biosynthesis is much simpler than that of the purines. Orotic acid, for example, is synthesised simply and then, in a reaction catalysed by orotate PRTase, reacts with PRPP to form orotidine-5'-monophosphate (OMP), which in turn can lead to the synthesis of other purine nucleotides, uridine, cytosine and thymidine. Again the other PRTases in this group are involved in salvage, rather than *de novo* pathways. However in mammals OPRTase catalyses the whole pyrimidine reutilization, while plants, bacteria and yeast also have a uracil specific enzyme.

1.7.8 Histidine and Tryptophan PRTases

Mammals are incapable of the *de novo* synthesis of histidine and tryptophan, relying on diet for their supply, but bacteria and other lower organisms can biosynthesise these compounds. Histidine and tryptophan PRTases utilise ATP and anthranilate respectively, and the products of these reactions undergo an interesting rearrangement which includes the opening of the phosphoribosyl ring. Modifications

of the ribose group occur such that two carbon atoms from the original ring are present in tryptophan, whereas in histidine all five are.

1.8 Biological Importance of Quinolinic acid

Quinolinic acid, which has been recognised as a naturally occurring compound for many years, is an intermediate in the formation of NAD from tryptophan. Lapin first reported its effect on the mammalian Central Nervous System (CNS) when he observed that quinolinic acid (and other metabolites on the tryptophan pathway) caused stimulant and convulsive effects in rodents.[59] The presence of quinolinic acid in human and rat brain has been shown,[60,61] but the actual source of quinolinic acid is still open to some discussion. The enzymes of the kynurenine pathway are mainly located in systemic tissues, in particular the liver. One of the features of quinolinic acid is that, because of its polar nature and a lack of a carrier mechanism, it is unable to penetrate the blood-brain barrier under physiological conditions.[62]

However, as quinolinic acid is present in both the cellular and extra-cellular components of the brain, cerebral mechanisms for the metabolism of quinolinic acid are likely to exist. Both 3-hydroxyanthranilic acid, and the enzyme 3-hydroxyanthranilic acid oxygenase (3-HAO) are present in the human and rat brain, and provide the most likely source of quinolinic acid. As described elsewhere, QPRTase is also present in the human brain.

3-HAO is 100 fold more active than QPRTase, implying that activity of the latter enzyme is rate limiting, although these relative activities may not be important factors of quinolinic acid concentration.[63] 3-HAO is not normally saturated, as administration of 3-hydroxyanthranilic acid results in an increase in quinolinic acid concentration.

In 1981, Stone and Perkins demonstrated that the introduction of quinolinic acid excited rat cerebral cortex neurones, and that this occurred through activation of receptors for excitatory amino acids (EAA).[64] These EAA are now regarded as the

major excitatory transmitters in mammalian CNS. Some agonists are known as "excitotoxins", to describe both their excitatory and neurotoxic effects.[65]

There are three main subtype of EAA receptor, named after their agonists, *N*-methyl-D-aspartic acid (NMDA), quisqualate and kianate. Quinolinic acid has been shown to be a selective agonist of the NMDA receptor.[66] Its action was shown when it was injected into rat striatum or hippocampus. Neurones exposed to quinolinic acid showed a massive swelling of dendrites, followed by degeneration of post-synaptic components.[67] Antagonists of the NMDA receptor reduced quinolinic acid responses therefore quinolinic acid acts primarily at the NMDA receptor.[68] NMDA receptors are located in the cerebral cortex, basal ganglia and hippocampus and are involved in long term potentiation, neuronal plasticity, learning and memory. Therefore an increase in quinolinic acid concentration could induce neuronal dysfunction in NMDA receptor activity in these areas.[69]

However, quinolinic acid is much more potent as a neurotoxin than would be suggested from its affinity for the NMDA receptor. The human brain has quinolinic acid concentrations of 10 nmol l^{-1} to 1 μmol l^{-1}, and is 10-60 times less potent than NMDA, yet it is equipotent as a neurotoxin. One theory is that local quinolinic acid concentrations at the synapses are much higher, and that this is not reflected in mean levels.

Quinolinic acid therefore does not act as a classic neurotransmitter, as it is not released on depolarisation, and no mechanism exists to remove it from the extracellular space. Schwarcz therefore considered quinolinic acid to be a potential neuromodulator whose role in excitatory neurotransmission must be investigated further.

Two theories were previously suggested for its action. The pre-synaptic hypothesis suggested that quinolinic acid activates specific receptors, causing release of a neurotransmitter, which in turn interacts with the NMDA receptor, leading to neuronal death.[70] Although no direct evidence supports this theory, it would explain why quinolinic acid induced neurotoxicity is prevented by blockade of the NMDA receptor by antagonists.[71]

The second, post-synaptic, hypothesis explains neurotoxicity on the basis of interaction between the EAA and post-synaptic membrane. The associated ion channels normally blocked by physiological Mg^{2+} concentration can be activated by injection of quinolinic acid which leads to degeneration of the neurones.

As quinolinic acid does not penetrate the blood-brain barrier it must be synthesised intracerebrally. Neurodegeneration actually occurs because of increased activity of the NMDA receptors as quinolinic acid acts at the receptors on the neuronal surface to produce the excitatory and neurotoxic effects.[72] Stimulation of the EAA receptors over a prolonged period of time degenerates the cells.[73]

A significant elevation in quinolinic acid concentration has been discovered in both the CSF and brain tissue of patients with inflammatory neurodegenerative diseases. These diseases include Huntington's disease, AIDS, poliovirus infection, Lyme disease and septicaemia. Injections of nM quinolinic acid concentration into specific areas of rat brain causes distinctive pattern nerve cell damage and seizures reminiscent of human neurodegenerative disorders.[26] Systemic administration of pokeweed mitogen to mice leads to the accumulation of quinolinic acid in the CNS and blood, implying that quinolinic acid is involved with neurodegeneration in inflammatory neurological diseases.[74]

Neuronal vulnerability to quinolinic acid actually increases with brain development.[75] With chronic increases in quinolinic acid concentration the integrity of the blood-brain barrier is eventually compromised. There are many reasons for a possible increase in quinolinic acid concentration:

i) An increase in the availability of quinolinic acid precursors.

ii) An increase in 3-HAO levels.

iii) A decrease in QPRTase levels.

iv) A dysfunction in the cerebral mechanism for the release of quinolinic acid.

v) An alteration in the balance of other systems which interact with quinolinic acid.

Quinolinic acid appears to be less effective as a neurotoxin in the cerebellum, hypothalamus and substantia nigra where there is high QPRTase activity, compared to areas of low QPRTase activity such as the cerebral cortex, striatum and hippocampus where it is very potent. Often an increase in astrocytic 3-HAO activity, due to astrocytic proliferation, is responsible for the increase in quinolinic acid.[76] Interestingly, the activity of 3-HAO increases 4 or 5 fold within days of excitotoxic lesion of rat striatum or hippocampus.[77]

1.8.1 Quinolinic acid and Neurological Diseases

The two main neurological diseases, associated with an elevation of quinolinic acid, studied are Huntington's disease (HD), and AIDS.

1.8.1.1 Huntington's disease

Features of the lesions caused by administration of quinolinic acid into experimental rats are similar to the neuronal degeneration occurring in HD patients.[78] HD is a neurodegenerative disorder, symptoms of which include dementia, development of choreiform movements, and psychiatric symptoms.[79] The disease is characterised neuropathologically by severe atrophy of striatal tissues. Quinolinic acid is proposed as the aetiological basis of the disease, and is the strongest candidate for the immediate cause of the disease. Another indication is that the activity of 3-HAO is increased in various brain regions of patients with HD. [80]

However, the role of quinolinic acid is far from proven. Excretion of quinolinic acid in HD patients is unchanged,[81] and QPRTase activity is unchanged in blood platelets and erythrocytes of patients.[82] There is no general increase in bodily levels of quinolinic acid in HD patients or any loss in QPRTase activity, so one possible explanation is that the levels of quinolinic acid increase transiently around the excitatory amino acid receptors. The quinolinic acid elaborating system is preferentially localised in astrocytes, therefore there is a possible involvement of proliferated astrocytes in HD as part of the disease process.[83]

1.8.1.2 HIV and AIDS

To investigate whether immune stimulation in man is associated with an increase in quinolinic acid concentration, Heyes studied the HIV-1 virus in some detail.[84] Patients with AIDS were found to have 3.5 times the normal quinolinic acid levels, with the increase in quinolinic acid correlating with the degree of motor impairment. Two thirds of all AIDS patients suffer from neurological problems, including dysfunction of cognition, movement and sensation. Azidothymidine (AZT) or anti-microbial therapy actually reduced the levels of quinolinic acid in the CSF and increased the neurological status of the patients, but those with latter stage AIDS dementia had 20 times the normal level of quinolinic acid. AZT inhibited HIV virus reproduction, causing the decrease in immunological response and therefore quinolinic acid synthesis.

Heyes also investigated the quinolinic acid concentration in SRV-D infected macaques and found that to be three times the normal level.[85,86] An increase in indolamine-2,3- dioxygenase level is associated with the increase in quinolinic acid concentration in the brain. This enzyme is induced by several factors, therefore the accumulation of quinolinic acid occurs across a broad spectrum of neurological diseases. Other diseases studied where increased quinolinic acid levels are observed were Lyme disease, poliovirus, auto-immune disease, sepsis and head trauma. The enzyme catalyses the first step of the kynurenine pathway (see section 1.9), and is actually activated by γ-interferon released during immune stimulation. One theory is that the extra quinolinic acid derives from macrophages.[63] These cells, which are employed by the non-specific immune system to neutralise foreign substances or cells can infiltrate the brain upon immune system activation. They have also been shown to synthesise quinolinic acid from L-tryptophan and indolamine-2,3-dioxygenase, the enzyme which catalyses the first step of the kynurenine pathway, and which has been shown to have been synthesised by macrophages. These factors may all be important in these inflammatory neurological diseases.

1.8.2 Kynurenic acid

Along with quinolinic acid, kynurenic acid is the other important neurologically active metabolite of the kynurenine pathway.[62] Kynurenic acid is a broad spectrum antagonist of the excitatory amino acid receptors, in particular the NMDA receptor, and increased concentrations of the acid lead to effects consistent with NMDA antagonist activity. As a natural constituent of the brain, it is a potential endogenous neuroprotective agent against excitatory neurotransmitters, including quinolinic acid.

An ongoing widely debated issue is whether kynurenic acid levels and quinolinic acid levels are actually finely balanced to maintain optimum NMDA receptor activity, implying that over stimulation of the receptor may arise from a decrease in kynurenic acid levels as well as an increase in quinolinic acid levels. Indeed recently HD patients have been observed to have lower kynurenic acid levels,[87] although this may arise from impaired biosynthesis rather than any other issue. In a similar way to quinolinic acid, kynurenic acid cannot penetrate the blood-brain barrier and therefore may be biosynthesised *in situ*. The main source of the acid is kynurenine, which can enter the brain via the enzyme kynurenine aminotransferase (KAT). This enzyme is localised in astrocytes in a system complicated by the fact that there are two distinct KAT enzymes, each with different properties.[88] Termination of the action of the acid appears to be by diffusion from the brain as no catabolic enzyme has been detected.

1.9 Biosynthetic Origin of Quinolinic acid: The Kynurenine Pathway

The source of quinolinic acid is the kynurenine pathway of tryptophan metabolism (Scheme 1.7).

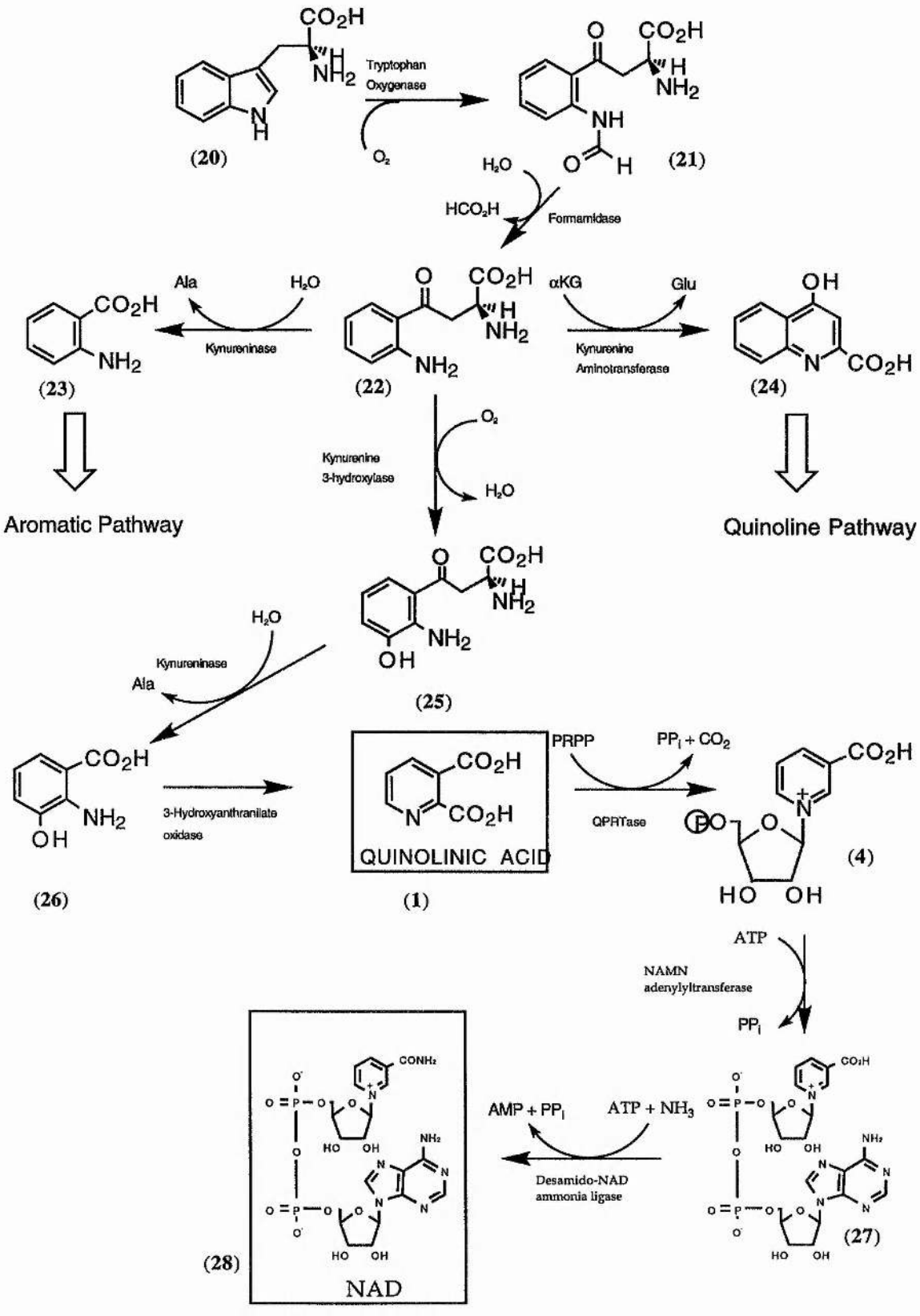

Scheme 1.7: Kynurenine pathway

The first step in the tryptophan pathway is the oxidation of tryptophan (**20**) to cleave the indole ring, by one of two enzymes. In the liver and kidney of mammals this oxidative cleavage is catalysed by tryptophan dioxygenase, but in most other tissues indolamine-2,3-dioxygenase catalyses this reaction.[89] Both of these enzymes are haem dependent, and the product of the catalysis is *N*-formylkynurenine (**21**).

Tryptophan dioxygenase (E.C. 1.3.11.11) is absolutely specific for L-tryptophan, and is actually the rate limiting enzyme for the kynurenine pathway. It has a bi-uni mechanism as tryptophan binds to the active holo-enzyme, followed by the binding of oxygen and only then does the reaction takes place.

The complementary enzyme indolamine-2,3- dioxygenase (E.C.1.3.11.17) is located in a wide range of mammalian tissues, including the distal ileum, stomach, lung and brain, but not in the liver or kidney. The enzyme has a broader substrate specificity, and will cleave other substrates such as D-tryptophan, D- and L-5-hydroxy tryptophan, melatonin and serotonin. However, the human enzyme does prefer L-tryptophan as the substrate. Hirati and Hayaishi demonstrated that the addition of superoxide dismutase inhibited the enzyme activity, proving that the enzyme is dependent on superoxide rather than oxygen.[90] The manner in which the enzyme is inhibited by different compounds than tryptophan dioxygenase implies that different substrate co-factor binding factors occur.

Kynurenine formamidase (E.C. 3.5.1.9) then catalyses the rapid conversion of *N*-formyl kynurenine to kynurenine (**22**) by hydrolysis and loss of the formate group.[91] Only slight variations of the enzyme occur from organism to organism, though with these there are differences in substrate specificity and inhibitor sensitivity. The enzyme actually has a wide substrate specificity and will hydrolyse a range of aryl formyl amines, including both D- and L- *N*-formylkynurenine and *N*-formylhydroxykynurenine.

Once kynurenine has been formed, it can undergo three very different reactions. Hydrolysis to anthranilic acid (**23**) is catalysed by kynureninase, transamination to kynurenic acid (**24**) by kynurenine aminotransferase, or hydroxylation by kynurenine

3-hydroxylase to give 3-hydroxykynurenine (**25**). This last transformation is the major fate of kynurenine in the tryptophan pathway, leading to the production of NAD.

Transamination of kynurenine by kynurenine aminotransferase (KAT, E.C. 2.6.1.7) is followed by cyclisation, dehydration and tautomerisation to lead to the production of kynurenic acid, a stable aromatic compound.[92] Kynurenic acid is an antagonist of the glycine site of the NMDA receptor, so increased levels of the acid may have neuroprotective action in some pathological conditions.

Kynurenine 3-hydroxylase (E.C. 1.14.13.9) competes for kynurenine as discussed above. In humans the enzyme is located in the outer mitochondrial membrane, and incorporates oxygen into kynurenine via a catalytic cycle mechanism. The enzyme is FAD dependent, and NADP or NADPH is used as a co-reductant. The purified enzyme is an oligomer, with 4 FAD molecules per sub-unit, and interestingly the monomer only has 10% of the catalytic activity of the dimer. In some circumstances the enzyme may be rate limiting for NAD production while the enzyme is inhibited by xanthurenic acid and the enzymic activity is decreased by hyperthyroidism.

Kynureninase (E.C. 3.7.1.3) catalyses the conversion of both kynurenine and 3-hydroxykynurenine to produce anthranilic acid and 3-hydroxyanthranilic acid (**26**) respectively. Anthranilic acid can then be metabolised into a variety of aromatic compounds such as quinoline, quinazoline or acridine alkaloids in plants. It can also be transformed into 3-hydroxyanthranilic acid, the product of catalysis by 3-hydroxykynureninase, and become a vital part of the NAD biosynthesis. In mammals and fungi where NAD biosynthesis is vital for production of the co-enzyme, there are low K_m and high v_{max} values for 3-hydroxykynurenine, whereas in micro-organisms where the *de novo* NAD route is not as important, there is a high activity towards kynurenine.

The enzyme is dependent upon PLP, and from some sources *N*-formyl kynurenic acid is a substrate and hydrolysed to *N*-formyl anthranilic acid, itself a substrate for formamidase. Synthesis of the enzyme is increased by growth in a

tryptophan rich medium,[93] and known PLP inhibitors such as β-chloro-2S-alanine and 2S-serine-*O*-sulfate inhibit kynureninase.[94]

3-Hydroxyanthranilic acid oxygenase (3-HAO) catalyses the cleavage of the benzene ring of 3-hydroxyanthranilic acid to produce a very unstable intermediate α-amino-β-carboxymuconic acid ω-semialdehyde.[95] Nishizuka and Hayaishi also investigated this conversion and were unable to find an enzyme that was responsible for the subsequent ring closure of the intermediate to form quinolinic acid (Scheme 1.8).[3] The rate limiting step for the conversion to quinolinic acid is the isomerisation of the double bond to produce the carboxylic acid groups in a cis formation, which allows condensation to form the stable pyridine ring.

The enzyme is widely distributed in the peripheral organs, e.g. liver and kidney, and like other groups on this pathway requires divalent iron for activity, but in this case not in the form of haem groups.

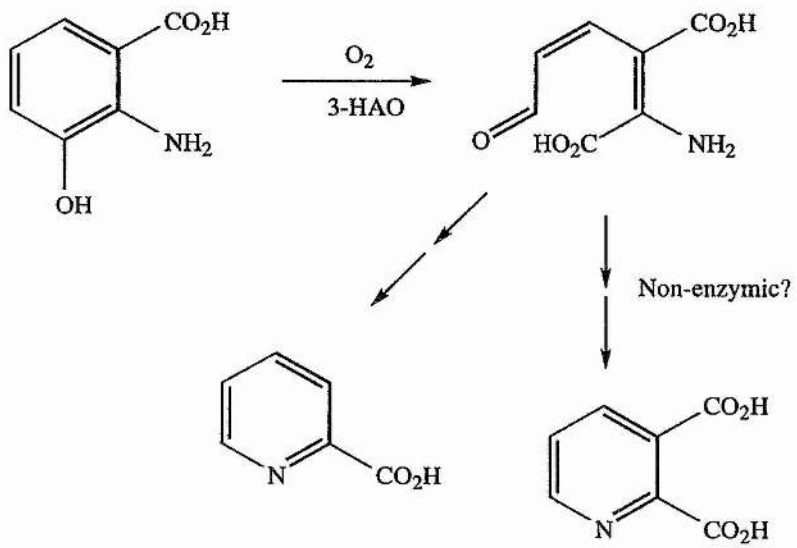

Scheme 1.8: 3-HAO reaction

The other fate of α-amino-β-carboxymuconic acid ω-semialdehyde is to be attacked by picolinic decarboxylase, where the acid is decarboxylated and then picolinic acid obtained by ring cyclisation. Picolinic decarboxylase is found in the liver and kidney of many mammals, therefore formation of NAD and other derivatives from quinolinic acid may have to compete with picolinic decarboxylase for α-amino-β-carboxymuconic acid ω-semialdehyde.

1.9.1 Modulating the Kynurenine Pathway

Modulation of the kynurenine pathway is one strategy to obtain useful pharmacological control of the central nervous system (CNS). The activity of the NMDA receptor can be controlled by altering the relative quinolinic acid and kynurenic acid concentrations. Two approaches to this situation have been employed. One is to investigate methods of inhibiting quinolinic acid synthesis as a way to produce drugs, whilst the other involves the development of analogues of kynurenic acid, which are more potent antagonists of the NMDA receptors. There have been several efforts to inhibit quinolinic acid biosynthesis by the synthesis of inhibitors of kynurenine pathway enzymes. One of those studied the most was nicotinoylalanine (**29**) which is reported to inhibit two enzymes - kynureninase and kynurenine 3-hydroxylase.

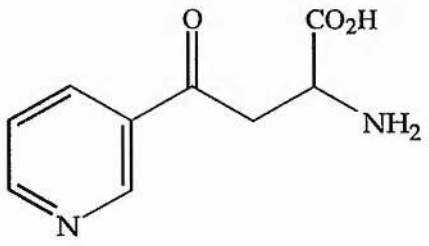

(29)

When it was administered to mice following a tryptophan dose, a large increase in kynurenic acid concentration was observed, along with behaviour consistent with exposure to NMDA antagonists.[88] The most obvious enzyme to inhibit, in order to

decrease quinolinic acid levels is 3-hydroxyanthranilate oxygenase (3-HAO), the enzyme directly responsible for quinolinic acid biosynthesis. 4-Chloro-3-hydroxyanthranilic acid is a very potent inhibitor and its *in vivo* effects have been examined. A dose dependent decrease in production of quinolinic acid in the hippocampus of rats was observed. When studied in more detail it was shown that quinolinic acid biosynthesis was inhibited following interferon stimulation. Inhibitors of indolamine 2,3-dioxygenase had similar effects. It therefore seems that inhibitors of the kynurenine pathway enzymes modulate the balance of kynurenic acid and quinolinic acid levels giving them potential as anti-convulsant agents and for treatment of various neurological diseases.

1.10 Metabolism of quinolinic acid: NAD Biosynthesis and the Pyridine Nucleotide pathway

NAD is ubiquitous in its role as an essential co-enzyme, and participates in many cellular oxidation and reduction reactions. It is important in cellular metabolism, functioning in many anabolic and catabolic reactions in biological systems.[96] The manner of NAD metabolism varies between eukaryotes and prokaryotes, and there is also a great deal of variation between different prokaryotes. However *E. coli* and *S. typhimurium* have a great deal of similarity in NAD metabolism,[97,98] and are the two bacteria investigated most often.

Gholson was the first to report the existence of the pyridine nucleotide cycle in a diversity of species,[99] and multiple forms of the cycle have since been examined through studies in *E. coli* and *S. typhimurium* .

Quinolinic acid is introduced into the NAD biosynthetic pathway by the QPRTase catalysed reaction to form NAMN. The two step pathway to NAD (**28**) from NAMN is known as the Priess-Handler pathway, with the intermediate being nicotinic acid adenine dinucleotide (NaADN)(**27**).[100,101] The conversion of NAMN to NaADN, also known as desamido NAD,[48] is catalysed by NAMN adenyltransferase

(E.C. 2.7.7.18). The enzyme has a much greater affinity for NAMN than nicotinamide mononucleotide (NMN), the rate of synthesis of NAD being 17 times faster than NaAD from NMN.[102] The final step to NAD is catalysed by the enzyme desamido-NAD: ammonia ligase (E.C. 6.3.5.1), also known as NAD synthetase. The enzyme requires both ATP and glucose, and involves the deamination of NaADN to NAD.

The major role of the pyridine nucleotide cycle (Scheme 1.9) is to provide a mechanism for regulation of NAD metabolism.[103] It is also a method of introducing other pyridine compounds into the cycle and therefore other ways of synthesising NAD, and is also a source of precursors for the biosynthesis of co-enzymes, including vitamin B_{12}.

The key enzymes in this cycle are subject to allosteric or feedback control, regulating NAD biosynthesis, whilst one of the unique features of the pathway is the manner in which the pyridine ring is conserved throughout the various cycles.

NAD may go through one of five distinct pyridine nucleotide cycles, of which three are known in *E. coli* and *S. typhimurium*. The cycles are 2, 3, 4, 5 and 6 membered cycles.

In pyridine nucleotide cycle II (PNC II), the two components are NAD and NMN. The inter conversion between the two is initiated by hydrolysis of the pyrophosphate bond in NAD by either NAD pyrophosphatase or DNA ligase, while an increase in DNA ligase obviously lends to an increase in NMN production. NMN does not occur in *E. coli* and *S. typhimurium*, therefore the two membered cycle is not present in these bacteria.

In PNC III, NAD is recycled via nicotinamide and NMN. The conversion of NAD to nicotinamide is catalysed by NAD glycohydrolase (E.C. 3.2.2.5) whilst nicotinamide phosphoribosyltransferase (NAmPRTase, E.C. 2.4.2.12) is the enzyme that catalyses the subsequent formation of NAD. Again this cycle is not observed in *E. coli* and *S. typhimurium* and if it exists is a very minor pathway.

PNC IV is the major intracellular NAD recycling pathway,[104-108] and represents 80 - 90 % of the total NAD recycling pathway. It also preserves the PRPP

moiety of NMN (**30**), the route with the minimum amount of energy. The rate of NAD turnover is eight times faster in PNC IV in *E. coli* than in the next fastest route PNC VI.

NAD is converted to NMN as before in PNC II, but is then converted to NAMN with the loss of ammonia, by NMN aminohydrolase (E.C. 3.5.1.00). NAD is then resynthesised via the Preiss-Handler pathway.

In PNC V deamination of nicotinamide (**31**) to nicotinic acid (**32**) by nicotinamide aminohydrolase (E.C. 3.5.1.19), and the nicotinic acid can then react with PRPP to form NAMN, via the action of NAPRTase (E.C. 2.4.2.11). Again the Preiss-Handler pathway allows NAD to be formed again.

PNC VI is very similar to PNC IV and PNC II, while NAPRTase appears to be the vital enzyme in PNC V and VI. Scheme 1.9 shows the NAD biosynthetic pathways and PNC IV, PNC V and PNC VI.

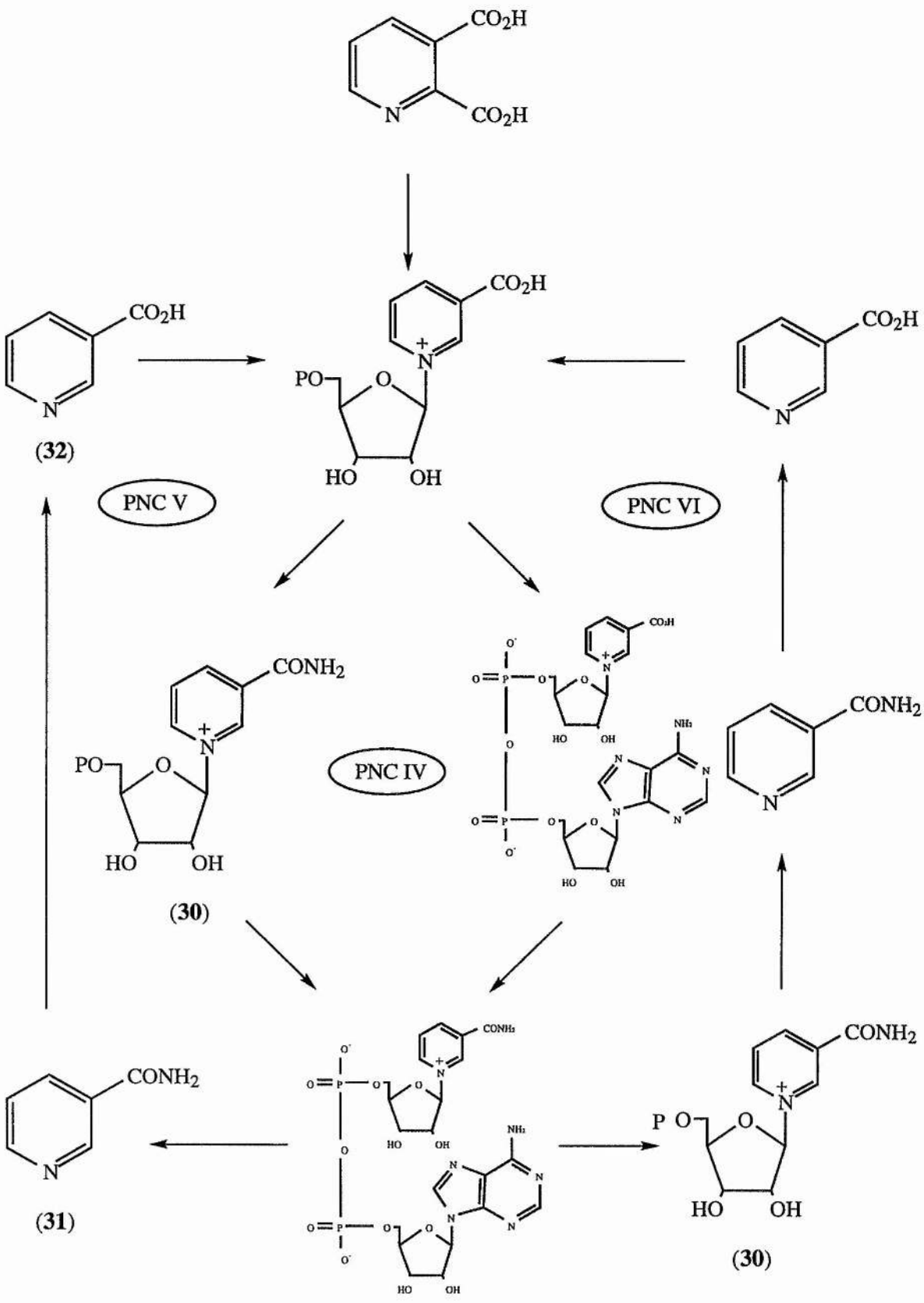

Scheme 1.9: Pyridine nucleotide cycle

CHAPTER 2

2. Synthesis of Quinolinic acid Analogues

As discussed, QPRTase lies on the kynurenine pathway of tryptophan metabolism. One of the end products of this pathway is the essential co-enzyme nicotinamide adenine dinucleotide (NAD).[99] Although animals acquire their NAD from dietary uptake and other sources, in fungi the kynurenine pathway is the sole biosynthetic route for production of all their NAD.[109] Therefore any compounds synthesised that can block enzymes along this pathway, including inhibitors of QPRTase, may have anti-fungal activity. Compounds that inhibit the enzyme could also be useful as biological "tools". These may allow the neurological effect of quinolinic acid to be investigated by blocking the active site of the enzyme, inhibiting its action and therefore artificially raising quinolinic acid levels. The biological effect of this increase can then be examined in model systems. The other use for inhibitors of QPRTase is to investigate the actual mechanism of the enzyme and its active site structure.

To study QPRTase inhibition it was intended to synthesise analogues of quinolinic acid that would allow the first of the two reactions catalysed by the QPRTase system, the phosphoribosyl transfer, to be examined in isolation from the decarboxylation reaction. Compounds were thus designed to mimic quinolinic acid by containing acidic groups at both the 2- and 3- position of the pyridine nucleus. However if the 2-substituent was not a carboxylic acid, this would mean that no decarboxylation could take place. Such analogues would therefore be able to undergo the first reaction, the phosphoribosyl transfer (Scheme 2.1), but be unable to decarboxylate.

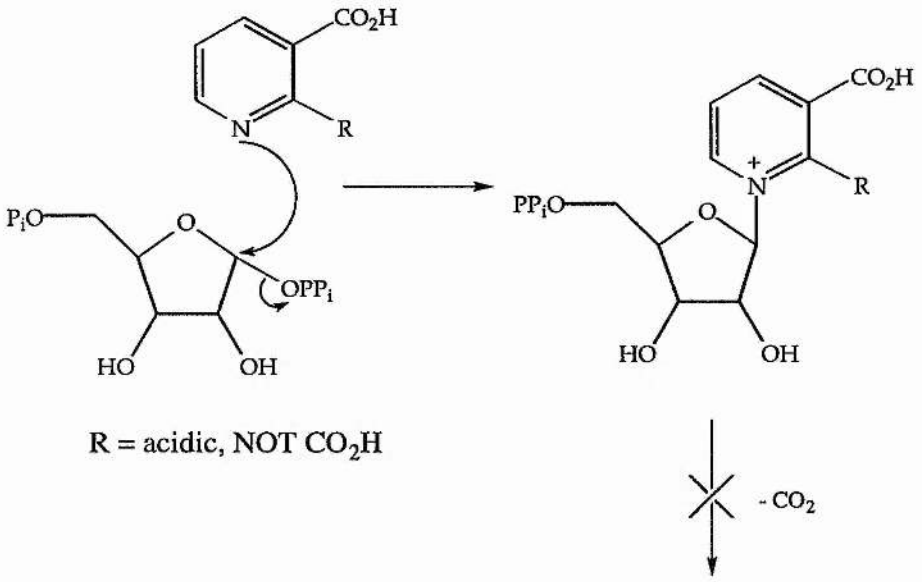

Scheme 2.1: Effect of analogues on QPRTase reaction

Initially two analogues were identified as suitable synthetic targets. These were 2-sulfonicotinic acid (**33**) and 2-phosphononicotinic acid (**34**). These compounds could thus be used to probe the mechanism of QPRTase. It would also be of interest to assess their neurological effects. Would they be neurotoxic as a result of QPRTase inhibition raising quinolinic acid levels, or neuroprotective by acting as agonists for the quinolinic acid binding site on the NMDA receptor?

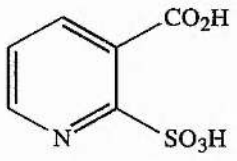

(**33**)

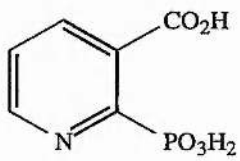

(**34**)

2.1 Synthesis of 2-sulfonicotinic acid

2.1.1 Literature Methods for Pyridine sulfonic acids

The most obvious route for the synthesis of sulfonic acid group was considered to be oxidation of a thiol group. Evans and Brown[110] investigated the synthesis of 2-, 3- and 4-pyridine sulfonic acids. Pyridine-2-sulfonic acid (**35**) was obtained by the oxidation of 2-mercaptopyridine,[111] which was itself prepared from 2-bromopyridine and aqueous alcoholic potassium sulfide in a sealed tube at 160-170 °C (Scheme 2.2).

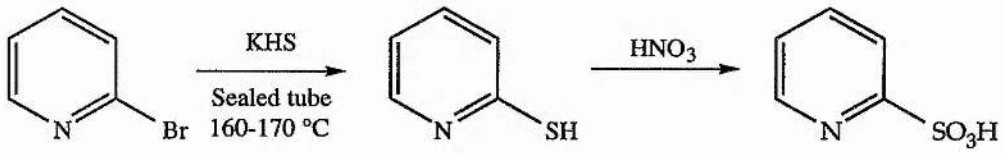

(35)

Scheme 2.2: Route to pyridine-2-sulfonic acid

More direct syntheses where the halogen is replaced by a sulfite group were also attempted, but even at high temperatures replacement by aqueous alcoholic sodium sulfite, in the cases of 2-chloropyridine and 2-fluoropyridine was only partial, and under the same conditions 2-bromopyridine decomposed extensively. If the halogenated pyridine was activated by *N*-oxide formation, nucleophilic displacement by the sulphite group occurred, but was also accompanied by reduction of the *N*-oxide linkage.

Pyridine-3-sulfonic acid was first synthesised by Fischer and co-workers in the late nineteenth century by heating pyridine with concentrated sulfuric acid, either in sealed tubes at 300-350 °C for a day, or for longer periods of time (30 hours to 20 days) at the boiling point of the mixture.[112-114] In the early twentieth century aluminium vanadyl and mercuric sulfates were used as catalysts for the sulfonation with fuming sulfuric acid,[115] both increasing yields and decreasing reaction times. The

sulfonation of pyridine and picolines was optimised by McElvain and Goese, by varying three factors, the catalyst mercuric sulfate levels, the length of time of the reaction and the amount of sulfur trioxide in the fuming sulfuric acid. As with the 2-substituted halogenated pyridines, the equivalent 3-substituted halogenated pyridine *N*-oxide was susceptible to attack by sodium sulfite to produce pyridine-3-sulfonic acid *N*-oxide, but 3-chloropyridine was stable under the same conditions.

Pyridine-4-sulfonic acid was first proposed by Koenigs and Kinne, who oxidised 4-mercaptopyridine with concentrated nitric acid.[116] However the melting point of the product was considerably less than that of the 4-mercaptopyridine, unlikely for a sulfonic acid. Evans and Brown successfully synthesised pyridine-4-sulfonic acid by oxidation with hydrogen peroxide in barium hydroxide solution.[110] It has also been produced on a large scale by a method developed by Tiesler,[117] where *N*-(4-pyridyl)pyridinium chloride was heated at 100 °C with sodium sulfite.

2.1.2 Oxidation of Thiols with Iodine

The ability of iodine to oxidise a thiol to a sulfonic acid, especially with the presence of a carboxylic acid group on an adjacent carbon is important in our aim to synthesise 2-sulfonicotinic acid. Shinohara[118] used Okuda's method of oxidation, with a large excess of iodine, to investigate the total oxidation to cysteic acid. This was a modified method of that suggested by Rosenheim and Davidshon[119] and first employed by Klason and Carlson.[120]

Danehy and Oester[121] also showed that a thiol with a free β-carboxylic acid group over oxidised without going through a disulfide, which is often the end product of oxidation of water soluble thiols without a β-carboxylic acid group. The ratio of this higher oxidation group, the sulfonic acid, to the disulfide increased as the initial thiol concentration decreased, i.e. increasing dilution. The corresponding sulfonic acids were synthesised from 3-mercaptopropionic acid (**36**), mercaptosuccinic acid (**37**) and *o*-mercaptobenzoic acid (**38**).

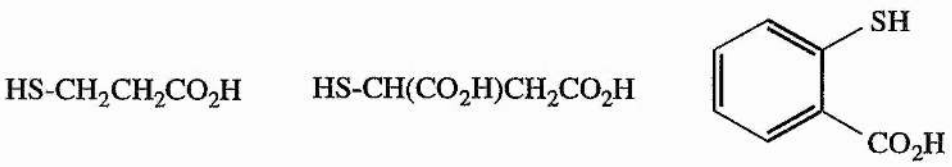

(36) **(37)** **(38)**

The mechanism of the oxidation of the thiol to disulfide is not widely reported. Kharasch[122] suggested the following possible mechanism (Scheme 2.3).

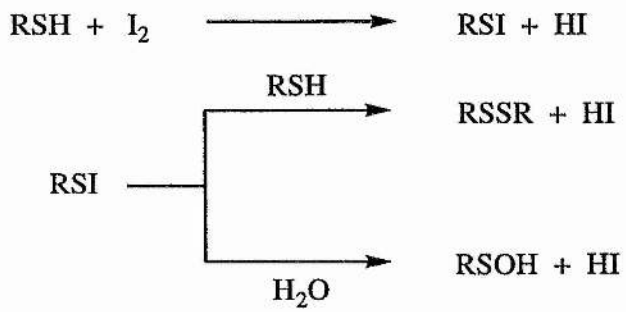

Scheme 2.3: Oxidation of thiol

If dilution and iodine levels allowed, the following overall reaction could occur:

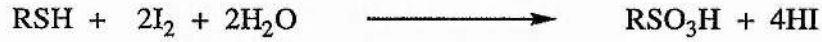

This further oxidation to the sulfonic acid, where more than the stoichiometric amount of iodine is consumed, is called overoxidation. Danehy's group proposed the following mechanism (Scheme 2.4).[123]

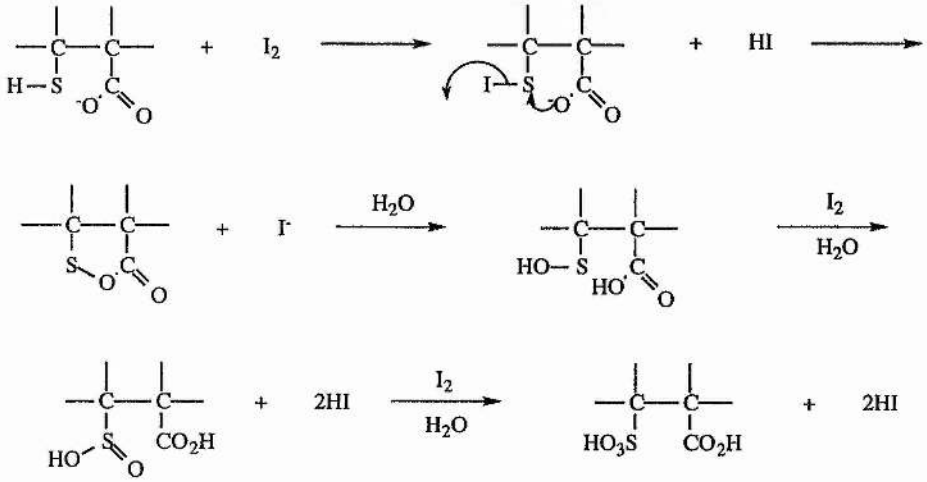

Scheme 2.4: Danehy's overoxidation mechanism

Attack on the disulfenyl iodide by the much less nucleophilic water is generally favoured as thiol ions become scarcer and the sulfonic acid is formed by further oxidation by iodine. It has been proposed that intramolecular attack by the carboxylate anion on the sulfenyl sulfur to displace the iodide ion and form a five membered cyclic intermediate occurs, followed after hydrolysis by oxidation.

The oxidation of *o*-mercaptobenzoic acid is an interesting case. Field *et al* investigated the disproportionation of 2-(phenyldithio)benzoic acid (**39**) to phenyl disulfide (**40**) and 2,2'-dithiodibenzoic acid (**41**),[124] and suggested that the ortho carboxylic acid group was involved (Scheme 2.5).

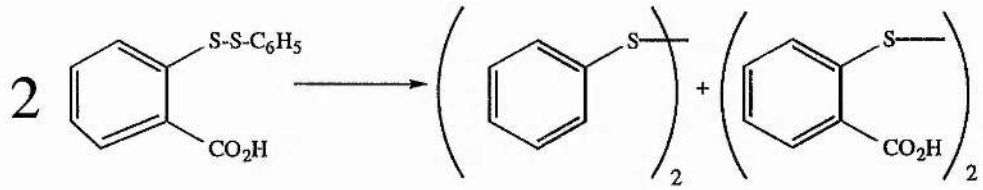

(39) **(40)** **(41)**

Scheme 2.5: Disproportionation of 2-(phenyldithio)benzoic acid

The five membered thioester has been isolated, confirming the involvement of the ortho carboxylic acid group. Dilution effects were minimal, implying that the rearrangement was intramolecular. The mechanism for the rearrangement is shown below (Scheme 2.6).

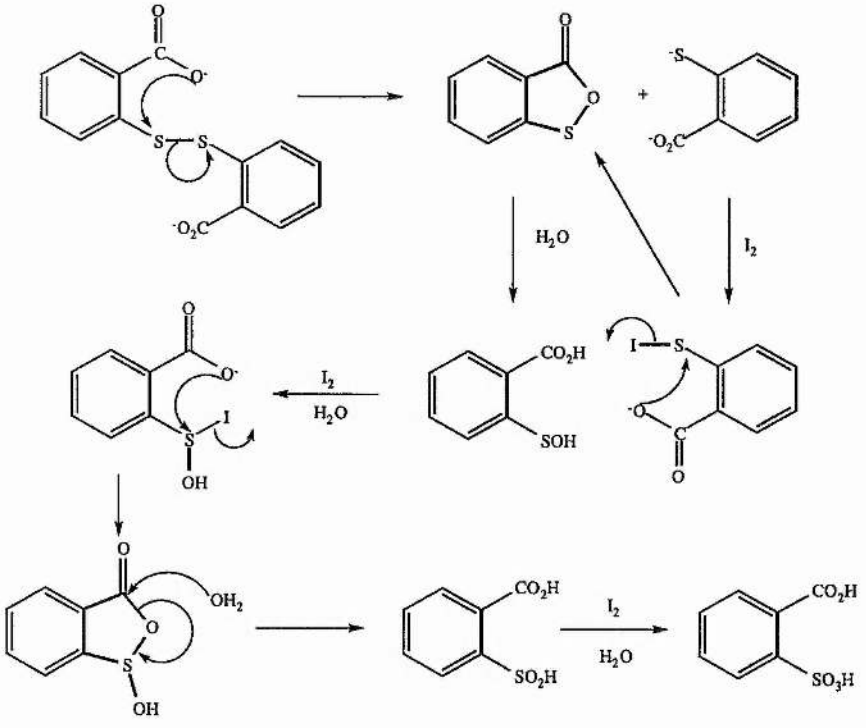

Scheme 2.6: Rearrangement mechanism

2.1.3 Synthetic Routes towards 2-Sulfonicotinic acid

Using this information, the oxidation of 2-mercaptonicotinic acid (**17**) to 2-sulfonicotinic acid was attempted, using a variety of oxidising agents (Scheme 2.7).

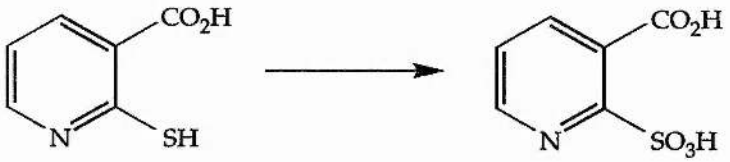

(17)

Scheme 2.7: Oxidation of 2-mercaptonicotinic acid

2.1.3.1 Oxidation with Nitric acid

Initially the oxidation of 2-mercaptopyridine (**42**) to pyridine-2-sulfonic acid was attempted, to confirm the work of Evans and Brown.[110] This was successful and gave the product in good yield (Scheme 2.8).

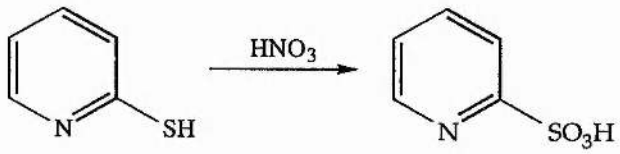

(42)

Scheme 2.8: Oxidation of 2-mercaptopyridine

The analogous oxidation of 2-mercaptonicotinic acid to 2-sulfonicotinic acid therefore seemed feasible. 2-Mercaptonicotinic acid was dissolved in concentrated nitric acid and heated to reflux for two hours. Upon cooling, needle-like crystals precipitated, which were recrystallised from boiling water. However, upon examination of the product by mass spectrometry, it became obvious the sulfonic acid had not been formed. The mass of the product was shown to be 139, much lower than expected if the sulfonic acid was formed. A significant fragment was produced at 121

(M-H_2O). Careful examination of these results revealed that the actual product to be 2-hydroxynicotinic acid (2-hydroxypyridine-3-carboxylic acid) (**15**), which was produced in 45% yield. This unexpected result was confirmed by the melting point of the product, 260 °C, identical to the literature value.[125] CHN Microanalysis also backed up these results, the actual composition, (C, 51.80; H, 3.62; N, 10.07%) was compared to the calculated values (C, 51.56; H, 3.26; N, 10.03%) to prove the product to be 2-hydroxynicotinic acid.

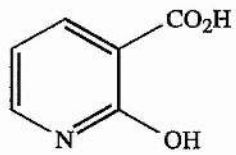

(15)

The proposed mechanism for the formation is shown in Scheme 2.9. The very acidic conditions promote the protonation of the thiol group. Nucleophilic attack by a water molecule at position 2 then leads to loss of the hydrogen sulfide group, and introduction of the hydroxyl group. The fact that this does not occur with 2-mercaptopyridine implies the significant effect of the 3-carboxylic acid substituent. The electron withdrawing effect of this group both makes the thiol more prone to protonation and more importantly increases the susceptibility of the 2-position to nucleophilic attack. The low pH employed presumably makes the latter effect more important.

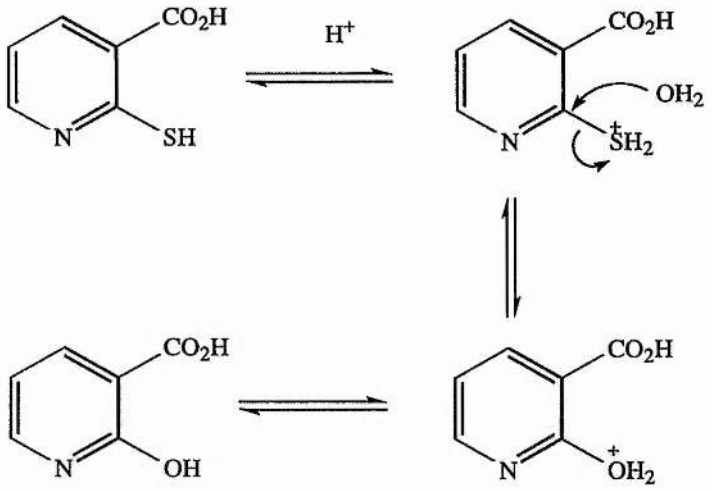

Scheme 2.9: Synthesis of 2-hydroxynicotinic acid

An alternative possibility is that oxidation to the sulfonic acid does actually occur, but in acidic conditions loss of sulfuric acid leads to the formation of 2-hydroxynicotinic acid.

2.1.3.2 Oxidation with Oxone

The oxidising agent oxone is a mixture of potassium sulfate salts ($2KHSO_5.KHSO_4.K_2SO_4$). When reacted with 2-mercaptonicotinic acid, examination by tlc showed that some oxidation had taken place. However, isolation of any product proved to be very difficult. The starting material, product and oxone are all barely soluble in water, and with ten equivalents of oxone required for complete oxidation, any oxidation product was not isolated, although ion exchange was attempted.

2.1.3.3 Oxidation with Iodine and Potassium permanganate

Following the previous unsuccessful attempts at oxidation, iodine[121] and potassium permanganate[125] were both examined as oxidising agents (Scheme 2.10).

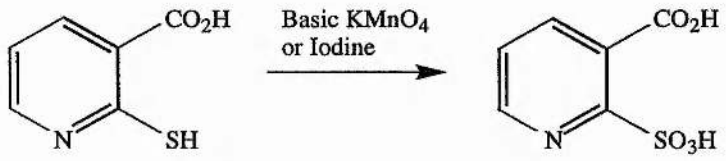

Scheme 2.10: Synthesis of 2-sulfonicotinic acid

2-Mercaptonicotinic acid was partially dissolved in distilled water and the pH adjusted to pH 6 with potassium hydroxide. This solution was added dropwise into a solution of iodine in distilled water. When addition was completed the solution was reduced to dryness, and then the product recrystallised from boiling water. Both 2-mercaptonicotinic acid and iodine are not very soluble in water, and so the reaction was not very efficient, giving only a 23% yield of product.

To facilitate oxidation by potassium permanganate, 2-mercaptonicotinic acid was dissolved in an aqueous sodium hydroxide solution. To this basic solution, potassium permanganate solution was added dropwise, and the resulting solution heated under reflux for one hour. Upon cooling manganese dioxide was removed by filtration, and the free acid generated by passing the solution through an Amberlite IR 120 ion exchange resin column to give the product in 25% yield.

^{1}H and ^{13}C NMR spectra were identical for both products, but did not confirm that oxidation had taken place. However fragments which corresponded to the loss of a sulfonic acid group and a carboxylic acid group, were detected in the mass spectrum. CHN Microanalysis for the compounds gave results suggesting that the synthesis of 2-sulfonicotinic acid was successful, (Found: C, 35.44; H, 2.00; N, 6.61%; Calculated for $C_6H_5NSO_5$; C, 35.47; H, 2.48; N, 6.89%) while the melting point of 254 °C was different from that of the product of the oxidation by nitric acid (260 °C). The structure

of the product was then confirmed by X-ray crystallography (see next page and Appendix for full data).

From the crystal structure (Figure 2.1) it is interesting to note that in the crystalline form, the sulfonic acid appears as a zwitterion, and that H-bonding occurs between the sulfonic acid and carboxylic acid groups.

These reactions were more successful as both of the oxidations were carried out in basic conditions, ensuring that the thiol group was not protonated. Therefore the nucleophilic attack by water, observed under acid conditions, did not take place. The oxidation with potassium permanganate appeared to be the better procedure. The reaction was considerably quicker and cleaner, and the yield could be much more easily optimised than the oxidation by iodine, where the lack of solubility of 2-mercaptonicotinic acid and iodine at the optimum pH is problematic.

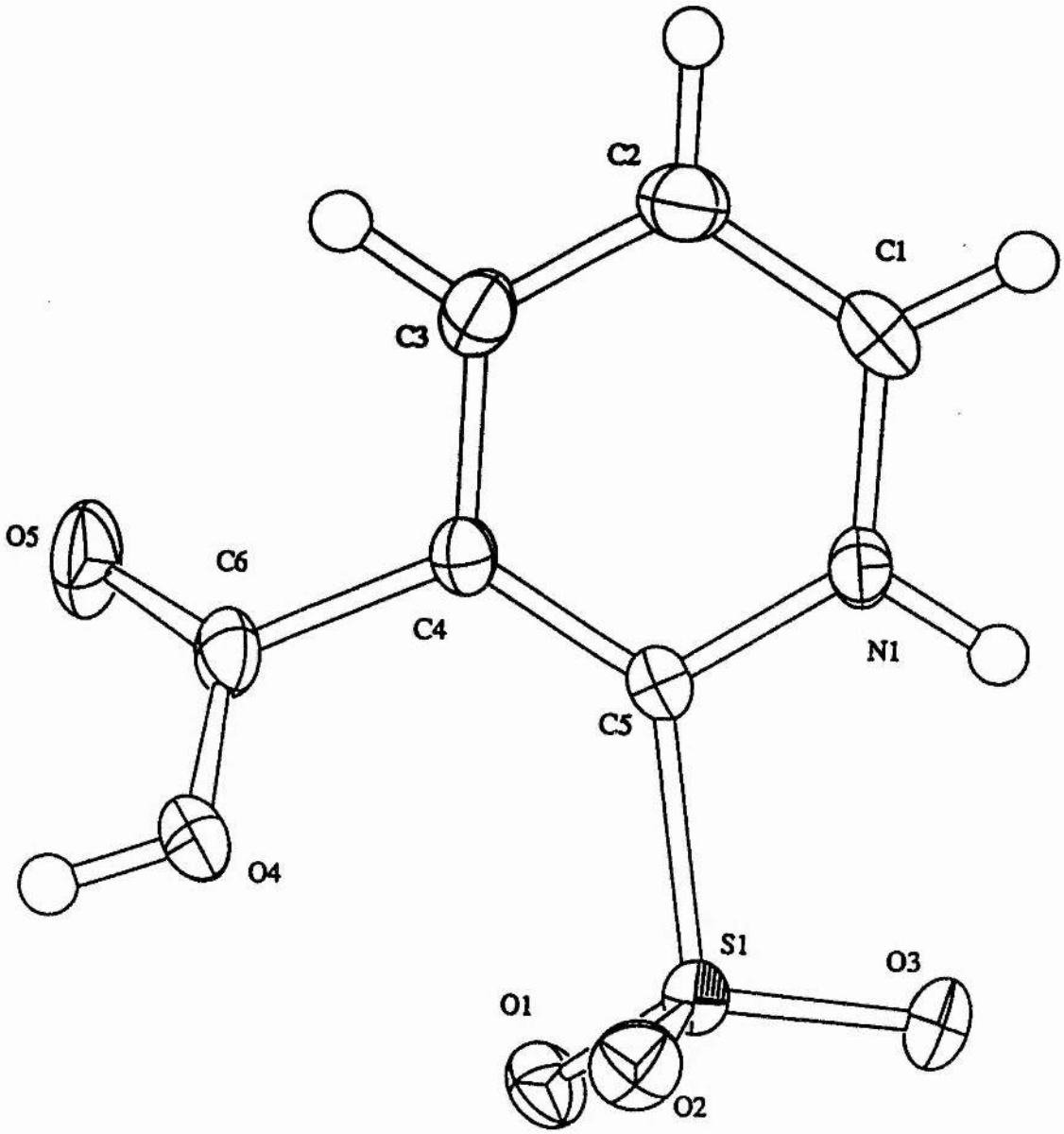

Figure 2.1: X-ray structure of 2-sulfonicotinic acid

2.1.4 Biological testing

A series of experiments were designed to screen quinolinic acid analogues, including 2-hydroxynicotinic acid and 2-sulfonicotinic acid, on primary cultures of mouse cerebellar granule cells. They were carried out in collaboration with Dr. Roger Griffiths in the Biochemistry department at the University of St. Andrews.[126] These were designed to assess the neurotoxic or neuroprotective effects of these compounds. The recognition of NMDA receptor was investigated by measurement of intracellular Ca^{2+} concentration and cell viability.

The NMDA receptor is one of the ionotrophic glutamate receptors, the others being the kainate and 3-(5-methylisoxazol-4-yl)propionic acid (AMPA), or quisqualate, receptors. The ionotrophic glutamate receptors all contain the agonist binding site and ion channel in the same macromolecular complex. The open NMDA channel is permeable to Ca^{2+} at a rate ten times greater than it is to monovalent cations (Na^{+} and K^{+}).

There are two agonist binding sites at the NMDA receptor. The first is for glutamate, although it is capable of binding NMDA and other short chain dicarboxylic acids, including quinolinic acid and aspartic acid. The second binding site is for glycine, which is required to bind simultaneously with glutamate. So that this effect is not a factor in laboratory experiments, glycine is added at a high level so that the site is saturated. There is also a third recognition site for polyamines, which appears to possess a regulatory role.

For these glutamate receptors, a common theme is an increase in intracellular Ca^{2+} levels. Elevated Ca^{2+} levels play a regulatory role through activation of Ca^{2+} dependent enzymes, but a large increase in intracellular Ca^{2+} levels leads to neuronal damage and death through the nature of the cascade of second messenger systems.

The link between the action of 2-hydroxynicotinic acid and 2-sulfonicotinic acid at the NMDA receptor and changes in intracellular Ca^{2+} was therefore examined. Thus, mouse cerebellar granular cells were tested against a range of concentrations of

quinolinic acid, 2-hydroxynicotinic acid and 2-sulfonicotinic acid and the intracellular Ca^{2+} levels measured. Quinolinic acid gave an increase in Ca^{2+} from a basal level of 129 nM to approximately 550 nM over a range of concentrations from 100 μM to 3 mM, after which the curve flattened off (see Graph 2.1). However, no rise in intracellular Ca^{2+} levels was seen for either 2-hydroxynicotinic acid or 2-sulfonicotinic acid over the same range of agonist levels. These results imply that although quinolinic acid is confirmed as an agonist of the NMDA receptor, 2-hydroxynicotinic acid and 2-sulfonicotinic acid appear not to be agonists of the NMDA receptor.

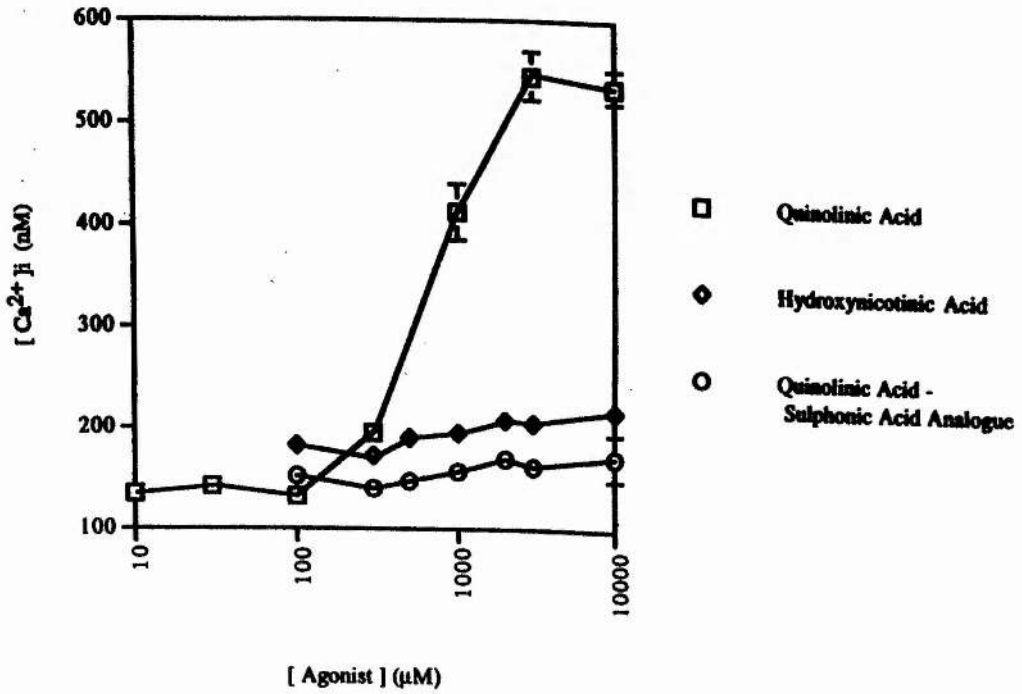

Graph 2.1

Quinolinic acid was applied to cells at a concentration of 2 mM, a level established as a concentration which produces a significant rise in intracellular Ca^{2+} levels. A range of other compounds were then added to the cells, to assess their ability to antagonise the effect of quinolinic acid. It was found that neither 2-hydroxynicotinic acid and 2-sulfonicotinic acid antagonised the 2 mM quinolinic acid mediated intracellular effects to a measurable extent.

The neurotoxicity of quinolinic acid and derivatives on mouse granule cells was then determined using a MTT assay. The MTT (3-(4,5-dimethylthiazolyl)-2,5-diphenyltetrazolium bromide) method for determining cytotoxicity is dependent on mitochondrial dehydrogenase activity. A solution of MTT is yellow in colour, but if the enzymes in viable cells cleave the tetrazolium ring purple crystals of formazan are produced. A quantitative measurement of cell damage is given by a spectrophotometric reading of the colour, and conclusions from these results can be drawn on the neurotoxicity of test compounds.

Graphs 2.2 and 2.3 show the results of MTT assays for quinolinic acid, 2-hydroxynicotinic acid and 2-sulfonicotinic acid. As the quinolinic acid concentration was increased then the absorbance as a percentage of the control decreased, demonstrating the neurotoxic effects of the increase in quinolinic acid levels. Under exactly the same conditions, the sulfonic acid analogue showed no statistical effect, a result also demonstrated for the MTT assay for 2-hydroxynicotinic acid. These results imply that these quinolinic acid analogues have no neurotoxic properties under these conditions.

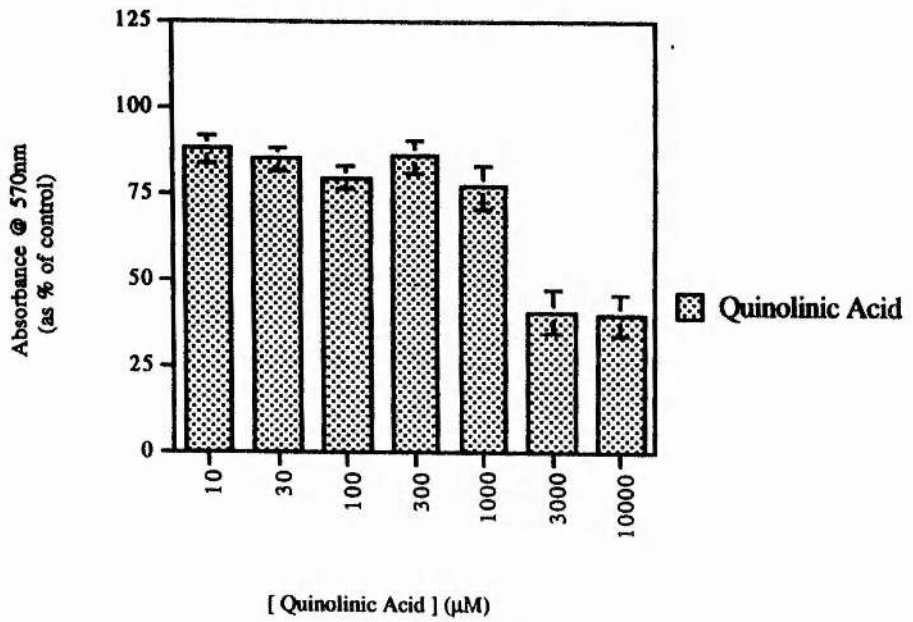

Graph 2.2: MTT assay for quinolinic acid

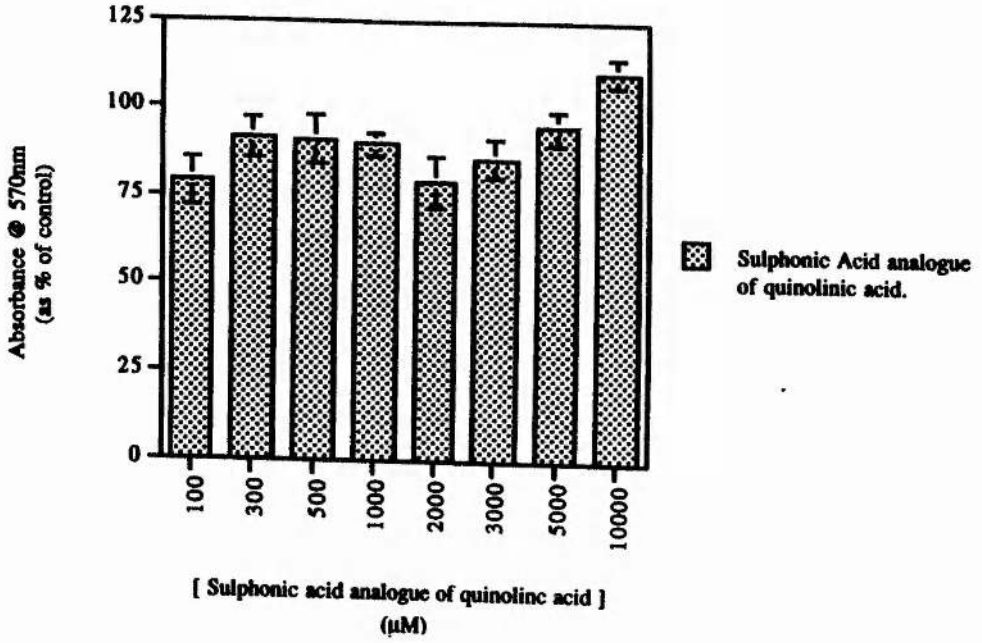

Graph 2.3: MTT assay for 2-sulfonicotinic acid

2-Hydroxynicotinic acid and 2-sulfonicotinic acid are therefore neither agonists nor antagonists of the NMDA receptor. It appears that replacement of the 2-carboxylic acid group greatly reduces the affinity of the compounds for the NMDA receptor. This is not unexpected for 2-hydroxynicotinic acid, as the hydroxyl group will be quite different in its binding properties to the carboxylate. Certainly a salt bridge or charge/charge interaction at the NMDA binding site will no longer exist. The sulfonic acid group, however, will have a negative charge at physiological pH as does the carboxylate. The problem in this case may be the increased size of the sulfonate over the carboxylate, and therefore unfavourable steric factors preventing binding.

2.2 Synthetic approaches to 2-Phosphononicotinic acid

This analogue of quinolinic acid, although seeming trivial, proved to be a more difficult and interesting synthetic challenge. Several synthetic routes to the compound were envisaged, incorporating a wide range of organic reactions.

2.2.1 Organometallic Strategies

During the last fifteen years, orthometallation has evolved into a significant position in organic chemistry.[127] The basic principle involves deprotonation by a strong base at a site adjacent to a heteroatom containing substituent, known as a directed metallation group (DMG). Normally an alkyl lithium base is required for generation of ortho-lithiated species, treatment of which with an electrophilic reagent provides the required 1,2-disubstituted product.

This can be condensed into three steps, the coordination of an alkyl lithium to a DMG heteroatom, followed by deprotonation at an adjacent carbon, leading to an ortho-lithiated species, and then reaction with a suitable electrophile (Scheme 2.11).

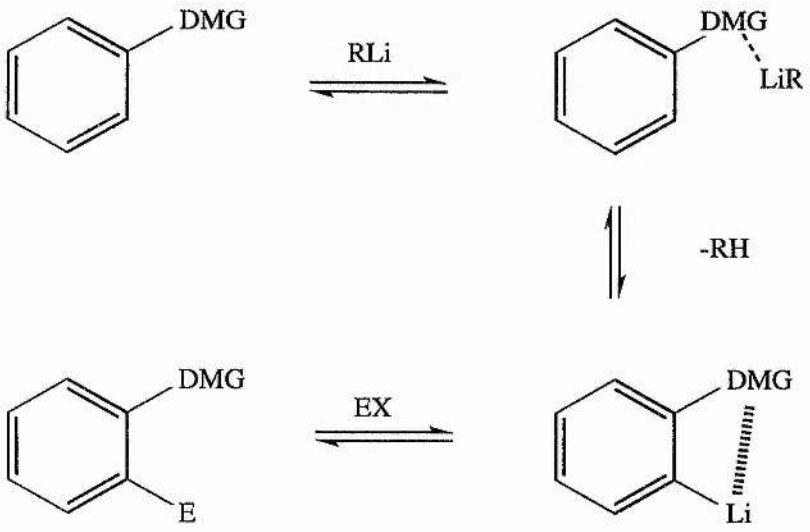

Scheme 2.11: Orthometallation strategy

Such a strategy could be used for the synthesis of the desired pyridine derivative. If a suitable DMG was incorporated at the 3-position, it could be used to direct a phosphorus substituent into the 2-position.[128]

Firstly, diisopropyl nicotinamide was successfully synthesised by treatment of nicotinic acid with thionyl chloride, followed by diisopropylamine. Epsztajn *et al* had previously demonstrated that when *ortho*-metallation was attempted on the 3-substituted pyridine, substitution was *ortho*- directed but to position 4 rather than position 2.[129]

To allow for this, a trimethylsilyl group was first added at position 4 as a protecting group. Diisopropyl nicotinamide (**43**) was thus lithiated using LDA and trapped out using trimethylsilyl chloride *in situ*. LDA was generated in dry THF, and trimethylsilyl chloride added prior to addition of the amide solution. This gave the product (**44**) in 76% yield, the TMS group easily observed in the ^{1}H NMR spectrum at 0.35 ppm. The TMS group at position 4 can easily be removed at a later stage by treatment with TBAF (Scheme 2.12).

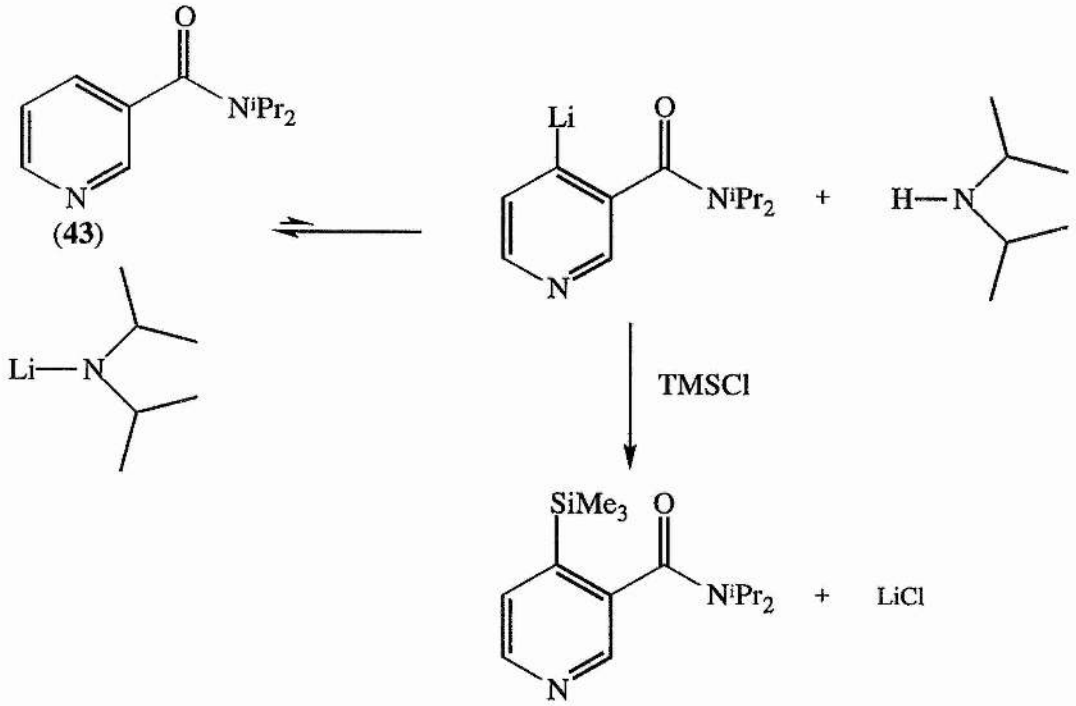

Scheme 2.12

After protection of the 4-position, a second *o*-metallation was attempted in order to get reaction at the 2-position. Lithium diisopropylamide (LDA) was initially used as the base, followed by treatment with diethyl chlorophosphonate, but no reaction took place, possibly because of a lack of deprotonation (Scheme 2.13). When the synthesis of the 2,4-disilyl derivative was attempted, so that a different electrophile was used to trap the anion, again no reaction was seen, which was an interesting result as previously when the 4-silylated diisopropyl nicotinamide was synthesised, the di-substituted product was present, albeit in a very small yield.

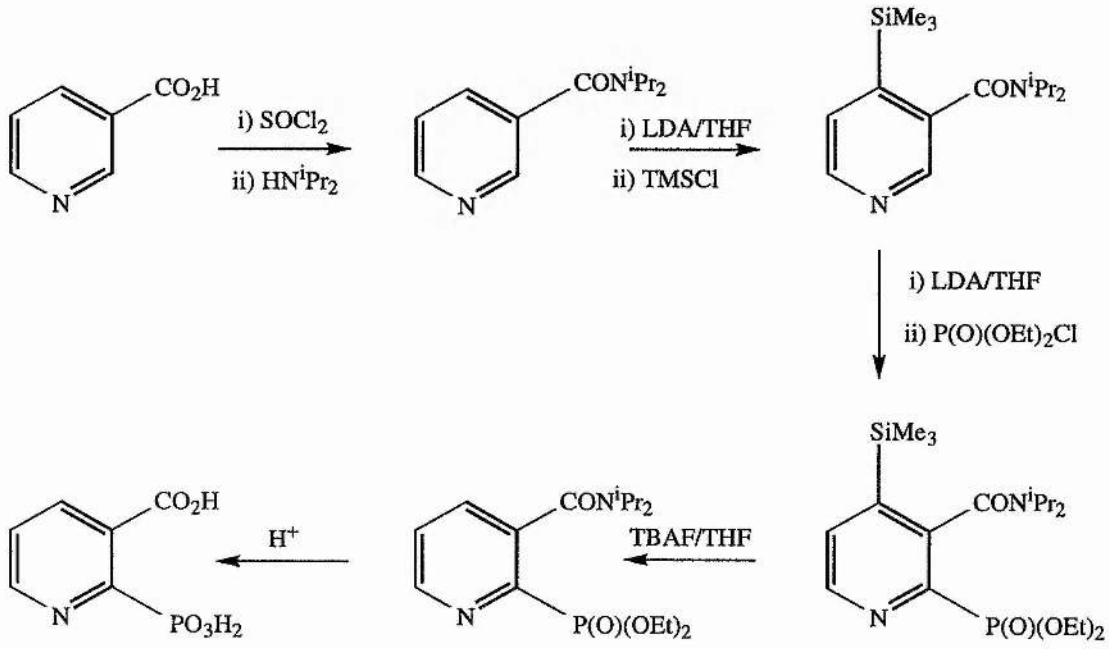

Scheme 2.13: Proposed route to 2-phosphononicotinic acid

LTMP (Lithium 2,2,6,6-tetramethylpiperidide), known to be suitable for efficient aromatic deprotonation, and *t*-BuLi were then used as bases, but again no reaction took place.[130] Similarly, mesityl lithium is known to lithiate the 2-position of 3-methoxypyridine,[131] but was not successful in this case. The rationalisation of using TMEDA (*N, N, N', N'*-tetramethyl-1,2-ethanediamine) as a base was that complexation of lithium with the nitrogen of the pyridine and TMEDA would allow lithiation to take place. However no reaction was seen.

The directing group was then changed to a cyclic oxazoline (**45**), to investigate whether the size of the diisopropyl group was too great and preventing reaction. The oxazoline protected nicotinic acid was synthesised from nicotinyl chloride (Scheme 2.14), which itself was obtained in the same manner as for the synthetic route to 4-silylated diisopropyl nicotinamide. Synthesis of the oxazoline group required two further steps. Nicotinyl chloride was treated with 2-amino 2-methylpropan-1-ol, and this reaction followed by chlorination of the terminal carbon, which upon treatment with base led to ring closure. However, attempted substitution of the 4-position in a manner analogous to the diisopropyl protecteed nicotinic acid gave similarly negative results.

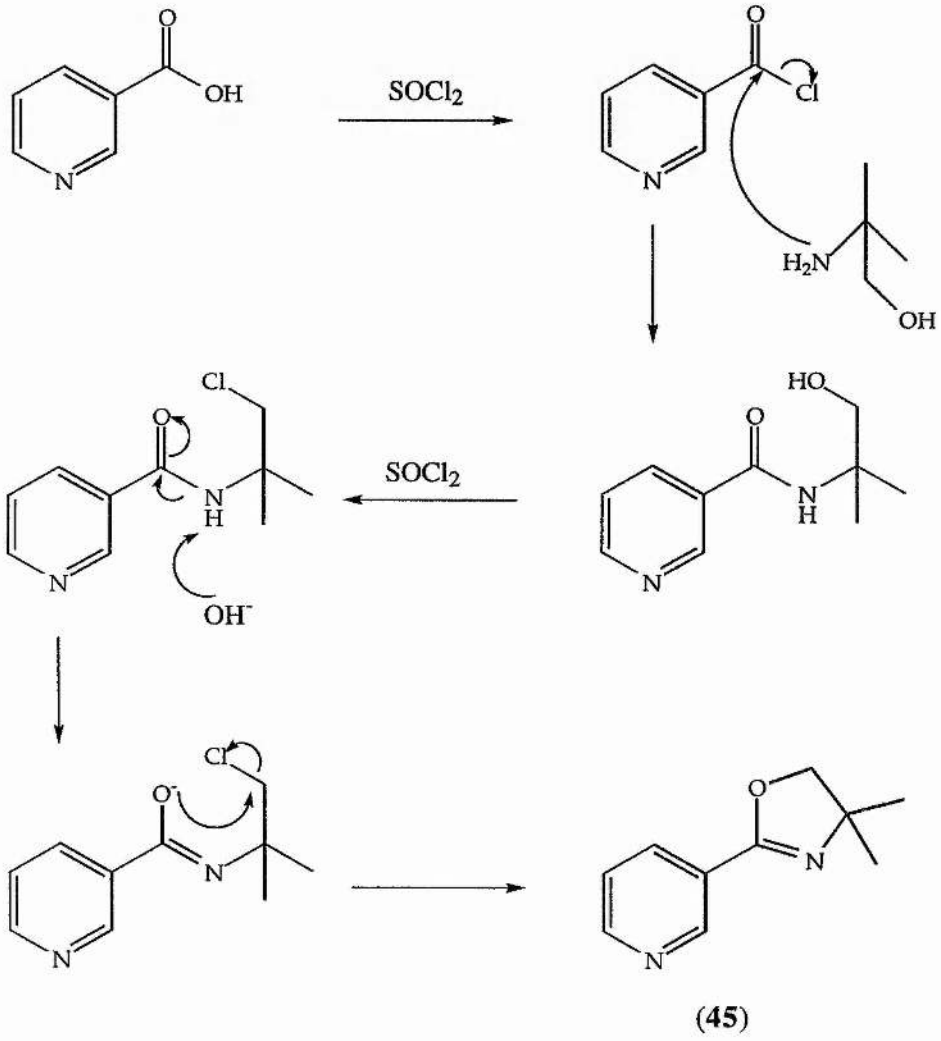

(45)

Scheme 2.14: Synthetic route to 2-(3-pyridyl)-4,4-dimethyl-oxazoline

2.2.2 Palladium Coupling Reactions

Although the Michaelis-Arbuzov reaction provides a well known route for the formation of carbon-phosphorus bonds, this method cannot be carried over to the formation of aryl carbon-phosphorus bonds. Indeed only a few methods have been reported for the synthesis of arenephosphonates.[132-138] Many include radical photolysis reactions,[134,135] Tavs used nickel catalysts nickel chloride or nickel bromide for the reaction,[136] while Kosalopoff and Roy carried out Michaelis-Arbuzov reactions to form pyrimidyl phosphonates.[138] However, Burger *et al* demonstrated that the Arbuzov-Michaelis reaction was not possible with 2-bromo- or 2-chloropyridine.[139]

Hirao *et al* discovered a novel synthetic route to dialkyl arene phosphonates using a palladium (0) catalyst.[140,141] The dialkyl arene phosphonates were synthesised in good yields by reaction of an aromatic bromide or iodide with the corresponding dialkyl phosphite and triethylamine in the presence of tetrakis(triphenylphosphine) palladium (Scheme 2.15).

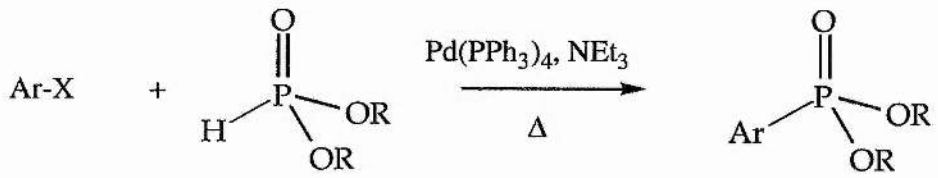

Scheme 2.15: Palladium coupling reaction

The reaction involving diethyl phosphite was successful for a number of substituted benzyl bromides and iodides, although chlorobenzenes did not react. These aryl phosphonates could also be synthesised with diisopropyl and dibutyl phosphites, and no significant effect on the yield was observed following the addition of substituents on the benzene ring. It was thus decided to investigate this methodology as a route to 2-phosphononicotinic acid.

In the literature diethyl pyridine-3-phosphonate was synthesised from 3-bromopyridine using this method. It was thus important to assess whether the same substitution reaction would occur at position two, where substitution is at the carbon adjacent to the pyridine nitrogen. Using the literature method diethyl pyridine-2-phosphonate was successfully synthesised from 2-bromopyridine in 41% yield. This was confirmed by NMR data showing the presence of the diethyl phosphonate group, and mass spectrometry gave the expected molecular ion at 215.

As this was successful, the synthesis of 2-phosphononicotinic acid was attempted. In order to prepare the correct compound, the necessary starting material was methyl 2-bromonicotinate (**46**). This was synthesised in the manner described by Bryson *et al* (Scheme 2.16).[142]

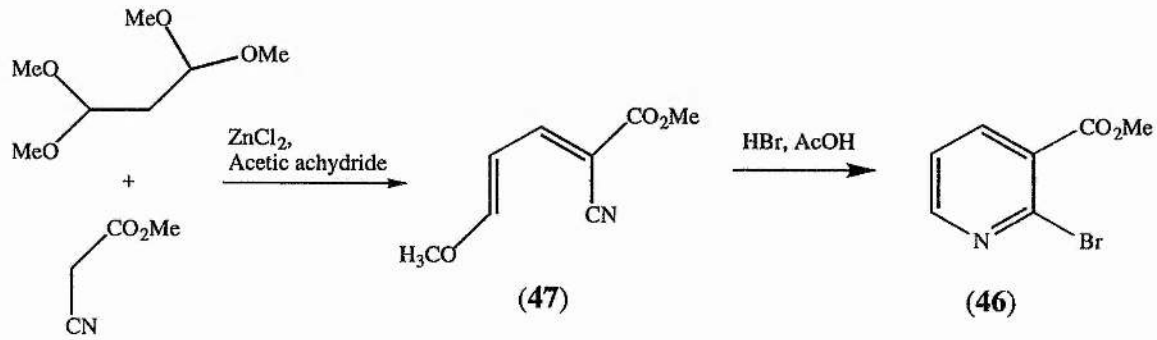

Scheme 2.16: Synthesis of methyl 2-bromonicotinate

The zinc chloride catalysed condensation of methyl cyanoacetate and 1,1,3,3-tetramethoxypropane in acetic anhydride led to the production of the enol ether methyl 2-cyano-5-methoxypentane-2,4-dienoate (**47**) in 90% yield (Scheme 2.17).[143]

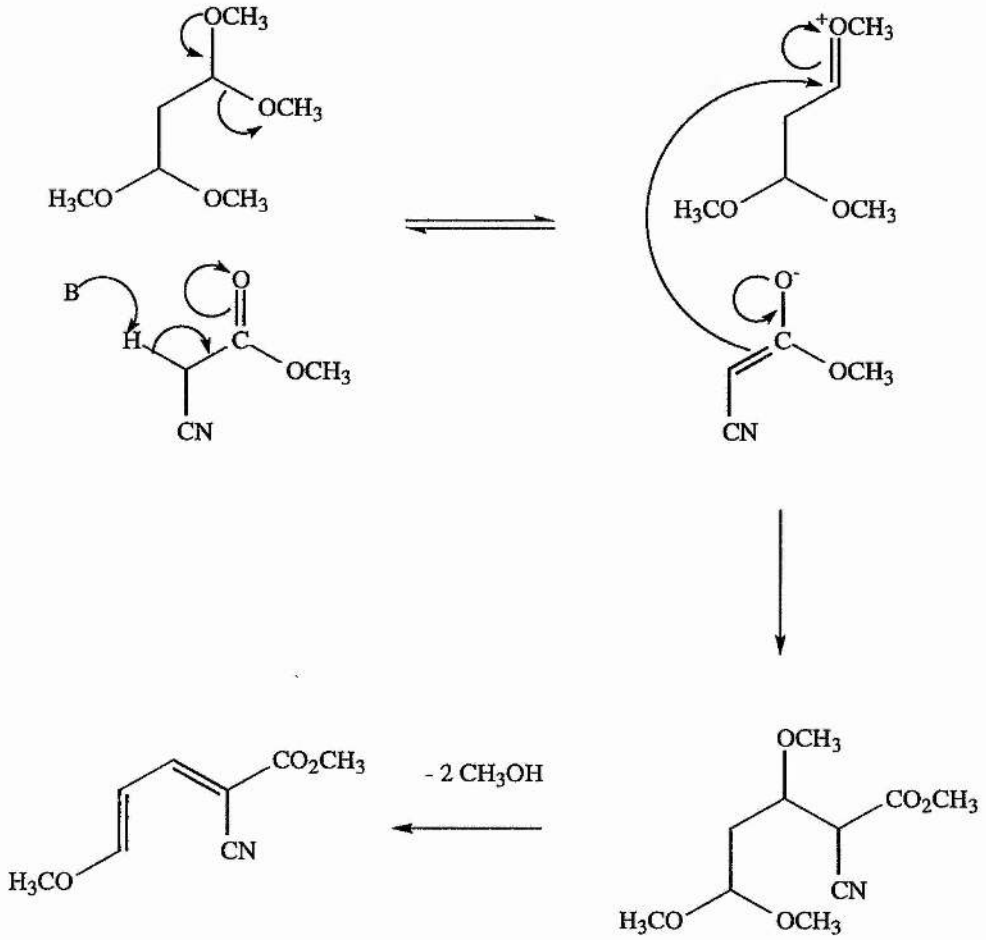

Scheme 2.17: Synthesis of methyl 2-cyano-5-methoxypentane-2,4-dienoate

Treatment with hydrobromic acid in acetic acid then resulted in the very facile intramolecular cyclisation-elimination reaction, to produce methyl 2-bromonicotinate in 97% yield. The cyclisation was initiated by addition of hydrobromic acid across the nitrile group, forming an iminobromide which, in a Michael type reaction, added to the terminus of the conjugated ester system. Methyl 2-bromonicotinate was then formed by elimination of methanol (Scheme 2.18).

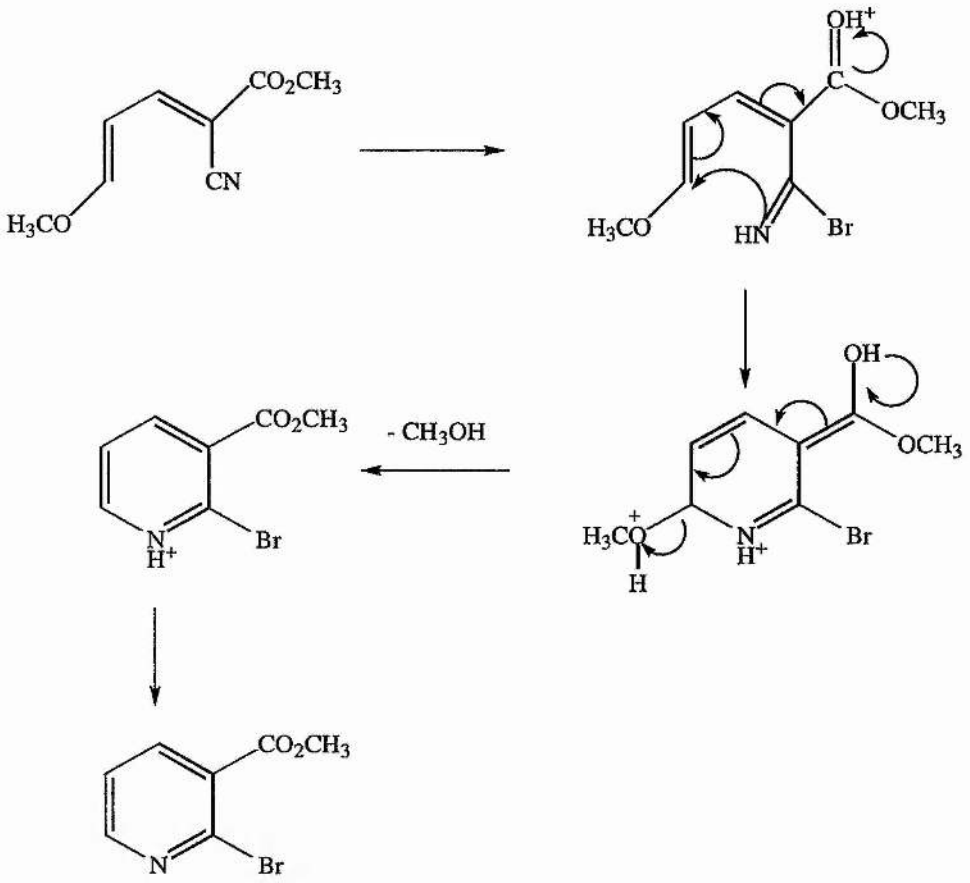

Scheme 2.18: Mechanism for methyl 2-bromonicotinate production

It is fortunate in the preparation of the enol ether that only one of the many possible geometric isomers form, as is confirmed by ^{1}H and ^{13}C NMR, leading to an explanation of the almost quantitative yield for cyclisation. Hydrobromic acid in acetic acid is quite a strong reagent, possibly making the geometry of the enol ether irrelevant. If malononitrile was used for the reaction, 2-bromonicotinonitrile would be formed.[143]

The palladium coupling reaction using methyl 2-bromonicotinate was then attempted. Methyl 2-bromonicotinate was heated with diethyl phosphite for three days in the presence of the palladium (0) catalyst and triethylamine. Although tlc suggested that some reaction had taken place, none of the expected product was isolated.

In order to rule out palladium catalyst contamination as a possible problem, the experiment was repeated with a newly opened sample of catalyst weighed out under nitrogen, but was not successful. The major hindrance to this reaction could be the size and position of the methyl ester group which prevented the palladium catalyst from coordinating the bromo-pyridine.

The mechanism for the synthesis of methyl 2-bromonicotinate involved the nucleophilic attack of bromide ions to initiate the cyclisation reaction. It was considered that a phosphorus nucleophile may have a similar effect, and provide a route that would introduce a phosphonate group into the desired 2-position on the pyridine ring. However a simple reaction in which hydrobromic acid was replaced by triethyl phosphite was not successful (Scheme 2.19).

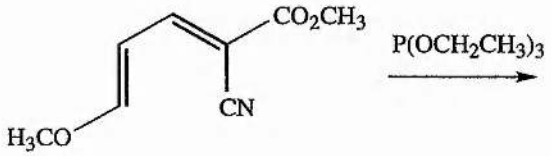

Scheme 2.19: Attempted nucleophilic addition

2.2.3 Nucleophilic Addition Reactions

Many substituted pyridines have been prepared via attack of nucleophiles on *N*-alkoxypyridine salts, prepared from the appropriate *N*-oxide.[144] For example, Redmore demonstrated that reaction of *N*-alkoxypyridinium salts with the alkali metal derivatives of dialkyl phosphonates provided a general route to the synthesis of dialkyl pyridine-2-phosphonates, which can then be hydrolysed in 18% hydrochloric acid to the corresponding phosphonic acids.[145] In particular it was found that *N*-methoxypyridinium methylsulfonate reacted with lithium diethyl phosphonates to form diethyl pyridine-2-phosphonate (**48**) in 67% yield (Scheme 2.20).

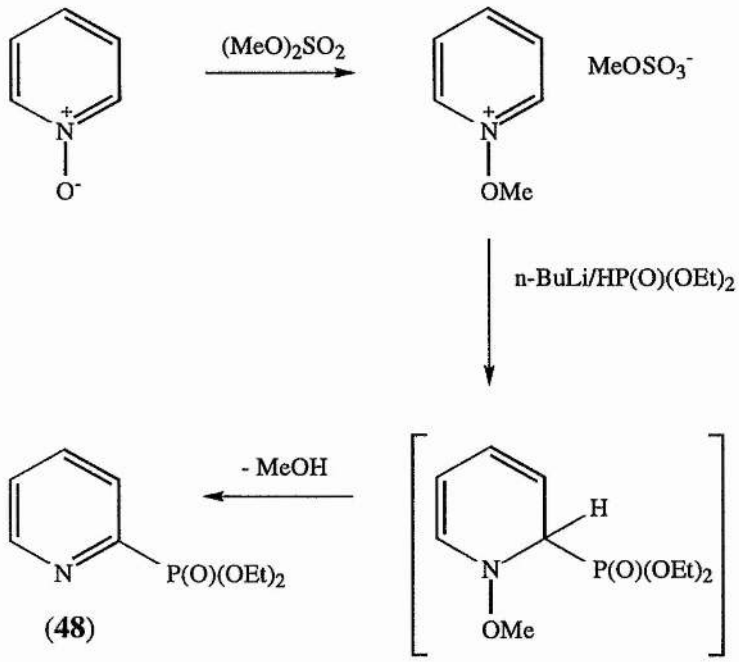

Scheme 2.20: Synthesis of diethyl pyridine-2-phosphonate

The temperature of the reaction is very important. The loss of methanol from the intermediate is rapid at room temperature, which leads to an increase in the concentration of methanol, which then competes with the *N*-methoxypyridine for the lithium diphosphonate salt.

$$LiP(O)(OEt)_2 + MeOH \rightleftharpoons LiOMe + HP(O)(OEt)_2$$

If the reaction temperature is lowered to - 20 to -30 °C then attack of the nucleophile on the *N*-methoxypyridine is much faster, giving higher yields. Diethyl pyridine-2-phosphonate has also been obtained by reaction of triethyl phosphite with 2-nitropyridine *N*-oxide.[146]

Redmore also carried out the reaction with 3-substituted pyridines. As expected a mixture of products was obtained, where substitution occurred at both the 2- and 6-positions. For example, 3-methylpyridine *N*-oxide (picoline *N*-oxide) was converted into a mixture of diethyl 3-methylpyridine-2-phosphonate (**49**) and diethyl 5-methylpyridine-2-phosphonate (**50**) in a ratio of 6:1 (Scheme 2.21).

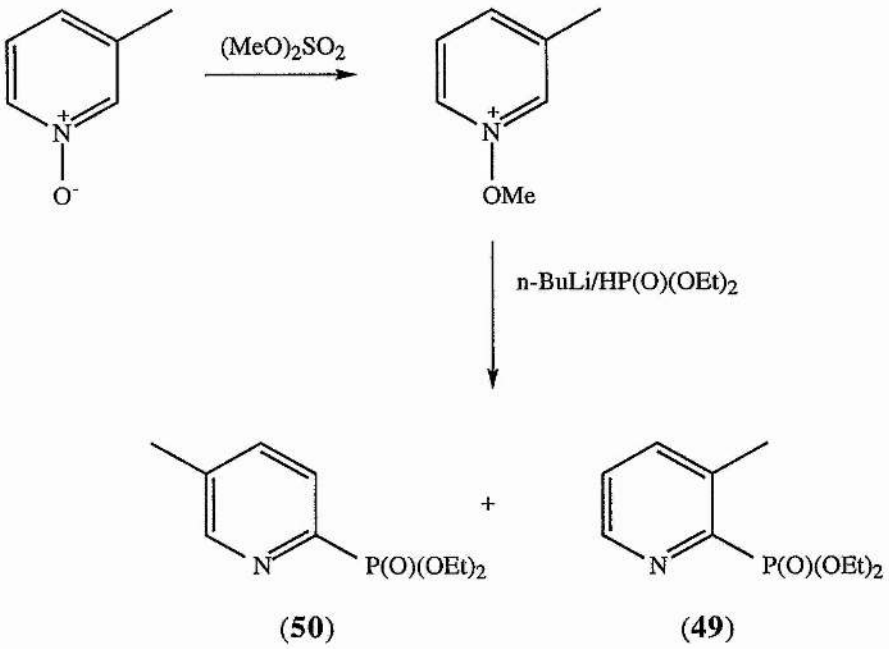

(50) **(49)**

Scheme 2.21: Redmore reaction

It was decided to investigate a similar reaction using ethyl nicotinate (Scheme 2.22). The *N*-oxide of ethyl nicotinate (**51**) was prepared in 75% yield using hydrogen peroxide and trifluoroacetic anhydride, and this was methylated in quantitative yield with dimethyl sulfate. Treatment of the ethyl *N*-methoxynicotinium methylsulfonate with lithium diethylphosphonate (from *n*-BuLi and diethyl phosphite) produced triethyl pyridine-5-carboxylate-2-phosphonate (**52**) as expected, shown by NMR. However no evidence of triethyl pyridine-3-carboxylate-2-phosphonate (**53**) was observed. The presence of **52** was confirmed by the singlet for the proton at position 2 of the pyridine ring, observed in the ^{1}H NMR spectrum at 7.75 ppm. The other pyridine protons were present as the expected doublets. If the substitution had been successful at position 2, then the triplet seen for the proton at position 5 would have been observed in ^{1}H NMR, and no singlets would have been present.

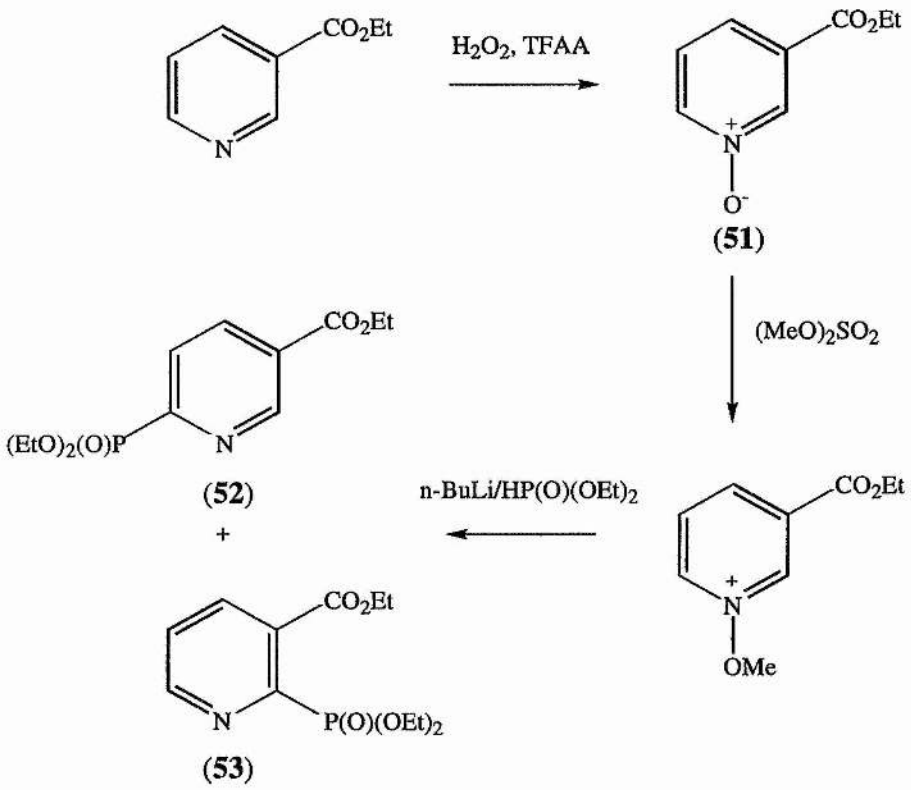

Scheme 2.22: Reaction using ethyl nicotinate

The size of the carboxylate ester group suggests that the bulky diethyl phosphonate group will preferentially attack the less hindered carbon at position 2, adjacent to the pyridine nitrogen.

An Arbusov type reaction was also attempted where triethyl phosphite was heated with methyl 2-bromonicotinate, prepared as in Section 2.2.2, (Scheme 2.23), but no reaction was observed. This implies that either the bromide was not sufficiently reactive for attack of the phosphonate group or that steric hindrance due to the ester was too great.

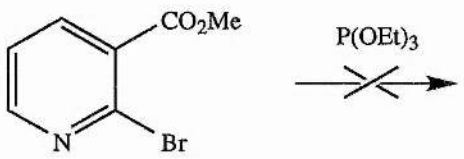

Scheme 2.23: Arbusov reaction

Burger *et al* had also shown that 2-bromopyridine was unreactive under these conditions, and methyl 2-bromonicotinate proved to be the same.[139] The Michaelis-Becker-Nylen reaction was also attempted with methyl 2-bromonicotinate (Scheme 2.24). The lithium salt of diethyl phosphite was formed in the usual way, but no reaction of the salt with methyl 2-bromonicotinate was seen.

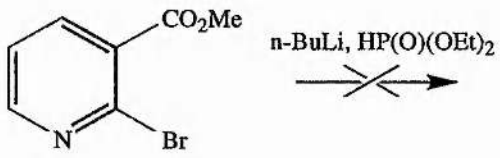

Scheme 2.24: Michaelis-Becker-Nylen

Both of these reactions were also attempted with 2-chloronicotinonitrile. It was thought that this group would provide less steric hindrance to attack by the phosphorus. The nitrile group could then be hydrolysed to the required carboxylic acid group at a later stage (Scheme 2.25).

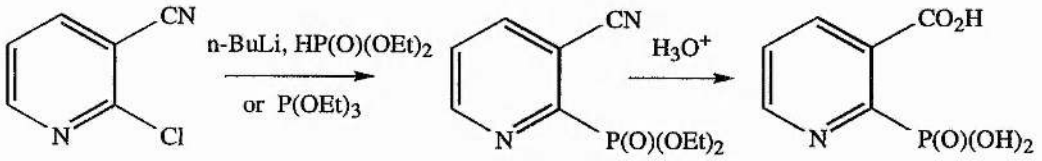

Scheme 2.25: Reaction using 2-chloronicotinonitrile

However under the same conditions as for methyl 2-bromonicotinate, no reaction occurred. 2-Chloronicotinonitrile again appears not to be sufficiently reactive.

Tavs and Karte heated 2-bromopyridine with triethyl phosphite, in the presence of a copper catalyst, and only obtained a 1% conversion to diethyl pyridine-2-phosphonate, which demonstrates the low reactivity of these compounds.[147]

2.2.4 Building up the Pyridine Ring

As discussed, routes to the formation of 2-phosphononicotinic acid involving the addition of the phosphorus-containing group to the pyridine ring were unsuccessful. Therefore, alternative methods were investigated which involved formation of the pyridine ring with the phosphorus-containing group already incorporated.

The initial investigation focused on the synthesis of α-aminophosphonic acids. It was envisaged that the amino acid could be incorporated into the pyridine ring by cyclisation, to give the carboxylic acid and phosphonic acid groups in the required positions. It was thought that 1,1,3,3-tetramethoxypropane could be utilised to effect the cyclisation, followed by aromatisation and deprotection to produce the product in a similar manner to that for methyl 2-bromonicotinate (Scheme 2.26). Therefore our initial synthetic target was (**54**).

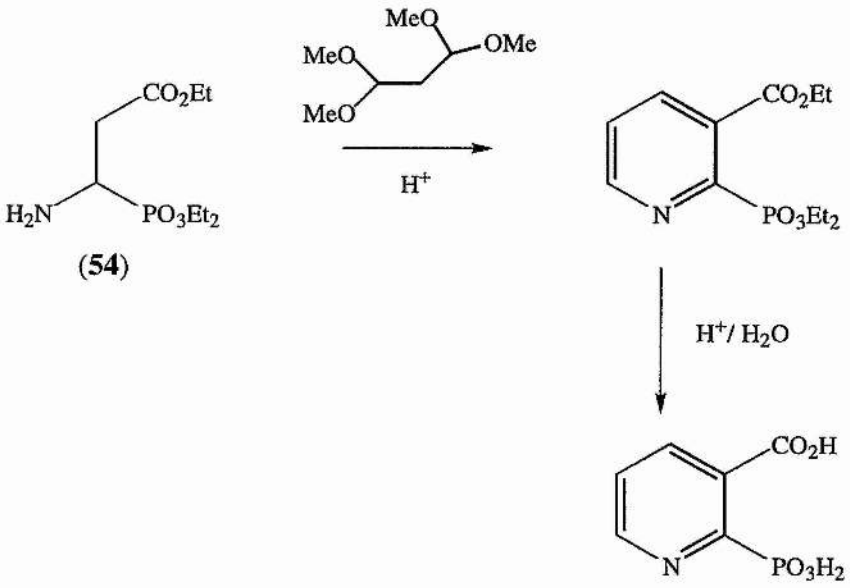

(**54**)

Scheme 2.26: Proposed cyclisation

2.2.4.1 α-Aminophosphonic acids

Many potent antibiotics,[148] enzyme inhibitors, herbicides and insecticides[149] are α-aminophosphonic acids.[150] Generally α-aminophosphonic acids are toxic in high concentrations, and differ from amino acids in that many tissues are unable to transform the phosphorus into phosphate.[151] The biological activity and uses of α-aminophosphonic acids have been widely reviewed.[152]

2.2.4.2 Synthetic Routes Towards α-Aminophosphonic acids

A proposed synthetic route to this protected α-aminophosphonic acid is described in Scheme 2.27 below.

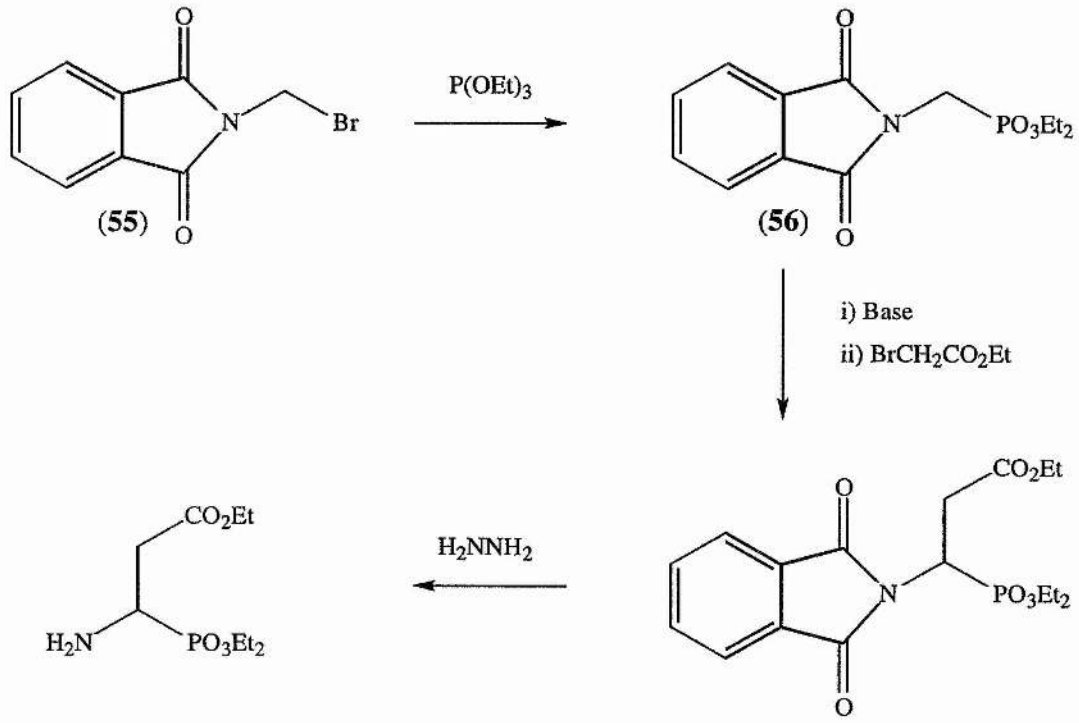

Scheme 2.27: Proposed route to protected α-aminophosphonic acid

N-Bromomethylphthalimide (**55**) was heated with triethyl phosphite over 3 days at 160 °C to produce diethyl *N*-phosphonomethylphthalimide (**56**) which was recrystallised from ethyl acetate and hexane to give a white powder in a good yield. The melting point corresponded to that from the literature confirming the identity.

It was expected that treatment of *N*-phosphonomethylphthalimide with a base, followed by addition of bromomethyl acetate would be successful. This reaction would allow the introduction of the protected carboxylic acid group on the carbon adjacent to the phosphonate group. The phthalimide group is a good protecting group for this function as there are no amide protons.

Initially *n*-BuLi and *t*-BuLi were employed as bases to carry out the deprotonation. However, little or no anion formation was observed, the only reaction observed being hydrolysis of the phosphonate ester groups. Lithium diisopropylamide (LDA), sodium hydride and sodium methoxide in methanol were also employed as bases, but again, only deprotection of the esters took place, preventing deprotonation, and causing great problems upon isolation. The attempts with these bases were repeated in a wide range of dry solvents to try and eliminate any possible solvent interference. These solvents included THF, DMF, ethanol, methanol and DME.

The much weaker bases potassium carbonate and KHMDS were also considered, but although no deprotection of the phosphonate esters occurred, neither did deprotonation. If substantial deprotonation, and subsequent incorporation of the ethyl acetate group, had taken place, then re-esterification of the hydrolysed product would have been an alternative, but no such reaction occurred.

Treatment of the product with hydrazine would deprotect the nitrogen to give the ester of an α-amino phosphonic acid. Cyclisation to form the pyridine ring with 1,1,3,3-tetramethoxypropane and hydrolysis of the esters would, as described earlier, produce 2-phosphononicotinic acid.

Due to the severity of the problems discussed, this route to the formation of an α-amino phosphonic acid was abandoned, and attention turned to alternative routes. Oleksyszyn *et al* developed a three component coupling route to produce an α-amino phosphonic acid (**57**) (Scheme 2.28).[153]

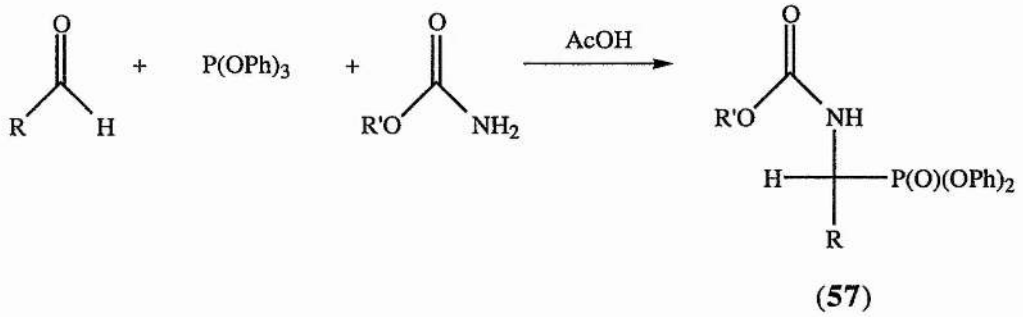

(**57**)

Scheme 2.28: Three component coupling route

A similar reaction, this time to synthesise phosphomethionine and other similar compounds as the phosphorus analogues of essential amino acids was developed by Tam *et al* (Scheme 2.29).[154]

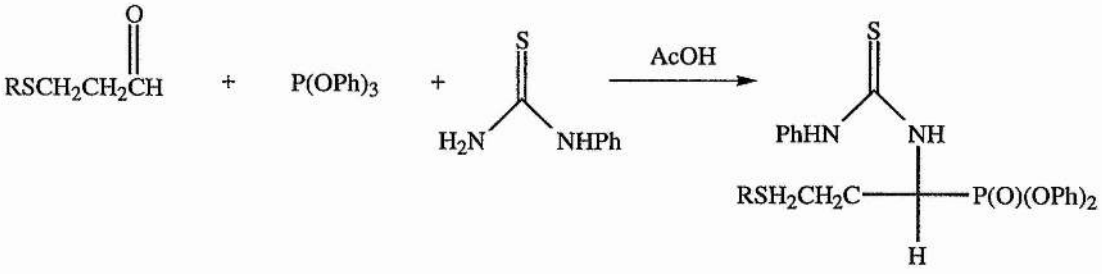

Scheme 2.29: Tam reaction

(*N*-Phenyl)thiourea was this time used as a protected source of the amino group, in reactions which gave good yields in producing both methionine and ethionine analogues. This work was adapted to develop a proposed route to 2-phosphononicotinic acid (Scheme 2.30).

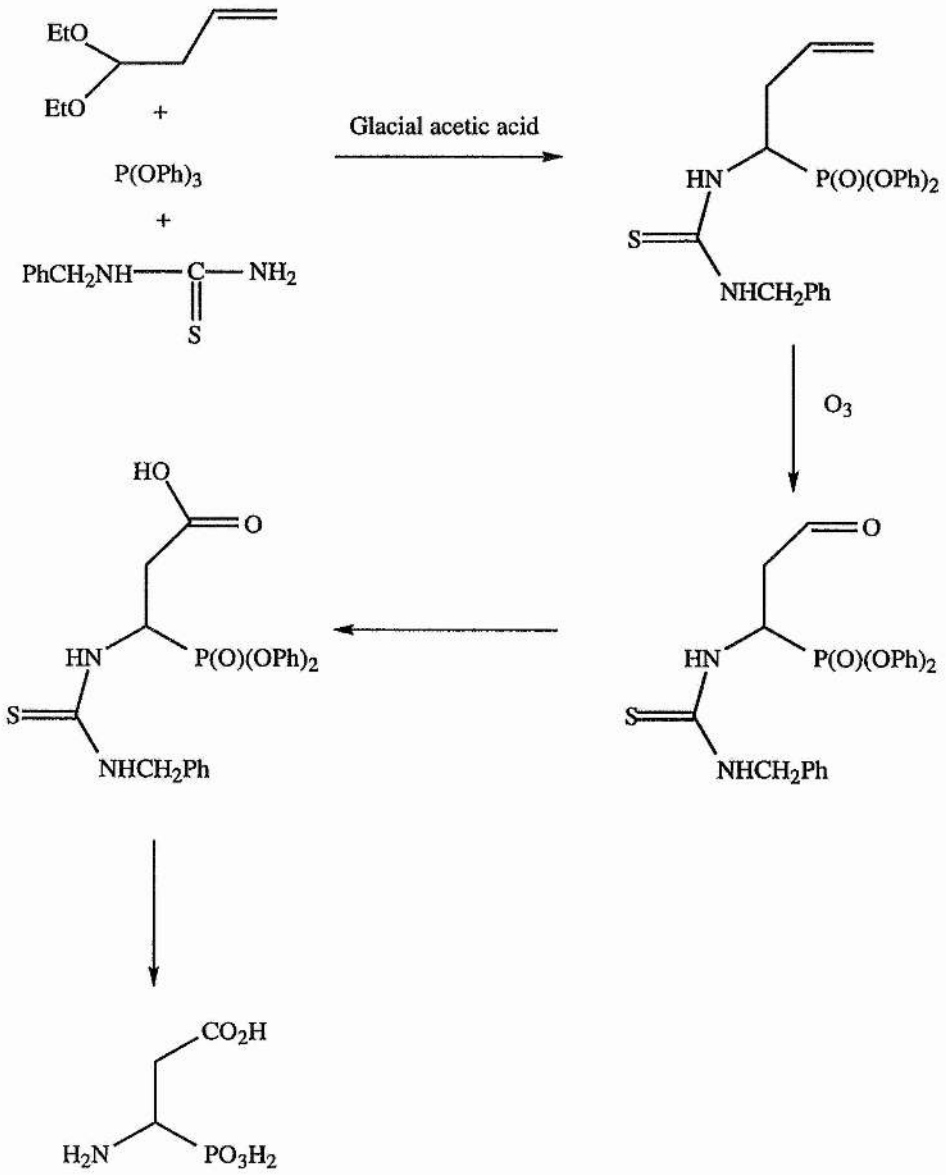

Scheme 2.30: Proposed route to 2-phosphononicotinic acid

Thus, benzylthiourea, triphenyl phosphite and 3-butenal diethylacetal were stirred for 16 hours in glacial acetic acid, heated to reflux for a further 2.5 hours and then the acetic acid removed. No reaction was detected by tlc or ^{1}H NMR. It was not possible to purchase, or easily synthesise butenal, which may have been a better component than the diethyl acetal, but it was hoped that the diethyl acetal would have been a successful alternative. When propanal had previously been used as a starting component the reaction occurred in good yield.

2.2.5 Alternative Routes to 2-Phosphononicotinic acid

Previously, attempts to introduce the phosphonate ester group into the pyridine ring have been highly specific, with introduction directed at the 2-position. However, as these were unsuccessful, routes which were potentially less efficient, but still produced 2-phosphononicotinic acid as one of a mixture of products, were considered.

Steric hindrance, in that the size of the carboxylate ester prevented the introduction of the phosphonate ester at the 2-position, was the main factor in these unsuccessful synthetic routes. Thus alternative groups for the 3-position small enough to allow substitution at position 2, but capable of conversion to a carboxylic acid group, were considered. The main focus of these involved compounds with a methyl group at the 3-position. The conversion of the 3-methyl group to a carboxylic acid group by oxidative methods would then produce the desired compound (Scheme 2.31).

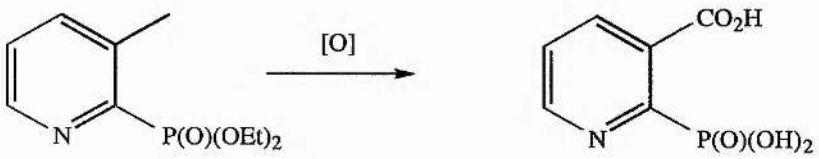

Scheme 2.31: Oxidation of methyl group

For this purpose, the reaction developed by Redmore,[145] to produce diethyl 3-methylpyridine-2-phosphonate, was employed to produce the diethyl 3-methylpyridine-2-phosphonate and diethyl 5-methylpyridine-2-phosphonate. This gave the two products in 89% yield, and in a ratio of 10:1, better ratio than that achieved by Redmore.

Firstly, picoline *N*-oxide (3-methylpyridine *N*-oxide) was methylated in quantitative yield, and the resulting *N*-methoxypicolininium salt dissolved in diethyl phosphite and added to a solution of n-BuLi and diethyl phosphite at - 20 to - 30 °C.

After addition was complete, the solution was stirred at - 20 to - 30 °C for a further 30 minutes and then the reaction allowed to warm to room temperature. The reaction was followed by tlc (3:2 40-60 pet. ether: ethyl acetate) and on completion excess diethyl phosphite removed under reduced pressure. Using Kugelrohr distillation, the two isomers were then separated giving a 10:1 ratio of products. Hydrolysis of the diethyl phosphonate was achieved by refluxing in concentrated hydrochloric acid for 6 hours to produce 3-methylpyridine-2-phosphonic acid (**58**) in 75% yield (Scheme 2.32).

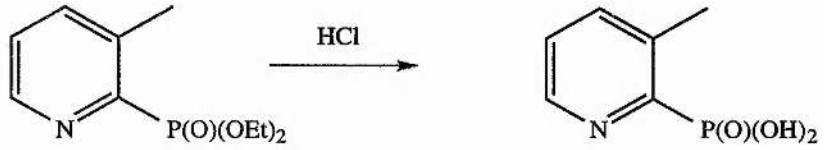

(**58**)

Scheme 2.32: Hydrolysis of ester

The focus then moved onto oxidation of the 3-methyl group to the carboxylic acid. DuPriest *et al* successfully synthesised 2-phenylpyridine-3-carboxylic acid (**59**), in moderate yields from the respective 3-methylpyridines, by oxidation with potassium permanganate (Scheme 2.33).[155]

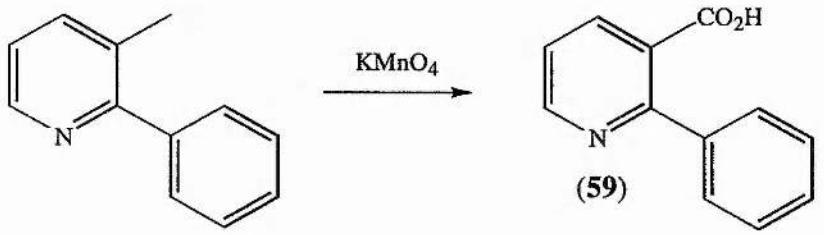

(**59**)

Scheme 2.33: DuPriest oxidation

This method was thus examined. 3-Methylpyridine-2-phosphonic acid and potassium permanganate were dissolved in water and heated to reflux and inspection by tlc appeared to show that oxidation had taken place (Scheme 2.34). No spot corresponding to starting material was observed.

When all the permanganate was consumed, the hot mixture was filtered through celite to remove manganese dioxide. When the water was removed under reduced pressure, a white solid formed. However this solid was insoluble in a wide range of NMR solvents, C^2HCl_3, ^2H_2O, d-6 DMSO and d-4 methanol.

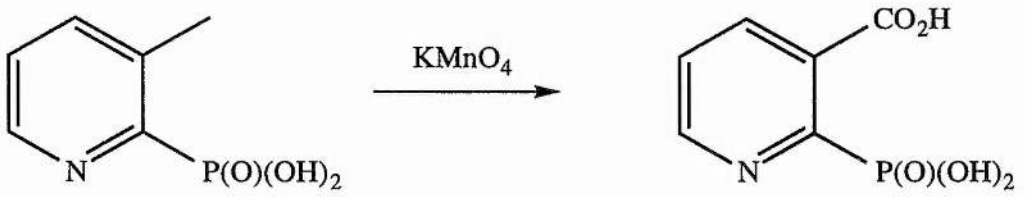

Scheme 2.34: Attempted oxidation

The lack of solubility of the oxidation product and the tlc result implied that perhaps the di-acid was formed, but could not be isolated. Analysis by mass spectrometry gave no further information on the identity of the oxidation product, whilst attempts at recrystallision from boiling water were unsuccessful.

In order to check the success of the reaction, the oxidation was repeated with picoline (3-methylpyridine), and nicotinic acid (pyridine-3-carboxylic acid) (**32**) was formed as expected, in good yield (Scheme 2.35) .

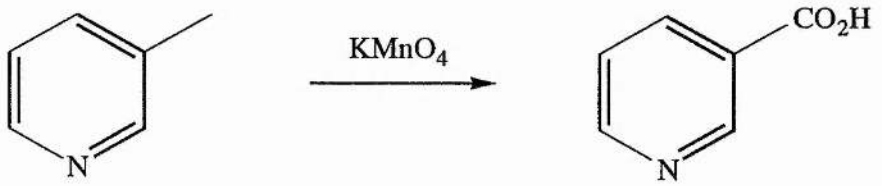

(**32**)

Scheme 2.35: Oxidation of 3-methylpyridine

An alternative oxidation method was investigated, involving bromination of the methyl group and subsequent oxidation of the bromomethyl group to the carboxylic acid (Scheme 2.36).

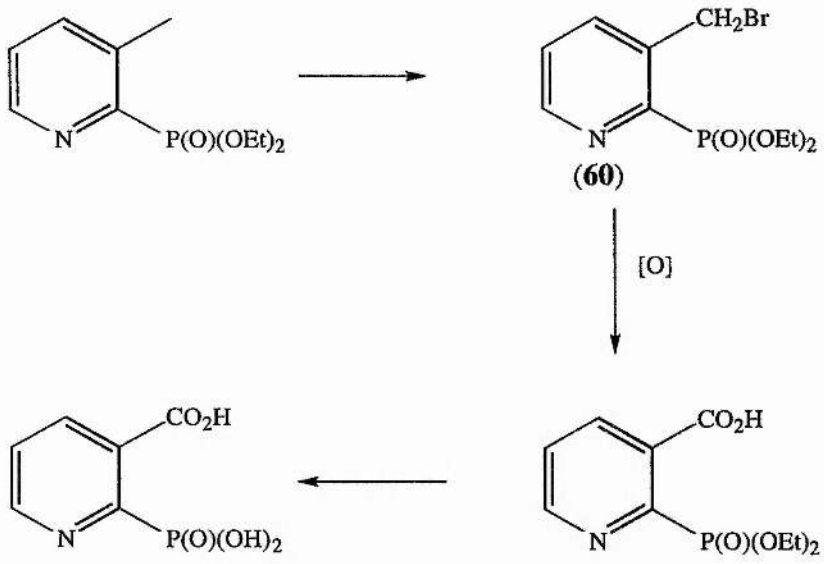

Scheme 2.36: Bromination route to 2-phosphononicotinic acid

In the synthesis of 2-carboxyquinoline-3-acetic acid by Gray *et al*,[156] the first step involved the bromination of methyl (3-methyl)quinoline-2-carboxylate (**61**) using *N*-bromosuccinimide to give methyl (3-bromomethyl)quinoline-2-carboxylate (**62**) in 22% yield (Scheme 2.37).[157] This presents a milder method for the desired oxidation and was therefore employed as an alternative method.

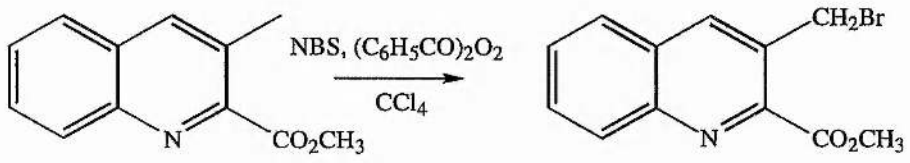

(**61**) (**62**)

Scheme 2.37: Bromination of methyl (3-methyl)quinoline-2-carboxylate

Thus diethyl (3-methyl)pyridine-2-phosphonate was dissolved in carbon tetrachloride and added to a solution of *N*-bromosuccinimide in carbon tetrachloride with 0.1 equivalents of catalytic dibenzoyl peroxide. The reaction was heated to reflux for two days, with further additions of 0.1 equivalent catalyst every 12 hours. On cooling the carbon tetrachloride was removed under reduced pressure and purification of the crude bromide on a silica gel column provided, on crystallisation, a pale orange

solid of diethyl (3-bromomethyl)pyridine-2-phosphonate (**60**) in 30% yield. The appearance of a singlet at 4.93 in the ^{1}H NMR spectrum, and the disappearance of one at 2.50 indicated that bromination had occurred. A pair of peaks at 307 and 309 in the mass spectrum confirmed this as did that at 228 (M-Br). Accurate mass data gave further weight to the data (Found: [*M*] 306.9969. $C_{10}H_{15}NO_3PBr$ requires 306.9972).

Matt *et al* described the transformation of primary alkyl bromides, including bromoethyl benzene (**63**), bromomethylbenzene and *N*-bromomethylphthalimide into the corresponding carboxylic acids (**64**) by treatment with sodium nitrite and acetic acid in dimethyl sulfoxide in good yields (Scheme 2.38).[158] The researchers claim that this method is the only synthetically useful one-pot oxidation of primary bromides to carboxylic acids.

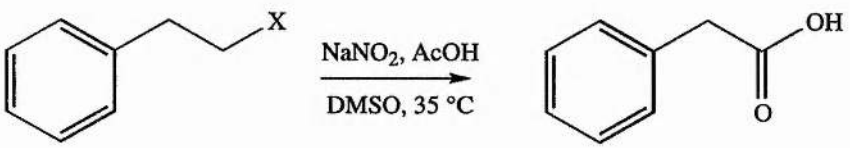

X= Br, NO_2

(63) **(64)**

Scheme 2.38: Matt oxidation

The following mechanism was proposed for the conversion of the nitroalkane formed by initial nucleophilic substitution to the acid (Scheme 2.39).

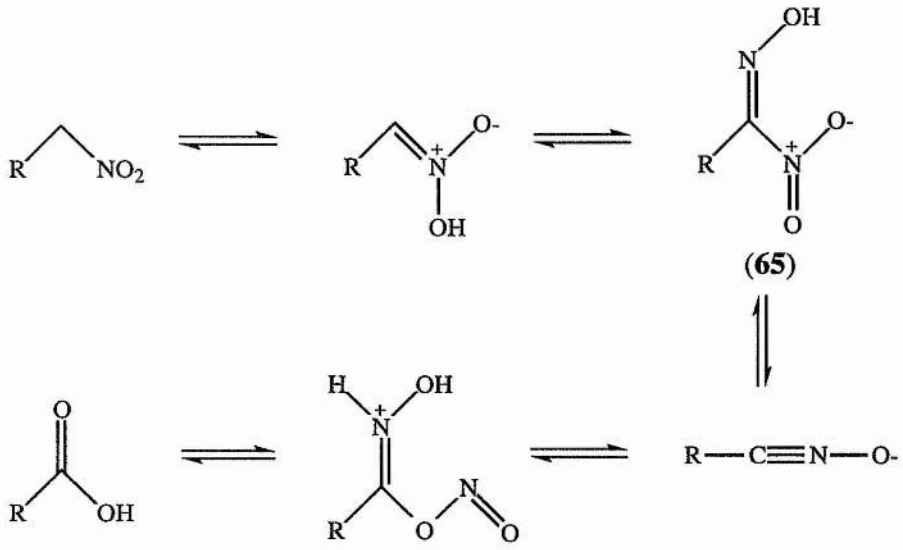

Scheme 2.39: Oxidation of nitroalkane

If the reaction was carried out at 18 °C rather than 35 °C, the nitrolic acid (**65**) was isolated. It was proposed that the reaction is not acid catalysed but that an equivalent of nitrosonium ion, generated *in situ* by reaction of sodium nitrite and acetic acid propels the reaction, a theory supported by the fact that reaction only occurs if both species are present.

Therefore, following the method of Matt *et al*, diethyl (3-bromomethyl)pyridine-2-phosphonate was dissolved in a mixture of sodium nitrite, acetic acid in dimethyl sulfoxide and stirred at 35 °C overnight, but no reaction was observed (Scheme 2.40).

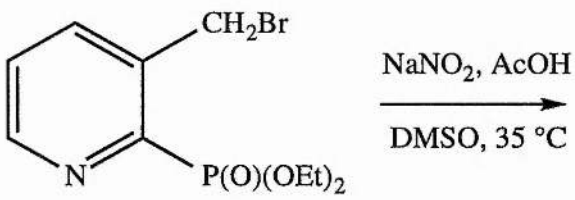

Scheme 2.40: Oxidation of diethyl (3-bromomethyl)pyridine-2-phosphonate

One obvious and simple explanation to the problem is that the size of the diethyl phosphonate group interferes and prevents reaction from taking place.

If time had allowed, other methods of oxidation of the bromide to the carboxylic acid would have been considered. For example, the Kornblum oxidation, involving heating of the halide in DMSO in the presence of a base, oxidises the bromide to the corresponding aldehyde (Scheme 2.41).

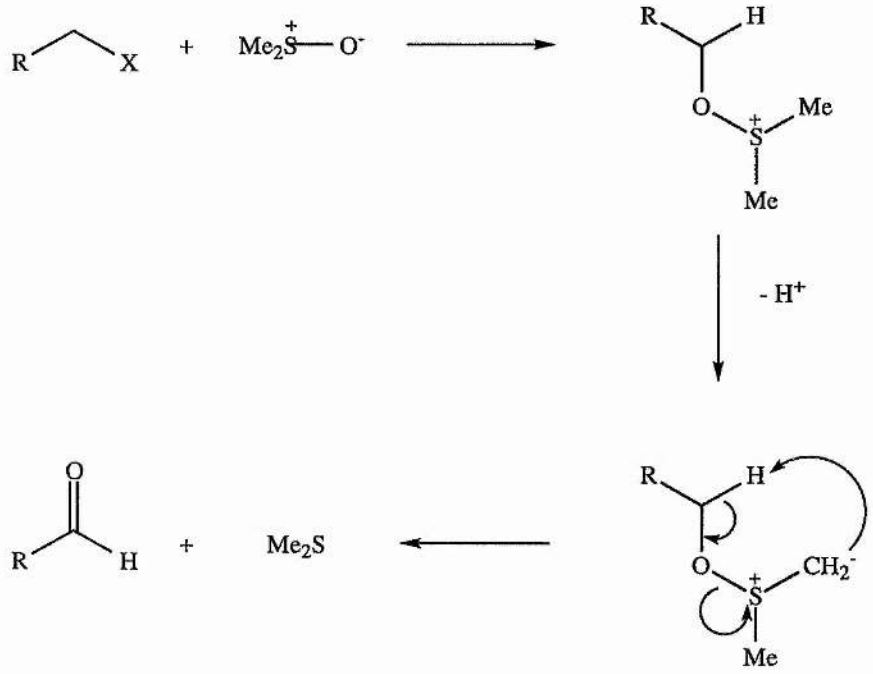

Scheme 2.41: Kornblum oxidation

The aldehyde could then be oxidised to the acid. The Kröhnke oxidation of a halide to an aldehyde involves three steps. Firstly, quaternization of the halide was completed using pyridine as the base. Deprotonation and reaction of the resulting pyridinium ylid with *N*,*N*-dimethyl-4-nitrosoaniline followed, and then finally acid hydrolysis led to the production of the carbonyl.

Benzyl halides were oxidised to the carboxylic acid with sodium hypochlorite,[159] while Borsotti *et al* described the electrochemical oxidation of some benzyl chlorides to the corresponding acids using a nickel hydroxide electrode.[160]

Other methods using transition metals included the use of perruthenate[161] and ruthenate anions[162] and the cobalt (III) ion.[163]

Further methods of oxidation of non-activated alkyl halides to the carbonyl derivatives include a variety of reagents, such as 2-nitropropane sodium salt, DMSO, *N*-phenyltrifluoromethane sulphonamide, soluble and supported chromate reagents, and dimethyl selenoxide.[159]

2.2.6 Synthesis of 2-(Phosphonomethyl)nicotinic acid

As the routes to 2-phosphononicotinic acid were all unsuccessful, 2-(phosphonomethyl)nicotinic acid (**66**) was considered as an alternative analogue of quinolinic acid. Scheme 2.42 shows the synthetic route to the novel phosphonic acid.

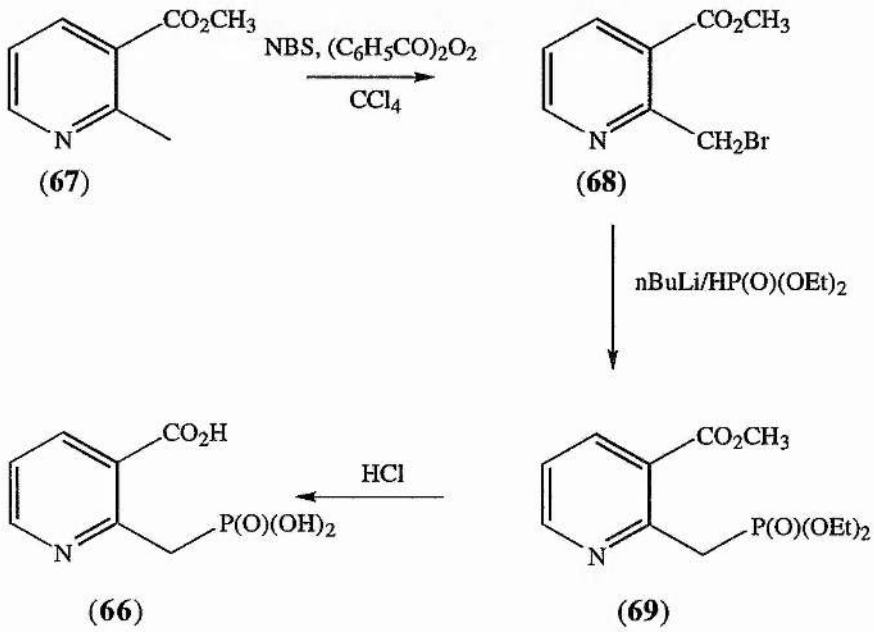

Scheme 2.42: Route to 2-(phosphonomethyl)nicotinic acid

Methyl 2-methylnicotinate (**67**) was brominated on the 2-methyl position, in an identical manner as described for diethyl 3-methylpyridine-2-phosphonate, in 30% yield (**68**). The singlet representing the methyl group shifted downfield to 5.02 ppm

upon bromination, in the ^{1}H NMR spectrum. When the product of this reaction was dissolved in diethyl phosphite and then treated with *n*-butyl lithium and diethyl phosphite at -20 to -30 °C, diethyl (3-methoxycarbonyl-2-pyridyl)methylphosphonate (**69**) was formed as an oil, in 20% yield. The methyl group shifted back upfield to 3.95 ppm in the ^{1}H NMR spectrum, indicating that nucleophilic substitution had taken place. A peak at 25.14 in the ^{31}P NMR spectrum and a peak at 1290 cm^{-1} in the IR spectrum, confirmed the presence of the diethyl phosphonate group. The final step was to hydrolyse the esters. Diethyl (3-methoxycarbonyl-2-pyridyl)methylphosphonate was dissolved in concentrated hydrochloric acid, and heated to reflux for 24 hours. Upon cooling and removal of the excess acid, the acid (**66**) was produced as a white solid in 90% yield from the ester (**69**). Again ^{1}H and ^{13}C NMR data confirmed the success of the reaction, as the peaks representing the ester groups disappeared.

2.3 Conclusions and Future Work

2-Sulfonicotinic acid and 2-hydroxynicotinic acid proved much easier to synthesise than 2-phosphononicotinic acid, though the efficiency of the routes towards these compounds could be improved through further work. Neither of these two compounds proved to be neuroprotective or to antagonise the effects of quinolinic acid during biological testing.

It would be interesting to evaluate the effect of 2-(phosphonomethyl)nicotinic acid under the same conditions. If the compound showed significant effects in any of the tests, either as an antagonist of quinolinic acid, or if the compound is neuroprotective, then a series of 2-phosphonoalkyl substituent compounds could be investigated.

2-Phosphononicotinic acid proved to be elusive, despite the large number of synthetic routes towards the target which were attempted. The oxidation of the 3-methyl group to the acid and methods of isolating the di-acid should be investigated further, as they may hold the key to the successful synthesis.

CHAPTER 3

3. Decarboxylation Studies on the QPRTase System and the Non-enzymic Decarboxylation of *N*-substituted Quinolinic acids

3.1 Introduction

The decarboxylation reaction for the QPRTase catalysed system has not been examined in great detail. It has been assumed to have the same mechanism as proposed for the decarboxylation of pyridine carboxylic acids. Dyson and Hammick were the first to investigate this reaction when they heated quinalidinic and isoquinaldinic acids with an excess of certain high boiling aldehydes and ketones (benzaldehyde, anisaldehyde and benzophenone).[38] These reactions resulted in evolution of carbon dioxide and production of α-pyridyl carbinols (**70**). This was followed by further investigation into the decarboxylation of pyridine carboxylic acids, including picolinic acid, by Ashworth, Daffern and Hammick.[164] Again the carboxylic acids were heated in the presence of high boiling aldehydes and ketones. The connection was made that only when the carboxylic acid group was on the carbon adjacent to the nitrogen was the loss of carbon dioxide observed. No decarboxylation took place with 3- or 4-substituted carboxylic acids.

It was recognised by Hammick that an intermediate involving an ylid (**71**) was produced, and that the rate of decarboxylation varied within the series. A mechanism for the decarboxylation and the subsequent reaction with the aldehyde or ketone was proposed (Scheme 3.1), where decarboxylation to form an ylid was followed by nucleophilic attack on the carbonyl to form the α-pyridyl carbinol.

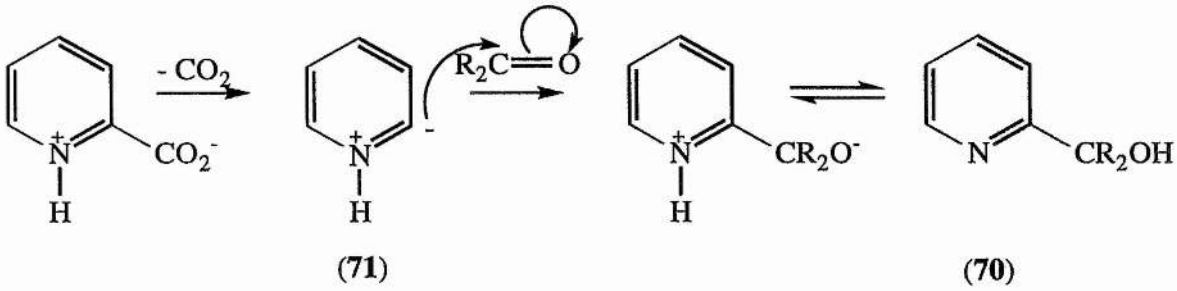

Scheme 3.1: Hammick reaction

Much of the work after Hammick has involved the evaluation of the timing of the proton transfer from the acid group to the nitrogen of the pyridine ring during decarboxylation. The two possibilities were sequential proton transfer and decarboxylation, (Scheme 3.2, path 1), or a concerted reaction, that is the decarboxylation of the neutral acid (Scheme 3.2, path 2). In both reactions there is increased positive charge on the nitrogen, thus reducing the electron density on the α-carbon and facilitating C-C bond cleavage and release of carbon dioxide.

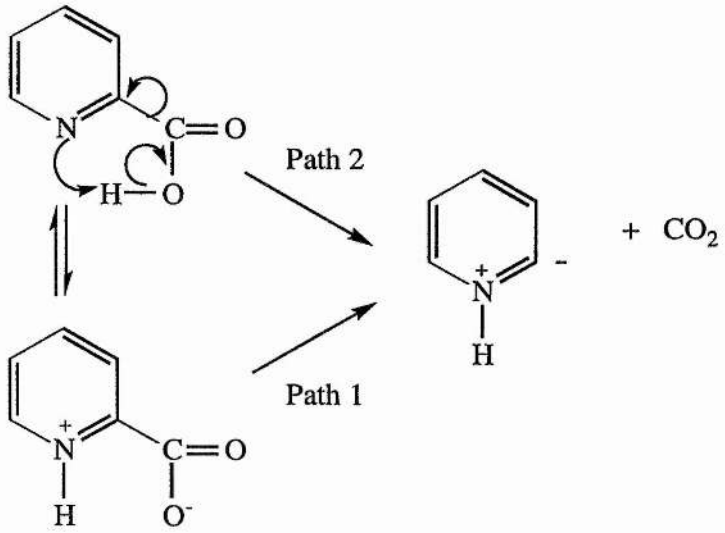

Scheme 3.2: Hammick mechanism

Cantwell and Brown reported the effect of solvents on the rate of decarboxylation of picolinic acid.[165] Both acidic (e.g. phenol) and basic (e.g. aniline) solvents lowered the rate of decarboxylation of picolinic acid. In the case of the acids, competition for the pyridine nitrogen from the pyridine carboxylic acid proton and the solvent acidic proton reduced the concentration of the initial reactant. Therefore higher levels of cation (**72**) present, reduced the amount of zwitterion leading to a slower reaction.

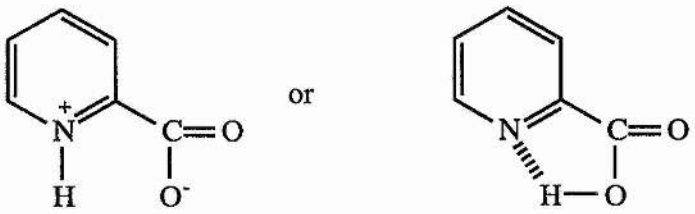

(**72**)

In the presence of base formation of the picolinate anion occurs, which lowers the rate of decarboxylation. Both these results support the theory that decarboxylation occurs through a zwitterion.

3.1.1 Effect of substituents on the pyridine ring

The effect of methyl substituents in the pyridine ring on the rate of decarboxylation of picolinic acid was also investigated.[166] 3-, 4-, 5-, 6-Methyl- and 4,6-dimethyl-picolinic acids (**73-77**) were synthesised and their rate of decarboxylation studied along with that of picolinic acid itself.

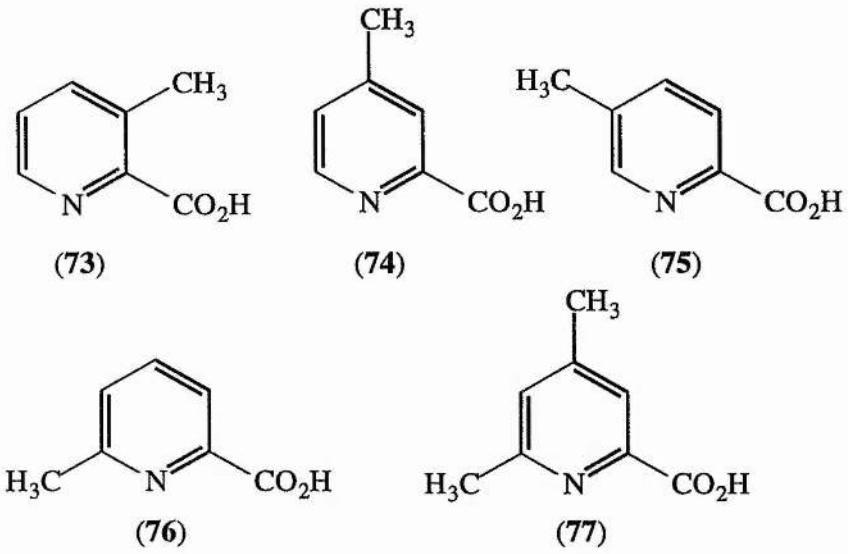

(73) (74) (75)

(76) (77)

When the methyl group is *ortho* or *para* to the nitrogen, inductive electron donation towards the nitrogen should reduce its pull on the α-carbon. This increases the energy required to break the C-C bond and therefore reduces the rate of decarboxylation, as was observed. The methyl groups *meta* to the nitrogen should also donate electrons towards the α-carbon although to a lesser extent, and again reducing the rate, as was observed for 5-methyl picolinic acid. However, 3-methyl picolinic acid produced an anomaly, in that the rate of decarboxylation increased with respect to picolinic acid, due to the steric effect of the presence of the methyl group at position 3.

Further studies on the decarboxylation of picolinic acid were carried out in polar solvents by Clark,[167] and led to the conclusion that the zwitterion was not favoured as the intermediate, but that the chelate form was. Previous studies by Clark also supported this theory.[168] The decarboxylation of picolinic acid in the molten state and polar solvents showed that the effect of these solvents was slight and that the reaction was bimolecular.

Brown and Moser examined the electronic effects in the transition states of the decarboxylation of pyridine-2-carboxylic acids.[37] The rate of decarboxylation of several 6-substituted pyridine-2-carboxylic acids in 3-nitrotoluene was determined. 6-Nitro, chloro, bromo, acetamido, methoxy and amino picolinic acids (**78-83**) were all

synthesised and their rate of decarboxylation used to deduce the structure of the intermediate in the transition state for the reaction.

It was proposed that if either the picolinate anion, or the zwitterion, were the transition states which lead to decarboxylation, then electron withdrawing effects would stabilise the transition states and lead to larger rate constants.

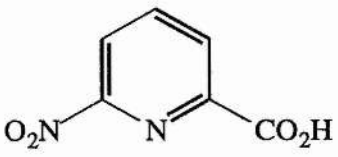

(78)

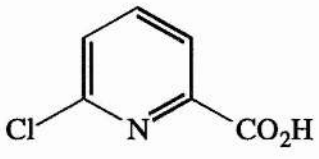

(79)

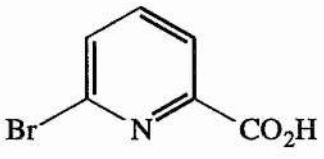

(80)

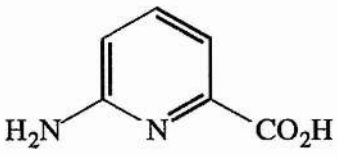

(81)

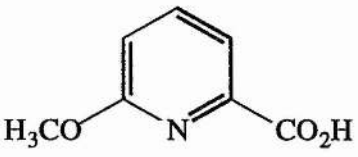

(82)

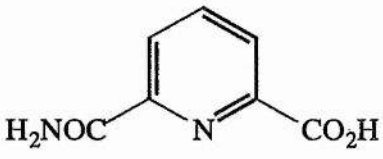

(83)

With a transition state where two events are occurring, i.e. N-H bond formation and C-C bond cleavage, there are three possibilities:

i) C-C bond cleavage leads N-H bond formation;

ii) C-C bond cleavage lags behind N-H bond formation;

iii) Both occur simultaneously.

The argument for the case of ii), where if C-C bond cleavage lags far enough behind N-H formation then a zwitterion is formed, was proposed as two-fold:

i) Amino acids exist in a stable form as zwitterions.

ii) If this were the case, an acid-base reaction would have a higher energy of activation than C-C bond cleavage.

6-Methoxy- and 6-acetamido- picolinic acids were selected to determine whether sterically hindering the lone electron pair on the ring nitrogen would have an effect on the rate of decarboxylation. Both compounds had a much lower rate of decarboxylation

than expected, as rotation of the substituent may be preventing access for the acidic proton to the nitrogen.

Brown and Moser reported that as the electron withdrawing ability of the 6-substituents increased, then the rate of decarboxylation decreased.[37] They also demonstrated that a linear relation existed between the σ values of Cl, Br, H and NO_2 and their rate constants, which indicated that a large positive charge develops in the transition state. This was proposed to be decarboxylation via the chelate intermediate, but with N-H formation slightly ahead of C-C bond cleavage.

Conclusions from Kilikin and Calvo's inhibition studies agree with the nitrogen ylid theory for decarboxylation.[33] The actual degree of inhibition correlated with the degree of ionisation at the 2-position, which implied that the negative charge at this position contributes significantly to tight binding to the enzyme. Kilikin and Calvo proposed that the inhibitor is mimicking the intermediate ylid formed following decarboxylation, but the size of the sulfide anion suggests that it may actually mimic the carboxylate group of the substrate.

3.1.2 Effect of *N*-methyl substituents

Haake and Mantecon investigated the effect of *N*-methyl substitution on the rate of decarboxylation of picolinic acid.[169] In a previous paper on the preparation of *N*-methyl pyridine carboxylic acids it was stated that *N*-methylpicolinic acid (homarine) (**84**) "must not be heated or decomposition takes place" which implied that there was rapid decarboxylation.[170] From this and the discovery that homarine was found to be present in large quantities in invertebrates,[171,172] Haake and Mantecon examined the rate of decarboxylation of picolinic acid derivatives in ethylene glycol at 134 °C.

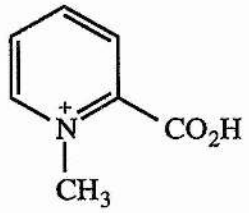

(84)

This work also recognised the studies of Brown and Hammick on the decarboxylation of *N*-methylquinaldinic acid,[173] but questioned the conclusions when it was shown that *N*-methylpicolinic acid decarboxylated 720 times faster than picolinic acid under the same conditions. The ΔH^* was almost 20 kJ mol^{-1} greater than that for picolinic acid, a combination of the increase in electron density on the ring and the electron donating ability of the *N*-methyl moiety.

Haake and Mantecon suggested a strong interaction between the *N*-methyl group and the carboxylic acid group. Any attempt by the methyl group to rotate leads to that interaction being lost. As a result, unlike picolinic acid the decarboxylation of *N*-methylpicolinic acid involves mainly rotational but also some vibrational degrees of freedom being gained going from the ground state to the transition state, increasing the rate of reaction.

This theory also supports the large difference in the rate of decarboxylation found by Brown and Hammick for quinaldinic (**85**) and isoquinaldinic acid (**86**). The carboxylate group in isoquinaldinic acid lies between two electron acceptors - the N-H group and the benzene ring. This raises the energy of the ground state, therefore less energy is required to reach the transition state.

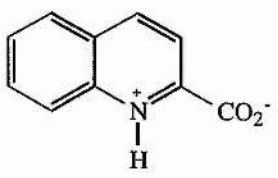

(85)

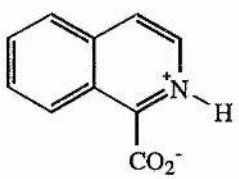

(86)

3.1.3 Other heterocyclic carboxylic acids

The rate of decarboxylation of other nitrogen heterocyclic 2-carboxylic acids was studied by Dunn and co-workers.[174,175] The decarboxylation of pyrrole-2-carboxylic acid (**87**) in aqueous solution at 50 °C, ionic strength 1.0, was studied. It was found to be first order and as the pH decreased from 3 to 1. The rate of decarboxylation increased gradually, but from pH 1 to 10 M hydrochloric acid the rate increased dramatically. The mechanism supported the same theory as proposed by Dunn for the decarboxylation of anthranilic acid (**23**), where the species undergoing the decarboxylation is protonated at the 2-position. At low acidity the rate of protonation is the rate determining step, but at high acidity it is the actual decarboxylation reaction (Scheme 3.3).

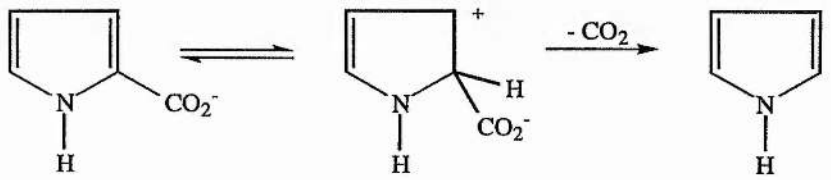

(**87**)

Scheme 3.3: Dunn decarboxylation

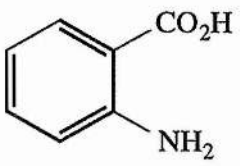

(**23**)

Pyrimidine 2-carboxylic acid undergoes a pseudo-first order decarboxylation. The reaction was studied from pH 2 to H_0 - 9.5, and whilst decarboxylation increased from pH 2 to H_0 - 3, it remained constant thereafter. The examination of pyrimidine-2-carboxylic acid allowed the effect of an electron withdrawing group at position 3 to be studied without the steric influence of a bulky substituent.

The main decarboxylating species is HA, but H_2A also decarboxylates. A Hammick type mechanism may account for this, as the mono-protonated pyrimidine-2-carboxylic acid undergoes the loss of carboxylic acid to form the ylid, which in aqueous solution is converted rapidly to pyrimidine.

3.1.4 Decarboxylation in aqueous solvents

Dunn, Lee and Thimm recognised that all the decarboxylation studies on pyridine 2-carboxylic acids had been carried out in non-aqueous solvents, where ionic species, ylids and zwitterions are not favoured.[176] Therefore the possibility of the cation or anion decarboxylating had not been considered, along with the possibility of electrophilic attack at the carbon, accompanying loss of carbon dioxide. The decarboxylating species can also be determined more accurately through pK_a data. Indeed, the decarboxylation of 6-methylpicolinic acid (**77**), 5-nitropicolinic acid (**88**) and picolinic acid (**7**) at 180 °C, ionic strength 1.0, produced interesting results.

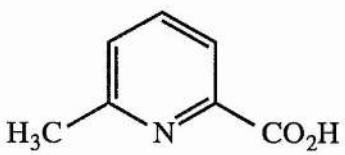

(**77**)

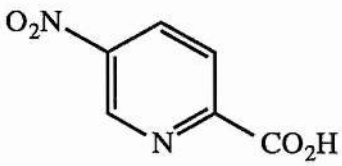

(**88**)

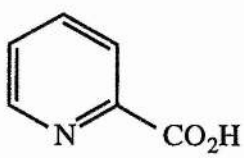

(**7**)

All three had a rate of decarboxylation with a maximum at an intermediate pH, which decreased at higher and lower acidities. The ylid decarboxylation mechanism predicted this result, where the decarboxylating species is isoelectric, although it cannot be proved whether this is correct as neither the pH or pK_a are known at 150 °C.

Significantly the rate constant versus pH profile was unsymmetrical. At low pH the rate decreased very sharply which implied that the cation did not decarboxylate, and that any unionised species did not decarboxylate very well. However, above the maximum, the rate decreased only slowly as the pH increased and above pH 5 was actually constant, at approximately half of the maximum. This unexpected result implied that the anion did decarboxylate. Decarboxylation thus occurred without nitrogen protonation, indicating that either protonation was not important or the isoelectric species contained little zwitterion.

The effect of the substituents was unusual. The 5-nitro group increased the rate of decarboxylation whereas it was decreased by a 6-methyl group, which was the expected result if negative charge developed at the site of reaction, but the effect was much smaller than that seen in the corresponding benzene species. The rate of decarboxylation was also slower than seen in non-aqueous solvents.

3.1.5 Decarboxylation of quinolinic acid

Quinolinic acid is actually the fastest of all the pyridine carboxylic acids so far studied, decarboxylating in aqueous hydrochloric acid (pH 1) at 95 °C with a half life of around 3 days. Quinolinic acid was shown to decarboxylate 500 times faster than picolinic acid or any other pyridine dicarboxylic acid at 95 °C and ionic strength 1.0. Although this is the fastest it is still a very slow rate under very harsh chemical conditions. The effect of the 3-carboxylic acid group seemed to be to disturb the coplanarity of the 2-carboxylic acid group and the aromatic ring, lowering bond order and thus facilitating bond breaking.

3.1.6 Kinetic isotope effect

The ^{13}C kinetic isotope effect on the rate of decarboxylation of quinolinic acid and picolinic acid was investigated. Dunn *et al* postulated that a reaction with rate maximum at the isoelectric pH is explained by either a rate-controlling decarboxylation of the isoelectric species postulated by Hammick,[176] or by the rate dependent step being the protonation of the monoanion. If the former is the case a ^{13}C kinetic isotope effect on the rate should be detected. At both the isoelectric pH and above, a significant carbon isotope effect was observed, implying that C-C bond breaking was the rate determining step for decarboxylation of both the isoelectric species and the anion. At both the isoelectric pH and higher values, the ^{13}C kinetic isotope effect ($100(K_{12}/k_{13}-1)$ was quite large. It was 1.0284 at pH 0, 1.0267 at pH 3.95 for quinolinic acid). The effect was slightly less for the anion for both quinolinic acid and picolinic acid, implying that the zero-point energy difference in the starting material is a smaller fraction of the activation energy for the slower reaction. The size of the effect suggested that C-C bond breaking was well advanced in both the transition states.

3.1.7 Decarboxylation of homarine

As neither 3- or 4- pyridine carboxylic acids decarboxylate, the nitrogen must have a profound effect on decarboxylation. *N*-Methyl picolinic acid (homarine) was studied in aqueous solution to complement the study in ethylene glycol by Haake and Mantecon.[169] Again it did not decarboxylate when unionised, but did when ionised. A rate constant of 1.3×10^{-4} s^{-1} was observed, and compared to a rate constant for the decarboxylation of picolinic acid of 5.0×10^{-7} s^{-1}. Thus, the effect of quaternisation of the picolinate nitrogen was to increase the rate of decarboxylation by around 250-fold, a considerable effect, although not as large as the effect of the presence of the 3-carboxyl group.

As protonation of picolinic acid only doubled the rate of decarboxylation, i.e. the maximum rate compared to the rate of decarboxylation of the anion, it seemed to be reasonable to suggest that protonation actually occurred on the acid, not the nitrogen, so that the decarboxylating species was actually the neutral acid, not the zwitterion. One possibility is that the positive charge on the protonated species was dissipated by solvation of the proton.

This work was followed up by Dunn and Thimm with studies on the decarboxylation of six 3-substituted picolinic acids in aqueous solution.[177] This was to investigate whether the effect of the 3-substituent, which in the case of quinolinic acid had increased the rate of decarboxylation by a factor of 500, was due to electronic, steric or neighbouring group effects.

The six substituted picolinic acids: amino (**89**), benzoyl (**90**), bromo (**91**), hydroxyl (**92**), methyl (**73**) and nitro (**93**) were synthesised and decarboxylated in buffered aqueous solution, ionic strength 1, at 150 °C and 95 °C.

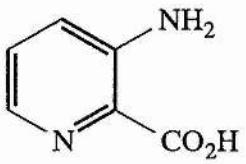

(**89**)

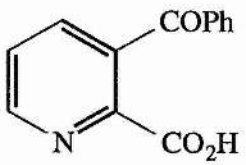

(**90**)

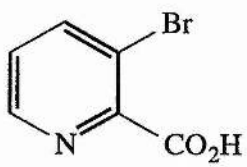

(**91**)

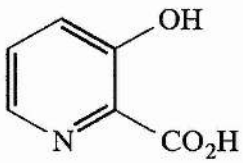

(**92**)

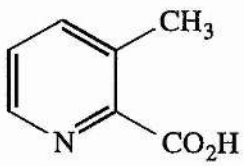

(**73**)

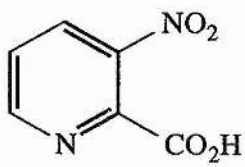

(**93**)

3-Amino and 3-hydroxy picolinic acids produced rate profiles very different to the other compounds. They were both thought to decarboxylate by an alternative mechanism from the others, which probably involved ring protonation, as was the case for the decarboxylation of amino- and hydroxy-benzoic acids.

3-Methylpicolinic acid produced a symmetrical rate profile. The rate maximum occurred at an intermediate pH, but the anion did not decarboxylate at all. The other three all decarboxylated very quickly. Interestingly none of the acids decarboxylated noticeably at high pH (9.2). The fact that electron withdrawing substituents all increased the rate of decarboxylation, despite their varied structures made it unlikely that neighbouring group effects were the main reason for the acceleration. The effect was thought to be partly steric, as 3-methyl picolinic acid increased the rate of decarboxylation, although 5- and 6-methyl picolinic acid retarded the rate.

The main cause however, was determined to be electronic. Although 3-bromo and 3-methylpicolinic acids are of similar size, the 3-bromo analogue showed a much larger rate increase. The electronic effect was more electrostatic than due to delocalisation effects, which is consistent with the mechanism proposed by Hammick. Upon decarboxylation, where negative charge at 2- position of the ylid develops, the transition state can be stabilised by a positive charge at 1 or 3, but cannot be delocalised by resonance structures on 3- or 5- position without the formation of a carbene. The increased rate of decarboxylation of 3-methylpicolinic acid demonstrated that the even more pronounced effect of *N*-methylpicolinic acid to increase the rate was not solely due to the quaternisation of nitrogen, but also due to some steric assistance.

Dunn and Thimm noted that significantly, none of the picolinate anions decarboxylate,[177] and suggested that as all anions, irrespective of the substituent, followed this pattern the effect may have been steric, with the substituent preventing coplanarity between the carboxylate group and the aromatic ring. In the case of the anion, this has a retarding effect, by interfering with the cyclic intramolecular electron shift.

3.1.8 Enzymic Decarboxylation

Understanding the mechanism of other enzyme catalysed decarboxylation reactions should enable analogies to the QPRTase system to be made and shed light on whether the decarboxylation is actually catalysed by the enzyme, and if so by which mechanism.

3.1.8.1 Orotate decarboxylase

The enzyme system which has been researched widely and that gives a very useful model for QPRTase is orotate decarboxylase (ODase). ODase (E.C. 4.1.1.23) is the catalyst for the conversion of orotidine 5'-monophosphate (OMP) (**95**) to uridine 5'-monophosphate (UMP) (**94**) in the final step of the *de novo* biosynthesis of pyrimidine nucleotides. The previous step is the conversion of orotic acid (**96**) to OMP by OPRTase (E.C. 2.4.2.10) (Scheme 3.4).[178]

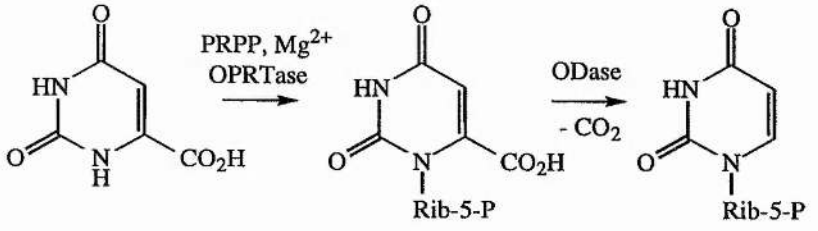

(**96**) (**95**) (**94**)

Scheme 3.4: ODase reaction

Therefore the two enzymes (OPRTase and ODase) catalyse the transfer of a phosphoribosyl group onto a nitrogen of a heterocycle, followed by decarboxylation, the reactions catalysed by the single QPRTase protein.

In their model studies, Beak and Siegel[39] investigated the decarboxylation of 1,3-dimethylorotic acid (**97**) to uracil (**98**) in sulfolane at 206 °C, and obtained a rate

constant of 7.6 x 10^{-4} s^{-1}. It was also shown that as the concentration of base (*N,N*-diethylaniline) increases so does the rate of decarboxylation (Scheme 3.5).

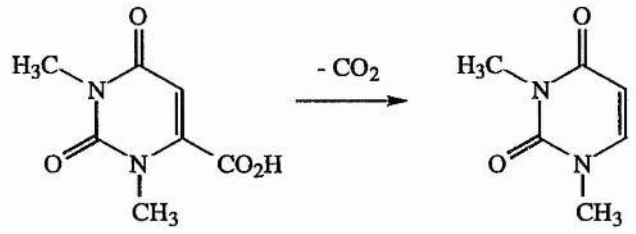

(97) **(98)**

Scheme 3.5: Decarboxylation of 1,3-dimethylorotic acid

The rate of decarboxylation of four other orotic acid analogues was also examined.

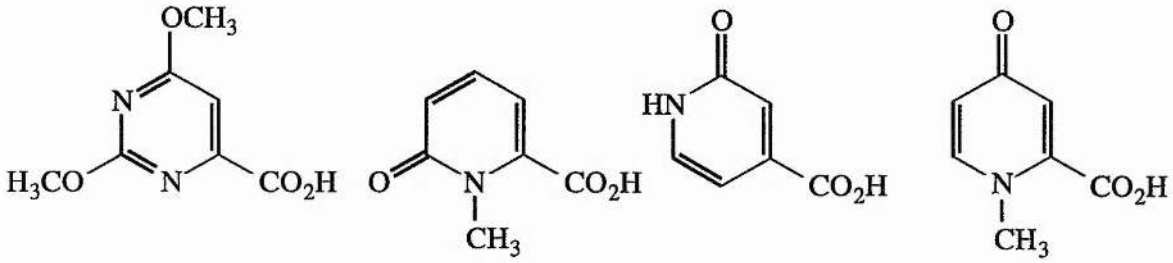

(99) **(100)** **(101)** **(102)**

In the base catalysed decarboxylation, compounds (**100**) and (**102**) can form dipole stabilised carbanions as intermediates, as seen in H-D exchange in pyridones and pyrimidones. However, compounds (**99**) and (**101**) could not form such stabilised species, and therefore did not undergo basic decarboxylation.

In the formally neutral conditions, the decarboxylation of (**99**) involves initial zwitterion formation, followed by a first order decarboxylation reaction to form an nitrogen ylid, which is reprotonated to give the final product. This is analogous to the decarboxylation mechanism of picolinic acid suggested by Haake and Mantecon.[169] Beak and Siegel therefore considered the role of the enzyme was to increase the

concentration of the zwitterion, through interactions at the active site.[39] These two pathways to the decarboxylation are shown below in Scheme 3.6.

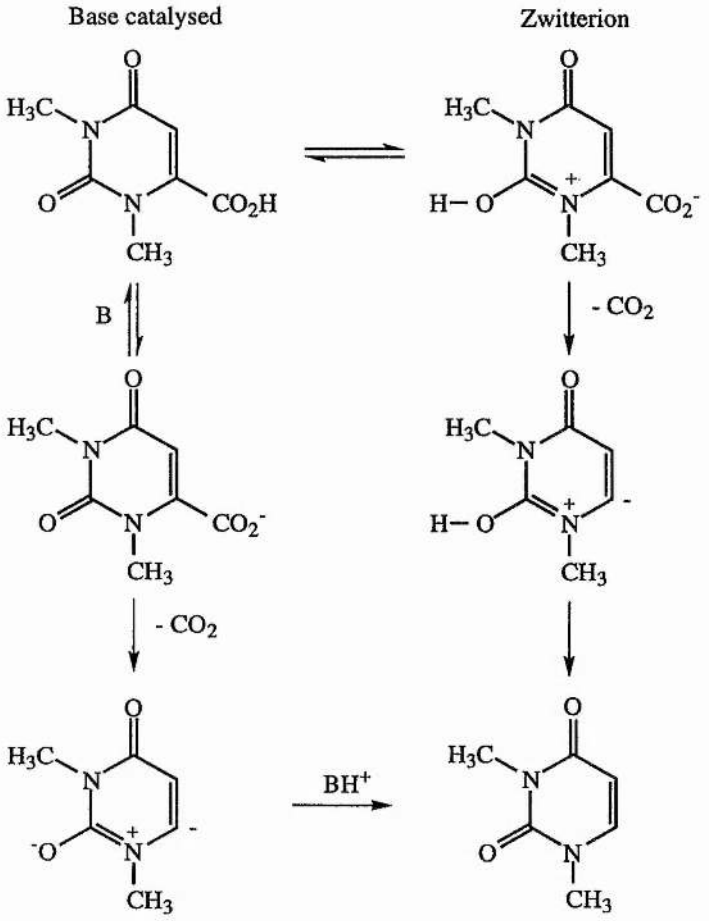

Scheme 3.6: Proposed decarboxylation mechanism

It is interesting to note that 6-aza-UMP (**103**) binds to ODase 10 times stronger than the actual substrate,[179] where electrons in the sp^2 orbital at C-6 can mimic the ylid intermediate, giving support to the zwitterion/ylid mechanism for decarboxylation.

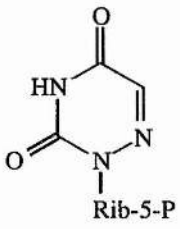

(103)

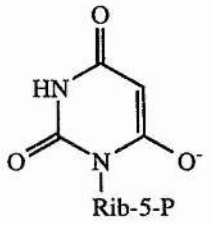

(104)

Levine *et al* demonstrated that barbituric monophosphate (BMP) (**104**) bound to ODase 100000 times more strongly than the actual substrate and that it was one of the strongest inhibitors observed.[40] In the rat brain enzyme it gave a K_i of 4.1 x10^{-9} M at pH 7.4.[180] In fact the inhibitor bound so tightly that the enzyme-inhibitor complex was purified by gel filtration with no dissociation. It was proposed that desolvation of substrate upon binding to the enzyme implied that the active site was hydrophobic, which based on Beak and Siegel's proposed mechanism would facilitate decarboxylation, or that the desolvation could result from electrostatic bonding of the phosphate to a cationic site on the enzyme.

It was also assumed that a negative charge at the 2-position on the pyrimidine ring was essential for binding, hence the affinity for BMP relative to OMP. This was also shown by the reduced inhibition at low pH, which reduces the concentration of ionised BMP. Stabilisation of the zwitterion in Beak and Siegel's proposed mechanism also required an increase in basicity of the position 4 oxygen, therefore the enzyme must have an acidic residue to "push protons" onto the substrate.

Silverman and Groziak proposed a greatly contrasting mechanism for the decarboxylation catalysed by ODase to that of Beak and Siegel.[181] They suggested that, because of the high temperature required in the model studies, a covalent catalytic mechanism was responsible for the decarboxylation reaction. This involved protonation of the acid followed by Michael attack by an active site nucleophile and acid-base catalysed elimination of carbon dioxide, and is shown in Scheme 3.7.

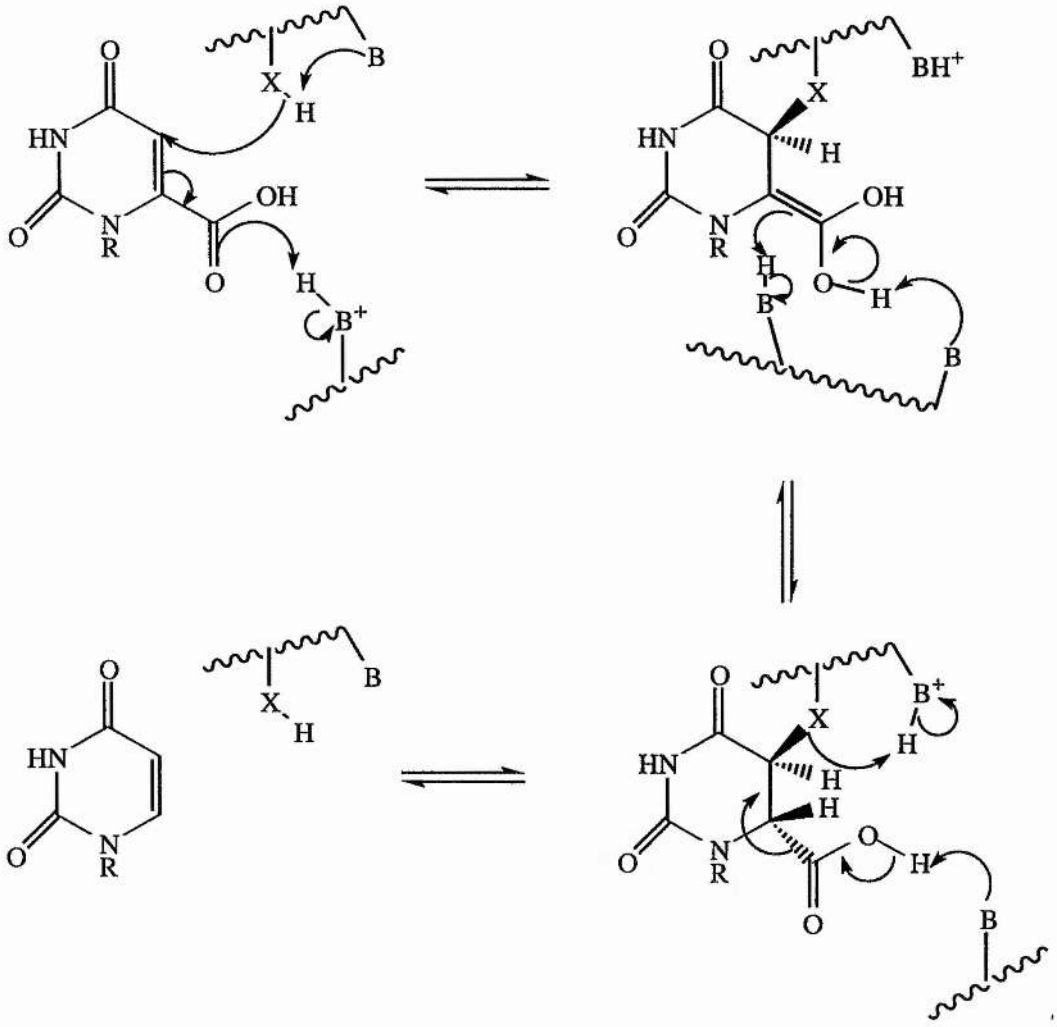

Scheme 3.7: Silverman and Groziak proposed mechanism

This mechanism was appealing to Silverman and Groziak for two main reasons. Firstly, the six acid-base catalytic steps could be controlled by the enzyme to influence the rate of decarboxylation, and also that this type of reaction has precedent in other enzymic reactions.

The two main parts of the reaction were considered independently. The results of Beak and Siegel actually supported the covalent mechanism, in that protonation of the nitrogen activates the substrate for Michael addition and decarboxylative elimination, and that enzyme catalysed protonation of N-6 of 6-azaUMP activated the C-5 position for nucleophilic addition.

To determine which of the suggested mechanisms was most reasonable for the decarboxylation reaction catalysed by ODase, Acheson *et al* reasoned that the NMR resonance at C-5 was important.[182] If nucleophilic attack at C-5 took place, i.e. the Silverman and Groziak theory, then the NMR resonance would shift upfield significantly, as sp^2 to sp^3 geometry change occurred at C-5. With the nitrogen ylid mechanism proposed by Beak and Siegel only a small shift in resonance would be expected as sp^2 hybridisation would be retained at C-5.

In fact only a 0.6 ppm resonance shift downfield was observed, suggesting no change in geometry. This supports Beak and Siegel's theory. Further confirmation came from the replacement of a hydrogen with deuterium at the 5-position. No significant change in rate, i.e. no secondary deuterium isotope effect, was observed, again suggesting no change in geometry.

Decarboxylation of 5-aza UMP, as studied by Shostak and Jones, also supports this theory.[183] As the aza moiety is not electrophilic, nucleophilic attack, proposed by the covalent mechanism, cannot take place, but because 5-azaUMP is a substrate for ODase, the result is consistent with the ylid mechanism.

Replacement of the 2-keto group with a thioketone to produce 2-thioOMP gave a compound that was neither a substrate nor an inhibitor. 5-FluoroOMP acted as a very good substrate, with a K_{cat} thirty times that of OMP probably due to an electronic effect, i.e. stabilisation of the carbanionic transition state by the fluorine.

This work also showed that there was a correlation between the activity of OPRTase with orotate analogues as substrates and ODase with the corresponding OMP analogues. Similarities between the protein sequences of the two enzymes were shown to give 20% homology and 43% similarity, and so a shared evolutionary relationship was proposed. This is interesting when it is related to QPRTase, a single enzyme which catalyses a combination of two reactions catalysed by OPRTase and ODase.

A third possible mechanism was proposed by Lee and Houk, based on quantum mechanics calculations on the energies of the ground states and possible intermediates in the decarboxylation.[184] This showed that in addition to protonation of the 2-oxygen accelerating the rate of decarboxylation, protonation at the oxygen at position 4 gave a very stable intermediate with both zwitterion and neutral carbene resonance structures. It is also predicted that positive charge on N-1 of OMP is not important, leading to studies by Wu *et al* on the role of N-1.[185]

The rate of decarboxylation of 1,3-dimethylorotic acid (**97**) and citrazinic acid (**105**) were compared to evaluate rate enhancement.

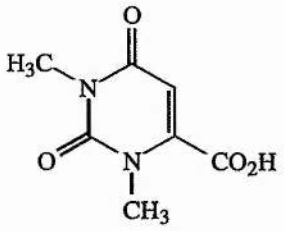

(**97**)

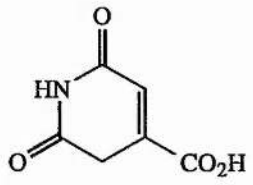

(**105**)

As expected, with the proposed ylid mechanism, 1,3-dimethylorotic acid decarboxylated faster than citrazinic acid, because of the zwitterion betaine formation at N-1. However, the increase in the rate was only a factor of 2 or 3, suggesting that the zwitterion formation was not as important as first thought. Both compounds can transfer protons onto C-4, an important discovery, confirmed as such when the higher basicity of 4-pyridone to 2-pyridone is shown.

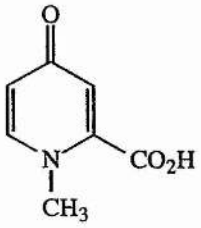

10^3 :

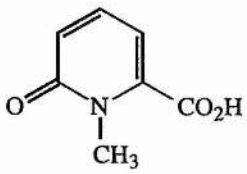

1

In a recent communication, Nakanishi and Wu isolated 6-benzyl-1,3-dimethyluracil (**106**) by trapping the reaction intermediate from the decarboxylation of 1,3-dimethylorotic acid with benzyl bromide.[186] The existence of the intermediate had never been shown, thus this reaction sought to gain insight into the model reaction. The decarboxylation of the acid was carried out in refluxing benzyl bromide, and after 3 hours 6-benzyl-1,3-dimethyluracil was isolated, by column chromatography in 10% yield.

No 6-benzyl-1,3-dimethyluracil was produced when uracil was heated with benzyl bromide, confirming that the product does not come from this reaction. This demonstrated for the first time that the intermediate is a carbon-6 centred nucleophile, and although this supports the carbanion nature of the intermediate, it still does not distinguish between ylid and carbene structures

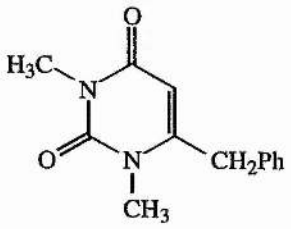

(106)

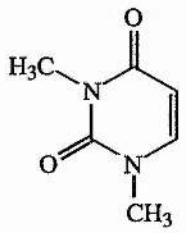

(97)

3.2 The QPRTase system

It can be seen that there is a good body of work on the decarboxylation of pyridine-2-carboxylic acids. However, this still falls short of providing information on the QPRTase catalysed decarboxylation of quinolinic acid mononucleotide, the intermediate in the QPRTase catalysed reaction. Also, even though there is mechanistic work on the related ODase, there is no clearly defined mechanism.

The aim of this study is to further investigate the uncatalysed decarboxylation of *N*-substituted quinolinic acids. The eventual aim is to examine the decarboxylation of quinolinic acid mononucleotide, the real intermediate in the QPRTase reaction. Kinetic studies of this reaction would provide very useful data, enabling a direct comparison to the enzymic reaction to be made. Any mechanistic differences would be observed and it may be possible to decide whether the reaction is actually enzyme catalysed, or spontaneous.

3.2.1 Decarboxylation studies on *N*-Alkyl quinolinic acids

Investigation of the pH versus rate profile for the decarboxylation of *N*-alkyl quinolinic acids was the obvious place to start in the investigation of substituents on the nitrogen of quinolinic acid. In particular the first two to be investigated were *N*-methylquinolinic acid (**107**) and *N*-ethylquinolinic acid (**108**).

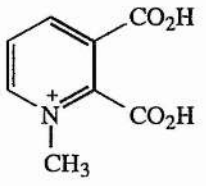

(107)

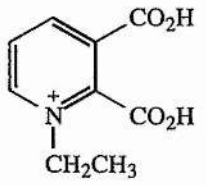

(108)

3.2.2 Synthesis

Both *N*-methylquinolinic acid and *N*-ethylquinolinic acid were synthesised in an identical manner (Scheme 3.8). Initially, the diethyl ester of quinolinic acid (**109**) was prepared by refluxing the acid in ethanol and hydrochloric acid for 24 hours. A crude oil was then distilled under Kugelrohr conditions to produce a colourless oil in 83% yield. Alkylation was achieved by heating diethyl quinolinate and a slight excess of the corresponding alkyl sulfate gently under a nitrogen atmosphere. The reactions were followed by tlc (Silica; 3:2 40/60 petroleum ether: ethyl acetate) and upon completion excess dialkyl sulfate was removed.

In the case of diethyl *N*-methylquinolinate methyl sulfonate, a white solid was formed upon cooling, in 83% yield. This was recrystallised from boiling methanol, and the structure of the white crystals produced confirmed by ^{1}H and ^{13}C NMR. The diethyl *N*-ethylquinolinate ethylsulfate was obtained as an oil.

The esters were then hydrolysed by refluxing with concentrated hydrochloric acid. The free acids were obtained as white solids on the removal of excess acid. When recrystallised from boiling water, white crystals of *N*-methylquinolinic acid and *N*-ethylquinolinic acid were produced in good yields of 81% and 76% respectively.

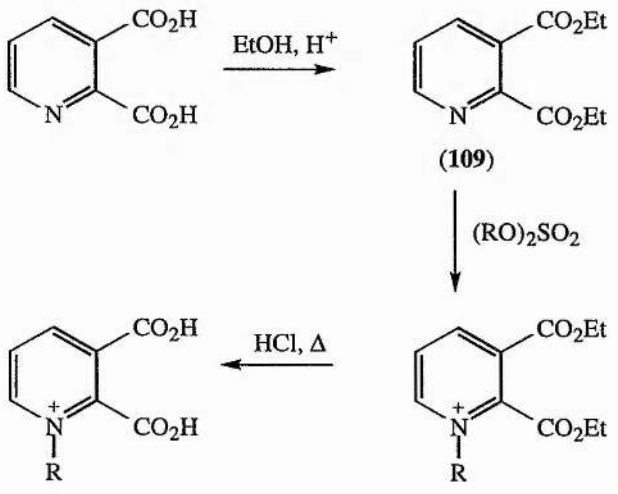

Scheme 3.8: Synthesis of *N*-alkylquinolinic acids

Interestingly, microanalysis data indicated that *N*-methylpyridinium-2,3-dicarboxylic acid and *N*-ethylpyridinium-2,3-dicarboxylic acid were actually present in the zwitterionic monohydrate form shown below.

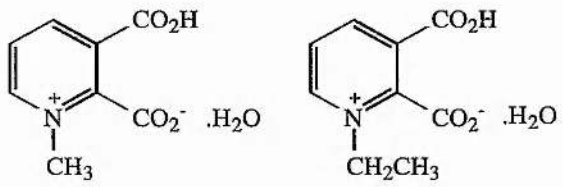

The decarboxylation products of *N*-methylpyridinium-2,3-dicarboxylic acid and *N*-ethylpyridinium-2,3-dicarboxylic acid, *N*-methylnicotinic acid (**110**) and *N*-ethylnicotinic acid (**111**), were synthesised in a similar manner (Scheme 3.9). These compounds were important reference compounds for the kinetic studies.

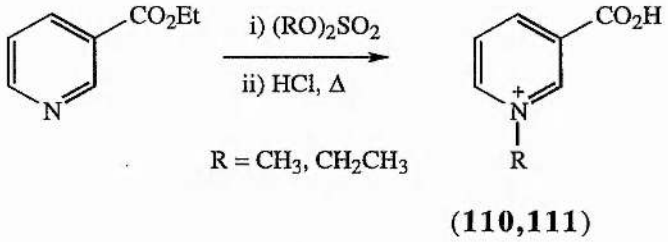

Scheme 3.9: Synthesis of *N*-alkylnicotinic acids

In addition, *N*-methylpicolinic acid (**84**) and *N*-ethylpicolinic acid (**112**) were also synthesised in a similar manner (Scheme 3.10).

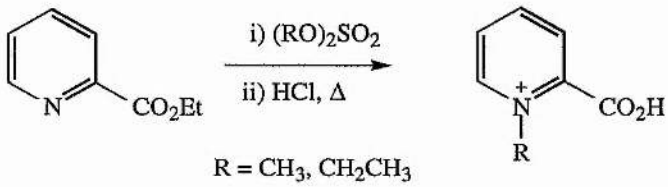

Scheme 3.10: Synthesis of *N*-alkylpicolinic acids

Microanalysis data showed that *N*-methylpicolinic acid and *N*-methylnicotinic acid both crystallised as the hydrogensulfate salts (*N*-methylpicolinium hydrogensulfate, *N*-ethylnicotinium hydrogensulfate). Confirmation came from the titration of known concentrations of the acids against aqueous base.

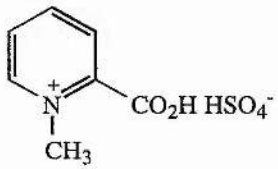

(84)

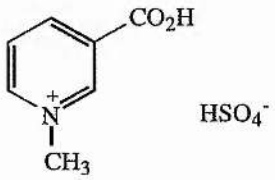

(110)

3.2.3 Kinetics studies on *N*-methylquinolinic acid and *N*-ethylquinolinic acid

The kinetics of the decarboxylation of *N*-methylpyridinium-2,3-dicarboxylic acid monohydrate and *N*-ethylpyridinium-2,3-dicarboxylic acid monohydrate were then investigated. An effective rate constant versus pH profile for both compounds was measured. This enabled determination of the effect of changes in hydrogen ion concentration on the rate of decarboxylation, and to compare the profile with that seen in previous studies on the rate of decarboxylation of other pyridine carboxylic acids. This included the work on the decarboxylation of *N*-methylpyridine carboxylic acids, in particular *N*-methylpicolinic acid, by Haake and Mantecon,[169] and Dunn and co-workers[176] on the rate profile of the decarboxylation of other heterocyclic 2-carboxylic acids and some substituted *N*-methylpicolinic acids.

From these rate profiles, the effect of increasing the size of the substituent on the nitrogen was examined, by comparing the rate of decarboxylation of *N*-methylquinolinic acid and *N*-ethylquinolinic acid under the same conditions.

The effect of temperature on the rate of decarboxylation of *N*-ethylquinolinic acid was also investigated. Rate constant versus pH profiles over a range of temperatures were measured. From these results, the activation energy for the decarboxylation reaction of *N*-ethylquinolinic acid was calculated.

Rate constant versus pH profiles have also been measured over a range of ionic strengths, to assess the effect of increasing the cation concentration on the rate of decarboxylation.

In solution many forms of the salt are present, therefore the salts are referred to as *N*-methylquinolinic acid and *N*-ethylquinolinic acid.

3.2.3.1 Method

The decarboxylation reactions were followed using methods similar to those of Dunn *et al.*[176] The crucial element is that the reactions could be followed directly by UV spectroscopy. Each of the pyridine carboxylic acids and their decarboxylation products absorb at different wavelengths in the ultra violet spectrum. Thus the change in absorbance at a particular wavelength can be followed over time. A suitable wavelength has to be chosen for each substrate by comparison of the starting material and the authentic decarboxylation product in basic solution. The wavelength chosen for both *N*-methylquinolinic acid and *N*-ethylquinolinic acid was 280 nm.

The correct choice of buffer for the decarboxylation reactions is also very important. The buffer must not absorb significantly in the ultra violet spectrum, and must not be affected by changes in temperature, as the reactions were carried out at high temperatures (90 ± 0.1 °C). For this reason the buffers employed were hydrochloric acid, 1 M sodium hydroxide solution and 50 mM potassium phosphate solution.

As the reactions were carried out at high temperatures, a problem was envisaged with evaporation. To eliminate this, the reactions were carried out in sealed ampoules. Thus, the acid to be studied was dissolved in the correct buffer. For measurements below pH 2.5, the acid was dissolved in distilled water, and potassium chloride added to adjust to constant ionic strength. Concentrated hydrochloric acid was added to adjust the pH to the required value and distilled water added to make up to 25 ml. The pH was checked again.

For pH 2.5 and 3.0 the same procedure was followed, except that 50 mM potassium phosphate solution replaced the distilled water. For pH values above 3.0, the acid was dissolved in 50 mM potassium phosphate solution, but the pH adjusted to the correct value with 1 M sodium hydroxide solution.

Aliquots of the solution (1 ml) were then placed into ampoules, these ampoules sealed, and then thermostatted at 90 ± 0.1 °C. At various time intervals, two ampoules were removed from the thermostatted vessel, chilled, and for each solution, 0.6 ml diluted into 10 ml of 1 M sodium hydroxide. The UV absorbance spectra of each was then measured at 280 nm at 25 °C and an average value taken.

Figure 3.1 shows the UV absorbance spectra for *N*-methylquinolinic acid at pH 2 (0 hours), and after 48 hours, where decarboxylation was complete and *N*-methylnicotinic acid produced.

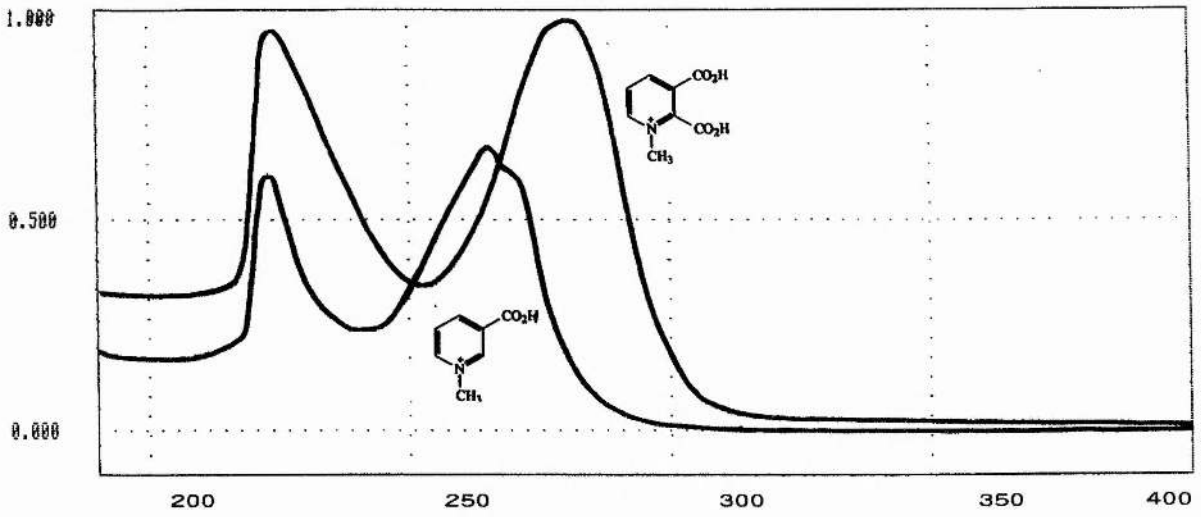

Figure 3.1: UV absorbance spectra for *N*-methylquinolinic acid and *N*-methylnicotinic acid at pH 2.

As reactions were carried out under pseudo first order conditions, values of k_{obs} could be obtained from plots of ln (A_{280} - A) versus time. A is the absorbance at 280 nm when the reaction is completed, and was obtained by measuring the absorbance at 280 nm due to the decarboxylation product at the same concentration as the compound investigated. As the reactions were carried out under pseudo-first order conditions, a straight line is obtained when the graph of time versus ln (A_{280} - A) is drawn. The gradient of this straight line represents the first order rate constant. Table

3.1 shows the results from a typical kinetic run for *N*-ethylquinolinic acid at pH 1.0, while Graph 3.1 represents the plot of ln (A_{280} - A) versus time.

time (s x10^3)	A_{280}	A_{280} - A	ln(A_{280} - A)	Average
0	0.968	0.773	-0.257	-0.261
	0.963	0.768	-0.264	
3.6	0.852	0.657	-0.420	-0.436
	0.831	0.636	-0.453	
7.2	0.718	0.523	-0.648	-0.648
12.6	0.694	0.499	-0.695	-0.704
	0.685	0.490	-0.713	
14.4	0.648	0.453	-0.792	-0.831
	0.613	0.418	-0.872	
18.0	0.570	0.375	-0.981	-0.973
	0.576	0.381	-0.965	
21.6	0.557	0.362	-1.016	-1.049
	0.534	0.339	-1.082	
27.0	0.470	0.275	-1.291	-1.277
	0.478	0.283	-1.262	
32.4	0.394	0.199	-1.614	-1.612
	0.395	0.200	-1.609	
37.8	0.370	0.175	-1.743	-1.743

Table 3.1: Typical kinetic run for decarboxylation of *N*-ethylquinolinic acid pH 1.0

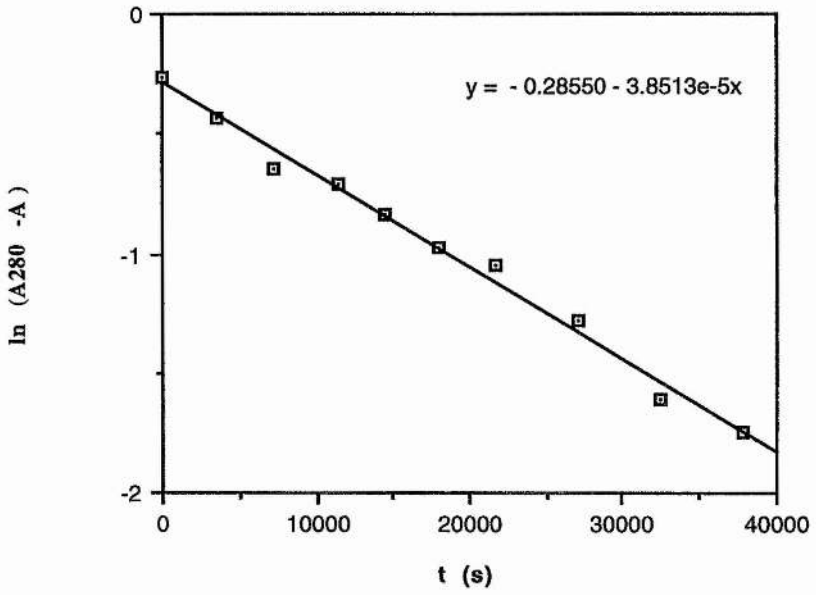

Graph 3.1: Typical kinetic run for decarboxylation of *N*-ethylquinolinic acid pH 1.0

It was necessary to establish that the reaction taking place was indeed the proposed decarboxylation reaction. Thus for both *N*-methylpyridinium-2,3-dicarboxylate and *N*-ethylpyridinium-2,3-dicarboxylate ampoules were incubated at 90 ± 0.1 °C for greater than 10 half-lives. The UV spectra were then measured as before and compared with those of the authentic products under identical conditions. These gave, within experimental error, identical UV spectra showing that the corresponding nicotinic acid had been formed in quantitative yield. Other samples from kinetic runs, left for greater than 10 half-lives were evaporated at reduced pressure and the residues examined by both ^{1}H and ^{13}C NMR spectroscopy. The observed spectra were identical to those of authentic products. There was no evidence for any by-products.

3.2.3.2 Effect of *N*-alkyl substituents on the rate of decarboxylation of quinolinic acid

The effect of introducing a methyl group onto the nitrogen of picolinic acid was investigated by Haake and Mantecon,[169] who demonstrated that *N*-methylpicolinic acid decarboxylated 700 times faster than picolinic acid under the same conditions (See Section 3.1.2).

Quinolinic acid decarboxylated 500 times faster than picolinic acid under the same conditions, the effect of the 3-carboxylic acid group being to disturb the planarity of the 2-carboxylic acid group and the aromatic ring, lowering bond order and thus facilitating bond breaking.

However, the effect of *N*-substitution on the rate of quinolinic acid decarboxylation has not been determined.

3.2.3.2.1 *N*-Methylquinolinic acid

The rate of decarboxylation at 90 °C of *N*-methylquinolinic acid was determined at several pH values from 0.5 to 5.0 to produce an extensive pH rate profile. Table 3.2 represents the overall data for the profile, which can be seen in graphical form in Graph 3.2.

pH	k_{obs} (10^{-5} s^{-1})	Average rate (10^{-5} s^{-1})
0.5	2.242 ± 0.076 2.086 ± 0.078 2.564 ± 0.150	2.297 ± 0.211
1.0	2.892 ± 0.226 2.521 ± 0.127	2.706 ± 0.186
1.5	2.681 ± 0.082 2.916 ± 0.132 2.995 ± 0.153	2.864 ± 0.183
2.0	2.260 ± 0.097 2.195 ± 0.145	2.228 ± 0.033
2.5	0.675 ± 0.017 0.871 ± 0.034	0.773 ± 0.098
3.0	0.251 ± 0.015 0.282 ± 0.011	0.267 ± 0.016
4.0	0.121 ± 0.007 0.135 ± 0.011	0.128 ± 0.007
5.0	0.043 ± 0.003	0.043 ± 0.003

Table 3.2: pH versus rate profile for the decarboxylation of *N*-methylquinolinic acid at 90 ± 0.1 °C

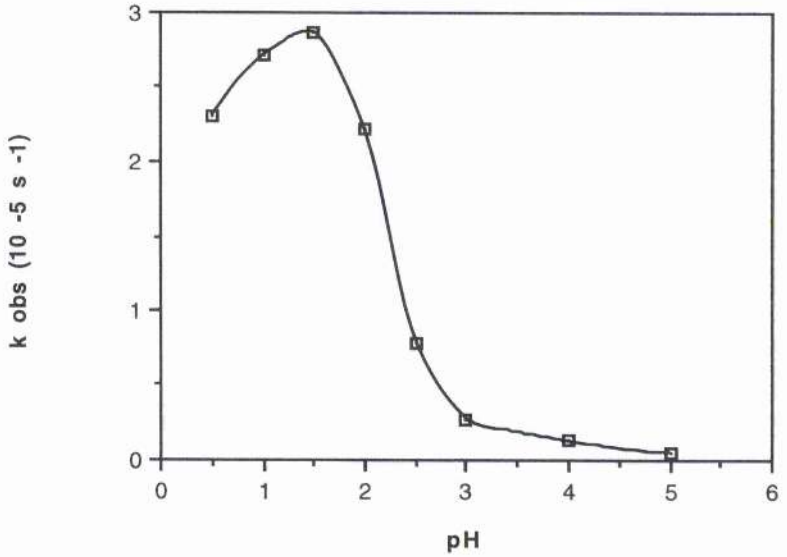

Graph 3.2: pH versus rate profile for the decarboxylation of *N*-methylquinolinic acid

From the Graph it can be seen that the rate of decarboxylation increases to a maximum of 2.86 x 10^{-5} s^{-1} at pH 1.5. This implied that the cation did decarboxylate, but at a much slower rate than the species that decarboxylated the fastest, the isoelectronic species.

Above pH 1.5, the rate of decarboxylation decreases sharply, down to a rate of 4.32 x 10^{-7} s^{-1} at pH 5.0. The shape of the graph is unlike that shown by Dunn *et al.* In that case decarboxylation was constant and independent of pH above 5.0, at a rate of about half the maximum. For *N*-methylquinolinic acid at pH 5.0, the rate is about 60 times less than that at the maximum rate. Although the curve appeared to flatten off, the rate of decarboxylation still decreased as pH increased. At pH 4.0 the rate of decarboxylation was 1.28 x 10^{-6} s^{-1} and at pH 5.0 it was 4.32 x 10^{-7} s^{-1}. It was only because the rates were very slow, compared to the rate at pH 1.5, that the differences between these two pH values was not obvious. This made it likely that the anion did not decarboxylate as the concentration of the anion increases with increasing pH.

Graph 3.3 shows the rate of decarboxylation of *N*-methylquinolinic acid, with the pH versus rate constant profile of picolinic acid, at 150 °C, ionic strength 1.0, overlaid. The maximum rate of decarboxylation of picolinic acid in water is 1 x 10^{-6} s^{-1} and above pH 5.0 it is constant at approximately half the maximum rate.

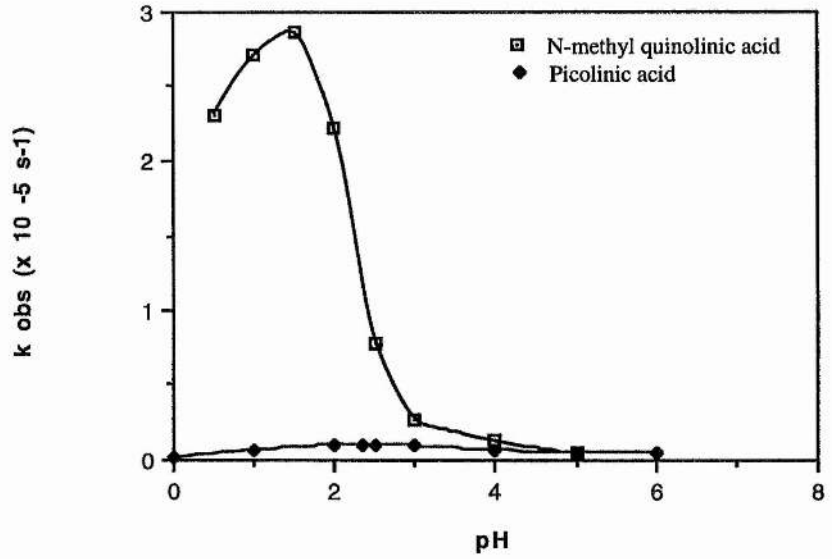

Graph 3.3: pH versus rate profile for the decarboxylation of *N*-methylquinolinic acid and picolinic acid

The pH versus rate profile for quinolinic acid at 95 °C, ionic strength 1.0 from pH 0.08 to pH 4.0 is shown in Graph 3.4 and compared to that for *N*-methylquinolinic acid.

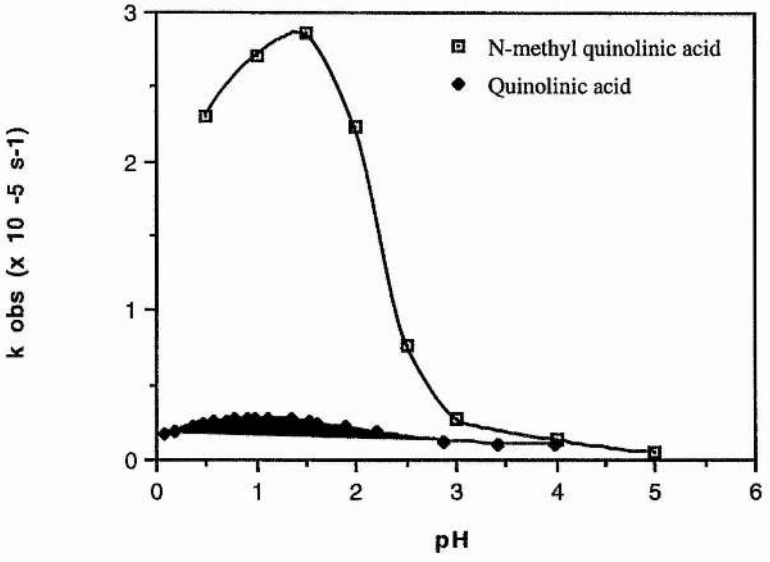

Graph 3.4: pH versus rate profile for *N*-methylquinolinic acid and quinolinic acid

The maximum value for the rate constant for quinolinic acid is 2.74 x 10^{-6} s^{-1} at pH 1.5. Thus the effect of introducing a methyl group onto the nitrogen of quinolinic acid was to increase the rate of decarboxylation by a factor of 10. As described before, the methyl group presumably interacts with the carboxylic acid group at position 2. If the methyl group attempts to rotate out of the plane of the ring, then this interaction is lost.

3.2.3.2.2 *N*-Ethylquinolinic acid

The pH versus rate profile was repeated for *N*-ethylquinolinic acid. In addition the rate constant was measured at pH 0.1 and pH 0.25, to further investigate the decarboxylation. Table 3.3 represents the data for the rate constant at the range of pH values studied, which can be seen in graphical form in Graph 3.5, where it is compared to the rate profile of *N*-methylquinolinic acid under identical conditions.

pH	k_{obs} (10^{-5} s^{-1})	Average rate (10^{-5} s^{-1})
0.1	1.465 ± 0.048	1.465 ± 0.048
0.25	2.562 ± 0.059 2.490 ± 0.070	2.526 ± 0.036
0.5	3.029 ± 0.060 3.383 ± 0.192 3.209 ± 0.078	3.207 ± 0.178
1.0	3.916 ± 0.157 3.958 ± 0.143 4.010 ± 0.248	3.961 ± 0.045
1.5	4.412 ± 0.180 4.608 ± 0.121 3.591 ± 0.120	4.204 ± 0.613
2.0	3.458 ± 0.079 3.074 ± 0.056 3.298 ± 0.085	3.277 ± 0.203
2.5	1.415 ± 0.033 1.661 ± 0.039 1.405 ± 0.036	1.494 ± 0.167
3.0	0.626 ± 0.039 0.675 ± 0.030 0.961 ± 0.025 0.474 ± 0.007	0.684 ± 0.227
4.0	0.082 ± 0.006 0.086 ± 0.004	0.084 ± 0.002
5.0	0.067 ± 0.004 0.069 ± 0.003	0.068 ± 0.001

Table 3.3: pH versus rate profile for the decarboxylation of *N*-ethylquinolinic acid

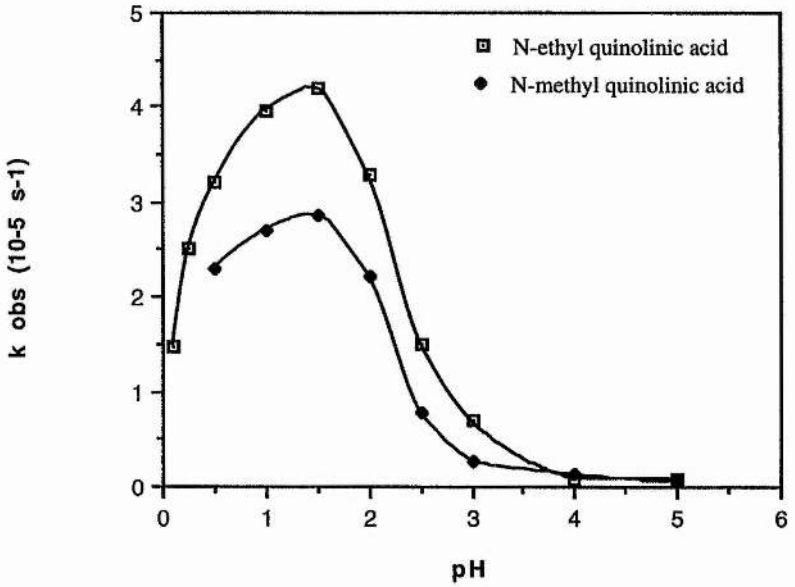

Graph 3.5: pH versus rate profile for the decarboxylation of *N*-methylquinolinic acid and *N*-ethylquinolinic acid

The most obvious point to note is that the effect of increasing the size of the alkyl group as substituent on the nitrogen from a methyl to an ethyl group was to increase the rate of decarboxylation by a factor of approximately 1.5. Presumably rotation of the $-CH_3$ portion of the ethyl group led to greater interaction between it and the carboxylic acid group, increasing the rate of decarboxylation.

The same pattern over the whole of the pH range was demonstrated for *N*-ethylquinolinic acid as was seen for *N*-methylquinolinic acid. For *N*-ethylquinolinic acid the maximum rate of decarboxylation was 4.20×10^{-5} s^{-1}, at pH 1.5. Below the rate maximum, the rate of decarboxylation decreased sharply in the range studied, which implied that the cation did not decarboxylate significantly. The rate also decreased sharply above the rate maximum pH. Again the curve flattened off at pH greater than 4.0, and for *N*-ethylquinolinic acid the rate of decarboxylation at pH 5.0 was again approximately 60 times slower than that at pH 1.5.

3.2.3.3 Kinetics

Dunn *et al* postulated that neither the rate profiles nor isotope effects require protonation at the α-C prior to the decarboxylation reaction.[176] The mechanism is shown below (Scheme 3.11), where unimolecular decomposition of the isoelectric species (HA), as demonstrated by Hammick, and the monoanion (A^-), occurs.

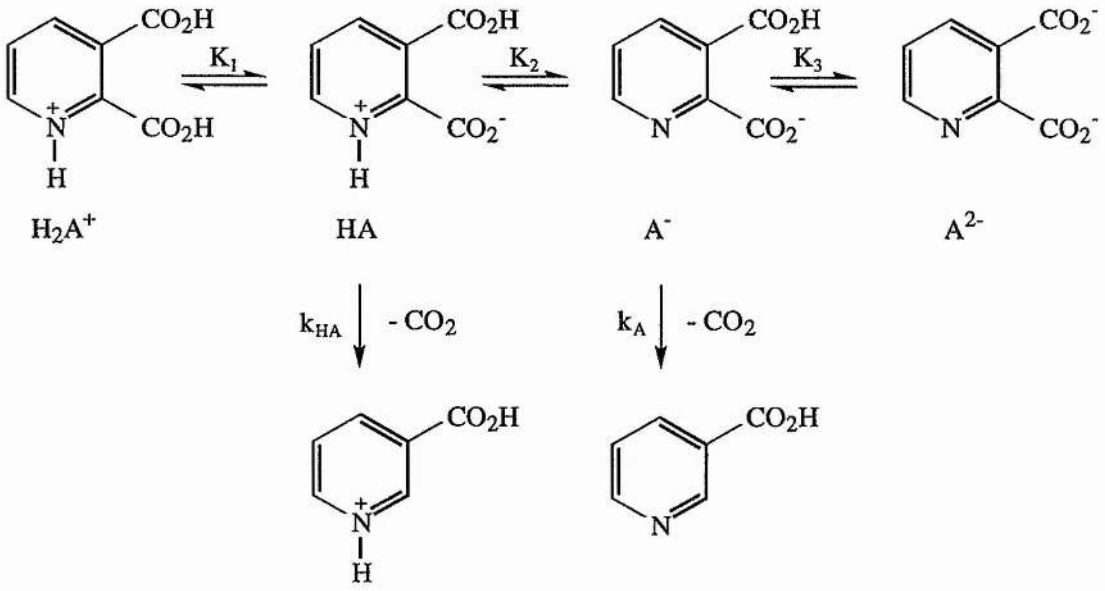

Scheme 3.11: Dunn postulation

Both HA and A^- exist in three isoprotonic forms, any of which can decarboxylate without affecting the pH profile. At the pH levels where the rate was measured, the concentration of dianion was very low, therefore A^{2-} can be omitted from the rate equation.

Therefore if $[C] = [H_2A^+] + [HA] + [A^-]$ = stoichiometric [pyridine carboxylic acid], then:

$$\frac{d[CO_2]}{dt} = k_{HA}[HA] + k_A[A^-]$$

$$= \frac{k_{HA} + \frac{k_A K_2}{[H^+]}}{\frac{[H^+]}{K_1} + 1 + \frac{K_2}{[H^+]}} [C] = k_{obs}[C] \qquad [1]$$

As k_A is much less than k_{HA}, K_2 can be neglected at pH < 0.9, simplifying the approximate equation to:

$$\frac{1}{k_{obs}} = \frac{[H^+]}{k_{HA}K_1} + \frac{1}{k_{HA}} \qquad [2]$$

From this equation values for k_{HA} and K_1 can be deduced. If this deduction is valid, then for pH > 1, equation [1] will reduce to:

$$k_{obs}([H^+] + K_{2)}) = k_{HA}[H^+] + k_A K_2 \qquad [3]$$

A similar mechanistic scheme to that postulated by Dunn can be envisaged for *N*-alkylquinolinic acids (Scheme 3.12).

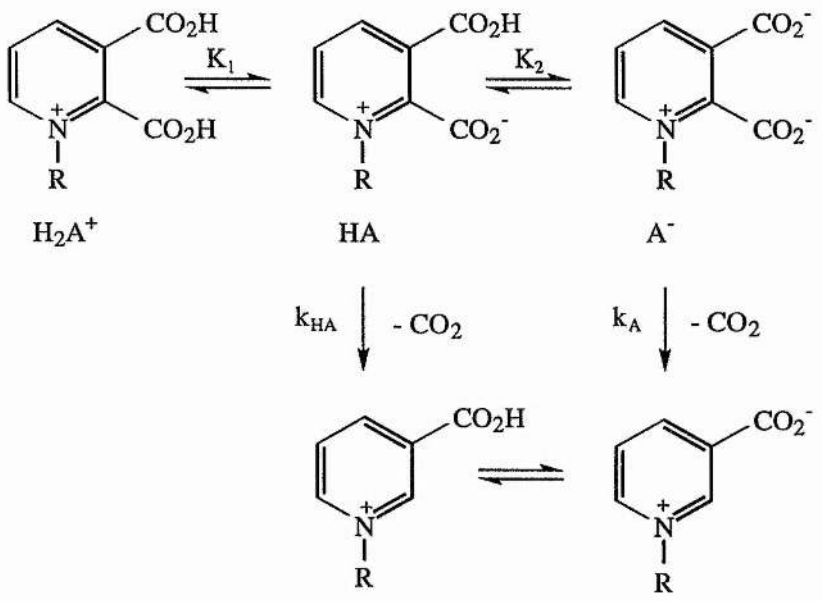

Scheme 3.12: Mechanistic postulation for *N*-alkylquinolinic acids

Using the equation [2], and the data obtained for *N*-ethylquinolinic acid at 90 °C, ionic strength 1.0, Graph 3.6 can be produced for pH < 0.9. Although there are only a few points, a linear relationship is shown. From the graph, it is calculated that for *N*-ethylquinolinic acid $k_{HA} = 4.58\ 10^{-5} \pm 1.6 \times 10^{-7}\ s^{-1}$, and $K_1 = 0.70 \pm 0.04$ ($pK_1 = 0.15$).

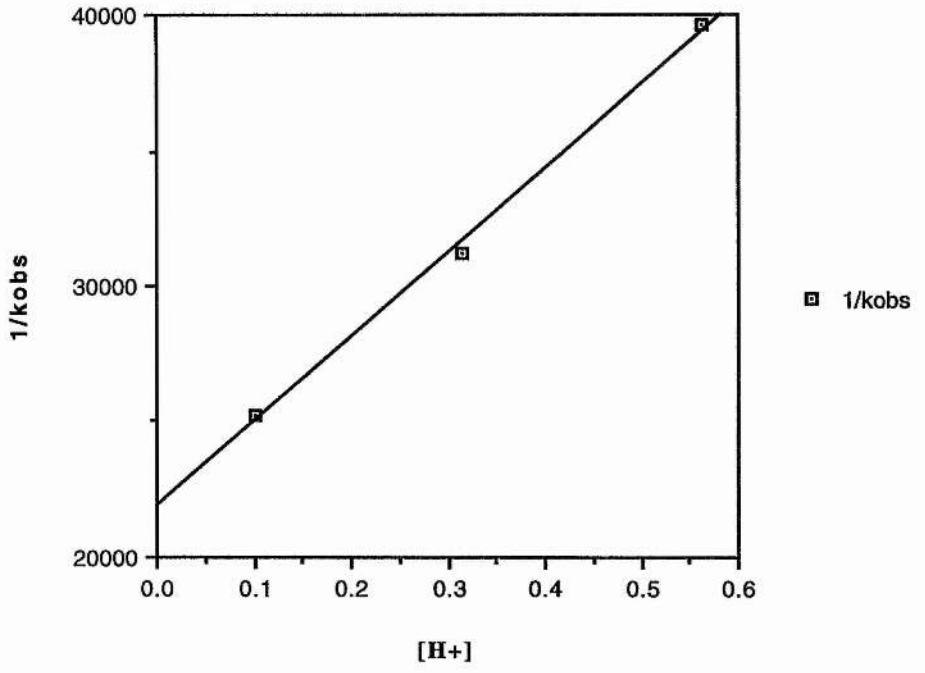

Graph 3.6: Plot to evaluate for k_{HA} and K_1 for *N*-ethylquinolinic acid.

Similarly, this was also calculated for *N*-methylquinolinic acid (Graph 3.7), although only two points are available, making the calculation only an approximation. For *N*-methylquinolinic acid at 90 °C, ionic strength 1.0, it is calculated that $k_{HA} = 2.95 \times 10^{-5}$ s^{-1}, and $K_1 = 0.90$ ($pK_1 = 0.05$).

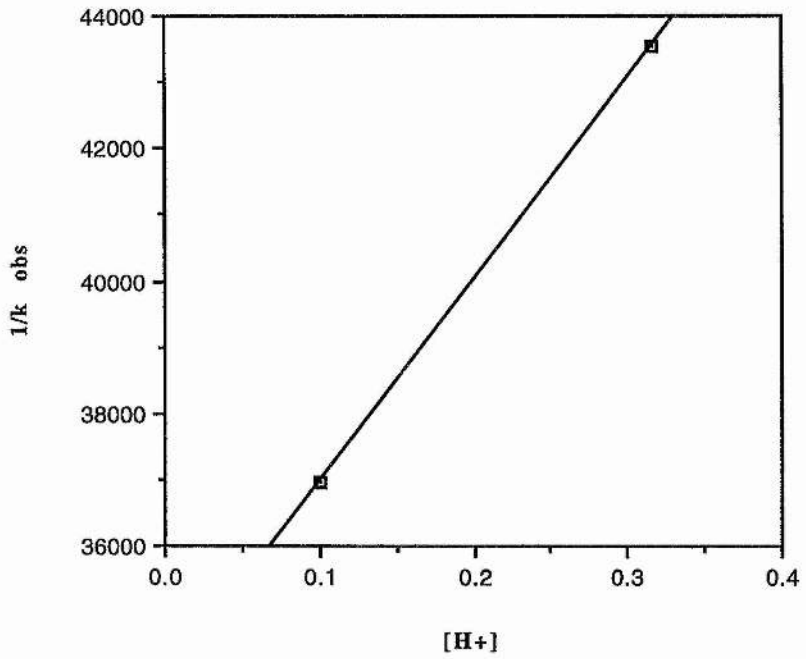

Graph 3.7: Plot to evaluate for k_{HA} and K_1 for *N*-methylquinolinic acid.

This data can be compared to the values of $k_{HA} = 3.30 \times 10^{-6}\ s^{-1}$ and $K_1 = 0.70$ ($pK_1 = 0.15$) for quinolinic acid at 90 °C, ionic strength 1.0. The differences between the k_{HA} values for the three compounds correspond to the observations, seen earlier, of the relative rate constants. The rate of decarboxylation of *N*-ethylquinolinic acid in particular is seen to be much faster.

The values of K_1 for *N*-ethylquinolinic acid and *N*-methylquinolinic acid are quite similar. This might be expected as the increase in size from the methyl group to the ethyl group should not have much effect on the dissociation of the 2-carboxylic acid.

As noted earlier the pH versus rate of decarboxylation profile for *N*-methylpicolinic acid flattens off, i.e. once the acid is ionised, decarboxylation is independent of pH. However it can be seen that for *N*-methylquinolinic acid and *N*-ethyl quinolinic acid the rate of decarboxylation decreases significantly as the

concentration of the carboxylate dianion increases. One possible explanation for this observation is that the negative charge is not well stabilised in the intermediate. This is analogous to that seen for picolinic acid and quinolinic acid.

Equation [3] can be rearranged in order to calculate k_A and K_2:

$$k_{obs} = \frac{(k_{HA}-k_{obs})[H^+]}{K_2} + k_A \qquad [4]$$

Due to the nature of the pH profile of *N*-methyl and *N*-ethylquinolinic acid, in that past the maximum, the rate decreases slowly then sharply, k_A and K_2 were evaluated at pH > 2.5. Graphs 3.8 and 3.9 show plots from equation [4] for *N*-methyl and *N*-ethyl quinolinic acid.

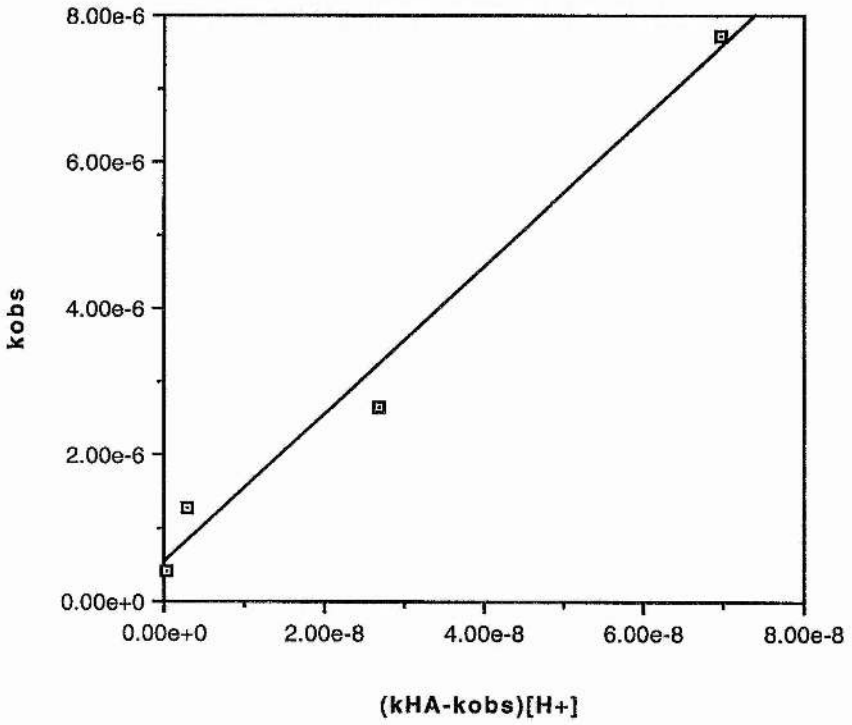

Graph 3.8: Plot to evaluate for k_A and K_2 for *N*-methylquinolinic acid.

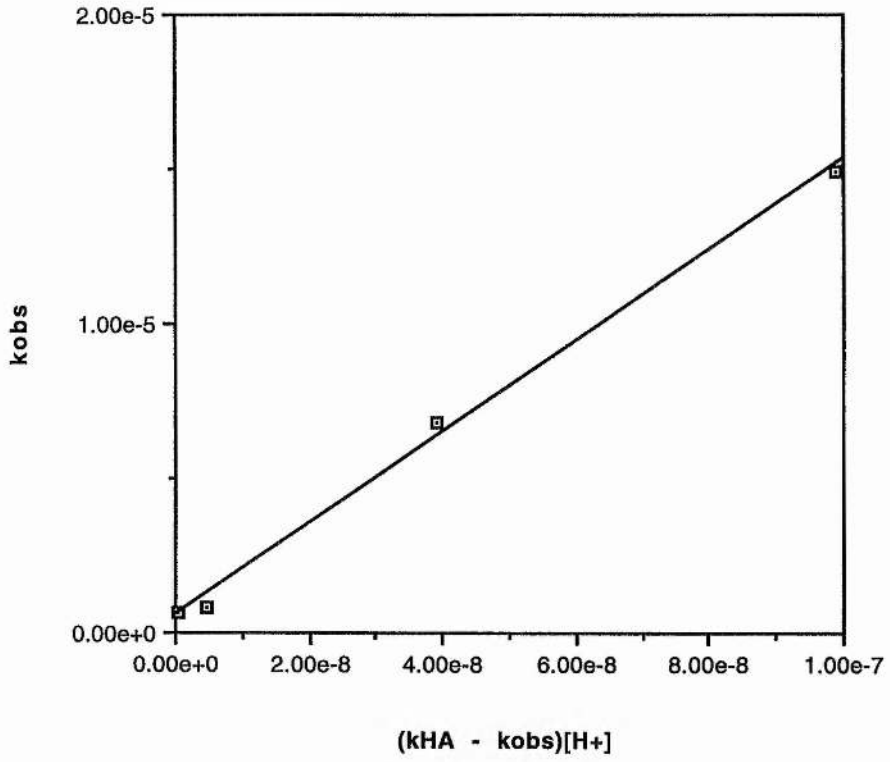

Graph 3.9: Plot to evaluate for k_A and K_2 for *N*-ethylquinolinic acid.

The plot for *N*-methylquinolinic acid gave $k_A = 5.19 \pm 3.60 \times 10^{-7}$ s^{-1} and $K_2 = 0.01 \pm 0.001$ ($pK_2 = 2.00$), whilst that for *N*-ethylquinolinic acid gave $k_A = 5.64 \pm 3.26 \times 10^{-7}$ s^{-1} and $K_2 = 6.8 \pm 0.3 \times 10^{-3}$ ($pK_2 = 2.17$). The values of k_A for *N*-methyl and *N*-ethylquinolinic acid are much lower than for k_{HA}, and are actually slower than that observed for quinolinic acid ($k_A = 5.64 \times 10^{-6}$ s^{-1}). The rate constants agree with the proposals that as the amount of the dicarboxylate anion increases then the rate of decarboxylation decreases, because of the lack of stabilisation of the ylid produced.

Again the pK_A values are very similar for the two acids, showing that the difference between the methyl and ethyl groups has very little effect on the rate of dissociation. They also correlate closely to that for quinolinic acid ($pK_2 = 2.43$ at 25 °C).[176]

3.2.3.4 Effect of temperature on rate of decarboxylation

The effect of temperature on the rate of decarboxylation of *N*-ethylquinolinic acid was determined. Measurement of the rate of decarboxylation at 60, 70, 75, 80, 85 and 90 °C for *N*-ethylquinolinic acid at pH 1.5, ionic strength 1.0, allowed the activation energy for the reaction to be calculated. The results of the studies are shown below in Table 3.4, and in graphical form in Graph 3.10.

T (°C)	k_{obs} (10^{-5} s^{-1})	k_{obs} (10^{-5} s^{-1})
60	0.042 ± 0.002 0.044 ± 0.001	0.043 ± 0.002
70	0.233 ± 0.009 0.232 ± 0.007	0.232 ± 0.009
75	0.490 ± 0.009 0.502 ± 0.020	0.496 ± 0.020
80	0.993 ± 0.030 1.030 ± 0.056	1.017 ± 0.056
85	2.068 ± 0.067 2.164 ± 0.064	2.116 ± 0.067
90	4.412 ± 0.180 4.608 ± 0.121 3.591 ± 0.120	4.204 ± 0.613

Table 3.4: Effect of temperature on the rate of decarboxylation of *N*-ethylquinolinic acid

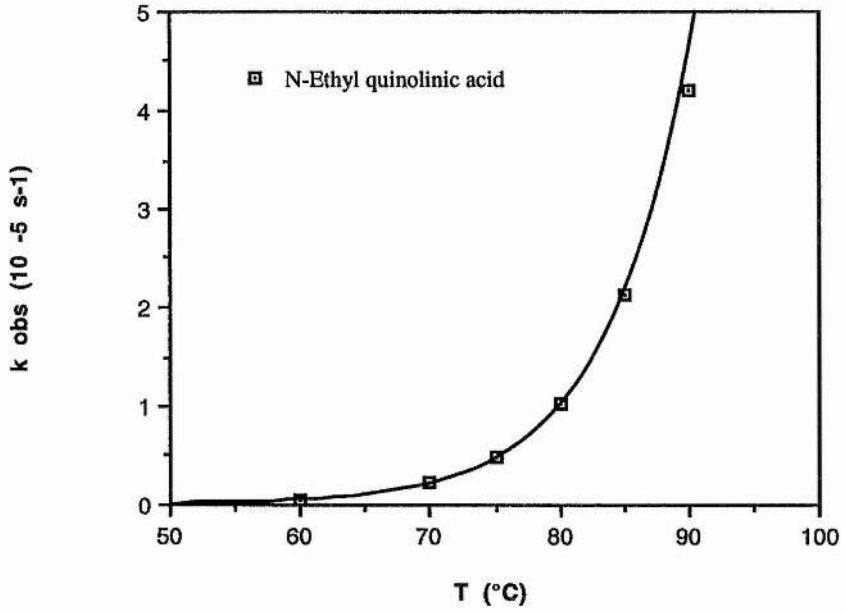

Graph 3.10: Effect of temperature on the rate of decarboxylation of *N*-ethylquinolinic acid

As expected, the rate of decarboxylation increased as the temperature was raised, by a factor of 2 as the temperature was raised by 5 °C.

The temperature dependence of the rate of reaction fits the expression proposed by Arrhenius.

$$k = Ae^{(-Ea/RT)} \qquad [5]$$

E_a, the activation energy for the reaction, and A, the pre-exponential factor, which is (almost) always independent of temperature, are determined from a plot of 1/T versus ln k.

$$\ln k = \ln A - \frac{E_a}{RT} \qquad [6]$$

Thus, from this Arrhenius plot the gradient of the straight line obtained is ($-E_a$ /R), and the intercept is ln A. Table 3.5 shows the data transformed into a suitable form for an Arrhenius plot (Graph 3.11).

T (°C)	T (K)	1/T (K^{-1})	k_{obs} (10^{-5} s^{-1})	ln k
60	333	0.003003	0.043 ± 0.002	-14.657
70	343	0.002915	0.232 ± 0.009	-12.973
75	348	0.002874	0.496 ± 0.020	-12.215
80	353	0.002833	1.017 ± 0.056	-11.502
85	358	0.002793	2.116 ± 0.067	-10.764
90	363	0.002755	4.204 ± 0.613	-10.094

Table 3.5: Table of data for Arrhenius plot

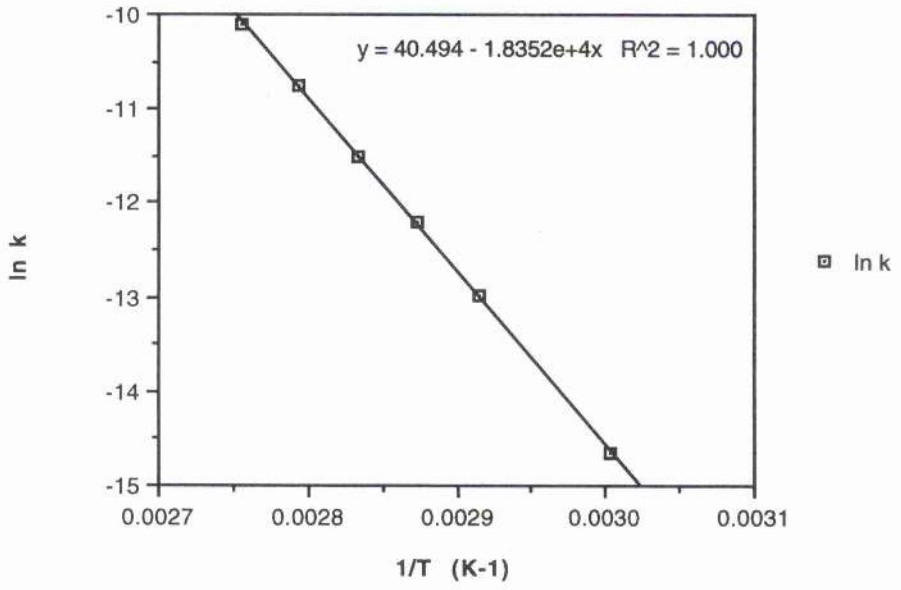

Graph 3.11: Arrhenius plot

From the equation of the graph

$$\frac{-E_a}{RT} = -1.835 \times 10^{-4} \qquad \text{(where } R = 8.314 \times 10^{-3} \text{ kJ mol}^{-1} \text{ K}^{-1}$$

$$E_a = 153 \text{ kJ mol}^{-1}$$

$$\ln A = 40.494$$

$$A = 3.858 \times 10^{17} \text{ s}^{-1}$$

The activation energy for the decarboxylation of *N*-ethylquinolinic acid is very similar to that for other pyridine-2-carboxylic acids.[169] Picolinic acid has an activation energy of 145 kJ mol^{-1}, whilst that for homarine is 148 kJ mol^{-1}.

3.2.3.5 Effect of ionic strength

The decarboxylation of *N*-ethylquinolinic acid at 90 °C, pH 1.5, was repeated over a range of ionic strengths, from 0.5 to 3.0. The ionic strength was adjusted for each experiment using potassium chloride. Table 3.6 shows the results from these experiments, which are placed in graphical form in Graph 3.12.

Ionic strength	k_{obs} (10^{-5} s^{-1})	k_{obs} (10^{-5} s^{-1})
0.5	4.970 ± 0.187 5.240 ± 0.151	5.105 ± 0.187
1.0	4.412 ± 0.180 4.608 ± 0.121 3.591 ± 0.120	4.204 ± 0.613
2.0	3.660 ± 0.101 3.644 ± 0.101	3.652 ± 0.101
3.0	3.025 ± 0.150 2.933 ± 0.104	2.979 ± 0.150

Table 3.6: Effect of ionic strength on the rate of decarboxylation of *N*-ethylquinolinic acid

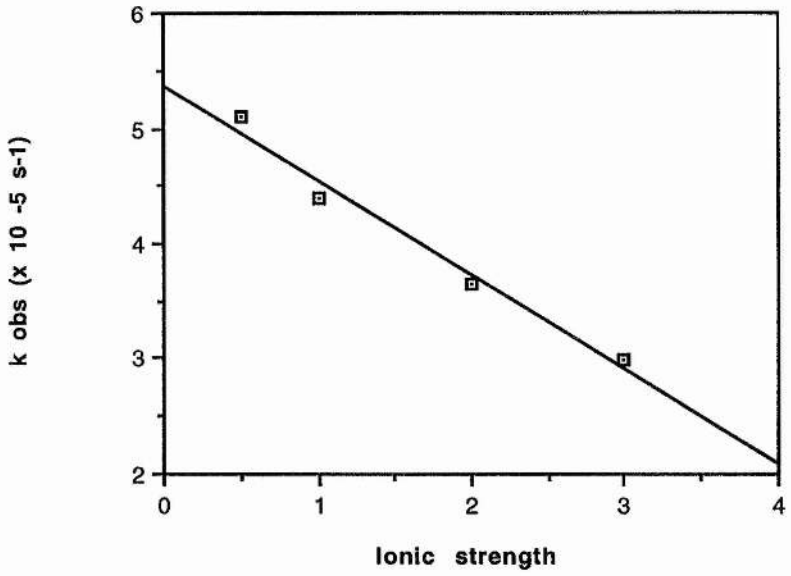

Graph 3.12: Effect of ionic strength on the rate of decarboxylation of *N*-ethylquinolinic acid

As ionic strength increases, the rate of decarboxylation decreases. This is the opposite effect to that expected. If a more charged intermediate is produced in the reaction then increasing the ionic strength should provide extra stabilisation which would be expected to increase the rate. The pk_a may change with a change in ionic strength, so affecting the rate of decarboxylation.

In the QPRTase system increasing the concentration of potassium cations leads to lower activity of the enzyme. In this case the cation is probably bound to the protein, altering the active site. Introduction of a chelating agent, such as EDTA, reverses the effect as the potassium cation is chelated. One alternative is that the increase in ionic stength actually inhibits the starting material from decarboxylating.

3.2.3.6 Effect of D_2O

The decarboxylation of *N*-ethylquinolinic acid at 90 °C, ionic strength 1.0, was carried out in D_2O. This allowed us to investigate the effect of the deuterated solvent. A change of solvent often has spectacular effects on the rate of a reaction, with solvent-solute interactions often responsible. Reactions with ionic species are particularly sensitive, because of the large ion-solvent interactions. Table 3.7 shows the rate of decarboxylation in the experiments, compared to the same decarboxylation in water.

	k_{obs} (10^{-5} s^{-1})	k_{obs} (10^{-5} s^{-1})
Water	4.412 ± 0.180 4.608 ± 0.121 3.591 ± 0.120	4.204 ± 0.613
D_2O	5.524 ± 0.239 4.728 ± 0.178	5.127 ± 0.398

Table 3.7: Effect of deuterated solvent on the rate of decarboxylation of *N*-ethylquinolinic acid

Although the effect of carrying out the reactions in D_2O has increased the rate of the reaction, it is not by such a significant amount to allow any further conclusions to be made.

3.2.4 *N*-Propylquinolinic acid

To approach the size of the quinolinic acid mononucleotide, the bulk of the group on the nitrogen must be increased. Following on from the synthesis and kinetic studies on *N*-methylquinolinic acid and *N*-ethylquinolinic acid, the next obvious synthetic target in the series of increasing the size of the nitrogen substituent, was *N*-propylquinolinic acid (**113**).

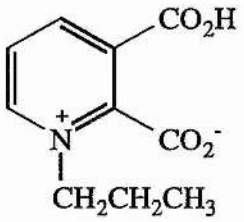

(113)

The initial route investigated was that identical to the method in which *N*-methylquinolinic acid and *N*-ethylquinolinic acid were produced.

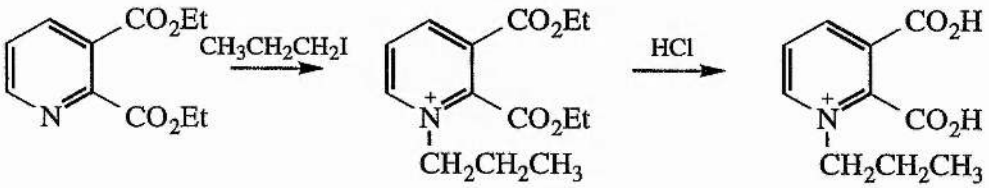

Scheme 3.13: Proposed route to *N*-propylquinolinic acid

Diethyl quinolinate was heated gently, under a nitrogen atmosphere with a slight excess of 1-iodopropane, but tlc analysis showed that no reaction had occurred even after extended times. It is possible that the size of the ethyl ester prevents nucleophilic attack by the nitrogen.

As this approach proved unsuccessful alternative routes for the synthesis were considered. There are very few literature references on 2-substituted *N*-alkylated pyridines. The majority of our approaches used quinolinic acid anhydride (pyridine

2,3-carboxylic acid anhydride) as a starting material (**114**). This was chosen because the two carboxylic acid groups are held in the plane of the ring and would hopefully avoid the steric problems. Also, following *N*-alkylation hydrolysis of the anhydride is carried out under very mildly acid aqueous conditions. To confirm the suitability of quinolinic acid anhydride to allow *N*-alkyl substitution, *N*-methylquinolinic acid was successfully synthesised in good yield in the following manner (Scheme 3.14). Successful production of *N*-methylquinolinic acid was confirmed by comparing spectral data to authentic *N*-methylquinolinic acid. Quinolinic acid anhydride was then reacted with an excess of 1-iodopropane under identical conditions to attempt to synthesise *N*-propylquinolinic acid (Scheme 3.15).

Scheme 3.14: Synthesis of *N*-methylquinolinic acid

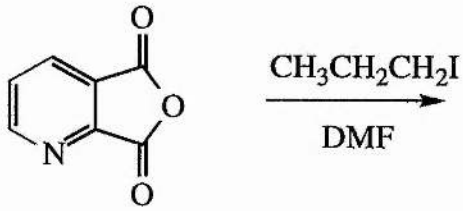

Scheme 3.15: Reaction of quinolinic acid anhydride and 1-iodopropane

The ^{1}H NMR data gave interesting results. Alkylation on the nitrogen did appear to have occurred, but it also seemed that the anhydride had been cleaved and that a propyl ester formed on one of the two acids. Two sets of propyl group peaks were observed, corresponding to the nitrogen substituent and the propyl ester. Thus, hydrolysis was still necessary to obtain the free acid.

However, even under relatively mild conditions (< 40 °C, in 1 M hydrochloric acid) decarboxylation also appeared to take place, to give *N*-propylnicotinium chloride (**115**) in 62% yield. The structure of the product was confirmed by comparing spectral data to that from authentic *N*-propylnicotinic acid in the manner described below (Scheme 3.16).

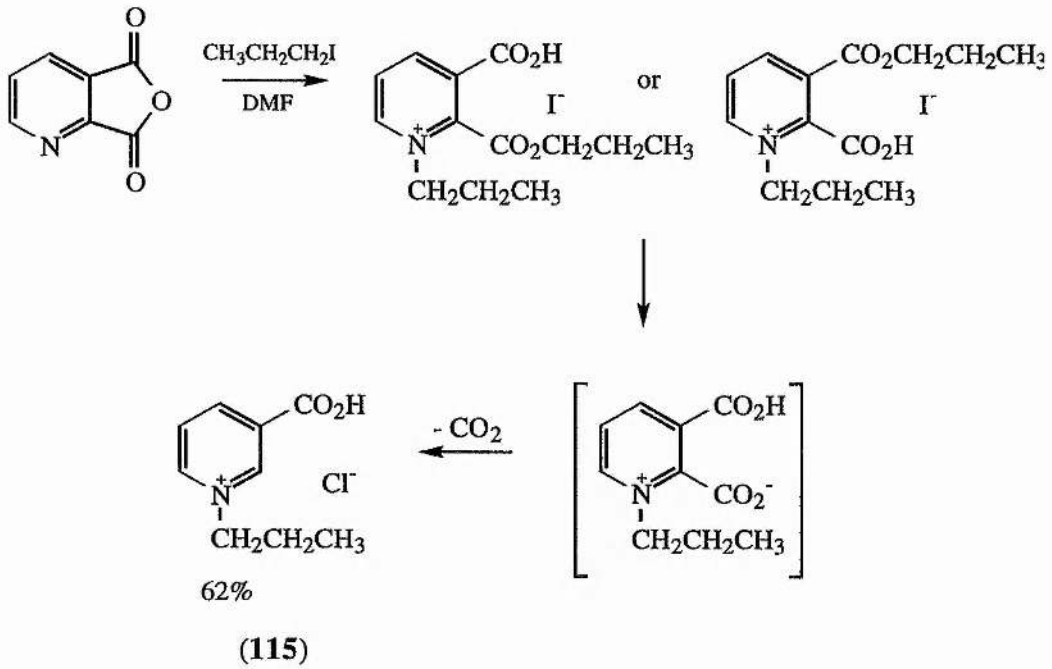

(**115**)

Scheme 3.16: Synthesis of *N*-propylnicotinium chloride

This result implied that decarboxylation does indeed get much faster with the increase in size from the ethyl group to the propyl. Indeed, the reaction seemed to be too fast to allow any measurements of the kinetics to be made, or the compound to be isolated

Further attempts to synthesise *N*-propylquinolinic acid were made. Altering the conditions for the reaction between quinolinic acid anhydride and 1-iodopropane proved unsuccessful. Reducing the temperature of the reaction slowed down any possible reaction significantly, while at higher temperatures the anhydride was cleaved. In one case some evidence of substitution onto the nitrogen was observed, but the product was very minor, and isolation was not possible by reverse phase tlc or HPLC.

Dimethyl quinolinate (**116**) was synthesised in an identical manner to diethyl quinolinate, with methanol replacing ethanol, to produce a white solid (Scheme 3.17), in a further attempt to reduce steric interactions.

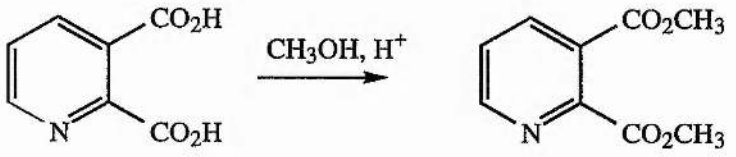

(116)

Scheme 3.17: Synthesis of dimethyl quinolinate

The dimethyl quinolinate was then heated with 1-iodopropane under a nitrogen atmosphere (Scheme 3.18). It was hoped that the smaller ester group would not sterically hinder addition of the propyl group onto the nitrogen. However, no reaction was detected by tlc.

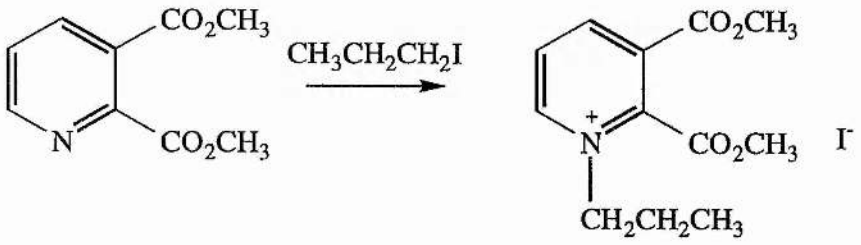

Scheme 3.18: Proposed synthesis of *N*-propyl quinolinic acid

3.2.5 Routes to other *N*-substituted quinolinic acids

In an attempt to increase the rate of the reaction, compounds with a better leaving group were considered. The synthesis of *n*-propyl trifluoromethanesulfonate (*n*-propyl triflate) was attempted but the product was too unstable. However, *n*-octyl triflate is a stable compound which would produce a larger *N*-alkyl substituent and a better leaving group.

n-Propyl triflate was synthesised in the manner of Gramstad and Haszeldine,[187] and octyl triflate by a method described by Beard, Baum and Grakauskas.[188]

For the synthesis of *n*-propyl triflate (**117**), silver triflate and 1-iodopropane were suspended in dry dichloromethane, and immediately a precipitate of silver iodide formed (Scheme 3.19). After stirring for a further 30 minutes to allow the reaction to complete, the precipitate was filtered off and the solvent removed. However, the *n*-propyl triflate proved to be unstable and was not suitable for use in further reactions.

$$CF_3SO_3Ag + CH_3CH_2CH_2I \longrightarrow CH_3CH_2CH_2OSO_2CF_3 + AgI$$

(117)

Scheme 3.19: Synthesis of propyl triflate

To synthesise *n*-octyl triflate (**118**), a solution of octan-1-ol and pyridine were dissolved in dry dichloromethane and added dropwise to a solution of triflic anhydride in dry dichloromethane at 0 °C (Scheme 3.20). After 30 minutes the solution was washed, dried and the solvent removed.

$$(CF_3SO_2)_2O + CH_3(CH_2)_6CH_2OH \xrightarrow{\text{py, DCM}} CH_3(CH_2)_6CH_2OSO_2CF_3 + CF_3SO_3H$$

(118)

Scheme 3.20: Synthesis of octyl triflate

However when *n*-octyl triflate was heated gently with quinolinic acid anhydride (Scheme 3.21), both with dry DMF and without solvent, no reaction occurred.

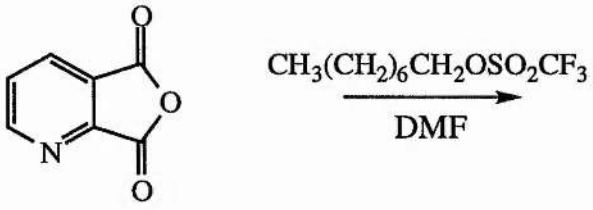

Scheme 3.21: Proposed route to *N*-octyl quinolinic acid

So far attempts to synthesise *N*-substituted quinolinic acids with larger groups on the nitrogen have also proved unsuccessful. 2,3,4,6-Tetra-O-acetyl-α-D-glucopyranosyl bromide (**119**) was synthesised from D-glucose, in a two step reaction, in 94% yield (Scheme 3.22). Acetylation was carried out by dissolving D-glucose in acetic anhydride followed by addition of 45% hydrogen bromide in acetic acid. Upon complete acetylation, further treatment with 45% hydrogen bromide in acetic acid afforded the brominated product, which on crystallisation from diethyl ether produced a white solid. ^1H and ^{13}C NMR and melting point confirmed the product to be 2,3,4,6-tetra-O-acetyl-α-D-glucopyranosyl bromide.

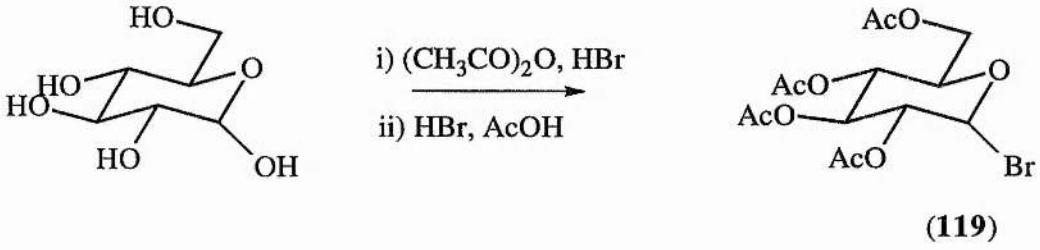

(119)

Scheme 3.22: Synthesis of 2,3,4,6-tetra-O-acetyl-α-D-glucopyranosyl bromide

It was envisaged that this sugar group would add on to the nitrogen of quinolinic acid, which would produce an excellent analogue of quinolinic acid mononucleotide, the intermediate in the QPRTase catalysed system.

This addition of the sugar group was attempted with both diethyl quinolinate (Scheme 3.23) and quinolinic acid anhydride (Scheme 3.24) under a variety of conditions, but unfortunately none were successful.

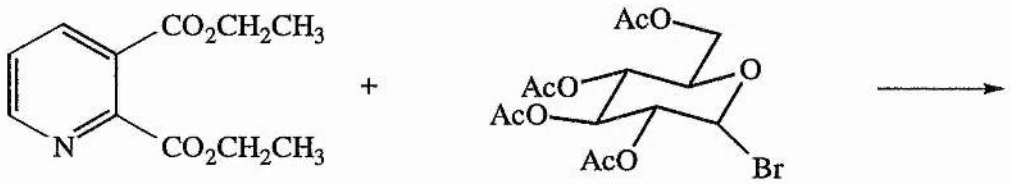

Scheme 3.23: Proposed synthetic route

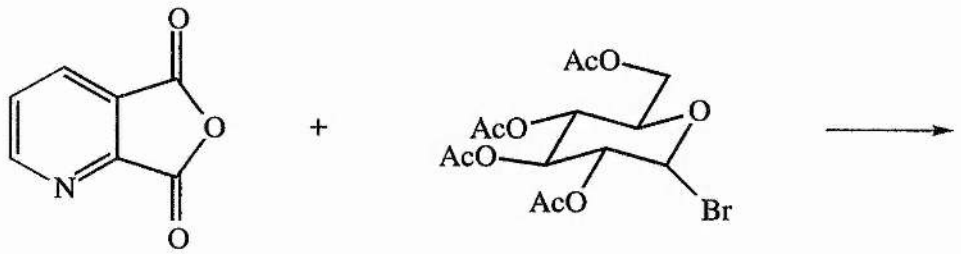

Scheme 3.24: Proposed synthetic route

3.3 Conclusions and Future Work

The kinetic studies on *N*-methyl and *N*-ethylquinolinic acid showed very interesting results, primarily that increasing the size of the substituent on quinolinic acid translates to an increase in the rate of decarboxylation, and secondly that a distinctive rate profile was obtained for both acids. To further investigate the effect of the substituent group on the rate of decarboxylation, much work needs to be done to successfully synthesise another *N*-substituted quinolinic acid. This should focus on the successful synthesis, and kinetic studies of, *N*-propylquinolinic acid.

Early results from our attempts to synthesise *N*-propylquinolinic acid indicate that it would indeed decarboxylate much faster than *N*-methyl and *N*-ethylquinolinic acid. *N*-Propylnicotinic acid was the only product isolated from the reaction of quinolinic acid anhydride and 1-iodopropane. When *N*-propylquinolinic acid is successfully synthesised and characterised, full kinetic studies will give further information on the effect of the increase in size of the alkyl group on decarboxylation.

The decarboxylation studies so far show that although there was an increase in rate from *N*-methyl to *N*-ethyl substituent, the actual rate was still quite slow when compared to an enzymic reaction ($t_{1/2}$ for *N*-methylquinolinic acid at pH 1.5 at 90 °C = 6.7 hours, $t_{1/2}$ for *N*-ethylquinolinic acid at pH 1.5 at 90 °C = 4.6 hours). However, as it was shown when routes to *N*-propylquinolinic acid were investigated, there seems to be a sharp increase in the rate of decarboxylation with this seemingly small increase in size. Presumably, the larger groups increase steric congestion around the 2-carboxylic acid, which is released upon decarboxylation. This would be even greater in the case of the intermediate in the QPRTase reaction (quinolinic acid mononucleotide). However it cannot yet be deduced whether there would be sufficient rate increase to make this reaction as rapid as an enzymatic reaction under physiological temperature and pH.

Ultimately the aim would be to synthesise quinolinic acid mononucleotide, the actual intermediate in the QPRTase system. Careful consideration must go into the route to this product. The nitrogen of quinolinic acid is not the strongest nucleophile, the acid groups must be protected to avoid steric hindrance, and conditions must be such that the decarboxylation reaction is measurable and does not occur spontaneously. This is not a trivial task, but if it was successful, it would establish whether or not decarboxylation is spontaneous or enzyme catalysed.

With the data so far it is probably more likely that it is enzyme catalysed. The rates of decarboxylation with the model compounds investigated are very slow. In addition, the X-ray structure also shows groups present at the active site, Lys 152 and Arg 175, which could be able to stabilise the ylid intermediate by interacting with the negative charge at the 2-position.

CHAPTER 4

4. Experimental

Melting points were determined using an electrothermal melting point apparatus and are uncorrected. Microanalyses were carried out by the University of St. Andrews microanalytical laboratory. NMR spectra were recorded on a Varian Gemini 200 f.t. spectrophotometer (^{1}H, 200 MHz; ^{13}C, 50.31 MHz) or a Bruker AM 300 f.t. spectrophotometer (^{31}P, 121.49 MHz). NMR spectra are described in parts per million downfield shift from TMS and are described consecutively as position (δ_H or δ_C), relative integral, multiplicity (s.-singlet, d.-doublet, t.-triplet, dd.-doublet of doublets and mult.-multiplet), coupling constant ($J_{x,y}$ Hz if applicable) and assignment. Infra-red spectra were recorded on a Perkin-Elmer series 1420 IR spectrophotometer. The samples were prepared as either Nujol mulls or thin films between sodium chloride discs. Absorption maxima are given in wavenumbers relative (cm^{-1}) to a polystyrene standard. Flash chromatography was performed according to the procedure of Still[189] using Sorbisil C60 (40-60 mm mesh) silica gel. Analytical thin layer chromatography was carried out on 0.25 mm precoated silica gel plated (Whatman PE SIL G/UV_{254}) or on 0.11 mm precoated cellulose plates (CEL Machery-Nagel 300/UV_{254}). Compounds were visualised by UV fluorescence, iodine vapour, aqueous potassium permanganate or 5% sulfuric acid in aqueous ethanol/charring. UV spectra assays were measured on a Kontron UVICON 932 scanning spectrophotometer.

2-Hydroxypyridine-3-carboxylic acid (15)

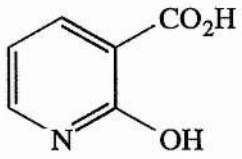

2-Mercaptonicotinic acid (5 g, 0.032 mol) was dissolved in water (69 ml) and then concentrated nitric acid (23 ml) was added. The solution was heated for 2 hours at 120 °C. On cooling, a precipitate of needle-like crystals appeared, which were filtered off and recrystallised from boiling water, to give colourless needle-like crystals (1.96 g, 45%). m.p. 258-260 °C (lit.[190] 260 °C); (Found: C, 51.56; H, 3.26; N, 10.03. Calc. for $C_6H_5NO_3$: C, 51.80; H, 3.62; N, 10.07%); υ_{max} (nujol/ cm^{-1}) 3460 (-OH), 1680 (C=O); δ_H (200 MHz; ^2H_2O) 6.57 (1H, t., $J_{4,5}$ =$J_{5,6}$ 7 Hz, 5-CH), 7.55 (1H, dd., $J_{4,5}$ 7 Hz, $J_{4,6}$ 2 Hz, 4-CH), 7.88 (1H, dd., $J_{5,6}$ 7 Hz, $J_{4,6}$ 2 Hz, 6-CH); δ_C (50.31 MHz; ^2H_2O) 108.9 (5-C), 116.9 (3-C), 141.7 (4-C), 146.4 (6-C), 164.8 (2-C), 165.3 (carbonyl); *m/z* (EI) 139 (*M*, 45%), 121 (18, *M*-H_2O), 95 (100, *M*-CO_2).

2-Sulfonicotinic acid (33)

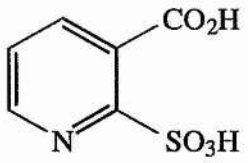

i) Using Potassium permanganate as oxidant

2-Mercaptonicotinic acid (1.25 g, 0.008 mol) was dissolved in a solution of sodium hydroxide (0.66 g) in distilled water (125 ml). A solution of potassium permanganate (2.75 g, 0.018 mol) in water (50 ml) was added dropwise, with stirring. After addition was complete, the solution was left to stir for 15 minutes at room temperature, and then heated for 1 hour at 75 °C.

On cooling, excess potassium permanganate was removed by adding ethanol to form MnO_2, which was removed by filtration, and the solid was washed with boiling water (50 ml). The free acid was then generated by passing the solution through an Amberlite IR-120 ion exchange column. The fractions with UV active components were reduced to dryness under reduced pressure and the solid formed was recrystallised from boiling water to give white crystals (0.32 g, 20%). m.p. 254 °C (lit.[125] 254 °C); (Found: C, 35.44; H, 2.00; N, 6.61; Calc., for $C_6H_5NSO_5$: C, 35.47; H, 2.48; N, 6.89%); υ_{max} (nujol/ cm^{-1}) 3420 (-OH), 1700 (C=O); δ_H (200 MHz; ^2H_2O) 7.56 (1H, dd., $J_{4,5}$ 9 Hz, $J_{5,6}$ 5 Hz, 5-CH), 7.92 (1H, d., $J_{4,5}$ 9 Hz, 4-CH), 8.53 (1H, d., $J_{5,6}$ 5 Hz, 6-CH); δ_C (50.31 MHz; ^2H_2O) 129.3 (5-C), 137.2 (3-C), 139.2 (4-C), 150.6 (6-C), 155.2 (2-C), 192.7 (carbonyl); *m/z* (EI) 185 (M-H_2O, 4%), 139 (23, M-SO_2), 105 (100, M-H_2O-SO_3), 95 (87, M- SO_2-CO_2), 78 (61, C_5H_4N).

ii) Using iodine as oxidant

Iodine (15.18 g, 0.06 mol) was partially dissolved in distilled water (200 ml). 2-Mercaptonicotinic acid (0.78 g, 0.005 mol) was partially dissolved in water and the pH adjusted to pH 6 using KOH. 2-Mercaptonicotinic acid is not very soluble in water

so parts were added slowly under stirring and then the excess 2-mercaptonicotinic acid was dissolved in water and then added. On completion of addition, the solution was left to stir for 3 hours, and then reduced to dryness under reduced pressure. The solid produced was recrystallised from boiling water to give white crystals (0.19 g, 19%). m.p. 254 °C; Spectral data as above.

Diisopropyl nicotinamide (43)

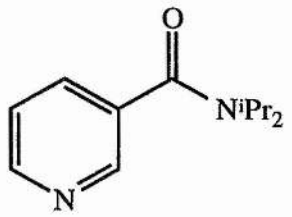

Nicotinic acid (10.0 g, 0.081 mol) was added to thionyl chloride (30 ml, distilled from sulfur) and this mixture stirred for 24 hours at room temperature. The excess thionyl chloride was removed under reduced pressure and the white acid chloride suspended in THF (200 ml). Diisopropylamine (44.8 ml, 0.32 mol) was added in excess at 0 °C and this solution stirred for a further 24 hours. The amine hydrochloride salt was filtered off and washed with a little THF. An aqueous work-up could not be employed due to the solubility of the amide. Removal of THF under reduced pressure produced the crude amide, which was recrystallised from ethyl acetate to give colourless crystals (11.8 g, 70%). m.p. 95-96 °C (lit.[191] 100 °C); ν_{max}(nujol/cm^{-1}) 1645 (C=O); δ_H (200 MHz; C^2HCl_3) 1.35 (12H, broad s., -CH($C\underline{H}_3$)$_2$), 3.70 (2H, broad s., -$C\underline{H}$(CH$_3$)$_2$), 7.32 (1H, m., 4-CH), 7.65 (1H, m., 2-CH), 8.60 (2H, m., 5-CH and 6-CH); δ_C (50.31 MHz; C^2HCl_3) 21.1 (-CH($C\underline{H}_3$)$_2$), 124.0 (5-C), 134.1 (4-C), 135.0 (3-C), 147.1 (6-C), 150.4 (2-C), 169.0 (carbonyl); *m/z* (EI) 206 (M$^+$, 10%), 191 (11, M-CH$_3$), 163 (21, M-CH(CH$_3$)$_2$), 149 (10, M-NCH(CH$_3$)$_2$), 106 (100, M-N(CH(CH$_3$)$_2$)$_2$), 78 (42, C_5H_4N), 44 (21, C_2H_5N).

4-(Trimethylsilyl)-*N*, *N*-diisopropylnicotinamide (44)

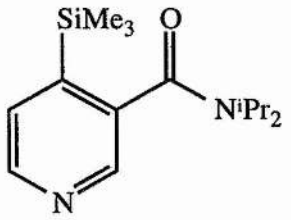

Dry diisopropylamine (20 mmol, 2.98 ml) was stirred in dry THF (15 ml) under a nitrogen atmosphere. *N*-Butyl lithium (22 mmol, 1.4 ml of 1.6 M solution in hexane) was added with stirring at -78 °C. After a further 20 minutes a solution of trimethylsilyl chloride (20 mmol, 2.53 ml) in THF (5 ml) was added, followed by the dropwise addition of a solution of diisopropylnicotinamide (10 mmol, 2.1 g) in dry THF (15 ml). The solution was stirred for a further 2 hours at -78 °C and then the reaction allowed to warm gradually to room temperature. The reaction was poured over 5% aqueous sodium hydrogen carbonate (10 ml), extracted with diethyl ether (3 x 60 ml), washed with water (15 ml), brine (2 x 20 ml) and dried ($MgSO_4$). Removal of the solvent under reduced pressure gave a pale yellow oil which crystallised spontaneously. Purification by column chromatography (silica gel, 3:2 ethyl acetate/40-60 petroleum ether) produced the white solid 4-trimethylsilyl diisopropyl nicotinamide (2.1 g, 76%) and the 2,4-disilyl derivative (0.6 g, 11%). m.p. 68-70 °C; (Found: C, 64.74; H, 9.72; N, 10.07; Calc., for $C_{15}H_{26}N_2OSi$: C, 64.70; H, 9.41; N, 10.03%); ν_{max}(nujol/cm^{-1}) 1645 (C=O), 840 (Si-$(CH_3)_3$); δ_H (200 MHz; C^2HCl_3) 0.35 (9H, s., -Si($C\underline{H}_3)_3$), 1.55 (6H, d., *J* 7.5 Hz, -CH($C\underline{H}_3)_2$), 3.50 (1H, broad m., -$C\underline{H}(CH_3)_2$), 7.52 (1H, d., $J_{5,6}$ 6 Hz, 5-CH), 8.35 (1H, s., 2-CH), 8.50 (1H, d., $J_{5,6}$ 6 Hz, 6-CH); δ_C (50.31 MHz; C^2HCl_3) 20.9, 21.1 (-CH($\underline{C}H_3)_2$), 48.0 (-$\underline{C}H(CH_3)_2$), 130.0 (5-C), 134.1 (4-C), 145.8 (3-C), 148.9 (6-C, 2-C), 170.3 (carbonyl); *m/z* (EI) 278 (M^+, 16%), 263 (17, M-CH_3), 251 (21, M-CHN), 219 (32, M-$HSi(CH_3)_2$), 205 (15, M-$(CH_3)_3Si$), 178 (100, M-$N(CH(CH_3)_2)_2$), 161 (13, C_5H_4N-CON-), 43 (21, $CH(CH_3)_2^+$).

2-(3-pyridyl)-4,4-dimethyl-oxazoline (45)

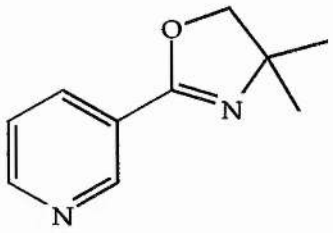

Nicotinoyl chloride was prepared in an identical manner to the first step described for diisopropyl nicotinamide, and then suspended in dichloromethane (200 ml). To this was added, dropwise at 0 °C, a solution of 2-amino-2-methyl propan-1-ol (21.7 g, 0.24 mol) in dichloromethane (50 ml). The mixture was stirred for 24 hours, and the amine hydrochloride filtered off and washed with dichloromethane. The combined filtrate and washings were concentrated to give the amide. Thionyl chloride was then added to the solid amide and the solution stirred until all the amide had dissolved. This solution was then added dropwise to an excess of 20% sodium hydroxide solution cooled in an ice bath. The aqueous solution was extracted with diethyl ether (5 x 50 ml), washed with brine and dried (K_2CO_3). The solvent was evaporated under reduced pressure to give a brown oil, which upon distillation under Kugelrohr conditions produced a clear oil (3.2 g, 44%). b.p. 92-95 °C/ 2 mmHg (lit.[192] 80 °C/ 2 mmHg); ν_{max}(thin film/cm^{-1}) 1635 (CN), 1070, 1020 (CO); δ_H (200 MHz; C^2HCl_3) 1.40 (6H, s., -C($\underline{C}H_3$)$_2$), 4.10 (2H, s., oxazoline-$C\underline{H}_2$), 7.30 (1H, m., 5-CH), 8.18 (1H, m., 6-CH), 9.10 (1H, s., 2-CH); δ_C (50.31 MHz; C^2HCl_3) 28.8 (-C($\underline{C}H_3$)$_2$), 68.3 (-$\underline{C}H(CH_3)_2$), 79.7 (oxazoline-CH_2), 123.6 (5-C), 124.6 (3-C), 136.1 (4-C), 149.9 (6-C), 152.3 (2-C), 160.6 (oxazoline-O-C=N); *m/z* (EI) 176 (M^+, 7%), 161 (64, M-CH_3), 146 (16, M-(CH_2O), 133 (27, M-$CH(CH_3)_2$), 105 (57, C_6H_5N), 78 (27, M-oxazoline), 56 (100, isobutene).

Methyl 2-cyano-5-methoxypentane-2,4-dienoate (47)

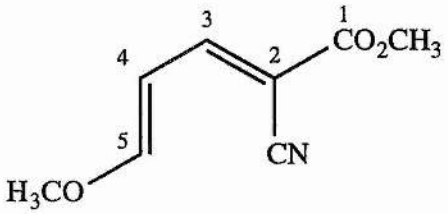

A mixture of tetramethoxypropane (12.3 g, 0.075 mol), acetic anhydride (25 ml), and dry zinc chloride (68 mg) was heated under reflux, and methyl cyanoacetate (4.5 g, 0.05 mol) was added dropwise. The reaction was maintained at reflux for 18 hours, after which time the volatiles were distilled off until the distillation temperature reached 122 °C. The residue was then cooled, and a crude brown solid apppeared. This crude product was used for the next step. m.p. 115 - 135 °C (lit.[142] 110 - 140 °C); δ_H (200 MHz; C^2HCl_3) 3.82 and 3.84 (6H, 2 x s., $-OCH_3$), 6.08 (1H, t., *J* 12 Hz, 4-CH), 7.32 (1H, d., *J* 12 Hz, 5-CH), 7.86 (1H, d., *J* 12 Hz, 3-CH); δ_C (50.31 MHz; C^2HCl_3) 53.2 ($CO_2\underline{C}H_3$), 58.9 (OCH_3), 98.7 (2-C), 103.6 (4-C), 115.6 (CN), 156.0 (3-C), 163.9 (1-C), 166.8 (1-C).

Methyl 2-bromonicotinate (46)

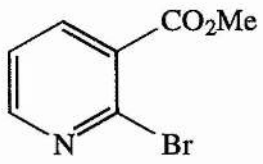

Methyl-2-cyano-5-methoxypentane-2,4-dienoate (4 g, 0.024 mol) was dissolved in acetic acid (20 ml) and warmed to 40 °C. HBr in acetic acid (40%, 40 ml) was added dropwise whilst the temperature of the reaction mixture was maintained at 40 - 45 °C. After addition was complete the temperature was raised to 55 °C and the solution heated for 30 minutes. Upon cooling, this solution was poured into water and neutralised by careful addition of sodium carbonate. The aqueous solution was extracted with dichloromethane (3 x 300 ml). The organic layers were combined, washed with water, dried ($NaSO_4$) and the solvent evaporated under reduced pressure. The residue was distilled in a Kugelrohr apparatus, producing a clear oil (2.2 g, 41%). υ_{max} (cm^{-1}) 2940 ($-OCH_3$), 1700 (C=O); δ_H (200 MHz; C^2HCl_3) 3.91 (3H, s., OCH_3), 7.29 (1H, dd., $J_{4,5}$ 8 Hz, $J_{5,6}$ 6 Hz, 5-CH), 8.01 (1H, dd., $J_{4,5}$ 8 Hz, $J_{4,6}$ 2 Hz, 4-CH), 8.40 (1H, dd., $J_{5,6}$ 6 Hz, $J_{4,6}$ 2 Hz, 6-CH); δ_C (50.31 MHz; C^2HCl_3) 53.4 (OCH_3), 122.8 (5-CH), 130.1 (3-CH), 140.1 (6-CH), 141.1 (2-CH), 152.5 (4-CH), 165.9 (carbonyl).

Reactions with methyl 2-bromonicotinate

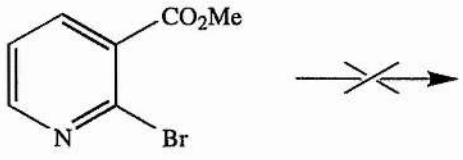

i) Methyl 2-bromonicotinate (2.16 g, 0.01 mol) and triethyl phosphite (2.04 g, 0.015 mol) were heated, under a nitrogen atmosphere, to 70 °C for 24 hours. The reaction

was followed by tlc (silica; 3:2 40-60 petroleum ether:ethyl acetate), but no reaction was detected.

ii) *n*-Butyl lithium (2.5 M in hexanes, 4.0 ml, 0.01 mol) was added dropwise to diethyl phosphite (2.0 g) at - 20 to - 30 °C under a nitrogen atmosphere over 2 hours. Methyl 2-bromonicotinate (2.16 g, 0.01 mol) was added, the reaction stirred and warmed to room temperature. The reaction was followed by tlc (silica; 3:2 40-60 petroleum ether:ethyl acetate), but no reaction was detected after 24 hours. The reaction was then warmed to 50 °C for 6 hours, but still no reaction was detected.

Reactions with 2-chloronicotinonitrile

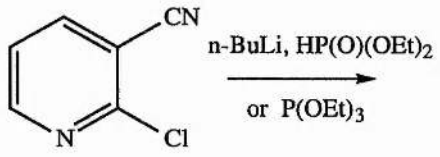

i) Sodium (0.06 g, 2.6 mmol) was dissolved in diethyl phosphite (5 ml) at 0 °C, the solution stirred and warmed to room temperature. 2-Chloronicotinonitrile (0.33 g, 2.38 mmol) was added, the solution stirred at room temperature for 6 hours, and the reaction followed by tlc (silica; 3:2 40-60 petroleum ether:ethyl acetate). No reaction was detected.

ii) The above reaction was repeated, with *n*-butyl lithium (2.5 M in hexanes, 0.95 ml, 2.6 mmol) replacing sodium. Again no reaction was detected.

iii) 2-Chloronicotinonitrile (1.33 g, 0.01 mol) and triethyl phosphite (1.68 g, 0.01 mol) were heated to 70 °C, under a nitrogen atmosphere, for 24 hours. The reaction followed by tlc (silica; 3:2 40-60 petroleum ether:ethyl acetate), but no reaction was detected.

Diethyl pyridine-2-phosphonate (48)

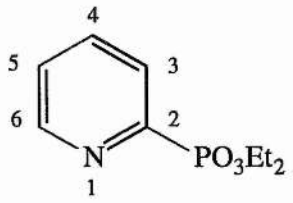

Tetrakis(triphenylphosphine)palladium (231 mg, 0.2 mmol) was added under a nitrogen atmosphere to a solution of diethyl phosphonate (0.61 ml, 4.4 mmol), toluene (2 ml) and dry triethylamine (0.61 ml, 4.4 mmol). 2-Bromopyridine (0.70 g, 4.4 mmol) was then added dropwise. This mixture was stirred under nitrogen at 90 °C for 5 days, and the reaction followed by t.l.c. (silica; 24:1 CH_2Cl_2: CH_3OH). On cooling diethyl ether (50 ml) was added, and the triethylamine hydrobromide removed by filtration. Evaporation of the solvent at reduced pressure, followed by column chromatography on silica gel, eluting with CH_2Cl_2: CH_3OH (24:1), gave a yellow oil as a product (2.20 g, 41%), which was analysed by ^1H and ^{13}C NMR. b.p. 120 °C/ 1 mm Hg; (Found: C, 49.77; H, 6.98; N, 6.51; Calc., for $C_9H_{14}NPO_3$: C, 50.23; H, 6.56; N, 6.51%); δ_H (200 MHz; C^2HCl_3) 1.23 (6H, t., *J* 8 Hz, $-OCH_2C\underline{H}_3$), 4.13 (4H, q., *J* 8 Hz, $-OC\underline{H}_2CH_3$), 7.34 (1H, m., 5-CH), 7.70 (1H, dd., $J_{3,4}$ 7 Hz, $J_{3,5}$ 4 Hz, 3-CH), 7.86 (1H, t., *J* 7 Hz, 4-CH), 8.70 (1H, d., $J_{5,6}$ 4 Hz, 6-CH); δ_C (50.31 MHz; C^2HCl_3) 16.8 ($-OCH_2C\underline{H}_3$), 63.4.($-OC\underline{H}_2CH_3$), 126.4 (5-CH), 128.6 (3-CH), 136.5 (4-CH), 151.0 (6-CH), 152.4 (2-CH); *m/z* (EI) 215 (M, 6%), 186 (20, M-CH_3CH_2), 171 (42, M-CH_3CHO), 142 (51, M-CH_3CH_2-CH_3CHO), 79 ($C_5H_5N^+$).

Diethyl *N*-phosphonomethylphthalimide (55)

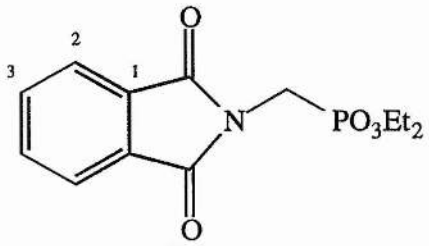

N-Bromomethylphthalimide (0.9 g, 3.8 mmol) and triethyl phosphite (0.6 g, 3.8 mmol) were heated to reflux for three days at 160 °C under nitrogen. On cooling, excess triethyl phosphite was removed by distillation using Kugelrohr apparatus. The remaining solid was crystallised from ethyl acetate/hexane to produce a white powder (0.40 g, 37%). m.p. 64 °C (lit.,[193] 64 °C). (Found: C, 52.53; H, 5.43; N, 4.71; Calc., for $C_{13}H_{16}NPO_5$: C, 52.53; H, 5.25; N, 4.90%); υ_{max} (nujol/ cm^{-1}) 1720 (C=O); δ_H (200 MHz; $^2H_6$-DMSO) 1.29 (6H, t., $C\underline{H}_3CH_2$), 4.08 (2H, d., N-CH_2-P), 4.16 (4H, q., $CH_3C\underline{H}_2$), 7.69 (2H, m., 3-CH), 7.83 (2H, m., 2-CH); δ_C (50.31 MHz; DMSO) 13.1 and 13.2 ($\underline{C}H_3CH_2$), 28.8 and 31.9 ($CH_3\underline{C}H_2$), 62.1 (N-CH_2), 121.2 (1-C), 132.3 (3-C), 132.6 (2-C), 164.0 (carbonyl); m/z (EI) 297 (*M*, 19%), 160 (100, *M*-PO_3Et_2).

Reactions with diethyl *N*-phosphonomethylphthalimide

Diethyl *N*-phosphonomethylphthalimide (0.40 g, 1.3 mmol) was dissolved in dry THF (20 ml) and the solution stirred at -78 °C, under a nitrogen atmosphere. 1.1 eq. *N*-Butyl lithium (2.5 M in hexanes, 0.095 g, 0.59 ml) was added dropwise and the reaction solution stirred at -78 °C for 30 minutes, after which ethyl bromoacetate (0.29 g, 1.3 mmol) was added, the reaction warmed to room temperature and left to stir for 24 hours. The reaction was followed by tlc (silica; ethyl acetate). The solution was reduced to dryness under reduced pressure, and diethyl ether (20 ml) and water (20 ml) added to the solid that remained. The two layers were separated, the solvents

evaporated to dryness under reduced pressure and the residues examined by ^{1}H NMR. No reaction, except hydrolysis of the ethyl ester, was detected.

The reaction was repeated using the same method, with a wide range of bases (*t*-Butyl lithium, LDA, sodium hydride, sodium methoxide/methanol, potassium carbonate and KHMDS) in a range of solvents (DMF, ethanol, methanol and DME). No reaction was detected in any of the reactions.

Ethyl nicotinate *N*-oxide (51)

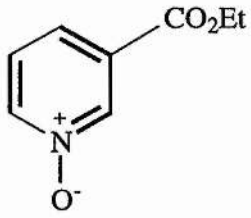

Hydrogen peroxide (100 volume, 24 ml) was dissolved in dichloromethane (56 ml) and the solution stirred at 0 °C. Trifluoroacetic anhydride (48 ml) was added slowly over 30 minutes, whilst maintaining the temperature at 0 °C. Ethyl nicotinate (2.00 g, 0.013 mol) was added dropwise, the solution allowed to warm to room temperature, and then refluxed for 5 hours. On cooling, the solution was evaporated to dryness under reduced pressure, and the residue redissolved in dichloromethane (20 ml). This was washed with distilled water (20 ml), the organic layer dried ($MgSO_4$), and evaporated under reduced pressure to leave a yellow solid (1.56 g, 72%). υ_{max} (nujol/ cm^{-1}) 1670 (C=O); δ_H (200 MHz; C^2HCl_3) 1.40 (3H, t., *J* 7 Hz, $OCH_2C\underline{H}_3$), 4.41 (2H, q., *J* 7 Hz, $OC\underline{H}_2CH_3$), 7.39 (1H, t., $J_{4,5}$ =$J_{5,6}$ 5 Hz, 5-CH), 8.31 (1H, d., $J_{4,5}$ 5 Hz, 4-CH), 8.77 (1H, d., $J_{5,6}$ 5 Hz, 6-CH), 9.23 (1H, s., 2-CH); δ_C (50.31 MHz; C^2HCl_3) 14.5 ($OCH_2\underline{C}H_3$), 62.6 (OCH_2), 125.3 (5-C), 131.0 (3-C), 140.8 (4-C), 148.0 (6-C), 150.2 (2-CH).

Diethyl 3-methylpyridine-2-phosphonate (49)

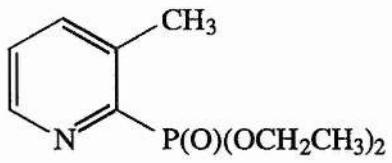

n-Butyl lithium (2.5 M in hexanes) (16.8 ml, 0.042 mol) was added dropwise to diethyl phosphite (7.0 g, 0.042 mol) at - 20 to - 30 °C under a nitrogen atmosphere over 2 hours. Meanwhile 3-methylpyridine *N*-oxide (5.33 g, 0.042 mol) and dimethyl sulfate (4.61 g, 0.042 mol) were heated together to 60 °C for 2 hours, under a nitrogen atmosphere. The resulting *N*-methoxy 3-methylpyridine methylsulfate was dissolved in diethyl phosphite (15 ml) and added dropwise to the diethyl lithium phosphonate at - 20 to - 30 °C under a nitrogen atmosphere over 2 hours. The reaction was allowed to warm to room temperature and stirred overnight. Water (50 ml) was added to the reaction mixture, which was then extracted with dichloromethane (3 x 50 ml). Extraction by acidification (4 M hydrochloric acid, 50 ml) was followed by basification and re-extraction with dichloromethane (3 x 30 ml). The solvent was removed under reduced pressure, and fractional distillation of the yellow oil using the Kugelrohr apparatus to produce a clear oil (8.53 g, 89%). (Found: C, 51.99; H, 7.56; N, 6.63; Calc. for $C_{10}H_{16}NO_3P$: C, 52.40; H, 7.04; N, 6.11%); υ_{max} (nujol/ cm^{-1}) 2960 (-OCH_2), 1480 (P-py), 1240 (P=O), 1020 (P-OCH_2); δ_H (200 MHz; C^2HCl_3) 1.22 (6H, t., *J* 7 Hz, $C\underline{H}_3CH_2$), 2.50 (4H, s., CH_3), 4.11 (4H, q., *J* 7 Hz, OCH_2), 7.19 (1H, dd., $J_{4,5}$ 6 Hz, $J_{5,6}$ 5 Hz, 5-CH), 7.44 (1H, t., $J_{4,5}$ 6 Hz, 4-CH), 8.46 (1H, d., $J_{5,6}$ 5 Hz, 6-H); δ_C (50.31 MHz; C^2HCl_3) 16.8 ($\underline{C}H_3CH_2$), 19.8 (CH_3), 63.2 (OCH_2), 126.1(5-C), 128.3 (3-C), 139.2 (4-C), 147.8 (6-C), 151.8 (2-C); δ_P (121.5 MHz; C^2HCl_3) 12.20; *m/z* (CI) 229 (*M*, 25%), 200 (30, [*M* - CH_2CH_3]), 185 (37, [*M* - C_3H_8]), 93 (100, C_6H_7N).

3-Methylpyridine-2-phosphonic acid (58)

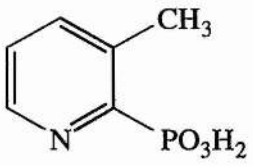

Diethyl 3-methylpyridine-2-phosphonate (0.80 g, 3.5 mmol) was dissolved in 6 M hydrochloric acid (15 ml) and heated to reflux for 6 hours. Upon cooling, the acid was evaporated under reduced pressure, and trituration of this resulting oil produced a white solid which was recrystallised from boiling water to produce white crystals (0.45 g, 75%). m.p. 284 °C (lit.,[145] 282 °C). (Found: C, 41.38; H, 4.67; N, 7.87; Calc., for $C_6H_8NO_3P$: C, 41.63; H, 4.68; N, 8.09%); δ_H (200 MHz; ^2H_2O) 2.60 (3H, s., CH_3), 7.87 (1H, t., $J_{5,6}$ 4 Hz, 5-CH), 8.34 (1H, dd., $J_{4,5}$ 4 Hz, $J_{4,6}$ 2 Hz, 4-CH), 8.46 (1H, d., $J_{5,6}$ 4 Hz, 6-CH); δ_C (50.31 MHz; ^2H_2O) 21.3 (CH_3), 130.5 (5-C), 141.3 (4-C), 144.1 (3-C), 149.8 (2-C), 151.3 (6-CH); δ_P (121.5 MHz; ^2H_2O) 2.52; *m/z* (EI) 173 (*M*, 60%), 155 (18, *M* - H_2O), 108 (64, *M* - C_5H_3NP), 93 (100, C_6H_7N).

Attempted oxidation of 3-methylpyridine-2-phosphonic acid

3-Methylpyridine-2-phosphonic acid (0.2 g, 1.16 mmol) was dissolved in water (10 ml) and 3 eq. potassium permanganate (0.55 g, 3.48 mmol) added. This reaction mixture was heated to reflux over 1.5 hours, and kept at reflux for a further 2 hours. On cooling, manganese dioxide was removed by filtering through celite and the residue washed with boiling water. The combined filtrates were evaporated to dryness under reduced pressure to produce a white solid. This solid could not be dissolved in any NMR solvent.

Diethyl (3-bromomethyl)pyridine-2-phosphonate (60)

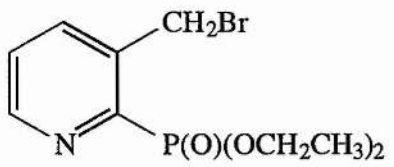

Diethyl 3-methylpyridine-2-phosphonate (1.00 g, 4.4 mmol) was dissolved in carbon tetrachloride (15 ml). This was added to a solution of dibenzoyl peroxide (0.11 g, 0.44 mmol) and *N*-bromosuccinimide (0.80 g, 4.4 mmol) in carbon tetrachloride (15 ml). This mixture was heated to reflux for two days, with benzoyl peroxide added at regular intervals, and the reaction followed by tlc (ethyl acetate). When no further reaction was detected, the reaction mixture was filtered and the carbon tetrachloride removed under reduced pressure. The dark oil remaining was purified by silica gel column chromatography, with ethyl acetate as elutant, to give a pale orange solid of diethyl (3-bromomethyl)pyridine-2-phosphonate as the product (0.35 g, 30%). *m/z* (EI^+) (Found: [*M*] 306.9969. $C_{10}H_{15}NO_3PBr$ requires 306.9972); υ_{max} (nujol/ cm^{-1}) 1300 (P=O); δ_H (200 MHz; C^2HCl_3) 1.27 (6H, t., *J* 8 Hz, CH_3CH_2), 4.17 (4H, q., *J* 8 Hz, OCH_2), 4.93 (2H, s., CH_2), 7.36 (1H, dd., $J_{4,5}$ 7 Hz, $J_{5,6}$ 6 Hz, 4-CH), 7.79 (1H, t., $J_{4,5}$ 7 Hz, 5-CH), 8.62 (1H, d., $J_{5,6}$ 6 Hz, 6-H); δ_C (50.31 MHz; C^2HCl_3) 16.7, 16.8 ($\underline{C}H_3CH_2$), 29.8 (CH_2Br), 63.7, 63.8 (OCH_2), 126.6(5-C), 138.8 (3-C), 139.8 (4-C), 149.6 (6-C), 152.0 (2-C); δ_p (121.5 MHz; C^2HCl_3) 10.1 *m/z* (EI^+) 307, 309 (*M*, 17%), 228 (79, [*M* - Br]), 154 (100, [*M* - $C_4H_{10}OBr$]), 93 (47, C_6H_7N).

Attempted oxidation of diethyl (3-bromomethyl)pyridine-2-phosphonate

Diethyl (3-bromomethyl)pyridine-2-phosphonate (0.13 g, 0.42 mmol), sodium nitrite (0.21 g, 3 mmol) and acetic acid (0.60 g, 10 mmol) were dissolved in dimethyl sulfoxide (2 ml), the solution stirred at 35 °C for 48 hours, and the reaction followed by tlc (cellulose; H_2O). The reaction was acidified (2 M hydrochloric acid) and the

solvents removed under reduced pressure. Prep. tlc (cellulose; 6:6:1 isopropanol:H_2O:NH_3) was attempted but no product isolated.

Methyl (2-bromomethyl)nicotinate (68)

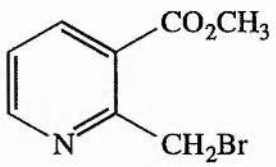

Methyl 2-methylnicotinate (3.02 g, 0.01 mol) was dissolved in carbon tetrachloride (25 ml). This was added to a solution of dibenzoyl peroxide (0.40 g) and *N*-bromosuccinimide (4.84 g, 0.01 mol) in carbon tetrachloride (25 ml). This mixture was heated to reflux for two days, with dibenzoyl peroxide added at regular intervals, and the reaction followed by tlc (3:2 40/60 petroleum ether:ethyl acetate). When no further reaction was detected, the reaction mixture was cooled and filtered. The carbon tetrachloride was removed under reduced pressure to leave a dark brown oil. Purification by silica gel column chromatography, using 3:2 40/60 petroleum ether:ethyl acetate as elutant, produced a reddish-brown solid as the product (1.32 g, 29%). *m/z* (EI^+) (Found: [*M*] 228.9731. $C_8H_8NO_2Br$ requires 228.9738); υ_{max} (cm^{-1}) 2850 ($-OCH_3$), 1745 (C=O); δ_H (200 MHz; C^2HCl_3) 3.93 (3H, s., OCH_3), 5.02 (2H, s., CH_2Br), 7.29 (1H, mult., 5-CH), 8.24 (1H, d., $J_{4,5}$ 8 Hz, 4-CH), 8.67 (1H, d., $J_{5,6}$ 7 Hz, 6-H); δ_C (50.31 MHz; C^2HCl_3) 32.9 (OCH_3), 53.2 (CH_2Br), 125.5 (5-C), 125.5 (3-C), 139.7 (4-C), 152.8 (6-C), 158.3 (2-C), 166.2 (carbonyl); *m/z* (EI^+) 228, 230 (*M*, 12, 11%), 150 (100, [*M* - Br]), 122 (26, [*M* - Br-C_2H_4]), 93 (32, C_6H_7N).

Diethyl (3-methoxycarbonyl-2-pyridyl)methylphosphonate (69)

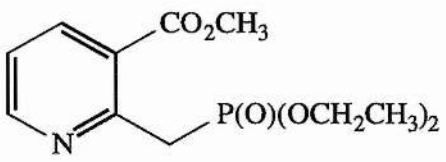

n-Butyl lithium (2.5 M in hexanes) (2.4 ml, 6 mmol) was added dropwise to diethyl phosphite (1.0 g, 6 mmol) at - 20 to - 30 °C under a nitrogen atmosphere over 2 hours. Methyl (2-bromomethyl)nicotinate (0.69 g, 3 mmol) was dissolved in diethyl phosphite (10 ml) and added dropwise to the diethyl lithium phosphonate at - 20 to - 30 °C under a nitrogen atmosphere over 2 hours. The reaction was allowed to warm to room temperature and stirred overnight, as the reaction was followed by tlc (silica; 9:1 ethyl acetate: methanol). Upon completion, water (10 ml) was added to the reaction mixture, which was then extracted with dichloromethane (2 x 20 ml). The organic layer was dried ($MgSO_4$) and the solvent removed under reduced pressure, and the yellow oil purified by silica gel column chromatography, elutant 9:1 ethyl acetate: methanol, to produce a clear oil (0.14 g, 14%). *m/z* (EI^+) (Found: [*M*] 288.1036. $C_{12}H_{19}NO_5P$ requires 288.2615); υ_{max} (cm^{-1}) 3500 (-OCH_3), 1730 (C=O), 1290 (P=O); δ_H (200 MHz; C^2HCl_3) 1.14 (6H, t., *J* 6 Hz, $OCH_2C\underline{H}_3$), 3.83 (3H, s., $CO_2C\underline{H}_3$), 3.95 (6H, mult., 2x $OC\underline{H}_2CH_3$ + CH_2P), 7.18 (1H, mult., 5-CH), 8.34 (1H, d., $J_{4,5}$ 8 Hz, 4-CH), 8.57 (1H, d., $J_{5,6}$ 8 Hz, 6-CH); δ_C (50.31 MHz; C^2HCl_3) 16.8 ($OC\underline{H}_2CH_3$), 35.2 (d., *J* 130 Hz, CH_2P), 52.2 ($CO_2C\underline{H}_3$), 62.5 (d., *J* 7 Hz, $POC\underline{H}_2CH_3$), 122.2 (5-C), 126.8 (3-CH), 138.2 (6-CH), 139.2 (4-C), 154.2 (2-CH); δ_P (121.5 MHz; C^2HCl_3) 25.14; m/z (EI) 288 (*M*, 7%), 183 (18, *M* - $O_3(CH_2CH_3)_2$), 136 (100, *M* - $O_3(CH_2CH_3)_2$ - CH_2P).

2-(Phosphonomethyl)nicotinic acid (66)

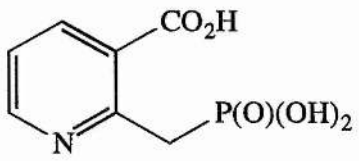

Diethyl (3-methoxycarbonyl-2-pyridyl)methylphosphonate (0.14 g, 0.49 mmol) was dissolved in concentrated hydrochloric acid (2 ml) and heated to 60 °C for 24 hours, as the reaction was followed by tlc (ethyl acetate). The excess acid was removed under reduced pressure, and the white solid produced recrystallised from boiling methanol to produce a white solid (0.10 g, 95%). m.p. 256-258 °C; υ_{max} (nujol/ cm^{-1}) 2700 (-OH), 1720 (C=O), 1280 (P=O); δ_H (200 MHz; $^2H_2O/NaO^2H$) 3.30 (2H, d., *J* 20 Hz, CH_2P), 7.12 (1H, t., $J_{4,5} = J_{5,6}$ 8 Hz, 5-CH), 7.68 (1H, d., $J_{4,5}$ 8 Hz, 4-CH), 8.67 (1H, d., $J_{5,6}$ 8 Hz, 6-H); δ_C (50.31 MHz; ^2H_2O) 40.1 (d., *J* 115 Hz, CH_2P), 123.4 (5-C), 137.5 (d.,$J_{C\text{-}P}$ 5 Hz, 3-C), 139.2 (4-C), 150.9 (6-C), 157.5 (d.,$J_{C\text{-}P}$ 9Hz, 2-C), 166.2 (carbonyl); δ_P (121.5 MHz; ^2H_2O) 16.30. *m/z* (EI^+) 219 (*M*, 15%), 200 (18, [*M* - H_2O]), 119 (100, C_5H_5NP).

Diethyl quinolinate (109)

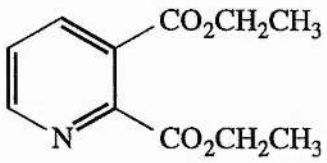

A mixture of quinolinic acid (3.0 g, 0.018 mol), ethanol (14 ml), and concentrated sulphuric acid (3 ml) was heated to reflux overnight. The solution was then cooled and poured onto crushed ice (10.0 g). Concentrated ammonia solution was added until the solution was strongly alkaline. Some of the ester separated as an oil but most remained dissolved in the solution. The mixture was extracted with ether (3x 40

ml), the ethereal layers were dried ($MgSO_4$), and then the sovent removed under reduced pressure. The oil produced was distilled using the Kugelrohr apparatus at water pump pressure to give a colourless oil, (2.53 g, 63%). υ_{max} (cm^{-1}) 2920 (OCH_3), 1700 (C=O); δ_H (200 MHz; C^2HCl_3) 1.35 and 1.39 (6H, 2x t., *J* 8 Hz, $C\underline{H}_3CH_2$-), 4.39 and 4.42 (4H, 2x q., *J* 8 Hz, $CH_3C\underline{H}_2$-), 7.45 (1H, dd., $J_{4,5}$ 8 Hz, $J_{5,6}$ 6 Hz, 5-CH), 8.17 (1H, dd., $J_{4,5}$ 8 Hz, $J_{4,6}$ 2 Hz, 4-CH), 8.71 (1H, dd., $J_{5,6}$ 6 Hz, $J_{4,6}$ 2 Hz, 6-CH); δ_C (50.31 MHz; C^2HCl_3) 14.05 ($\underline{C}H_3CH_2$-), 62.0 and 62.1 ($CH_3\underline{C}H_2$-), 125.0 (5-C), 126.0 (3-C), 137.8 (4-C), 151.5 (2-C), 151.9 (6-C), 165.0 and 166.4 (carbonyl).

Diethyl *N*-methylquinolinium methylsulfonate

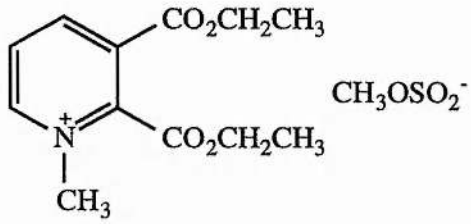

Dimethyl sulfate (1.13 g, 9 mmol) was added slowly, with stirring, to diethyl quinolinate (2.0 g, 9 mmol) and the reaction stirred overnight at 60-70 °C. The solution was then cooled and placed in an acetone/ $CO_{2(s)}$ bath where a glass formed, which on removal from the acetone/ $CO_{2(s)}$ bath crystallised out to a white solid. This was then recrystallised from ethanol to give the product as white crystals (2.50 g, 83%). δ_H (200 MHz; C^2HCl_3) 1.34 and 1.38 (6H, 2 x t., *J* 7 Hz, CH_3's), 3.53 (3H, s., S-OCH_3), 4.40 (2H, q., *J* 7 Hz, 3-$CO_2C\underline{H}_2$), 4.50 (3H, s., NCH_3), 4.54 (2H, q., *J* 7 Hz, 2-$CO_2C\underline{H}_2$), 8.21 (1H, t., $J_{4,5}$=$J_{5,6}$ 8 Hz, 5-CH), 9.07 (1H, d., $J_{4,5}$ 8 Hz, 4-CH), 9.12 (1H, d., $J_{5,6}$ 8 Hz, 6-CH); δ_C (50.31 MHz; C^2HCl_3) 16.1 and 16.4 (CH_3's), 50.2 ($SOCH_3$), 58.0 (NCH_3) 67.5 and 68.8 (OCH_2's), 131.8 (3-C), 132.2 (5-C), 149.3 (2-C), 150.6 (6-C), 153.1 (4-C), 163.6 and 165.1 (carbonyl).

N-Methylquinoliniium-2,3-dicarboxylic acid (107)

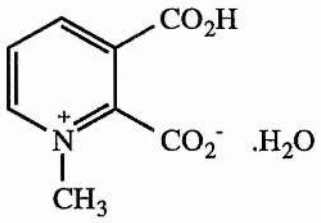

Diethyl *N*-methylquinolinium methylsulfonate (2.5 g, 0.01 mol) was dissolved in concentrated hydrochloric acid (27.5 ml) and heated to reflux for 2 hours at 100 °C. Upon cooling, excess acid was removed under reduced pressure to produce a white solid. This was recrystallised from methanol, to give the product as white crystals (1.86 g, 81%). m.p. 156-8 °C; (Found: C, 48.55; H, 4.60; N, 7.02. Calc. for $C_8H_9NO_5$: C, 48.25; H, 4.55; N, 7.02%); υ_{max} (nujol/ cm^{-1}) 3420 (O-H), 1650 (C=O); δ_H (200 MHz; ^2H_2O) 4.35 (3H, s., NCH_3), 7.93 (1H, t., $J_{4,5}$=$J_{5,6}$ 6 Hz, 5-CH), 8.78 (1H, d., $J_{4,5}$ 6 Hz, 4-CH), 8.91 (1H, d., $J_{5,6}$ 6 Hz, 6-CH); δ_C (50.31 MHz; ^2H_2O) 49.6 (NCH_3), 128.9 (3-C), 131.6 (5-C), 150.1 (2-C), 150.3 (4-C and 6-C), 151.1 and 151.9 (carbonyl).

Ethyl *N*-methylpicolinium methylsulfonate

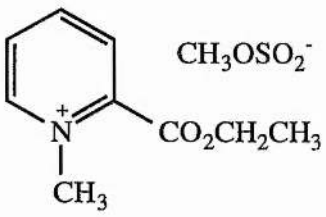

Dimethyl sulfate (6.3 g, 0.05 mol) was added slowly, with stirring, to ethyl picolinate (7.6 g, 0.05 mol) and the reaction stirred overnight at 60-70 °C. The solution was then cooled and placed in an acetone/ $CO_{2(s)}$ bath where a glass formed, which on removal from the acetone/ $CO_{2(s)}$ bath crystallised out to a white solid. This was then

recrystallised from ethanol to give the product as white crystals (12.3 g, 88 %). υ_{max} (nujol/ cm^{-1}) 1710 (C=O); δ_H (200 MHz; C^2HCl_3) 1.33 (3H, t., *J* 8 Hz, $-OCH_2\underline{C}H_3$), 3.49 (3H, s., $SOCH_3$), 4.46 (2H, q., *J* 9 Hz, $-OC\underline{H}_2CH_3$), 4.60 (3H, s., $N-CH_3$), 7.38 (1H, t., $J_{4,5} = J_{5,6}$ 6 Hz, 5-CH), 7.73 (1H, d., *J* 8 Hz, 3-CH), 8.04 (1H, t., $J_{4,5}$ 6 Hz, 4-CH), 8.65 (1H, d., $J_{5,6}$ 6 Hz, 6-CH); δ_C (50.31 MHz; C^2HCl_3) 13.9 ($\underline{C}H_3CH_2O$), 49.1 (CH_3OS), 54.0 (NCH_3), 64.4 ($CH_3\underline{C}H_2O$), 130.3 (3-C), 130.8 (5-C), 142.5 (2-C), 147.2 (6-C), 150.0 (4-C), 159.6 (carbonyl).

N-Methylpicolinium hydrogensulfate (84)

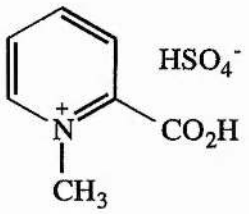

Ethyl *N*-methylpicolinium methylsulfonate (12.3 g, 0.045 mol) was dissolved in concentrated hydrochloric acid (27.5 ml) and heated to reflux for 2 hours at 100 °C. This was then crystallised in the same way as *N*-methylpyridinium-2,3-dicarboxylic acid, and recrystallised from methanol, to give the product as a white solid (7.96 g, 95%). m.p. 169-171 °C (lit.[194] 170-173 °C); (Found: C, 35.64; H, 3.74; N, 5.91. Calc for $C_7H_9NSO_6$: C, 35.74; H, 3.85; N, 5.95%); υ_{max} (nujol/ cm^{-1}) 3050 (-OH), 1760 (C=O); δ_H (200 MHz; ^2H_2O) 4.39 (3H, s., $N-CH_3$), 7.90 (1H, t., $J_{3,4} = J_{4,5}$ 8 Hz, 4-CH), 8.08 (1H, d., $J_{3,4}$ 8 Hz, 3-CH), 8.43 (1H, t., $J_{4,5} = J_{5,6}$ 8 Hz, 5-CH), 8.66 (1H, d., $J_{5,6}$ 8 Hz, 6-CH); δ_C (50.31 MHz; ^2H_2O) 50.7 ($N-CH_3$), 131.6 (3-C), 132.0 (5-C), 147.5 (2-C), 149.1 (6-C), 150.5 (4-C), 164.9 (carbonyl).

Ethyl *N*-methylnicotinium hydrogensulfate

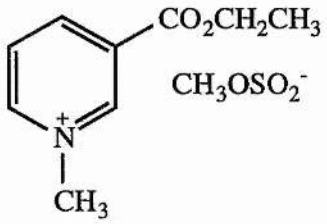

This was synthesised in the identical manner as for ethyl *N*-methylpicolinium methyl sulfate, except using ethyl nicotinate, to give the product as white crystals (12.5 g, 90%). υ_{max} (nujol/ cm^{-1}) 1710 (C=O); δ_H (200 MHz; C^2HCl_3) 1.19 (3H, t., *J* 8 Hz, $-OCH_2C\underline{H}_3$), 3.29 (3H, s., $SOCH_3$), 4.24 (2H, q., *J* 7 Hz, $-OC\underline{H}_2CH_3$), 4.38 (3H, s., $N-CH_3$), 8.08 (1H, t., *J* 6 Hz, 5-CH), 8.73 (1H, d., *J* 7 Hz, 4-CH), 8.97 (1H, d., *J* 6 Hz, 6-CH), 9.19 (1H, s., 2-CH); δ_C (50.31 MHz; C^2HCl_3) 14.3 ($\underline{C}H_3CH_2O$), 49.5 (CH_3OS), 54.6 (NCH_3), 63.5 ($CH_3\underline{C}H_2O$), 128.9 (5-C), 130.7 (3-C), 145.1 (2-C), 147.0 (6-C), 149.5 (4-C), 162.1 (carbonyl C).

N-Methylnicotinium hydrogensulfate (110)

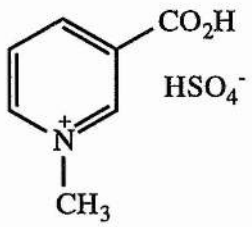

This was synthesised in the identical manner as for *N*-methylpicolinium hydrogensulfate, except using ethyl *N*-methylnicotinium methylsulfonate (12.3 g, 0.045 mol) in concentrated hydrochloric acid to give the product as white crystals (7.80, 90%). m.p. 167 °C; (Found: C, 36.14; H, 3.90; N, 6.00. Calc for $C_7H_9NSO_6$: C, 35.74; H, 3.85; N, 5.95%); υ_{max} (nujol/ cm^{-1}) 3050 (-OH), 1760 (C=O); δ_H (200 MHz; ^2H_2O) 4.44 (3H, s., N-CH_3), 8.13 (1H, t., $J_{4,5}$=$J_{5,6}$ 5 Hz, 5-CH), 8.94 (2H, t., $J_{4,5}$, 4-CH), 8.97 (1H, t., $J_{5,6}$ 5 Hz, 6-CH), 9.35 (1H, s., 2-CH); δ_C (50.31 MHz; ^2H_2O) 51.3 (N-CH_3), 130.9 (5-C), 147.7 (3-C), 148.3 (2-C), 149.5 (6-C), 150.8 (4-C), 164.2 (carbonyl).

N-Ethylpyridinium-2,3-dicarboxylic acid monohydrate (108)

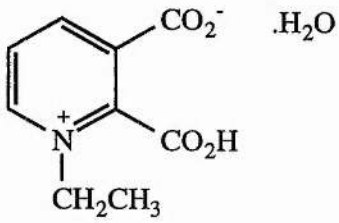

Diethyl sulfate (1.38 g, 8.96 mmol), was added slowly to diethyl quinolinate (1.00 g, 4.48 mmol) and this mixture stirred for 24 hours at 40-45 °C, under a nitrogen atmosphere. The reaction was followed by tlc (3:2 40/60 petroleum ether/ ethyl acetate), and upon completion excess diethyl sulphate was removed under reduced pressure. The structure of *N*-ethylquinolinium ethylsulfonate was confirmed by ^1H

and ^{13}C n.m.r but not isolated. δ_H (200 MHz; C^2HCl_3) 1.26 (3H, t., *J* 7 Hz, $COCH_2C\underline{H}_3$), 1.42 (6H, 2x t., *J* 7 Hz, $SOCH_2C\underline{H}_3$), 1.71 (3H, t., *J* 8 Hz, $NCH_2C\underline{H}_3$), 4.10 (2H, q., *J* 7 Hz, $SOC\underline{H}_2CH_3$), 4.46 and 4.60 (4H, 2x q., *J* 7 Hz, $COC\underline{H}_2CH_3$), 4.78 (2H, q., *J* 8 Hz, $NC\underline{H}_2CH_3$), 8.55 (1H, t., $J_{4,5}= J_{5,6}$ 6 Hz, 5-CH), 9.10 (1H, d., $J_{4,5}$ 6 Hz, 4-CH), 9.63 (1H, d., $J_{5,6}$ 6 Hz, 6-CH); δ_C (50.31 MHz; C^2HCl_3) 14.1 and 14.4 ($COCH_2C\underline{H}_3$), 15.6 ($SOCH_2C\underline{H}_3$), 17.6 ($NCH_2C\underline{H}_3$), 53.4 ($SOC\underline{H}_2CH_3$), 63.9 and 64.4 ($COC\underline{H}_2CH_3$), 65.6 ($NC\underline{H}_2CH_3$), 129.0 (5-C), 131.1 (3-C), 146.9 (4-C), 147.7 (6-C), 151.0 (2-C), 160.1 and 161.1 (carbonyl).

Diethyl *N*-ethylquinolinium ethylsulfonate (1.5 g, 3.8 mmol) was dissolved in concentrated HCl (12.5 ml) and refluxed for 12 hours at 100 °C. Upon cooling, excess acid was removed under reduced pressure to produce a white solid. This was recrystallised from methanol, to give the product as white crystals (1.86 g, 81%). m.p. 146 °C; (Found: C, 50.89; H, 5.03; N, 6.47. Calc. for $C_9H_{11}NO_5$: C, 50.71; H, 5.20; N, 6.57%); υ_{max} (nujol/ cm^{-1}) 3020 (O-H), 1720 (C=O); δ_H (200 MHz; ^2H_2O) 1.54 (3H, t., *J* 7 Hz, $NCH_2C\underline{H}_3$), 4.06 (2H, q., *J* 7 Hz, $NC\underline{H}_2CH_3$), 8.01 (1H, t., $J_{4,5}=J_{5,6}$ 7 Hz, 5-CH), 8.89 (1H, d., $J_{4,5}$ 7 Hz, 4-CH), 8.94 (1H, d., $J_{5,6}$ 7 Hz, 6-CH); δ_C (50.31 MHz; ^2H_2O) 18.8 ($NCH_2C\underline{H}_3$), 58.6 ($NC\underline{H}_2CH_3$), 129.2 (3-C), 129.4 (5-C), 148.5 (4-C), 150.2 (2-C and 6-C), 176.7 and 178,6 (carbonyls).

N-Ethylpicolinium hydrogensulfate (112)

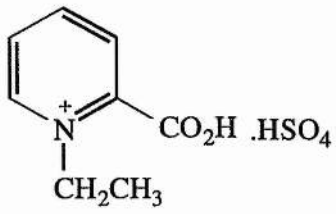

N-Ethyl picolinic acid was synthesised in an identical manner to *N*-ethyl quinolinic acid, except that ethyl picolinate (3.02 g, 0.02 mol) was heated with diethyl sulfate (3.08 g, 0.02 mol). The intermediate ethyl *N*-ethylpicolinium ethylsulfonate was confirmed by ^{1}H and ^{13}C nmr, but not isolated. δ_H (200 MHz; C^2HCl_3) 1.26 (3H, t., *J* 7 Hz, $COCH_2C\underline{H}_3$), 1.47 (3H, t., *J* 8 Hz, $SOCH_2C\underline{H}_3$), 1.68 (3H, t., *J* 8 Hz, $NCH_2C\underline{H}_3$), 4.05 (2H, q., *J* 7 Hz, $COC\underline{H}_2CH_3$), 4.54 (2H, q., *J* 8 Hz, $COC\underline{H}_2CH_3$), 5.06 (2H, q., *J* 8 Hz, $NC\underline{H}_2CH_3$), 8.38 (1H, mult., 5-CH), 8.47 (1H, d., $J_{3,4}$ 9 Hz, 3-CH), 8.76 (1H, t., $J_{3,4} = J_{4,5}$ 9 Hz, 4-CH), 9.50 (1H, d., $J_{5,6}$ 8 Hz, 6-CH); δ_C (50.31 MHz; C^2HCl_3) 14.3 ($COCH_2C\underline{H}_3$), 15.4 ($SOCH_2C\underline{H}_3$), 17.4 ($NCH_2C\underline{H}_3$), 58.5 ($CSOC\underline{H}_2CH_3$), 65.0 ($SOC\underline{H}_2CH_3$), 65.1 ($NC\underline{H}_2CH_3$), 131.1 (5-C), 132.0 (3-C), 142.5 (2-C), 147.8 (4-C), 149.3 (6-C), 159.9 (carbonyl).

This was then treated with hydrochloric acid (25 ml) and the solid produced upon removal of excess hydrochloric acid recrystallised from boiling methanol to form *N*-ethyl picolinic acid (2.11 g, 62%). υ_{max} (nujol/ cm^{-1}) 3000 (O-H), 1720 (C=O); δ_H (200 MHz; ^2H_2O) 1.29 (3H, t., *J* 8 Hz, $NCH_2C\underline{H}_3$), 4.53 (2H, q., *J* 8 Hz, $NC\underline{H}_2CH_3$), 7.78 (1H, t., $J_{4,5} = J_{5,6}$ 6 Hz, 5-CH), 7.94 (1H, d., $J_{3,4}$ 9 Hz, 3-CH), 8.30 (1H, t., $J_{3,4} = J_{4,5}$ 9 Hz, 4-CH), 8.58 (1H, d., $J_{5,6}$ 6 Hz, 6-CH); δ_C (50.31 MHz; ^2H_2O) 18.6 ($NCH_2C\underline{H}_3$), 58.6 ($NC\underline{H}_2CH_3$), 130.8 (5-C), 131.5 (3-C), 148.3 (4-C), 149.0 (6-C), 150.9 (2-C), 166.6 (carbonyl).

N-Ethylnicotinium hydrogensulfate (111)

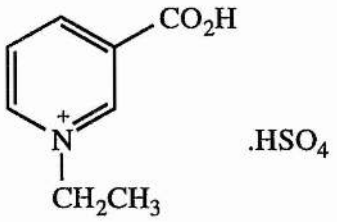

N-Ethylnicotinium hydrogensulfate was synthesised in an identical manner to *N*-ethyl quinolinic acid, except that ethyl nicotinate (3.02 g, 0.02 mol) was heated with diethyl sulfate (3.08 g, 0.02 mol). The intermediate ethyl *N*-ethylnicotinium ethylsulfonate was confirmed by ^{1}H and ^{13}C nmr, but not isolated. δ_H (200 MHz; C^2HCl_3) 1.21 (3H, t., *J* 8 Hz, $SOCH_2C\underline{H}_3$), 1.50 (3H, t., *J* 8 Hz, $COCH_2C\underline{H}_3$), 1.70 (3H, t., *J* 7 Hz, $NCH_2C\underline{H}_3$), 4.03 (2H, q., *J* 8 Hz, $SOC\underline{H}_2CH_3$), 4.45 (2H, q., *J* 8 Hz, $COC\underline{H}_2CH_3$), 4.88 (2H, q., *J* 7 Hz, $NC\underline{H}_2CH_3$), 8.27 (1H, t., $J_{4,5}= J_{5,6}$ 6 Hz, 5-CH), 8.90 (1H, d., $J_{4,5}$ 6 Hz, 4-CH), 9.33 (1H, s., 2-CH), 9.36 (1H, d., $J_{5,6}$ 6 Hz, 6-CH); δ_C (50.31 MHz; C^2HCl_3) 14.5 ($COCH_2C\underline{H}_3$), 15.7 ($SOCH_2C\underline{H}_3$), 17.4 ($NCH_2C\underline{H}_3$), 58.8 ($SOC\underline{H}_2CH_3$), 63.5 ($COC\underline{H}_2CH_3$), 63.8 ($NC\underline{H}_2CH_3$), 129.6 (5-C), 131.5 (3-C), 145.4 (4-C), 145.9 (6-C), 149.2 (2-C), 161.7 (carbonyl).

This was then dissolved in hydrochloric acid (25 ml) and the solution heated to 50 °C for 12 hours. The solid produced upon removal of excess hydrochloric acid was recrystallised from boiling methanol to form *N*-ethylnicotinium hydrogensulfate (2.43 g, 72%). m.p. 234-236 °C; υ_{max} (nujol/ cm^{-1}) 3000 (O-H), 1730 (C=O); δ_H (200 MHz; ^2H_2O) 1.54 (3H, t., *J* 7 Hz, $NCH_2C\underline{H}_3$), 4.52 (2H, t., *J* 7 Hz, $NC\underline{H}_2CH_3$), 8.08 (1H, t., $J_{4,5}=J_{5,6}$ 7 Hz, 5-CH), 8.88 (1H, d., $J_{4,5}$ 7 Hz, 4-CH), 8.95 (1H, d., $J_{5,6}$ 7 Hz, 6-CH), 9.34 (1H, s., 2-CH); δ_C (50.31 MHz; ^2H_2O) 18.3 ($NCH_2C\underline{H}_3$), 60.6 ($NC\underline{H}_2CH_3$), 131.2 (5-C), 134.0 (3-C), 148.0 (4-C), 148.4 (6-C), 149.8 (2-C), 167.1 (carbonyl).

Dimethyl quinolinate (116)

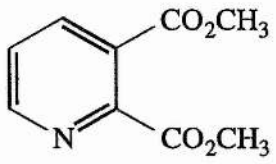

A mixture of quinolinic acid (6.0 g, 0.0368 mol), methanol (30 ml), and concentrated sulfuric acid (6 ml) was refluxed overnight. The solution was then cooled and poured onto crushed ice (20 g). Concentrated ammonia solution was added until the solution was strongly alkaline.This solution was extracted with ether (3x 40 ml), the ethereal layers dried ($MgSO_4$), and then the solvent removed under reduced pressure to preduce a white solid, (5.43 g, 78%). Recrystallisation from diethyl ether produced white crystals upon filtration. m.p. 55 °C; (Found: C, 55.55; H, 4.72; N, 7.13; Calc., for $C_9H_9NO_4$: C, 55.39; H, 4.65; N, 7.18%); υ_{max} (nujol/cm^{-1}) 1760 (C=O); δ_H (200 MHz; C^2HCl_3) 3.88 (3H, s., CH_3) 3.95 (3H, s., CH_3), 7.46 (1H, dd., $J_{4,5}$ 8 Hz, $J_{5,6}$ 3 Hz, 5-CH), 8.12 (1H, d., $J_{4,5}$ 8 Hz, 4-CH), 8.71 (1H, d., $J_{5,6}$ 3 Hz, 6-CH); δ_C (50.31 MHz; C^2HCl_3) 53.48 and 53.62 (CH_3), 125.5 (5-C), 126.9 (3-C), 138.1 (4-C), 151.0 (2-C), 152.2 (6-C), 166.2 and 167.0 (carbonyl); *m/z* (CI) 195 (M, 11%), 164 (100, M-OCH_3), 136 (86, M-CO_2CH_3), 107 (67, M-CO_2CH_3-CHO), 79 (83, C_5H_5N).

N-Propylnicotinium chloride (115)

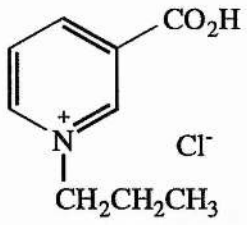

i) 1-Iodopropane with ethyl nicotinate

1-Iodopropane (3.40 g, 0.02 mol) was added slowly to ethyl nicotinate (1.51 g, 0.01 mol) and the mixture heated for 24 hours under a nitrogen atmosphere. The reaction was followed by tlc (3:2 40/60 petroleum ether: ethyl acetate) and upon completion excess 1-iodopropane was removed under reduced pressure. A yellow solid was obtained (2.61 g, 81%). m.p. 68-70 °C; υ_{max} (nujol/ cm^{-1}) 1730 (C=O); δ_H (200 MHz; C^2HCl_3) 0.92 (3H, t., *J* 8 Hz, $COCH_2C\underline{H}_3$), 1.33 (3H, t., *J* 7 Hz, $NCH_2CH_2C\underline{H}_3$), 2.04 (2H, sextet, *J* 7 Hz, $NCH_2C\underline{H}_2CH_3$), 4.36 (2H, q., *J* 8 Hz, $COC\underline{H}_2CH_3$), 4.97 (2H, t., *J* 7 Hz, $NC\underline{H}_2CH_2CH_3$), 8.31 (1H, t., $J_{4,5}= J_{5,6}$ 7 Hz, 5-CH), 8.89 (1H, dd., $J_{4,5}$ 7 Hz, $J_{4,6}$ 2Hz, 4-CH), 9.58 (1H, s., 2-CH), 9.72 (1H, d., $J_{5,6}$ 7 Hz,$J_{4,6}$ 2Hz, 6-CH); δ_C (50.31 MHz; C^2HCl_3) 11.0 ($COCH_2C\underline{H}_3$), 14.8 ($NCH_2CH_2C\underline{H}_3$), 25.7 ($NCH_2C\underline{H}_2CH_3$), 64.1 ($COC\underline{H}_2CH_3$), 64.3 ($NC\underline{H}_2CH_2CH_3$), 129.6 (5-C), 131.3 (3-C), 145.8 (4-C), 148.9 (6-C), 1619.2 (2-C), 170.2 (carbonyl).

The propyl *N*-propylnicotiniumiodide (2.00 g, 6.3 mmol) was dissolved in concentrated hydrochloric acid (10 ml) and this solution heated for 24 hours. Upon completion, excess acid was reoved under reduced pressure to produce an off-white solid, which upon recrystallisation gave white crystals (1.05 g, 90% from ester). m.p. 81 °C; υ_{max} (nujol/ cm^{-1}) 3000 (O-H), 1710 (C=O); δ_H (200 MHz; ^2H_2O) 0.87 (3H, t., *J* 8 Hz, $NCH_2CH_2C\underline{H}_3$), 1.97 (3H, sextet., *J* 8 Hz, $NCH_2C\underline{H}_2CH_3$), 4.58 (2H, t., *J* 8 Hz, $NCH_2C\underline{H}_2CH_3$), 8.12 (1H, t., $J_{4,5}=J_{5,6}$ 7 Hz, 5-CH), 8.94 (1H, m., 6-CH, 4-CH), 9.33 (1H, s., 2-CH); δ_C (50.31 MHz; ^2H_2O) 6.3 ($NCH_2CH_2C\underline{H}_3$), 20.8

($NCH_2C\underline{H}_2CH_3$), 60.5 ($NC\underline{H}_2CH_2CH_3$), 125.3 (5-C), 128.7 (3-C), 142.6 (4-C), 144.0 (6-C), 144.1 (2-C), 161.6 (carbonyl).

ii) 1-Iodopropane with quinolinic acid anhydride

Quinolinic acid anhydride (0.5 g, 3.3 mmol) was dissolved in dry DMF (10 ml), excess 1-iodopropane added, and this solution heated gently (35 - 40 °C) for 2 days under a nitrogen atmosphere. The reaction was followed by tlc (silica; ethyl acetate) and upon completion excess 1-iodopropane and DMF were removed under reduced pressure to produce propyl *N*-propyl quinolinate as a brown oil (0.67 g, 67%). δ_H (200 MHz; C^2HCl_3) 0.88 (3H, t., *J* 8 Hz, $COCH_2CH_2C\underline{H}_3$), 1.28 (3H, t., *J* 7 Hz, $NCH_2CH_2C\underline{H}_3$), 1.84 (2H, sextet, *J* 7 Hz, $COCH_2C\underline{H}_2CH_3$), 2.00 (2H, sextet, *J* 7 Hz, $NCH_2C\underline{H}_2CH_3$), 4.36 (2H, q., *J* 8 Hz, $COC\underline{H}_2CH_2CH_3$), 4.97 (2H, t., *J* 7 Hz, $NC\underline{H}_2CH_2CH_3$), 8.27 (1H, t., $J_{4,5}$= $J_{5,6}$ 8 Hz, 5-CH), 8.80 (1H, dd., $J_{4,5}$ 8 Hz, $J_{4,6}$ 3 Hz, 4-CH), 9.67 (1H, d., $J_{5,6}$ 8 Hz, $J_{4,6}$ 3 Hz, 6-CH).

The ester was dissolved in concentrated hydrochloric acid and heated gently (< 40 °C) for 24 hours. Excess acid was removed under reduced pressure, again with gentle heat, to produce a white solid (0.40 g, 62% from anhydride). Spectral data as above.

n-Propyl trifluoromethanesulfate (*n*-propyl triflate)(117)

$CH_3CH_2CH_2OSO_2CF_3$

1-Iodopropane (1.99 g, 0.012 mol) was added to a suspension of silver trifluoromethanesulfate (3.0 g, 0.012 mol) in dry dichloromethane (15 ml). A precipitate of iodide was observed, and the reaction left to stir for 30 minutes until the reaction was completed. The precipitate was filtered through celite, and dichloromethane removed under reduced pressure, to produce an unstable brown oil (1.52 g, 66%). δ_H (200 MHz; C^2HCl_3) 1.02 (3H, t., *J* 7 Hz, $SOCH_2CH_2C\underline{H}_3$), 1.85 (2H, sextet, *J* 7 Hz, $SOCH_2C\underline{H}_2CH_3$), 4.51 (2H, t., *J* 7 Hz, $SOC\underline{H}_2CH_2CH_3$).

n-Octyl trifluoromethanesulfate (*n*-octyl triflate)(118)

$CH_3(CH_2)_6CH_2OSO_2CF_3$

A solution of *n*-octanol (1.30 g, 0.01 mol) and pyridine (0.79 g, 0.01 mol) in dichloromethane (5 ml) was added, dropwise over 45 minutes, to a solution of trifluoromethanesulfonic anhydride (2.82 g, 0.01 mol) in dichloromethane (20 ml) at 0 °C. The insoluble pyridinium salt was removed by filtration, and the dichloromethane removed by distillation to produce an oil (1.90 g, 71%). δ_H (200 MHz; C^2HCl_3) 0.90 (3H, t., *J* 6 Hz, $SOCH_2(CH_2)_6C\underline{H}_3$), 1.29 (10H, m., $SOCH_2CH_2(C\underline{H}_2)_5CH_3$), 1.83 (2H, quintet, *J* 7 Hz, $SOCH_2C\underline{H}_2(CH_2)_5CH_3$), 4.42 (2H, t., *J* 7 Hz, $SOC\underline{H}_2CH_2(CH_2)_5CH_3$); δ_C (50.31 MHz; C^2HCl_3) 14.2 ($SOCH_2(CH_2)_6C\underline{H}_3$), 21.0 ($SOCH_2(CH_2)_5C\underline{H}_2CH_3$), 25.8 ($SOCH_2(CH_2)_4CH_2C\underline{H}_2CH_3$), 29.9 ($SOCH_2CH_2(C\underline{H}_2)_3CH_2CH_2CH_3$), 32.1 ($SOCH_2C\underline{H}_2(CH_2)_5CH_3$), 53.8 ($SOC\underline{H}_2(CH_2)_6CH_3$).

2,3,4,6-Tetra-O-acetyl-α-D-glucopyranosyl bromide (119)

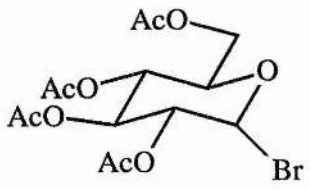

D-Glucose (19.5 g, 0.11 mol) was dissolved in acteic anhydride (75 ml), and 45% hydrogen bromide in acetic acid (30 ml) added dropwise. This solution was stirred under a nitrogen atmosphere at room temperature, and the reaction followed by tlc (3:2 40-60 petroleum ether: ethyl acetate, developed using 5% sulfuric acid in ethanol). When acetylation was complete further 45% hydrogen bromide in acetic acid (90 ml) was added, the solution stirred for 16 hours and the reaction followed by tlc as above. On completion dichloromethane (150 ml) was added to the solution and this solution poured onto ice/water, with stirring. The two layers were separated, and the organic layer washed twice with an ice/saturated sodium hydrogen carbonatate solution. The organic layer was separated, the organic layer dried ($MgSO_4$), and the solvent removed under reduced pressure to produce a white solid, which was recrystallised from diethyl ether to give a white powder (41.6 g, 94%). m.p. 87 °C (lit.[195] 88 °C); $[\alpha]_D$ +195.9° (c 2.42 in $CHCl_3$) (lit.[196] +197.84° (c 2.42 in $CHCl_3$)); ν_{max}(nujol/cm^{-1}) 1730 (CO); δ_H(200 MHz, C^2HCl_3) 2.04 (12 H, 4 x s., $COOCH_3$), 4.09 (1 H, m., 5-CH), 4.29 (2 H, m., 6^a,6^b-CH), 4.81 (1 H, dd., $J_{1,2}$ 4 Hz, $J_{2,3}$ 10 Hz, 2-CH), 5.14 (1 H, t., $J_{3,4} = J_{4,5}$ 10, 4-CH), 5.53 (1 H, t., $J_{2,3} = J_{3,4}$ 10 Hz, 3-CH), 6.59 (1 H, d., $J_{1,2}$ 4 Hz, 1-CH); δ_C(50.31 MHz, C^2HCl_3) 21.06, 21.16 (CH_3), 61.37 (6-C), 67.55 (4-C), 70.57 (2-C), 71.01 (5-C), 72.56 (3-C), 87.04 (1-C), 169.96, 170.28, 170.35, 171.00 (CO); *m/z* (CI) 428, 430 ($[M+NH_4]^+$, 18%), 331 (8, $[M-Br]^+$) and 213 (29, $[M-Br-2\ OAc]^+$).

Kinetics

Spectra

Ultraviolet absorption spectra were obtained using a Uvikon 932 spectrophotometer. Spectra were measured from 580 - 190 nm, and the change in absorption at 280 nm measured.

General Procedure

For measurements at pH 0.1, 0.25, 0.5, 1.0, 1.5, and 2.0, the acid to be studied (*ca.* 0.015 g) was dissolved in distilled water (23 ml), and potassium chloride added to adjust to constant ionic strength (1.0). Concentrated hydrochloric acid was then added to adjust the pH to the required value, and distilled water added to make up to 25 ml. The pH was then re-checked.

For pH 2.5 and 3.0, the acid (*ca.* 0.015 g) was dissolved in 50 mM potassium phosphate (24 ml), and potassium chloride added to adjust to constant ionic strength (1.0). Concentrated hydrochloric acid added to adjust the pH to the required value, and 50 mM potassium phosphate added to make up to 25 ml. The pH was then re-checked.

For pH values of 4.0, 5.0 and 6.0, the acid (*ca.* 0.015 g) was dissolved in 50 mM potassium phosphate (24 ml), and potassium chloride added to adjust to constant ionic strength (1.0). 1 M Sodium hydroxide solution added to adjust the pH to the required value, and 50 mM potassium phosphate added to make up to 25 ml. The pH was then re-checked.

Approximately 0.8 ml of the required solution was added to each 1 ml ampoule which was then sealed. The ampoules (except two, used to measure the absorbance at t = 0) were placed in a water bath at 90 °C to initiate reaction.

Pairs of ampoules were removed at regular intervals. After cooling, an ampoule was opened, 0.6 ml of the solution diluted to 10 ml with 1 M sodium hydroxide solution, and the UV absorbance spectra at 25 °C measured at the required wavelength. This was repeated for each ampoule.

For each result, A was removed from the figure obtained for the absorbance at 280 nm, the natural log of this figure calculated, and the average of the pair of results noted. A was the absorbance at 280 nm of the decarboxylation product of the acid, at the same concentration. A pseudo-first order plot of ln (A_{280}- A) versus time was drawn for each run. The best straight line was fitted by regression Each run was repeated at least once for the whole pH range, and on completion of these a pH versus observed rate constant plot was calculated.

This method was repeated at pH 1.5 for *N*-ethyl quinolinic acid over a range of temperatures from 60 - 90 °C. It was also repeated at pH 1.5 for *N*-ethyl quinolinic acid over a range of ionic strengths from 0.5 to 3.0, and at pH 1.5 for *N*-ethyl quinolinic acid replacing distilled water with deuterated water (D_2O).

The identity of the decarboxylation products of the kinetic experiments was determined by UV absorbance and NMR. A sample kinetic run of each of the acids studied was carried out until completion. The solvent was removed under reduced pressure, and the absorbance at 280 nm of the product measured, along with the ^{1}H and ^{13}C NMR spectra. These were then compared to the authentic spectra of the decarboxylation products to confirm that it was decarboxylation that had taken place.

CHAPTER 5

5. References

1. D. M. Bonner and C. Yanofsky, *Proc. Natl. Acad. Sci. U.S.*, 1949, **35**, 576-581.
2. Y. Nishizuka and O. Hayaishi, *J. Biol. Chem.*, 1963, **238**, 483-485.
3. Y. Nishizuka and O. Hayaishi, *J. Biol. Chem.*, 1963, **238**, 3369-3375.
4. S. Nakamura, M. Ikeda, H. Tsuji, Y. Nishizuka and O. Hayaishi, *Biochem. Biophys. Res. Commun.*, 1963, **13**, 285-290.
5. R. K. Gholson, I. Ueda, N. Ogasawara and L. M. Henderson, *J. Biol. Chem.*, 1964, **239**, 1208-1214.
6. E. M. Kosower and J. A. Skorcz, *J. Am. Chem. Soc.*, 1960, **82**, 2195-2203.
7. A. J. Andreoli, M. Ikeda, H. Tsuji, Y. Nishizuka and O. Hayaishi, *Biochem. Biophys. Res. Commun.*, 1963, **12**, 87-92.
8. K. Iwai and H. Taguchi, *J. Nutri. Sci. Vitaminol.*, 1973, **19**, 491-499.
9. D. F. Mann and R. U. Byerrum, *J. Biol. Chem.*, 1974, **249**, 6817-6823.
10. H. Taguchi and K. Iwai, *Biochim. Biophys. Acta*, 1976, **422**, 29-37.
11. K. Iwai and H. Taguchi, *Biochem. Biophys. Res. Commun.*, 1974, **56**, 884-891.
12. K. Shibata and K. Iwai, *Biochim. Biophys. Acta*, 1980, **611**, 280-288.
13. K. Shibata and K. Iwai, *Agric. Biol. Chem.*, 1980, **44**, 301-308.
14. K. Iwai, K. Shibata, H. Taguchi and T. Ikatura, *Agric. Biol. Chem.*, 1979, **43**, 345-350.
15. R. Wagner and K. G. Wagner, *Phytochemistry*, 1984, **23**, 1881-1883.
16. E. Okuno and R. Schwarcz, *Biochim. Biophys. Acta*, 1985, **841**, 112-119.
17. A. C. Foster, W. O. Whetsell, E. D. Bird and R. Schwarcz, *Brain Res.*, 1985, **336**, 207-214.
18. E.Okuno, R. J. White and R. Schwarcz, *J. Biochem.*, 1988, **103**, 1054-1059.
19. K. Hughes, A. Dessen, P. Gray and C. Grubmeyer, *J. Bacteriol.*, 1993, **175**, 479-486.

20. P. M. Packman and W. B. Jakoby, *J. Biol. Chem.*, 1965, **240**, 4107-4108.

21. P. M. Packman and W. B. Jakoby, *J. Biol. Chem.*, 1967, **242**, 2075-2079.

22. K. Iwai, K. Shibata, H. Taguchi and T. Ikatura, *Agric. Biol. Chem.*, 1979, **43**, 351-355.

23. Y. Nishizuka and S. Nakamura, *Methods in Enzymology*, 1970, **17**, 491-500.

24. H. Taguchi and K. Iwai, *J. Nutri. Sci. Vitaminol.*, 1974, **20**, 269-281.

25. S. H. Moyed and H. E. Umbarger, *Physiol. Recs.*, 1962, **42**, 444-466.

26. A. C. Foster, W. C. Zinkland and R. Schwarcz, *J. Neurochem.*, 1985, **44**, 446-454.

27. P. M. Packman and W. B. Jakoby, *Methods in Enzymology*, 1970, **17**, 501-505.

28. S. Kunjara, C. S. Lee, G. W. Smithers, K. Shibata, K. Iwai and W. J. O'Sullivan, *Int. J. Biochem.*, 1986. **18**, 489-491.

29. G. W. Smithers and W. J. O'Sullivan, *Biochemistry*, 1984, **23**, 4767-4773.

30. K. Shibata and K. Iwai, *Agric. Biol. Chem.*, 1980, **44**, 2785-2791.

31. J. S. Myers and W. B. Jakoby, *J. Biol. Chem.*, 1975, **250**, 3875-3879.

32. K. Shibata and K. Iwai, *Agric. Biol. Chem.*, 1980, **44**, 293-300.

33. L. Kilikin and K. C. Calvo, *Biochem. Biophys. Res. Commun.*, 1988, **152**, 559-564.

34. H. Taguchi and K. Iwai, *Agric. Biol. Chem.*, 1976, **40**, 385-389.

35. P. M. Packman and W. B. Jakoby, *Biochem. Biophys. Res. Commun.*, 1965, **18**, 710-715.

36. R. A. Alberty, *Adv. Enzymology*, 1956, **17**, 1-34.

37. E. V. Brown and R. J. Moser, *J. Org. Chem.*, 1971, **36**, 454-457.

38. P. Dyson and D. L. Hammick, *J. Chem. Soc.*, 1937, 1724-1725.

39. P. Beak and B. Siegel, *J. Am. Chem. Soc.*, 1976, **98**, 3601-3606.

40. H. L. Levine, R. S. Brady and F. H. Westheimer, *Biochemistry*, 1980, **19**, 4993-4999.

41. W. D. L. Musick, *J. Mol. Biol.*, 1977, **117**, 1101-1107.

42. H. Taguchi and K. Iwai, *Agric. Biol. Chem.*, 1975, **39**, 1493-1500.

43. J. C. Eads, D. Ozturk, T. B. Wexler, C. Grubmeyer and J. C. Sacchettini, *Structure*, 1997, **5**, 47-58.

44. R. K. Goitein, D. Chelsky and S.M. Parsons, *J. Biol. Chem.*, 1978, **253**, 2963-2971.

45. S. Scheppele, *Chem. Rev.*, 1972, **72**, 511-523.

46. A. Fry in "*Isotope Effects in Chemical Reactions*", eds. C. J. Collins and N. S. Bowman, Van Nostrand Reinhold Co., New York, 1970, 364-414.

47. V. F. Raaen, T. Juhlke, F. J. Brwon and C. J. Collins, *J. Am. Chem. Soc.*, 1974, **96**, 5928-5930.

48. A. Maccoll, *J. Chem. Soc. A*, 1974, 77-101.

49. W. D. L. Musick, *CRC Crit. Rev. Biochem.*, 1981, **11**, 1-34.

50. M. Kori and J. F. Henderson, *J. Biol. Chem.*, 1966, **241**, 3404-3408.

51. J. Victor, L. B. Greenberg and D. L. Sloan, *J. Biol. Chem.*, 1979, **254**, 2647-2655.

52. T. Honjo, S. Nakamura, Y. Nishizuka and O. Hayaishi, *Biochem. Biophys. Res. Commun.*, 1966, **25**, 199-204.

53. A. Kosaka, H. O. Spivey and R. K. Gholson, *J. Biol. Chem.*, 1971, **246**, 3277-3283.

54. L. D. Smith and R. K. Gholson, *J. Biol. Chem.*, 1969, **244**, 68-71.

55. J. Preiss and P. Handler, *J. Biol. Chem.*, 1958, **233**, 488-492.

56. M. C. Powanda, O. Muniz and L. S. Dietrich, *Biochemistry*, 1969, **8**, 1869-1873.

57. S. Singer and E. W. Holmes, *J. Biol. Chem.*, 1977, **252**, 7959-7963.

58. G. L. King, C. G. Bounous and E. W. Holmes, *J. Biol. Chem.*, 1978, **253**, 3933-3938.

59. I. Lapin, *Epilepsia*, 1981, **22**, 257-265.

60. F. Moroni, G. Lombardi, V. Carla and G. Monetti, *Brain Res.*, 1984, **195**, 352-355.

61. M. Wolfensberger, U. Amsler, M. Cuenod, A. C. Foster, W. O. Whetsell and R. Schwarcz, *Neurosci. Lett.*, 1983, **38**, 85-90.

62. R. Schwarcz, *Biochem. Soc. Trans.*, 1993, **21**, 77-82.

63. N. P. Botting, *Chem. Soc. Rev.*, 1995, 401-412.

64. T. W. Stone and M. N. Perkins, *Eur. Pharmacology*, 1981, **72**, 411-412.

65. A. C. Foster and R. Schwarcz, in *Quinolinic acid and the Kynurenines*, ed. T. W. Stone, CRC Press, Boca Raton, 1989, 173-192.

66. S. R. Birley, J. F. Collins, M. N. Perkins and T. W. Stone, *Br. J. Pharmacol.*, 1982, **77**, 7-12.

67. R. Schwarcz, W. O. Whetsell and R. M. Mangano, *Science*, 1983, **219**, 316-318.

68. M. N. Perkins and T. W. Stone, *J. Pharmacol. Exp. Theor.*, 1983, **226**, 551-557.

69. M. P. Heyes, M. Gravell, M. April, D. Blackmore, W. T. London, J. A. Yergey and S. P. Markey, in *"Kynurenine and Serotonin Pathways"*, eds. R. Schwarcz, S. N. Young and R. R. Brown, Plenum Press, New York, 1991, 555-561.

70. A. C. Foster, J. F. Collins and R. Schwarcz, *Neuropharmacology*, 1983, **22**, 1331-1342.

71. V. I. Teichberg, M. Beaujean and O. Goldberg, in *Quinolinic acid and the Kynurenines*, ed. T. W. Stone, CRC Press, Boca Raton, 1989, 161-172.

72. A. C. Foster, L. P. Miller, W. H. Oldendorf and R. Schwarcz, *Exp. Neurol.* 1984, **84**, 428.

73. R. P. M. Bruyn and J. C. Stoof, *J. Neuro. Sci.*, 1990, **95**, 29-30.

74. M. P. Heyes, P. Kim and S. P. Markey, *J. Neurochem.*, 1988, **51**, 1946-1948.

75. R. Schwarcz and F. Du, in *"Kynurenine and Serotonin Pathways"*, eds. R. Schwarcz, S. N. Young and R. R. Brown, Plerum Press, New York, 1991, 185-199.

76. R. Schwarcz, E. Okuno and R. J. White, *Brain Res.*, 1989, **490**, 103-109.

77. C. Speciale and R. Schwarcz, *Abs. Soc. Neurosci.*, 1986, **12**, 243.

78. M. F. Beal, N. W. Kowall, D. W. Ellison, M. F. Mazarek, K. J. Schwartz and J. B. Martin, *Nature*, 1986, **231**, 168-171.

79. G. P. Reynolds, S. J. Pearson, J. Halket and M. Sandler, *J. Neurochem.*, 1988, **50**, 1959-1960.

80. R. Schwarcz, E. Okuno, R. J. White, E. D. Bird and W. O. Whetsell, *Proc. Natl. Acad. Sci. (USA)*, 1988, **85**, 4079-4081.

81. M. P. Heyes, E. J. Garnett and R. R. Brown, *Life Sci.*, 1985, **37**, 1811-1816.

82. A. C. Foster and R. Schwarcz, *J. Neurochem.*, 1985, **45**, 199-205.

83. W. O. Whetsell, C. Kohler, E. Okuno and R. Schwarcz, *Clin. Neuropath.*, 1988, **7**, 222.

84. M. P. Heyes, *Biochem. Soc. Trans.*, 1993, **21**, 82-89.

85. M. P. Heyes, *Ann. N.Y. Acad.Sci.*, 1993, **679**, 211-216.

86. M. P. Heyes, D. Rubinow, C. Lane and S. P. Markey, *Ann. Neurol.*, 1989, **26**, 275-277.

87. D. Jauch, E. H. Urbanska, P. Guidetti, E. D. Bird, J. P. G. Vonsattel, W. O. Whetsell and R. Schwarcz, *J. Neurol. Sci.*, 1995, **130**, 39-47.

88. J. H. Connick, G. C. Heywood, G. J. Sills, G. G. Thompson, M. J. Brodie and T. W. Stone, *Gen. Pharmacol.*, 1992, **23**, 235-239.

89. D. A. Bender, *Quinolinic acid and the Kynurenines*, ed. T. W. Stone, CRC Press, Boca Raton, 1989, 3-38.

90. F. Hirati and O. Hayaishi, *J. Biol. Chem.*, 1971, **246**, 7825-7826.

91. N. Eguchi, Y. Watanabe, K. Kawanash, Y. Hashimoto and O. Hayaishi, *Arch. Biochem. Biophys.*, 1984, **232**, 602-609.

92. L. D. Buckbery, B. W. Bycroft, P. N. Shaw and I. S. Blagborough, *Bioorg. Med. Chem. Lett.*, 1992, **2**, 1225-1230.

93. F. C. Ross, *Ph.D. Thesis*, University of St. Andrews, 1996.

94. G. M. Kishore, *J. Biol. Chem.*, 1984, **259**, 10669-10741.

95. A. H. Mehler, *J. Biol. Chem.*, 1956, **218**, 241-254.

96. J. G. Foster and A. G. Moat, *Microbiological Rev.*, 1980, **44**, 83-105.

97. G. J. Tritz, *E. Coli and S, Typhimurium Cellular and Molecular Biology, Vol. 1,* eds. F. C. Niedhart, J. L. Ingraham, K. Blow, B. Magasanik, M. Schaechter and H. C. Umbarger, Am. Soc. for Microbiology, Washington D. C., 1987, 557-563.

98. H. B. White, *Pyridine nucleotide coenzymes*, eds. J. Everse, B. M. Anderson and K. S. You, Academic Press Inc., New York, 1982, 1-17.

99. R. K. Gholson, *Nature*, 1966, **212**, 933-935.

100. J. Preiss and P. Handler, *J. Biol. Chem.*, 1958, **233**, 488-492.

101. J. Preiss and P. Handler, *J. Biol. Chem.*, 1958, **233**, 493-500.

102. W. Dahmen, B. Webb and J. Preiss, *Arch. Biochem. Biophys.*, 1967, **120**, 440-450.

103. J. W. Foster, D. M. Kinney and A. G. Moat, *J. Bacteriol.*, 1979, **138**, 957-961.

104. T. Penfound and J. W. Foster, *E. Coli and S. Typhimurium Cellular and Molecular Biology, Vol. 1,* ed. F. C. Niedhart, Am. Soc. for Microbiology, Washington D. C., 1995, 721-730.

105. A. J. Andreoli, T. Grover, R. K. Gholson and T. S. Matney, *Biochim. Biophys. Acta*, 1969, **193**, 539-541.

106. J. W. Foster and A.M. Baskowsky-Foster, *J. Bacteriol.*, 1980, **142**, 1032-1035.

107. D. Hillyard, M. Rechsteiner, P. Manlapaz-Ramos, J. S. Imperial, L. J. Cruz and B. M. Olivera, *J. Biol. Chem.*, 1981, **256**, 8491-8497.

108. P. Manlapaz-Ramos and B. M. Olivera, *J. Biol. Chem.*, 1973, **248**, 5067-5073.

109. L. S. Hanna, S. L. Hess and D. L. Sloan, *J. Biol. Chem.*, 1983, **258**, 9475-9454.

110. R. F. Evans and H. C. Brown, *J. Org. Chem.*, 1962, **27**, 1329-1332.

111. W. Marckwald, W. Klemm and H. Trabert, *Ber.*, 1900, **33**, 1556-1566.

112. O. Fischer *et al, Ber.*, 1882, **15**, 62-64.

113. O. Fischer *et al, Ber.*, 1883, **16**, 1183-1185.

114. O. Fischer *et al*, *Ber.*, 1884, **17**, 763-764.

115. S. M. McElvain and M. E. Goese, *J. Am. Chem. Soc.*, 1943, **65**, 2233-2236.

116. E. Koenigs and G. Kinne, *Ber.*, 1921, **54**, 1357-1362.

117. A. F. Tiesler, U.S. Patent, **2,330,641**; *Chem. Abstr.*, 1944, **38**, 1249.

118. K. Shinohara, *J. Biol. Chem.*, 1932, **96**, 285-297.

119. A. Rosenheim and I. Davidsohn, *Z. anorg. Chem.*, 1904, **41**, 231.

120. P. Klason and T. Carlson, *Ber.*, 1906, **39**, 738.

121. J. P. Danehy and M. Y. Oetser, *J. Org. Chem.*, 1967, **37**, 1491-1495.

122. N. Kharasch, in "Organic Sulfur Compounds", ed. N. Kharasch, Pergamon Press, Oxford, 1961, 387.

123. J. P. Danehy, B. T. Doherty and C.P. Egan, *J. Org. Chem.*, 1971, **25**, 2525-2530.

124. L. Field, P. M. Giles and D. L. Tuleen, *J. Org. Chem.*, 1971, **25**, 623-626.

125. J. Delarge and C. L. Lapiere, *Bull. Chem. Soc. Belges*, 1986, **75**, 321-327.

126. A. Stewart, Unpublished results, University of St. Andrews, 1997.

127. V. Snieckus, *Chem. Rev.*, 1990, **90**, 879-883.

128. M. A. M. Easson, and N. P. Botting, unpublished results.

129. J. Epsztajn, E. Bieniek, J. Z. Brezinski and A Jozwiak, *Tetrahedron Lett.*, 1983, **24**, 4735-4738.

130. S. Sengupta and V. Snieckus, *Tetrahedron Lett.*, 1990, **31**, 4267-4270.

131. D. L. Comins and D. H. LaMunyon, *Tetrahedron Lett.*, 1988, **29**, 773-776.

132. K. H. Worms and M. Schmidt-Dunker, in "Organic Phosphorus Compounds" vol. 7, eds. G. M. Kosolapoff and I. Maier, J. Wiley & Sons, New York, 1976, 1.

133. L. D. Freedman and G. O. Doak, *Chem. Rev.*, 1957, **57**, 479-523.

134. E. F. Jason and E. K. Fields, *J. Org. Chem.*, 1962, **27**, 1402-1405.

135. A. G. Vargolis, *Tetrahedron Lett.*, 1972, 31-32.

136. P. Tavs, *Chem. Ber.*, 1970, **103**, 2428-2436.

137. R. A. Naylor and A. Williams, *J. Chem. Soc., Perkin Trans. II*, 1976, 1908-1913.

138. G. M. Kosolapoff and C. H. Roy, *J. Org. Chem.*, 1961, **26**, 1895-1898.

139. A. Burger, J. B. Clements, N. D. Dawson and R. B. Henderson, *J. Org. Chem.*, 1955, **20**, 1383-1386.

140. T. Hirao, T. Masanaga, Y. Oshiro and T. Agawa, *Synthesis*, 1981, 56-57.

141. T. Hirao, T. Masanaga, N. Yanada, Y. Oshiro and T. Agawa, *Bull. Chem. Soc. Japan*, 1982, **55**, 909-913.

142. T. A. Bryson, J. C. Wisawaty, R. B. Dunlop, R. R. Fisher and P. D. Ellis, *J. Org. Chem.*, 1974, **39**, 3436-3438.

143. T. B. Windholz, L. H. Peterson and G. J. Kent, *J. Org. Chem.*, 1963, **28**, 1443.

144. A. R. Katrizky and E. Lunt, *Tetrahedron*, 1969, **25**, 4291-4305.

145. D. Redmore, *J. Org. Chem.*, 1970, **35**, 4114-4117.

146. J. I. G. Cadogan, D. J. Sears and D. M. Smith, *J. Chem. Soc. C*, 1969, 1314-1318.

147. P. Tavs and F. Korte, *Tetrahedron*, 1967, **23**, 4677-4679.

148. D. J. Hunter, J. Bird, F. Cassidy, R. C. DeMello, G. P. Harper, E. H. Karran, R. E. Markwell, A. J. Miles-Williams and R. W. Ward, *Bioorg. Med. Chem. Lett.*, 1994, **4**, 2833-2836.

149. P. A. Bartlett and C. K. Marlowe, *Biochemistry*, 1983, **22**, 4618-4624.

150. S. Hanessian and Y. L. Bennani, *Tetrahedron Lett.*, 1990, 6465-6468.

151. V. L. Ryzhkov, M. I. Kabacknik, L. M. Tarasevich, N. A. Medved, N. K. Zeitenok, J. K. Marchenko, V. A. Vagzhanova, E. F. Vianova and N. V. Cherburkina, *Doklady Akad. Nauk U.S.S.R.*, 1954, **98**, 849-852.

152. D. N. Moothoo, M. Sc. Literature Report, University of St. Andrews, 1995.

153. J. Olefsyszyn, L. Subotkowska and P. Mastalerz, *Synthesis*, 1979, 985-986.

154. C. C. Tam, K. L. Mattocks and M. Tischler, *Synthesis*, 1982, 188-190.

155. M. T. DuPriest, C. L. Schmidt, D. Kuzmich and S. B. Williams, *J. Org. Chem.*, 1985, **50**, 2021-2023.

156. N. M. Gray, M. S. Dappen, B. K. Cheng, A. A. Cordi, J. P. Biesterfeldt, W. F. Hood and J. B. Monahan, *J. Med. Chem.*, 1991, **34**, 1283-1292.

157. S. Danishefsky, T. A. Bryson and J. J. Puthenpurayil, *J. Org. Chem.*, 1975, **40**, 796-797.

158. C. Matt, A. Wagner and C. Mioskowski, *J. Org. Chem.*, 1997, **62**, 234-235.

159. S. Cacchi and F. L. Torre, *Chem. Ind.*, 1986, 286-287.

160. G. P. Borsotti, M. Foa and N. Gatto, *Synthesis*, 1990, 207-208.

161. A. J. Bailey, W. P. Griffith, S. I. Mostaya and P. A. Sherwood, *Inorg. Chem.*, 1983, **32**, 268-271.

162. A. Onopchenko, J. G. D. Schulz and R. Seekircher, *J. Org. Chem.*, 1972, **37**, 1414-1417.

163. L. Garuti, A. Ferranti, M. Roberti, E. Katz, R. Budriesi and A. Chiarni, *Pharmazie*, 1992, **47**, 295-297.

164. M. R. F. Ashworth, R. P. Daffern and D. L. Hammick, *J. Chem. Soc.*, 1939, 809-812.

165. N. H. Cantwell and E. V. Brown, *J. Am. Chem. Soc.*, 1953, **75**, 4466-4468.

166. N. H. Cantwell and E. V. Brown, *J. Am. Chem. Soc.*, 1952, **74**, 5967-5970.

167. L. W. Clark, *J. Phys. Chem.*, 1965, **69**, 2277-2280.

168. L. W. Clark, *J. Phys. Chem.*, 1962, **66**, 125-127.

169. P. C. Haake and J. Mantecon, *J. Am. Chem. Soc.*, 1964, **86**, 5230-5234.

170. E. M. Kosower and J. W. Patten, *J. Org. Chem.*, 1961, **26**, 1318-1319.

171. F. A. Hoppe-Seyler, *Z. Physiol. Chem.*, 1933, **222**, 105-115.

172. E. L. Gasteiger, P. C. Haake and J. A. Gergen, *Proc. N.Y. Acad. Sci.*, 1960, **90**, 622-636.

173. B. R. Brown and D. L. Hammick, *J. Chem. Soc.*, 1949, 649-653.

174. G. E. Dunn and G. J. K. Lee, *Can. J. Chem.*, 1971, **49**, 1032-1035.

175. G. E. Dunn, E. A. Lawler and A. B. Yamashito, *Can. J. Chem.*, 1977, **55**, 2478-2481.

176. G. E. Dunn, G. J. K. Lee and H. F. Thimm, *Can. J. Chem.*, 1972, **50**, 3017-3027.

177. G. E. Dunn and H. F. Thimm, *Can. J. Chem.*, 1977, **55**, 1342-1347.

178. G. Scapin, C. Grubmeyer and J. Sacchettini, *Biochemistry*, 1994, **33**, 1287-1294.

179. R. E. Handshucmacher, *J. Biol. Chem.*, 1960, **235**, 2917-2929.

180. B. W. Potvin, H. J. Stern, S. R. May, G. R. Lam and R. S. Krooth, *Biochem Pharmacol.*, 1978, **27**, 655-665.

181. R. B. Silverman and R. P. Groziak, *J. Am. Chem. Soc.*, 1982, **104**, 6434-6439.

182. S. A. Acheson, J. B. Bell, M. E. Jones and R. Wolfenden, *Biochemistry*, 1990, **29**, 3198-3202.

183. K. Shostak and M. E. Jones, *Biochemistry*, 1992, **31**, 12155-12161.

184. J. K. Lee and K. N. Houk, *Science*, 1997, **276**, 942-945.

185. W. Wu, A. Ley-Kam, F. M. Wong, T. J. Austin and S. M. Miller, *Bioorg. Med. Chem. Lett.*, 1997, **7**, 2623-2628.

186 M. P. Nakanishi and W. Wu, *Tetrahedron Lett.*, 1998, **39**, 6271-6272.

187. T Gramstad and R. N. Haszeldine, *J. Chem. Soc.*, 1956, 173-180.

188. C. D. Beard, K. Baum and V. Grakauskas, *J. Org. Chem.*, 1973, **38**, 3673-3677.

189. W. C. Still, M. Khan and A. Mitra, *J. Org. Chem.*, 1978, **43**, 2923-2925.

190. J. D. Crum and C. H. Fuchsman, *J. Het. Chem.*, 1966, **3**, 252-256.

191. A. P. Swain and S. K. Nagele, *J. Am. Chem. Soc.*, 1957, **79**, 5250-5253.

192. A. I. Meyers and R. A. Gabel, *J. Org. Chem.*, 1982, **47**, 2633-2637.

193. K. Yanauchi, M. Kinoshita and M. Imoto, *Bull. Chem. Soc. Japan*, 1972, **45**, 2531-2534.

194. H. Neunberg, *Ber.*, 1935, **68**, 1474.

195. S. Karayala and K. P. Link, *J. Am. Chem. Soc.*, 1940, **62**, 917-920.

196. D. H. Brauns, *J. Am. Chem. Soc.*, 1925, **47**, 1280-1284.

CHAPTER 6

6. Appendix

Full experimental data for the crystal structure of 2-sulfonicotinic acid is given in this appendix.

Experimental

Data Collection

A colourlessblock block crystal of $C_6H_5NSO_5$ having approximate dimensions of 0.20 x 0.20 x 0.10 mm was mounted on a glass fiber. All measurements were made on a Rigaku AFC7S diffractometer with graphite monochromated Mo-Kα radiation.

Cell constants and an orientation matrix for data collection, obtained from a least-squares refinement using the setting angles of 17 carefully centered reflections in the range $7.39 < 2\theta < 15.34°$ corresponded to a primitive monoclinic cell with dimensions:

a = 5.950(2) $\AA$

b = 9.335(3) $\AA$ $\quad \beta = 92.51(3)°$

c = 13.115(3) $\AA$

V = 727.7(4) $\AA^3$

For Z = 4 and F.W. = 203.17, the calculated density is 1.85 g/cm^3. The systematic absences of:

h0l: h+l $\neq$ 2n

0k0: k $\neq$ 2n

uniquely determine the space group to be:

$P2_1/n$ (#14)

The data were collected at a temperature of 20 $\pm$ 1°C using the ω-2θ scan technique to a maximum 2θ value of 50.0°. Omega scans of several intense reflections, made prior to data collection, had an average width at half-height of 0.28° with a take-off angle of 6.0°. Scans of (1.10 + 0.35 tan θ)° were made at a speed of 16.0°/min (in omega). The weak reflections ($I < 15.0\sigma(I)$) were rescanned (maximum of 4 scans) and the counts were accumulated to ensure good counting statistics. Stationary background counts were recorded on each side of the reflection. The ratio of peak counting time to background counting time was 2:1. The diameter of the incident beam collimator was 1.0 mm and the crystal to detector distance was 235 mm, The computer-controlled slits were set to 9.0 mm (horizontal) and 13.0 mm (vertical).

Data Reduction

Of the 1501 reflections which were collected, 1364 were unique ($R_{int} = 0.020$). The intensities of three representative reflection were measured after every 150 reflections. No decay correction was applied.

The linear absorption coefficient, μ, for Mo-Kα radiation is 4.1 cm^{-1}. An empirical absorption correction based on azimuthal scans of several reflections was applied which resulted in transmission factors ranging from 0.93 to 1.00. The data were corrected for Lorentz and polarization effects.

Structure Solution and Refinement

The structure was solved by direct methods[1] and expanded using Fourier techniques[2]. The non-hydrogen atoms were refined anisotropically. Some hydrogen atoms were refined isotropically, the rest were included in fixed positions. The final cycle of full-matrix least-squares refinement[3] was based on 1048 observed reflections ($I > 3.00\sigma(I)$) and 122 variable parameters and converged (largest parameter shift was 0.08 times its esd) with unweighted and weighted agreement factors of:

$$R = \Sigma||Fo| - |Fc||/\Sigma|Fo| = 0.031$$

$$R_w = \sqrt{(\Sigma w(|Fo| - |Fc|)^2/\Sigma wFo^2)} = 0.030$$

The standard deviation of an observation of unit weight[4] was 2.13. The weighting scheme was based on counting statistics and included a factor (p = 0.003) to downweight the intense reflections. Plots of $\Sigma w(|Fo| - |Fc|)^2$ versus $|Fo|$, reflection order in data collection, $\sin\theta/\lambda$ and various classes of indices showed no unusual trends. The maximum and minimum peaks on the final difference Fourier map corresponded to 0.26 and -0.33 $e^-/\AA^3$, respectively.

Neutral atom scattering factors were taken from Cromer and Waber[5] . Anomalous dispersion effects were included in Fcalc[6]; the values for $\Delta f'$ and $\Delta f''$ were those of Creagh and McAuley[7]. The values for the mass attenuation coefficients are those of Creagh and Hubbel[8]. All calculations were performed using the teXsan[9] crystallographic software package of Molecular Structure Corporation.

References

(1) SIR92: Altomare, A., Burla, M.C., Camalli, M., Cascarano, M., Giacovazzo, C., Guagliardi, A., Polidori, G. (1994). J. Appl. Cryst., in preparation.

(2) DIRDIF92: Beurskens, P.T., Admiraal, G., Beurskens, G., Bosman, W.P., Garcia-Granda, S., Gould, R.O., Smits, J.M.M. and Smykalla, C. (1992). The DIRDIF program system, Technical Report of the Crystallography Laboratory, University of Nijmegen, The Netherlands.

(3) Least-Squares:

Function minimized: $\Sigma w(|Fo| - |Fc|)^2$

where w = $\frac{1}{\sigma^2(Fo)} = \frac{4Fo^2}{\sigma^2(Fo^2)}$

$\sigma^2(Fo^2) = \frac{S^2(C+R^2B)+(pFo^2)^2}{Lp^2}$

S = Scan rate

C = Total integrated peak count

R = Ratio of scan rime to background counting time

B = Total background count

Lp = Lorentz-polarization factor

p = p-factor

(4) Standard deviation of an observation of unit weight:

$$\sqrt{\Sigma w(|Fo| - |Fc|)^2/(No - Nv)}$$

where: No = number of observations

Nv = number of variables

(5) Cromer, D. T. & Waber, J. T.; "International Tables for X-ray Crystallography", Vol. IV, The Kynoch Press, Birmingham, England, Table 2.2 A (1974).

(6) Ibers, J. A. & Hamilton, W. C.; Acta Crystallogr., 17, 781 (1964).

(7) Creagh, D. C. & McAuley, W.J .; "International Tables for Crystallography", Vol C, (A.J.C. Wilson, ed.), Kluwer Academic Publishers, Boston, Table 4.2.6.8, pages 219-222 (1992).

(8) Creagh, D. C. & Hubbell, J.H..; "International Tables for Crystallography", Vol C, (A.J.C. Wilson, ed.), Kluwer Academic Publishers, Boston, Table 4.2.4.3, pages 200-206 (1992).

(9) teXsan: Crystal Structure Analysis Package, Molecular Structure Corporation (1985 & 1992).

EXPERIMENTAL DETAILS

A. Crystal Data

Empirical Formula	$C_6H_5NSO_5$
Formula Weight	203.17
Crystal Color, Habit	colourlessblock, block
Crystal Dimensions	0.20 X 0.20 X 0.10 mm
Crystal System	monoclinic
Lattice Type	Primitive
No. of Reflections Used for Unit Cell Determination (2θ range)	17 (7.4 - 15.3°)
Omega Scan Peak Width at Half-height	0.28°
Lattice Parameters	a = 5.950(2)Å b = 9.335(3) Å c = 13.115(3) Å β = 92.51(3)° V = 727.7(4) Å^3
Space Group	$P2_1/n$ (#14)
Z value	4
D_{calc}	1.854 g/cm^3
F_{000}	416.00
μ(MoKα)	4.12 cm^{-1}

B. Intensity Measurements

Diffractometer	Rigaku AFC7S
Radiation	MoKα (λ = 0.71069 Å) graphite monochromated
Attenuator	Zr foil (factors = 1.00, 8.53, 8.53, 8.53)
Take-off Angle	6.0°
Detector Aperture	9.0 mm horizontal 13.0 mm vertical
Crystal to Detector Distance	235 mm
Temperature	20.0°C
Scan Type	ω-2θ
Scan Rate	16.0°/min (in ω) (up to 4 scans)
Scan Width	(1.10 + 0.35 tan θ)°
$2\theta_{max}$	50.0°
No. of Reflections Measured	Total: 1501 Unique: 1364 (R_{int} = 0.020)
Corrections	Lorentz-polarization Absorption (trans. factors: 0.9334 - 1.0000)

C. Structure Solution and Refinement

Structure Solution	Direct Methods (SIR92)
Refinement	Full-matrix least-squares
Function Minimized	$\Sigma w(\|Fo\| - \|Fc\|)^2$
Least Squares Weights	$\frac{1}{\sigma^2(Fo)} = \frac{4Fo^2}{\sigma^2(Fo^2)}$
p-factor	0.003
Anomalous Dispersion	All non-hydrogen atoms
No. Observations (I>3.00σ(I))	1048
No. Variables	122
Reflection/Parameter Ratio	8.59

Residuals: R; Rw	0.031 ; 0.030
Goodness of Fit Indicator	2.13
Max Shift/Error in Final Cycle	0.08
Maximum peak in Final Diff. Map	0.26 $e^-/\AA^3$
Minimum peak in Final Diff. Map	-0.33 $e^-/\AA^3$

Table 1. Atomic coordinates and B_{iso}/B_{eq}

atom	x	y	z	B_{eq}
S(1)	1.2456(1)	0.02291(8)	0.70666(5)	1.54(1)
O(1)	1.4745(3)	0.0570(2)	0.6809(1)	2.04(5)
O(2)	1.1582(3)	-0.1069(2)	0.6610(1)	2.16(5)
O(3)	1.2043(3)	0.0369(2)	0.8144(1)	2.33(5)
O(4)	1.2805(3)	0.0429(2)	0.4675(2)	2.07(5)
O(5)	1.3140(4)	0.2718(2)	0.4192(2)	2.79(5)
N(1)	0.9236(4)	0.2180(2)	0.7144(2)	1.61(5)
C(1)	0.7648(5)	0.3141(3)	0.6870(2)	1.97(7)
C(2)	0.7537(5)	0.3668(3)	0.5898(2)	2.14(7)
C(3)	0.9113(5)	0.3215(3)	0.5227(2)	1.96(6)
C(4)	1.0730(4)	0.2191(3)	0.5522(2)	1.45(6)
C(5)	1.0732(4)	0.1649(3)	0.6502(2)	1.33(6)
C(6)	1.2373(5)	0.1801(3)	0.4729(2)	1.81(6)
H(1)	0.9311	0.1855	0.7831	1.9336
H(2)	0.6605	0.3456	0.7350	2.3705
H(3)	0.6401	0.4332	0.5689	2.5612
H(4)	0.9096	0.3601	0.4556	2.3743
H(5)	1.367(6)	0.021(4)	0.415(3)	6(1)

$$B_{eq} = \frac{8}{3}\pi^2(U_{11}(aa^*)^2 + U_{22}(bb^*)^2 + U_{33}(cc^*)^2 + 2U_{12}aa^*bb^*\cos\gamma + 2U_{13}aa^*cc^*\cos\beta + 2U_{23}bb^*cc^*\cos\alpha)$$

Table 2. Anisotropic Displacement Parameters

atom	U_{11}	U_{22}	U_{33}	U_{12}	U_{13}	U_{23}
S(1)	0.0200(4)	0.0214(4)	0.0172(4)	0.0015(3)	0.0023(3)	0.0010(3)
O(1)	0.017(1)	0.031(1)	0.029(1)	0.0007(9)	0.0033(9)	-0.0011(9)
O(2)	0.032(1)	0.021(1)	0.029(1)	-0.0025(9)	0.0002(10)	-0.0007(9)
O(3)	0.037(1)	0.037(1)	0.015(1)	0.006(1)	0.0043(9)	0.0039(9)
O(4)	0.027(1)	0.027(1)	0.024(1)	0.0056(10)	0.0091(9)	-0.0012(10)
O(5)	0.047(1)	0.033(1)	0.027(1)	-0.007(1)	0.019(1)	0.003(1)
N(1)	0.022(1)	0.023(1)	0.016(1)	0.000(1)	0.005(1)	0.000(1)
C(1)	0.021(2)	0.026(2)	0.029(2)	0.003(1)	0.007(1)	-0.006(1)
C(2)	0.026(2)	0.026(2)	0.029(2)	0.006(1)	-0.001(1)	0.000(1)
C(3)	0.030(2)	0.024(2)	0.020(2)	-0.001(1)	0.002(1)	0.002(1)
C(4)	0.019(1)	0.019(1)	0.018(1)	-0.002(1)	0.003(1)	-0.001(1)
C(5)	0.016(1)	0.018(1)	0.017(1)	-0.001(1)	0.003(1)	-0.002(1)
C(6)	0.023(2)	0.032(2)	0.015(1)	0.000(1)	0.001(1)	-0.004(1)

The general temperature factor expression:

$$\exp(-2\pi^2(a^{*2}U_{11}h^2 + b^{*2}U_{22}k^2 + c^{*2}U_{33}l^2 + 2a^*b^*U_{12}hk + 2a^*c^*U_{13}hl + 2b^*c^*U_{23}kl))$$

Table 3. Bond Lengths($\AA$)

atom	atom	distance	atom	atom	distance
S(1)	O(1)	1.453(2)	S(1)	O(2)	1.439(2)
S(1)	O(3)	1.451(2)	S(1)	C(5)	1.814(3)
O(4)	C(6)	1.309(3)	O(5)	C(6)	1.211(3)
N(1)	C(1)	1.340(4)	N(1)	C(5)	1.347(3)
C(1)	C(2)	1.365(4)	C(2)	C(3)	1.380(4)
C(3)	C(4)	1.398(4)	C(4)	C(5)	1.381(4)
C(4)	C(6)	1.503(4)			

Table 4. Bond Lengths($\AA$)

atom	atom	distance	atom	atom	distance
O(4)	H(5)	0.90(4)	N(1)	H(1)	0.95
C(1)	H(2)	0.95	C(2)	H(3)	0.95
C(3)	H(4)	0.95			

Table 5. Bond Angles(°)

atom	atom	atom	angle	atom	atom	atom	angle
O(1)	S(1)	O(2)	114.4(1)	O(1)	S(1)	O(3)	114.0(1)
O(1)	S(1)	C(5)	105.3(1)	O(2)	S(1)	O(3)	114.1(1)
O(2)	S(1)	C(5)	104.9(1)	O(3)	S(1)	C(5)	102.4(1)
C(1)	N(1)	C(5)	123.8(2)	N(1)	C(1)	C(2)	119.7(3)
C(1)	C(2)	C(3)	118.6(3)	C(2)	C(3)	C(4)	120.8(3)
C(3)	C(4)	C(5)	118.7(3)	C(3)	C(4)	C(6)	115.8(2)
C(5)	C(4)	C(6)	125.5(3)	S(1)	C(5)	N(1)	113.0(2)
S(1)	C(5)	C(4)	128.7(2)	N(1)	C(5)	C(4)	118.2(2)
O(4)	C(6)	O(5)	125.5(3)	O(4)	C(6)	C(4)	114.2(3)
O(5)	C(6)	C(4)	120.3(3)				

Table 6. Bond Angles(°)

atom	atom	atom	angle	atom	atom	atom	angle
C(6)	O(4)	H(5)	112(2)	C(1)	N(1)	H(1)	118.1
C(5)	N(1)	H(1)	118.1	N(1)	C(1)	H(2)	120.3
C(2)	C(1)	H(2)	120.0	C(1)	C(2)	H(3)	120.6
C(3)	C(2)	H(3)	120.8	C(2)	C(3)	H(4)	119.6
C(4)	C(3)	H(4)	119.6				

Table 7. Torsion Angles(°)

atom	atom	atom	atom	angle	atom	atom	atom	atom	angle
S(1)	C(5)	N(1)	C(1)	-173.7(2)	S(1)	C(5)	C(4)	C(3)	174.7(2)
S(1)	C(5)	C(4)	C(6)	-6.7(4)	O(1)	S(1)	C(5)	N(1)	-133.8(2)
O(1)	S(1)	C(5)	C(4)	48.4(3)	O(2)	S(1)	C(5)	N(1)	105.2(2)
O(2)	S(1)	C(5)	C(4)	-72.6(3)	O(3)	S(1)	C(5)	N(1)	-14.2(2)
O(3)	S(1)	C(5)	C(4)	168.0(2)	O(4)	C(6)	C(4)	C(3)	-137.9(3)
O(4)	C(6)	C(4)	C(5)	43.5(4)	O(5)	C(6)	C(4)	C(3)	40.6(4)
O(5)	C(6)	C(4)	C(5)	-138.0(3)	N(1)	C(1)	C(2)	C(3)	-1.5(5)
N(1)	C(5)	C(4)	C(3)	-3.0(4)	N(1)	C(5)	C(4)	C(6)	175.6(3)
C(1)	N(1)	C(5)	C(4)	4.3(4)	C(1)	C(2)	C(3)	C(4)	2.7(5)
C(2)	C(1)	N(1)	C(5)	-2.1(4)	C(2)	C(3)	C(4)	C(5)	-0.5(4)
C(2)	C(3)	C(4)	C(6)	-179.2(3)					

Table 8. Non-bonded Contacts out to 3.60 Å

atom	atom	distance	ADC	atom	atom	distance	ADC
S(1)	N(1)	3.588(2)	74602	O(1)	O(4)	2.651(3)	85603
O(1)	C(1)	2.957(4)	65501	O(1)	N(1)	3.080(3)	65501
O(1)	C(1)	3.211(3)	74602	O(1)	N(1)	3.492(3)	74602
O(1)	C(6)	3.493(3)	85603	O(1)	C(2)	3.567(4)	65501
O(1)	O(5)	3.587(3)	85603	O(2)	C(6)	2.954(3)	75603
O(2)	O(4)	3.103(3)	75603	O(2)	C(3)	3.146(4)	75603
O(2)	C(4)	3.235(3)	75603	O(2)	O(5)	3.333(3)	75603
O(2)	N(1)	3.344(3)	74602	O(2)	C(1)	3.360(3)	64602
O(2)	O(3)	3.436(3)	74602	O(2)	C(5)	3.589(3)	74602
O(3)	C(3)	3.230(3)	4	O(3)	O(5)	3.278(3)	45504
O(3)	C(2)	3.439(4)	64602	O(3)	C(1)	3.480(4)	64602
O(4)	O(4)	2.827(4)	85603	O(4)	C(5)	3.208(3)	75603
O(4)	C(4)	3.229(3)	75603	O(4)	O(4)	3.572(4)	75603
O(4)	N(1)	3.584(3)	75603	O(4)	C(3)	3.592(4)	75603
O(5)	N(1)	2.793(3)	55404	O(5)	C(1)	3.149(4)	55404
O(5)	C(2)	3.400(4)	76603	O(5)	C(2)	3.482(4)	65501
C(3)	C(3)	3.555(6)	76603				

The ADC (atom designator code) specifies the position of an atom in a crystal. The 5-digit number shown in the table is a composite of three one-digit numbers and one two-digit number: TA (first digit) + TB (second digit) + TC (third digit) + SN (last two digits). TA, TB and TC are the crystal lattice translation digits along cell edges a, b and c. A translation digit of 5 indicates the origin unit cell. If TA = 4, this indicates a translation of one unit cell length along the a-axis in the negative direction. Each translation digit can range in value from 1 to 9 and thus ± 4 lattice translations from the origin (TA=5, TB=5, TC=5) can be represented.

The SN, or symmetry operator number, refers to the number of the symmetry operator used to generate the coordinates of the target atom. A list of symmetry operators relevant to this structure are given below.

For a given intermolecular contact, the first atom (origin atom) is located in the origin unit cell and its position can be generated using the identity operator (SN=1). Thus, the ADC for an origin atom is always 55501. The position of the second atom (target atom) can be generated using the ADC and the coordinates of the atom in the parameter table. For example, an ADC of 47502 refers to the target atom moved through symmetry operator two, then translated -1 cell translations along the a axis, +2 cell translations along the b axis, and 0 cell translations along the c axis.

An ADC of 1 indicates an intermolecular contact between two fragments (eg. cation and anion) that reside in the same asymmetric unit.

Symmetry Operators:

(1)	X,	Y,	Z	(2)	1/2-X,	1/2+Y,	1/2-Z
(3)	-X,	-Y,	-Z	(4)	1/2+X,	1/2-Y,	1/2+Z